



THE UNIVERSITY OF
WAIKATO
Te Whare Wānanga o Waikato

Research Commons

<http://researchcommons.waikato.ac.nz/>

Research Commons at the University of Waikato

Copyright Statement:

The digital copy of this thesis is protected by the Copyright Act 1994 (New Zealand).

The thesis may be consulted by you, provided you comply with the provisions of the Act and the following conditions of use:

- Any use you make of these documents or images must be for research or private study purposes only, and you may not make them available to any other person.
- Authors control the copyright of their thesis. You will recognise the author's right to be identified as the author of the thesis, and due acknowledgement will be made to the author where appropriate.
- You will obtain the author's permission before publishing any material from the thesis.

Processing Extrudable Sheets using Decoloured Bloodmeal

A thesis
submitted in fulfilment
of the requirements for the degree
of
Doctor of Philosophy in Engineering
at
The University of Waikato
by
Izuchukwu Sandra Chinenye Peace



THE UNIVERSITY OF
WAIKATO
Te Whare Wānanga o Waikato

2019

Abstract

This study investigated the feasibility of blending decoloured bloodmeal thermoplastic (DBT), a thermoplastic protein material, with poly (lactic acid) (PLA), a semi-crystalline polymer, and subsequently processing the blend into a sheet using extrusion. Free radical grafting was used to graft itaconic anhydride onto PLA to create reactive side groups. Blends of DBT and PLA compatibilized with itaconic anhydride were produced using different processing conditions, different formulations of DBT and different blend compositions. Decoloured bloodmeal thermoplastic powder (DBTP) was easier to process into injection mouldable samples than were decoloured bloodmeal thermoplastic granules (DBTG).

The compatibility between the produced material blends was investigated using mechanical testing, scanning electron microscopy (SEM), differential scanning calorimetry (DSC), dynamic mechanical analysis (DMA) and wide-angle X-ray scattering (WAXS). Blending DBT with PLA increased the tensile strength and modulus of DBT while strain at break decreased. The glass transition temperature of the blends increased compared to neat DBT. SEM revealed a more homogenous microstructure, which provided evidence of enhanced interfacial adhesion between both phases in the blends with PLA grafted with itaconic anhydride (PLA-g-IA). An insignificant decrease in the crystallinity of the blends compared to neat material was observed in the WAXS result, indicating that blending with PLA has no structural effect on DBT.

Ratios (DBP:PLA) of 30:70 (DP37), 50:50 (DP55), 70:30 (DP73) and 90:10 (DP91), with and without compatibilizer (PLA-g-IA), were examined to determine the optimal blend ratio for DBT/PLA blends. DBP content below 30 wt.% was considered to defeat the main aim of maximizing the use of decoloured bloodmeal. Below 50 wt.% and above 70 wt. % DBT content, either DBT or PLA overwhelmed the compatibilizing effect of itaconic anhydride resulting in poor mechanical properties of the blends. Four DBT formulations with varying water, SDS and TEG content were blended with PLA or PLA-g-IA to determine the best DBT formulation for DBT/PLA blend system. From the mechanical properties and digested surface morphology obtained, a compatibilized DBT formulation

containing 40 parts per hundred DBM (pph_{DBM}), 3 pph_{DBM} SDS and 20 pph_{DBM} TEG (F2)/PLA showed a considerable increase in tensile strength, elongation at break and impact strength compared to other formulations trialled. Also, an improvement in interfacial interaction, evidenced by a finer phase structure with relatively uniform void, was observed for this blend. However, a balance can be achieved between this blend and a compatibilized blend containing 40 PPH_{DBM} , 6 PPH_{DBM} SDS and 30 PPH_{DBM} , if elongation at break is compromised depending on the desired material properties and functionality of the desired end product.

The data obtained from SEM and WAXS of the blends indicated an improvement in the blend's compatibility with the addition of itaconic anhydride. However, no significant effect was observed in the blend's mechanical properties with the addition of compatibilizer. This led to the investigation of possible ways to improve the blend's mechanical properties.

Compatibility between DBT and PLA, the effect of different compatibilizer type, and plasticizer type used were investigated using mechanical testing, SEM and DMA. DBT/PLA blends were produced using three different compatibilizers: itaconic anhydride grafted PLA (PLA-g-IA), poly (2-ethyl-2-oxazoline) (PEOX) and poly (phenyl isocyanate)-co-formaldehyde (pMDI). Compatibilizing DBT/PLA blend with PEOX or PLA-g-IA was relatively straightforward, while using dual compatibilizer (PEOX and pMDI) required the addition of compatibilizer at different stages of blending to achieve a compatible blend. PLA-g-IA produced high tensile and impact strength as well as an evenly dispersed DBT domain and finer morphology compared to PEOX/pMDI and PEOX only. Two compatibilization approaches were used for DBT/PLA blends; one in which a compatibilizer (PLA-g-IA) was added as a third blend component and another in which a reactive group (itaconic anhydride) capable of interacting with the DBT and PLA phase was grafted onto PLA to improve the interfacial interaction between both phases. The data obtained suggested that adding the compatibilizer as a third blend component may be a successful approach. Two plasticizer types, tri ethylene glycol (TEG) and glycerol, were trialled to determine the best for the DBT/PLA blend system. The washed surface morphology of blends plasticized with TEG revealed finer morphology with more evenly distributed pores and small DBT domain sizes than blends plasticized with glycerol.

The feasibility of sheet extruding DBT/PLA blends was assessed, and the properties of the sheets produced were measured. The effects of different processing methods and different processing steps on the produced sheets were investigated in terms of mechanical, structural and water absorption properties. With a fundamental understanding of the blending method for DBT/PLA blends, different sheet processing methods (M₁, M₂, M₃, M₄ and M₅) and processing steps (2- and 3-step processing) were used to successfully process D463.4.1 (DBT/PLA blend containing 50 parts DBT, 40 parts PLA and 10 parts compatibilizer) into a sheet using extrusion. The viscosity of the blends produced using different methods was measured, to better understand the sheet processing of DBT/PLA blends. M₄ produced the most promising sheet, with better consolidation and a relatively smooth surface, as revealed by SEM topography of DBT/PLA blends sheet. The tensile properties and water absorption of the produced sheets suggested that the collective effects of reduced heat processing (method M₄) and 2-step processing improved the sheet properties.

This study demonstrated the feasibility of blending DBT with PLA, improving the properties of DBT/PLA blends and processing the produced blends into sheets for use in agricultural (such as weed mat) and packaging applications.

Acknowledgments

First and most importantly, I would like to thank my almighty Father and God, who gave me this opportunity to pursue my dream despite the obstacles. He kept me and saw me through to this level. My God, you brought light and direction into my path in the darkest hours during this study.

Doctoral study is truly demanding. It always seems impossible until it is done. I have been privileged to work with some wonderful, supportive people. I wish to express my sincere gratitude to my chief supervisor, Associate Professor Johan Verbeek, for making me persist and for his encouragement, ensuring that I gave my best during the time available to write this thesis. This would not have been possible without his endless guidance and professionalism. Thank you, Johan, for pushing me beyond my limits and believing that I could do this regardless.

I would also like to thank my co-supervisor, Dr James Michael Bier. Thank you for looking after me; for your support, friendship, advice, and encouragement.

I also want to thank my family. Firstly, to my husband Engr, Happiness Okoro; thank you for your endless support and comfort during the days when I felt low. You always reminded me why I was here and doing this. Thank you for always having my back. Thanks to my mum, Rev Mrs. N. D Nwawulu-Izuchukwu, for all your support and encouragement to the family and me, ensuring this dream became a reality. Thanks go too to my son Zephaniah Okoro, for being a lovely child, putting a smile on my face during the hard times, and understanding that mum had to do this for herself.

I also want to thank other staff members at the School of Engineering, University of Waikato for their technical assistance: Mary Dalbeth, for administrative help and a warm welcome in the Engineering office; Chris Wang and Yuanji Zhang for technical support in Large Scale Lab; Helen Turner for support with SEM; and Lisa Li for technical support. Thank you to Cheryl Ward, for assistance with ordering and sorting appropriate books and reading materials, help with EndNote and Microsoft Word and the last-minute formatting and organizing of this thesis; and to

Dr Debby Dada for assistance in sorting my reading materials and organizing this thesis.

Thanks also go to Deonne Taylor and Thomas McDonald for ensuring that I settled easily in New Zealand and that I was well looked after.

I am very grateful for the financial support and scholarship from MFAT under the commonwealth agreement with my country, and to my country Nigeria for choosing me to represent it. I will always love you, my fatherland. Without your support, it would not have been practically possible for me to pursue my dreams.

I am grateful to have been part of a great research group. I have made friends that I will never forget by being a part of this group. I would like to acknowledge my friends Chawa, Safiya, Anu and Tommy Sunny for having my back and being there when I needed someone to talk to. Thanks also to Herman, Chanelle, Talia, Wade, Francis, Tim, Matthew, Jussi, Maria and Alex.

Lastly, thank you Ijeoma Esther Izuchukwu for being a true friend and encouraging me when I needed it.

Table of Contents

Abstract	i
Acknowledgments	iv
Table of Contents	vi
List of Figures	ix
List of Tables.....	xiv
1 Chapter 1	1
Introduction	2
2 Chapter 2	6
Bio-polymers and Blends	7
2.1 Introduction.....	7
2.2 Bio-polymers	7
2.2.1 Micro-organisms	8
2.2.2 Polymers synthesized from bio-monomers	9
2.2.3 Polymers extracted from biomass	12
2.3 Bloodmeal-based thermoplastics	20
2.3.1 Novatein®	22
2.3.2 Decoloured bloodmeal thermoplastic (DBT).....	23
2.4 Polymer Blends.....	27
2.4.1 The concept of polymer blends	27
2.4.2 Blends of bio-polymers	39
2.4.3 Blends of protein-based polymers.....	41
2.4.4 Blend characterization.....	43
2.5 Film/Sheet forming	47
2.5.1 Film or sheet formation	48
2.5.2 Films manufactured from proteins	50
2.5.3 Properties of protein-based sheets/films	51
2.5.4 Enhancement methods.....	53

2.5.5	Factors influencing sheet formability of polymer blend	56
3	Chapter 3	62
	Preparation and Properties of Decoloured Blood-meal/Poly (lactic) Acid Blends modified with Itaconic Anhydride	63
3.1	Abstract.....	63
3.2	Introduction.....	64
3.3	Materials and Methods.....	66
3.3.1	Materials.....	66
3.3.2	Sample preparation.....	67
3.3.3	Sample testing	72
3.4	Results and Discussion	73
3.4.1	Decoloured blood-meal thermoplastic processing	73
3.4.2	Blending and processing	75
3.4.3	Blend composition ratio determination	77
3.4.4	DBT formulation determination.....	90
3.5	Conclusion	105
4	Chapter 4	107
	Mechanical Properties of Decoloured Bloodmeal Thermoplastic Protein and Poly(lactic) acid Blends	108
4.1	Abstract.....	108
4.2	Introduction.....	108
4.3	Material and Methods	110
4.3.1	Materials.....	110
4.3.2	Sample Preparation	111
4.3.3	Sample Analysis.....	114
4.4	Results and Discussion	116
4.4.1	Morphological properties	117
4.4.2	Mechanical properties	126
4.4.3	Dynamic mechanical properties	130

4.4.4	Intrinsic viscosity	135
4.5	Conclusion	136
5	Chapter 5	138
	Sheet Extrusion of DBT/PLA Blends	139
5.1	Abstract.....	139
5.2	Introduction.....	139
5.3	Material and Methods	141
5.3.1	Materials.....	141
5.3.2	Sample Preparation	142
5.3.3	Sample Analysis.....	146
5.4	Results and Discussion	148
5.4.1	Sheet formation	149
5.4.2	Surface morphology	154
5.4.3	Mechanical properties	157
5.4.4	Water absorption	158
5.4.5	Rheology characterization.....	159
5.4.6	Conclusion.....	162
6	Chapter 6	164
	Conclusion and Recommendations	165
	References.....	170
	Appendices.....	195
	Appendix 1	197
	Appendix 2.....	216
	Appendix 3.....	231
	Appendix 4.....	248

List of Figures

Figure 1: Classification of bio-polymers [27; 28].....	8
Figure 2: General structure of PHAs.....	9
Figure 3: Structure of PLA.....	10
Figure 4: Structure of D-lactic acid.....	10
Figure 5: Structure of L-lactic acid	10
Figure 6: Ring-opening polymerization of PLA	11
Figure 7: Structure of cellulose.....	13
Figure 8: Structure of amylose.....	14
Figure 9: Structure of amylopectin	14
Figure 10: Structure of chitin	15
Figure 11: Structure of chitosan.....	16
Figure 12: General molecular structure of an amino acid, with variation occurring only at the R group.....	16
Figure 13: Protein structures [62].	17
Figure 14: Image of produced Novatein® parts	23
Figure 15: Injection moulded sample of decoloured thermoplastic protein processed using TEG, SDS, and water.....	26
Figure 16: Agricultural plant pots and injection moulded samples made from decoloured thermoplastic	27
Figure 17: Phase diagram of a binary polymer blend indicating different phase regions, the lower critical solution temperature (LCST) and upper critical solution temperature (UCST).....	31
Figure 18: Structure of conformation of block (a; diblock and b; triblock) and grafted (c; single graft and d; multi-graft) copolymers at the interface of a heterogeneous polymer blend.	34
Figure 19: Dispersed phase size variation in a known polymer blend as a function of polymer b concentration [127]	36
Figure 20: Viscosity behaviour of different fluids as the applied shear rate varies.	57
Figure 21: Flowchart of the experimental plan showing different blend approach, varying blend ratio and content (Table 3).	71

Figure 22: Injection moulded samples produced from the different DBT formulations	74
Figure 23: Mechanical properties of DBT formulations with different ratios of additives (Table 2).	75
Figure 24: DBT/PLA blend extrudates produced using DBTP as a starting material.....	76
Figure 25: SEM micrographs of the cryo-fractured surface of DBTP/ PLA blends with and without compatibilizer. a and a': PLA and DBT; b and b': DP37 and DgP37; c and c': DP55 and DgP55; d and d': DP73 and DgP73; e and e': DP91 and DgP91	80
Figure 26: Mechanical properties of DBT, PLA and varying compositions of DBT/PLA blends with (DBT/PLA-g-IA) and without compatibilizer (DBT/PLA)	81
Figure 27: Tan δ (a) PLA and PLA-g-IA, (b) DBT, and storage modulus (a') of PLA, PLA-g-IA, and DBT	83
Figure 28: Tan δ (a and a') and storage modulus (b and b') of blends. DP: uncompatibilized and DgP: Compatibilized with itaconic anhydride.....	84
Figure 29: Loss modulus of pure material (A) and blends without (B) and with (C) compatibilizer	87
Figure 30: WAXS diffractograms of DBT/PLA blends without (a) and with compatibilizer (a'), PLA and DBT (b), and summation of DBT and PLA (b').....	89
Figure 31: Unsuccessful washed surface of F3P, DP and DgP blend in chloroform.....	92
Figure 32: SEM cryo-fracture surfaces of DBTP/PLA blends with and without itaconic anhydride.....	93
Figure 33: SEM Digested surface micrographs of DBP/PLA blends with and without Itaconic anhydride.....	94
Figure 34: The mechanical properties of DBT/PLA blends with and without itaconic anhydride.	96
Figure 35: Glass transition temperature (T_g), crystallization peak (T_{cc}) and melting endotherms (T_m) of PLA and DBT	99
Figure 36: Glass transition temperature (T_g) of different formulations of DBT/PLA blends (DSC first heat scan thermograms).....	100
Figure 37: DSC first heat scan thermograms of different formulations of DBT/PLA blends showing crystallization peak (T_{cc}) and melting endotherm (T_m).....	101

Figure 38: WAXS diffraction patterns for DBT/PLA blends without (A) and with (B) itaconic anhydride, pure PLA, DBP (C), and summation of PLA and DBT (D).....	103
Figure 39: Scanning electron micrographs of cryo-fractured surfaces of pure DBT, pure PLA and their blends without compatibilizer. 432 represents 40 parts water, 3 parts SDS and 20 parts plasticiser and 463 represents 40 parts water, 6 parts SDS and 30 parts plasticisers.	117
Figure 40: Blends of DBT/PLA with different compatibilization approaches. (D432.5 and D463.5 had itaconic anhydride grafted onto the PLA in the blend while D432.4.1 and D463.4.1 had PLA-g-IA added as a third component in the blend).	118
Figure 41: The fractured surfaces of DBTP and PLA blends plasticized with tri-ethylene glycol and having different compatibilizers. D432.IA and D463.IA were compatibilized with PLA-g-IA, D432.PEOX and D463.PEOX were compatibilized with PEOX alone, and D432.PP and D463.PP were compatibilized with pMDI and PEOX.	122
Figure 42: The fractured surfaces of DBTP and PLA blends plasticized with glycerol having different compatibilizers. Dg432.IA and Dg463.IA were compatibilized with PLA-g-IA, Dg432.PEOX and Dg463.PEOX were compatibilized with PEOX alone, and Dg432.PP and Dg463.PP were compatibilized with pMDI and PEOX.	123
Figure 43: The digested surfaces of DBTP and PLA blends plasticized with tri-ethylene glycol having different compatibilizers. D432.IA and D463.IA were compatibilized with PLA-g-IA, D432.PEOX and D463.PEOX were compatibilized with PEOX alone, and D432.PP and D463.PP were compatibilized with pMDI and PEOX.	124
Figure 44: The digested surfaces of DBTP and PLA blends plasticized with glycerol having different compatibilizers. Dg432.IA and Dg463.IA were compatibilized with PLA-g-IA, Dg432.PEOX and Dg463.PEOX were compatibilized with PEOX alone, and Dg432.PP and Dg463.PP were compatibilized with pMDI and PEOX.	125
Figure 45: Mechanical properties of DBT/PLA blends with different compatibilization approaches. (D432.5 and D463.5 had itaconic anhydride grafted onto the PLA in the blend while D432.4.1 and D463.4.1 had PLA-g-IA added as a third component in the blend)	126
Figure 46: Mechanical properties of DBT and PLA blends with different compatibilizers and plasticizers. 432.IA and 463.IA were compatibilized with PLA-g-IA, 432.PEOX and 463.PEOX were	

compatibilized with PEOX alone, and 432.PP and 463.PP were compatibilized with pMDI and PEOX.....	129
Figure 47: Tan δ of DBT, PLA and DBTP/PLA blends with different plasticizers and different compatibilizers. Sample names starting with D were plasticized with TEG while those with Dg were plasticized with glycerol. 432.IA and 463.IA were compatibilized with PLA-g-IA, 432.PEOX and 463.PEOX were compatibilized with PEOX alone, and 432.PP and 463.PP were compatibilized with pMDI and PEOX.....	132
Figure 48: Storage and loss moduli of DBTP/PLA blends with different plasticizers and different compatibilizers. Sample names starting with D were plasticized with TEG while those with Dg were plasticized with glycerol. 432.IA and 463.IA were compatibilized with PLA-g-IA, 432.PEOX and 463.PEOX were compatibilized with PEOX alone, and 432.PP and 463.PP were compatibilized with pMDI and PEOX.....	133
Figure 49: Intrinsic viscosity of PLA (dried, grafted and extruded) and different blends of PLA and DBTP. Sample names starting with D were plasticized with TEG while those with Dg were plasticized with glycerol. 432.IA were compatibilized with PLA-g-IA, and 432.PP were compatibilized with pMDI and PEOX.	136
Figure 50: Summary of sheet extrusion methods trialed	144
Figure 51: Twin-screw extrusion of DBT/PLA sheet using a LabTech twin screw co-rotating extruder.....	149
Figure 52: Image of poorly formed DBT/PLA sheets processed at die temperatures above 140 °C.....	151
Figure 53: Photograph of DBT/PLA sheets produced using different processing methods (M ₁ – M ₅) and different processing steps (two or three steps). (see Figure 50)	152
Figure 54: Image of produced DBT/PLA blend sheets produced using different methods (M ₁ and M ₄ respectively).	154
Figure 55: Surface morphology of DBT/PLA sheets processed using different methods (M ₁ - M ₅) and different processing steps (two or three step process). (see Figure 50).....	156
Figure 56: Mechanical properties of DBT/PLA sheets processed using different methods (M ₁ – M ₅) and different processing steps (two or three steps). (see Figure 50).....	157
Figure 57: Water absorption (wt.%) of DBT/PLA sheets produced using different processing methods (M ₁ - M ₅)and steps (two or three step process). (Figure 50).....	158

Figure 58: Shear viscosity of DBT/PLA sheets material using different processing steps (two or three step process) and different methods (M₁ - M₅) (see Figure 50)..... 160

List of Tables

Table 1: Proteins used for biodegradable sheets/films and their sources.....	50
Table 2: DBT formulations and additive contents	68
Table 3: Blend composition	70
Table 4: Injection moulding temperatures determined during trial runs.....	72
Table 5: Description of injection moulding of sampled blends	77
Table 6: Glass transition temperatures, cold crystallization peaks and melting endotherms of blends, PLA and DBT.....	102
Table 7: Composition of the blends sampled.....	113
Table 8: Mechanical properties of other thermoplastic proteins and polyester blends.....	127
Table 9: Power law indices of DBT/PLA sheet material using different processing methods ($M_1 - M_5$) and processing steps (two or three step process) (see Figure 50).....	161

Chapter 1

Introduction

Introduction

There is ever-increasing concern about economic issues and environmental pollution in today's society. This has resulted in an increased interest in natural polymers as an alternative to synthetic polymers [1; 2], which contribute to environmental pollution when disposed of. Natural polymers from plants and animals, including those based on proteins, starch, lipids, and cellulose, have been processed into thermoplastics [3-6].

Currently, bioplastics are used in specific applications where biodegradability is required, such as packaging (laminated paper, film wrapping, foams, and industrial packaging), agriculture (composting bags, agricultural pegs, mulch films, nursery pots), and general use (disposable tableware such as cups, cutlery, plates and straws, and cotton swabs) [7-9].

Proteins are natural polymers that have received renewed attention with regard to possible thermoplastic applications over the last two decades [4]. The protein-based feedstock can be renewably derived from agricultural or horticultural activities. However, if dedicated growth of crops is required for polymeric materials, this may result in competition for land use with food and biofuel production. In the quest for an alternative feedstock, sourced from either waste streams or low-value by-products of existing activities, bloodmeal was identified as a potential raw material [5]. Bloodmeal is a by-product of animal slaughtering, containing 90 to 95% protein [6; 10].

Bloodmeal can be successfully processed into a thermoplastic material that can be extruded and injection moulded on conventional polymer processing equipment. The processing of bloodmeal into thermoplastic requires the addition of water and another small polar molecule such as urea or tri-ethylene glycol (TEG) to act as plasticizers and disrupt hydrogen bonding between protein chains; sodium sulphite (SS) to reduce cross-linking by cleaving disulphide bridges; and sodium dodecyl sulphate (SDS) to disrupt hydrophobic interactions [4].

Recently, blood meal has been decoloured using a pre-treatment with peracetic acid (PAA) to eliminate its odour and reddish black colour, thereby increasing its applications and acceptability [11]. The treated bloodmeal is referred to as decoloured bloodmeal (DBM). DBM has been processed into a conventional thermoplastic known as decoloured bloodmeal thermoplastic (DBT) using water, TEG, and SDS. The processing of DBT does not rely on the addition of SS for the reduction of cross-linkage because of the significant reduction in the covalent network-forming amino acids after treatment [11; 12].

DBT is sensitive to moisture and can easily biodegrade due to the hydrophilic nature of protein [13]. However, its mechanical properties are poor compared to conventional polymers. The ability of DBT to easily degrade makes it an ideal starting material in biodegradable polymer blends.

Blending is the most favoured approach for improving material properties or for producing novel materials because of its ability to use conventional technology at low cost, compared to synthesizing new polymers. The ability to tailor end-product properties is another reason why blending is widely preferred in industry. However, there are major challenges facing polymer blending, such as miscibility [14; 15]. Most polymers are thermodynamically immiscible and to achieve a miscible blend, a compatibilizer capable of reacting with the different components of the blend is incorporated.

This study explores the blending of DBT with another hydrophobic biodegradable polymer, poly (lactic acid) (PLA) with the aim of improving DBT's mechanical properties and sheet formability.

Most commercially available sheets are synthetic-based, such as low-density polyethylene (LLPE). Because of economic and environmental issues, natural protein polymers such as zein, gelatin, cottonseed, wool keratin, collagen, soy, whey, casein, egg white, and fish myofibrillar proteins [3; 16] have been investigated and successfully processed into edible and non-edible film and sheet materials.

Most available protein films/sheets are produced by solution casting [16; 17], which is based on dispersing and solubilizing proteins in various solvents followed by casting then drying. However, this process is highly capital intensive, unsuitable for sheet processing and challenging to scale up. Therefore, an alternative processing method is required for the acceptance and industrial production of protein-based films/sheets. In addition, DBM is not soluble in aqueous solutions. Therefore, solution casting could not be explored as an alternative method of DBM film/sheet formation. In contrast, sheet extrusion of DBM was worth investigating due to the advantages of the extrusion process: it is a continuous and versatile process, capable of mass production. Sheet extrusion of DBM based material is expected to enable its economic transformation into usable products.

Extrusion is widely used in the plastics industry for the production of most synthetic polymer films/sheets. The processing of protein-based films or sheets by extrusion has been a challenge to researchers because of the complex association and dissociation phenomena of proteins under induced shear and heat treatment. However, protein films/sheets derived from zein, sunflower isolate, collagen and soy [18-21] have been processed successfully using extrusion.

The main objectives of this research were to study the feasibility of blending DBT and PLA; measure the blend's properties; and evaluate the possibility of using extrusion processing for fabrication of DBM-based sheets. The ability to sheet extrude DBM based products would make it adaptable to production lines applied in the plastics industry, with advantages such as low cost and easy processability.

This thesis is presented as six chapters and four conference publications (which are attached as Appendices):

Chapter 1 gives a general overview of the study, which includes an introduction, research objectives, research goals and an outline of the thesis.

Chapter 2 presents a review of relevant research and knowledge within the scope of this research. It includes an overview of bio-polymers, proteins, polymer blends and concepts, protein sheet process formation, and factors that affect sheet formability.

In Chapter 3, the feasibility of blending DBT and poly (lactic acid) (PLA) is assessed. PLA is among the most promising and abundant thermoplastic polyesters. It is biodegradable; therefore, blending it with DBT will not compromise the biodegradability of the final product. PLA has been used in various applications such as packaging, coatings for paper, compost bags and single-use cutlery, due to its excellent properties. Improvement in the material properties of DBT is expected when it is blended with PLA. PLA grafted with itaconic anhydride using reactive extrusion was used as a compatibilizer to improve the compatibility and properties of the blends.

Chapter 4 expands on the concept presented in Chapter 3 by thoroughly drying DBT before blending with PLA to control for PLA hydrolysis during processing. Also, the effect of different compatibilizers, compatibilization approaches and different plasticizers on the blends' properties were assessed with the aim of producing improved material properties. Compatibilizer types were assessed using three different compatibilizers: PLA-g-IA; poly-2-ethyl-2-oxazoline (PEOX); and poly (phenyl isocyanate)-co-formaldehyde (pMDI). Compatibilization approaches were assessed by either adding compatibilizer as a third component in the blend or grafting a reactive group onto the PLA in the blend. The effect of different plasticizers on blends' properties were assessed using two plasticizers: tri-ethylene glycol (TEG) and glycerol to optimize blend properties.

Chapter 5 investigates the feasibility of sheet extruding DBT/PLA blends and measures the properties of the sheets produced. Chapter 5 investigates the effect of processing methods on the mechanical, structural, and water absorption properties of the produced sheet. Measurements also include shear viscosity as this plays an important role in understanding the sheet processability of the blended material. The rheology of protein or protein-based materials with a focus on sheet processing is a rarely studied area. Therefore, there is limited literature in this area. Sheet extrusion of the blends is assessed based the understanding of DBT/PLA blends as presented in Chapter 4.

Chapter 6 draws the main conclusions of the study and provides some recommendations for future work based on the findings of the present study.

Chapter 2

Literature review: Bio-polymers and Blends

Bio-polymers and Blends

2.1 Introduction

Polymers are macromolecules consisting of repeating structural units known as monomers. They play an essential role in our everyday life because of their useful properties, which include resistance to weather, ease of processing, low density, and thermal and electrical insulation [22; 23]. Increasing environmental concerns and diminishing natural energy reserves have shifted research interest from non-renewable petroleum-based resources to renewable, biologically-based resources for sustainable development.

Polymers are classified into two categories based on their origin: non-renewable resources, which are feedstocks derived from by-products of petroleum processing; and renewable resources, which are feedstocks from natural resources. Natural polymers are extracted mostly from biological resources and are considered to be biodegradable. Therefore, they are often referred to as bio-polymers or biodegradable polymers [24]. Conventional polymers synthesized from either bio-derived or synthetic monomers are also often referred to as bio-polymers as they break down over time into environmentally friendly components. However, in the context of this study, the term bio-polymers refers to polymers from natural sources that are either extracted from biomass, synthesized from bio-based monomers or produced by microorganisms.

2.2 Bio-polymers

Attention has been drawn to bio-polymers since the 19th century due to the increasing economic and environmental issues surrounding petroleum-based polymers [16, 23]. However, they became widely used on an industrial scale in the 20th century [1].

Biodegradation, as defined by Albertsson and Karlsson [25], is a process that occurs through the actions of enzymes and/or chemical decomposition associated with living organisms and their secretion products. However, some researchers also include abiotic reactions such as photo-degradation, oxidation and hydrolysis,

which alter polymeric material, as biodegradation processes. Different authors agree to either the former or the latter description, while some accept both as true definitions of polymer biodegradation. However, ISO 14855-1/2 presents standardised methods for the determination of the ultimate aerobic/anaerobic biodegradability of plastic materials under controlled composting conditions, using continuous infrared analysis, gas chromatography or titration to measure the amount of carbon dioxide evolved.

It is essential to consider abiotic reactions such as photo-degradation, oxidation, and hydrolysis, which alter polymeric material, in addition to biodegradation. Therefore, the term 'biodegradable' in this work refers to bio-polymers that can degrade in a composting environment through the action of enzymes and/or chemical decomposition.

Bio-polymers are mostly derived from animal or plant sources [24]. They can be classified into three groups based on their origin and production [26][25, 26] as shown in Figure 1. However, the main renewable sources of bio-polymers are polysaccharides (such as starch), cellulose, and proteins [16, 24].

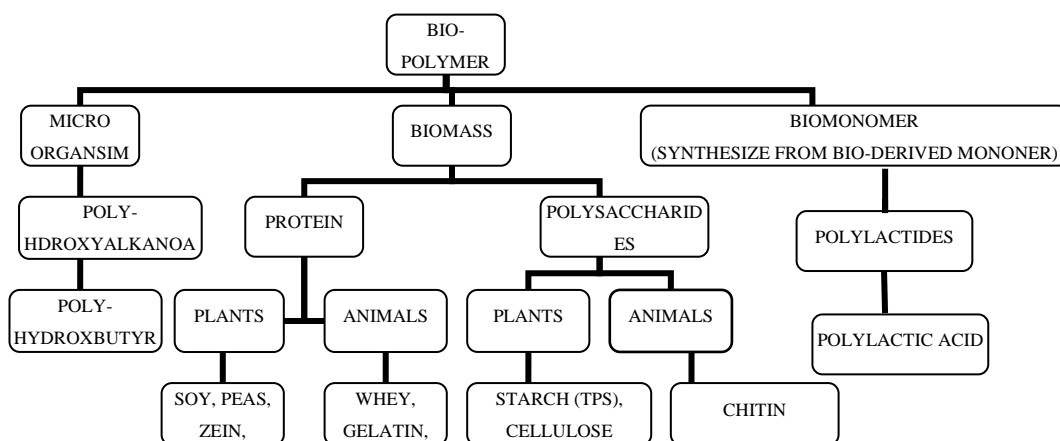


Figure 1: Classification of bio-polymers [27; 28]

2.2.1 Micro-organisms

Polymers derived directly from micro-organisms under various growth conditions [28] are referred to as microbial polymers. The most common microbial polymers

are polyhydroxyalkanoates (PHAs), as shown in Figure 2. They are produced directly by microbes as carbon storage and intercellular energy reserves [26; 29; 30]. PHAs build up in response to nutrient limitations when carbon is present in excess. They are then consumed when no external carbon source is available. The biosynthesis of PHAs occurs in three metabolic phases when a suitable carbon source is introduced into the cellular environment. The compound is converted into hydroxyacyl co-enzyme A thioester (PHA synthase substrate) through either anabolic or catabolic reactions or both. The formation of an ester bond is then catalyzed by PHA, followed by the sequent release of co-enzyme A.

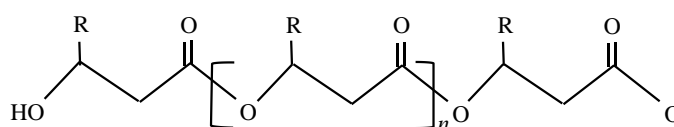


Figure 2: General structure of PHAs

Poly-3-hydroxybutyrate (PHB) is the most abundant PHA, produced commercially by fermentation when glucose or sucrose (carbon sources) are fed to microorganisms in a bioreactor [26; 31]. PHAs are natural thermoplastic polyesters with a wide range of performance and commodity applications because of their physical properties. PHAs are water-insoluble, biodegradable storage polymers. They have good resistance to hydrolytic degradation, good moisture and odour barrier properties, and excellent resistance to UV, water, and heat [28; 31; 32]. PHAs have found uses in applications including controlled drug release, scaffolding in tissue engineering, surgical sutures, packaging materials, lawn and leaf bags, food service ware, paints, and disposal diapers [31; 32].

2.2.2 Polymers synthesized from bio-monomers

Polymerization techniques are used to produce bio-polymers from bio-monomers. The bio-monomers used for processing into bio-polymers are molecules from renewable sources, capable of polymerization, and are biodegradable.

Poly(lactic acid (PLA) is one of the most promising and abundant thermoplastic polyesters [26; 28]. It is synthesized from lactic acid (2-hydroxypropionic acid, which is the monomer), and its chemical structure is shown in Figure 3. Lactic acid

is produced through microbial fermentation using polysaccharides from agricultural by-products such as corn, potato or sugar beets, whey, sugar cane and spent grain as a feedstock [26; 28; 31; 33; 34]. Lactic acid is a chiral molecule which exists as two stereoisomers: D-lactic acid (Figure 4) and L-lactic acid (Figure 5). The polymerization of lactic acid into PLA can be through condensation polymerization, ring opening polymerization, or a combination of both. Ring-opening polymerization (ROP) (Figure 6) involves ring opening of lactide, which uses the removal of water without solvents under milder conditions to produce lactide, which is then purified by vacuum distillation and ring opening under heat [35; 36]. Ring-opening polymerization reactions produce high molecular weight PLAs with high mechanical properties, glass transition temperatures, and degradation temperatures. Condensation polymerization involves the condensation of L- and D-Lactic acid isomers to produce low molecular weight PLA, with water removed using solvents under high temperature, and vacuum distillation [26; 28].

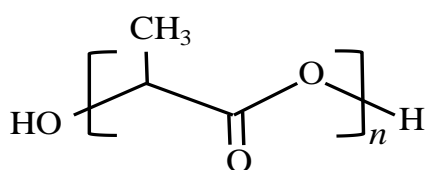


Figure 3: Structure of PLA

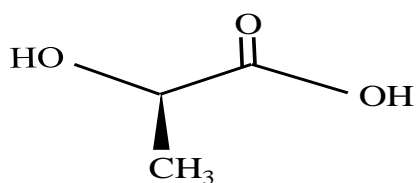


Figure 4: Structure of D-lactic acid

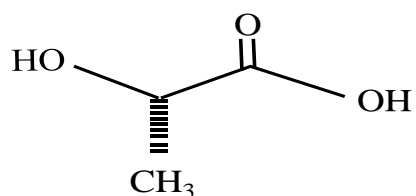


Figure 5: Structure of L-lactic acid

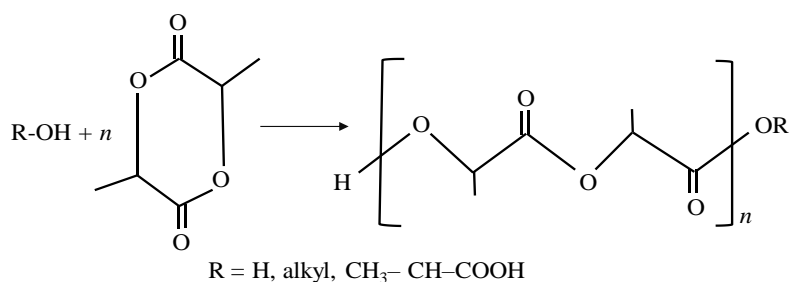


Figure 6: Ring-opening polymerization of PLA

PLA has found uses in various applications including fibre for clothing, filtration systems (as a flocculating agent), medical sutures and screws, packaging applications, drug delivery for controlled delivery of drugs, coatings for paper, carpet tiles, compost bags for yard trimmings, disposable single-use cutlery, vascular grafts, orthopaedic implants, stent development and tissue engineering [28; 31; 37].

The ratios of the three stereochemical forms of lactic acid monomer (poly(L-lactide), poly(D-lactide) and poly(DL-lactide)) are strongly related to PLA properties. Poly(L-lactide) and poly(D-lactide) are semi-crystalline polymers. Synthesizing pure L-lactide will produce a PLA with high crystallinity and a high melting point. However, a mixture of L-lactide and D-lactide (poly(DL-lactide)) produces a more amorphous PLA [26; 31].

PLA is insoluble in water and soluble in chlorinated and fluorinated solvents. It has good moisture and grease barrier properties, and its mechanical properties can be modified by varying its molecular weight and crystallinity [26; 28; 31; 35]. The incorporation of -CH₃ groups makes PLA hydrophobic. PLA's molecular weight influences its susceptibility to microbial attack. Higher molecular weight PLA is less susceptible to microbial attack than low molecular weight PLA. Also, PLA's degree of crystallinity is another factor that influences its properties, including degradation rate in water and biodegradation [26]. PLA crystallinity is controlled by slow cooling or annealing above its glass transition temperature.

PLA can be processed using various common techniques such as extrusion, injection moulding, blow moulding, thermoforming and fibre spinning. PLA can be

recycled back into its monomer, it degrades by hydrolysis, is biodegradable in controlled environments, and is compostable [38; 39].

PLA was selected for this research as it is a front runner in the emerging bio-plastic market for packaging applications. It is more readily available and is cheaper than most bio-synthesised polymers.

2.2.3 Polymers extracted from biomass

Most polymers extracted from biomass exist in the environment in their natural state. These types of polymers are extracted and/or modified from plants, animals, marine and agricultural origin. Proteins and polysaccharides are the most abundant in nature. Most natural polymers from biomass are hydrophilic and therefore present processing and performance difficulties. The production of bio-polymers from biomass involves extraction and purification.

2.2.3.1 POLYSACCHARIDES

Polysaccharides are characterized by long chains of carbohydrate molecules composed of repeating units of either monosaccharide or di-saccharide, bound together by glycosidic linkages [40; 41]. Polysaccharides form a large class of natural degradable polymers. Their structures are mostly linear but can include varying degrees of branching. The general formula of polysaccharides is based on repeat units of sugar and is represented as $C_x(H_2O)_y$ [42; 43], where x is usually between 200 and 2500. However, when the repeating units in the polymer backbone are six-carbon monosaccharides, the general formula is simplified to $(C_6H_{10}O_5)_n$ where $40 \leq n \leq 3000$. The saccharide repeat units in polysaccharides are connected via the oxygen on carbon 1, which forms a glycosidic bond to carbon 4 on another molecule, with subsequent elimination of water. Polysaccharides can be grouped based on their primary sources: plants, animals and micro-organisms. Starch is the most abundant plant-based polysaccharide while chitin and chitosan are the most abundant animal-based polysaccharides [44-46].

Cellulose is one of the most abundant polysaccharides. Cellulose is the major constituent of plant cell walls and is the most common component of cotton. It is the most abundant organic compound on earth, and accounts for 40% of all organic

matter. D-glucose is the building block of cellulose, which is linearly linked by β -1, 4-D-glucosidic bonds. Cellulose is the same at the molecular level regardless of its origin. Each cellulose molecule is an unbranched polymer of 10^3 - 10^6 D-glucose units [34].

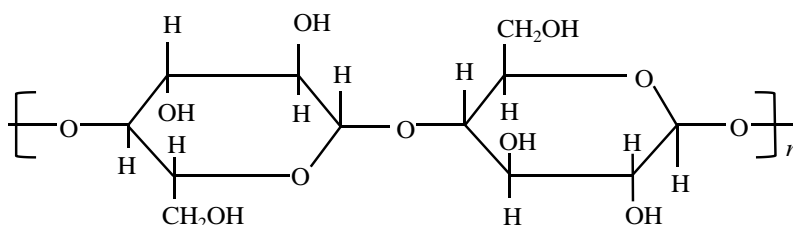


Figure 7: Structure of cellulose

Cellulose can be produced either by plants or in bacteria by fermentation. Cellulose produced by bacteria via fermentation can be chemically modified to provide improved properties. Therefore, producing cellulose from bacterial sources is the most widely used commercial method. This process involves the modification of the OH groups on the polymer backbone using an acid anhydride, resulting in various degrees of substitution and producing an ester functionalized cellulose [31; 47; 48]. Presently, only two groups of cellulose material are widely available: cellulose bio-composites and cellulose acetate [49]. Cellulose acetate is obtained through the reaction of cellulose with acetic anhydride [33] while cellulose bio-composites involve the reinforcement of cellulose with another natural renewable polymer [50; 51].

Cellulose is relatively resistant to biodegradation compared to starch. It is not soluble in water. Cellulose hydrolyses to yield glucose. Cellulose fibres are used in bio-composites as reinforcing material, and in the manufacture of paper and paper products, while modified celluloses are used in paint manufacturing, plaster, clear adhesive tape, adhesives, eyeglass frames, ceramics, toothbrushes, cosmetics, tool handles and film coatings [31; 33; 48; 52].

Starch is a major plant storage form of glucose, and it is an abundant component of plant biomass. Starch contains two polysaccharides: linear amylose linked by α -1'4-D-glucosidic bonds (15 – 20%), and branched amylopectin linked by α -1,4-D-

glucosidic and α -1,6-D-glucosidic bonds (80 – 85%), making amylopectin the dominant component in starch. However, genetics and sources determine the relative amount, structure and molar mass of the amylose (Figure 8) and amylopectin components (Figure 9) in starch. Starch-based materials account for 85 to 90% of biodegradable materials from renewable sources, dominating the industry today [53].

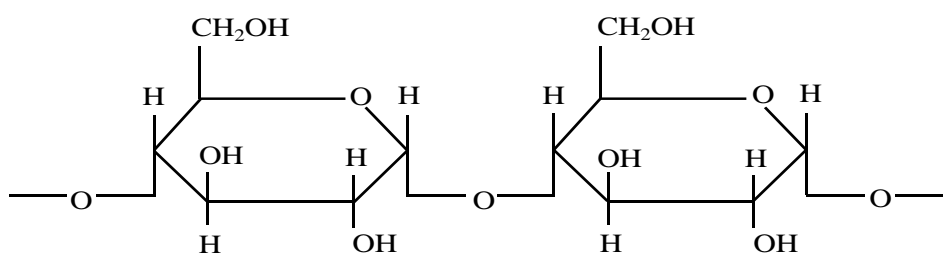


Figure 8: Structure of amylose

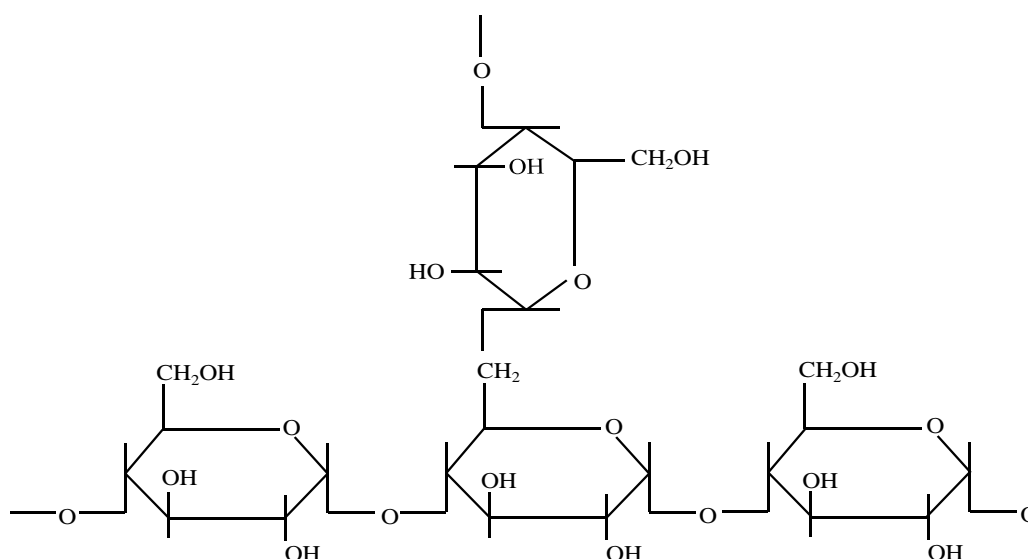


Figure 9: Structure of amylopectin

The major sources of starch used in bio-process applications are corn (maize), rice, wheat, potato, tapioca (cassava), sorghum, barley and peas [31; 54]. Partially hydrolyzed starch is used to manufacture corn syrup and dextrose (glucose) sweeteners, and as a feedstock in chemical, pharmaceutical and brewing industries. Modified or native state starch is used in food applications such as cake mixes,

puddings, glazes, baby foods and confectionery, and in non-food applications such as paper coatings, compostable bags, cardboard and paper manufacturing, agricultural mulch films, textile and carpet sizing, while foamed starch is used as an antistatic, insulating and shock absorbing material, in packaging applications, and in sheets for thin-walled products [31].

Thermoplastic starch is stable in oils, alcohols, and fats, and it is fully biodegradable. It has mechanical properties comparable to synthetic polymers such as polyethylene and can be processed using conventional processing equipment such as blow and injection moulding, extrusion and thermoforming.

Chitin is the second most abundant polysaccharide next to cellulose. It acts as a structural component in many animals, and is found in marine invertebrates, insects, yeast, and fungi. Chitin is mostly extracted from the shells of crustaceans and the cell walls of fungi. Chitin is a homopolymer of 2-acetamido-2-deoxy- β -D-glucopyranose. Figure 10 shows the structure of chitin. Chitosan is a derivative of chitin, which is obtained in a base-catalyzed deacetylation reaction where acetate is removed from the molecule, resulting in a deacetylated form; 2-amino-2-deoxy- β -D-glucopyranose. The structure of chitosan is shown in Figure 11.

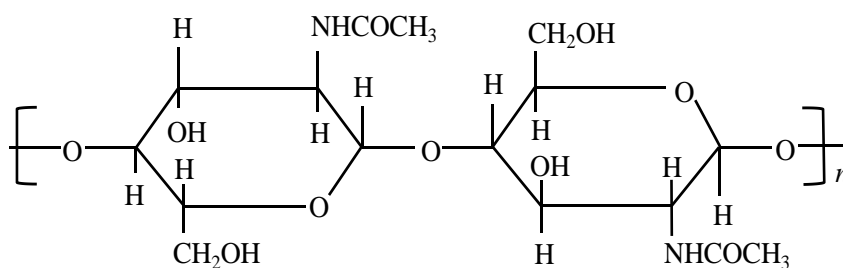


Figure 10: Structure of chitin

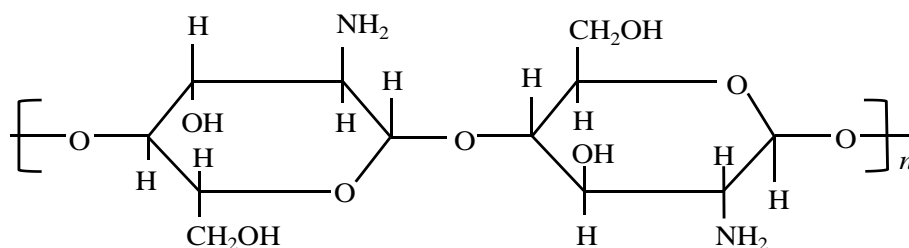


Figure 11: Structure of chitosan

Chitosan has antibacterial, antifungal and medicinal properties, making it a high-interest material for wound care. Chitin and chitosan have versatile chemical and physical properties, and have been made into fibres and films used in membranes, medical gauze, sutures, beads, wound dressings, paper and fibrids [55-59].

2.2.3.2 *PROTEINS*

Protein-based polymers are simply polymers derived from a protein feedstock. Proteins are thermoplastic hetero-polymers constituting of various polar and non-polar α -amino acids (Figure 12). Proteins play important roles in biological systems as biocatalysts, structural components of cells and organ, contractile fibres, hormones, transport molecules, antibodies, and have a range of protective and storage functions [60]. Proteins have complex molecular structures in their native states, which are stabilized by interactions between amino acid functional groups.

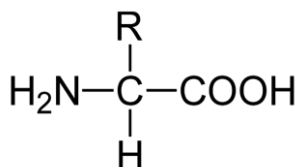


Figure 12: General molecular structure of an amino acid, with variation occurring only at the R group.

The amine and carboxylic acid groups in a protein's repeat units are linked by peptide bonds [61]. Proteins have four different structures: primary, secondary, tertiary and quaternary, as shown in Figure 13.

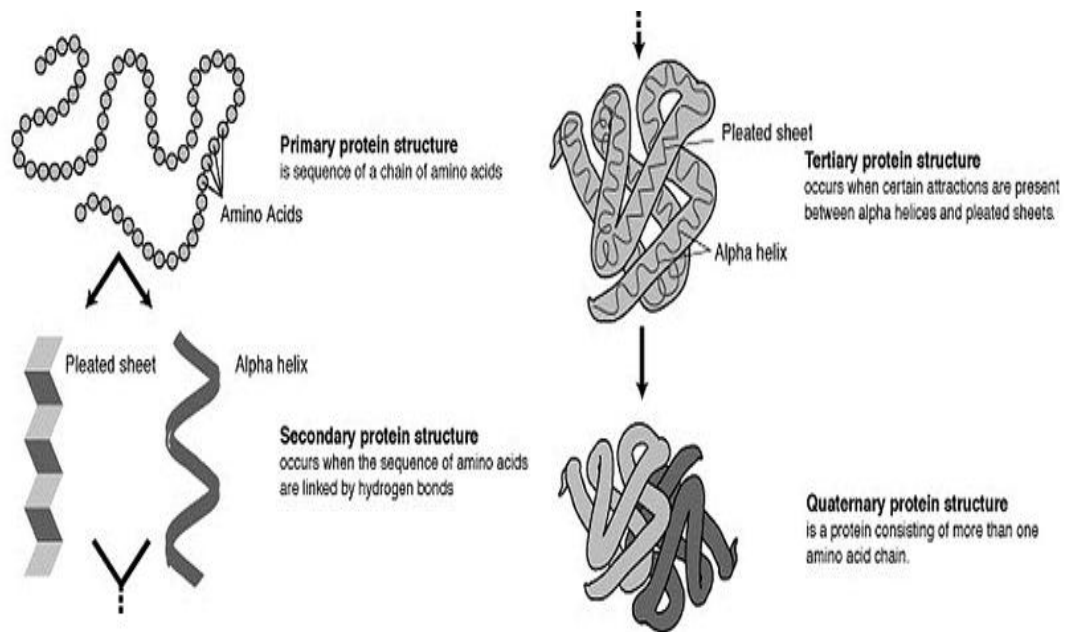


Figure 13: Protein structures [62].

A protein's primary structure is determined by the amino acids that form it, and the sequence of their linkage. The secondary structure is the localized coiling and bending of the polypeptide chain due to hydrogen bonding between a carbonyl group of one amino acid and an amine group of a different amino acid. The most common stable conformations seen in the secondary structures of proteins are α -helices, β -sheets, β -turns and random coils [63; 64]. The way in which protein chains fold and bend into more complex three-dimensional shapes because of the positioning of α -helices and β -pleated sheets is referred to as their tertiary structure. Quaternary structures result from multiple polypeptide chains aggregating into a globular structure.

Proteins are classified into two groups; fibrous and globular proteins. Fibrous proteins are made up of polypeptide chains that are elongated and have a sheet-like

structure (long and narrow). They have repetitive amino acid sequences that favour specific kinds of secondary structures, which confer particular mechanical properties on the protein [65]. Fibrous proteins have low water solubility and they do not denature easily, while globular proteins have spherical structures and display irregular amino acid sequences. Globular proteins are highly soluble in water and they denature easily. Fibrin, collagen, myosin, actin and keratin are examples of fibrous proteins while enzymes, haemoglobin, insulin and immunoglobulins are examples of globular proteins [66]. Fibrous proteins are mostly used in commodity applications because they are readily available and are abundant in nature [67; 68].

The process of converting protein into a thermoplastic requires three basic steps: the disruption of protein-protein interactions; plasticization; and retention of the thermoplastic nature [69-72].

A protein's various functional groups and heat sensitivity leave a very small window of feasible processing conditions. The processing of protein-based polymers requires denaturation of the protein, either by thermal or chemical means [61]. A protein is said to be denatured when disruption occurs in the secondary, tertiary or quaternary structures, leading to new interactions by means of hydrogen bonding. A protein is said to be degraded when the primary structure is broken. The temperature of denaturation depends mainly on the amino acid sequence, chemical additives, processing methods, and the amount of water used. Proteins have a softening temperature that is often higher than their denaturation temperature. This makes them difficult to process as the processing temperature should be within the softening temperature and above the denaturation temperature of protein to avoid material degradation.

There are various sources of protein polymers, but the most widely used are those found in greatest abundance [73]. Common sources of proteins used as biomaterials for processing are animal proteins such as collagen, keratin, casein, whey protein and blood meal, and plant proteins such as corn gluten meal, wheat gluten meal, sunflower and soybean. Bacterial sources such as dehydrogenase, chymotrypsin, and fumarase have also been used for bio-polymer processing, although they are not found in abundance.

Soy proteins consist of four major protein fractions known as 2S, 7S (conglycinin), 11S (glycinin) and 15S, based on their ultra-centrifugal sedimentation rates [74]. Both the conglycinin and glycinin fractions contain cysteine residues, which leads to the formation of disulphide crosslinks. Soy proteins are produced commercially as soy flour, soy protein concentrate, and soy protein isolate.

Soy flour contains over 53% protein on a dry basis. It is a fat-free, low fibre protein obtained by dehulling soybeans, followed by defatting with solvents and finally grinding. Soy protein concentrate contains about 68 – 72% protein, and it is produced by leaching out water- and alcohol-soluble sugars from soy flour. Soy protein isolate has the highest protein content, of approximately 90% [31; 33; 74]. It is extracted from soy protein concentrate with alkali and reprecipitated by acidification.

Soybean-based polymers have high modulus and can be processed using injection and compression moulding. Soy proteins can be modified to suit required applications; they have been used in industry in adhesives, paper and paperboard coating, and in cast film and foam products [33; 74].

Collagen constitutes 30% of the protein found in mammals, and it is abundant in nature [75; 76]. It provides mechanical stability, toughness, and strength to a range of connective tissues in animals and is found in tendons and ligaments, skin, cornea, bone, and dentin. It is also found in animal hides and blood vessels.

The basic building block of collagen is the collagen fibril, which is a fibre ranging from about 50 to a few hundred nanometers in thicknesses. Fibrils in collagen are formed by the arrangement of triple helices created from the long chains of polypeptide. These fibrils are assembled in a variety of more complex structures with different mechanical properties.

Whey proteins are a mixture of globular proteins isolated from whey, a by-product of cheese production. Whey proteins are rich in β -lactoglobulin. Whey protein makes up 20% of the protein in cow's milk while 80% is casein [77]. Whey has a high nutritional value, and it is commonly marketed as a dietary supplement. Whey

proteins have been investigated as edible coating and films. Also, they have potential as exterior coating films and are readily processable.

Protein bio-polymers have excellent gas barrier properties. However, their mechanical properties are influenced by relative humidity due to their hydrophilic nature. This drawback can be overcome by chemical modification, blending or laminating with other bio-polymers [78-83].

Protein bio-polymers are used in biomedical and agricultural applications, fibre industries, packaging and coating applications, automobile applications and in horticulture as an absorbent [2; 20; 84-87].

2.3 Bloodmeal-based thermoplastics

Bloodmeal is a by-product of animal slaughtering and is produced by drying blood at a temperature above 100 °C to remove water and destroy any pathogenic organisms; this process results in a denatured protein. This protein is not collected in a hygienic way that is fit for human consumption. Therefore, it is mostly used as animal feed or fertilizer.

Blood contains compounds with potential commercial value [88]. Blood is a major source of protein, containing 17.3% protein, 80.9% water, 0.23% fat, 0.07% carbohydrate and 0.62% minerals [89; 90]. Blood components are separated into two fractions; plasma and cellular fractions [90]. The plasma is the liquid fraction of blood and it contains up to 60% of the blood components, while the cellular fraction makes up about 30% to 40% of blood's wet weight and is dispersed within the plasma fraction [91]. The cellular fraction consists of red blood cells, white blood cell and platelets. Blood from different sources such as cattle, sheep, pigs and deer consists of between 50.5% to 72% plasma and 23% to 49.5% cellular mass [90; 91].

The protein content of bovine whole blood ranges between 3.61 – 3.80% albumin, 0.19 – 0.59% α -globulins, 0.47 – 0.53 β -globulins, 0.63 – 0.95% γ -globulins, 0.46 – 0.65% fibrinogen and 9.3 – 14.2 % haemoglobin, depending on its source [92; 93]. The main protein component of red blood cells is haemoglobin [91].

Haemoglobin consists of polypeptides that form α - and β -chains arranged in a globular (spherical) structure [94], known as globins. Each globin has an iron-containing heme group, which binds oxygen to haemoglobin tetramer molecules and makes it possible to transport 4 oxygen molecules together [90; 91]. Dehydrated plasma contains about 7% moisture, 80% protein, 7.9% minerals and approximately 1% fat, of which the main proteins are albumins, α - and β - globulins, immunoglobulins and fibrinogen [91; 95]. Globular proteins such as haemoglobin have four structural levels: primary, secondary, tertiary and quaternary as previously described (see Figure 13).

Centrifugation and clotting of blood to separate red blood cells from serum are the two main processes used to separate whole blood into fractions. Bloodmeal is produced through filtration of the blood to remove fragments. The product is then coagulated using steam injection at about 90°C, centrifuged and dried at a temperature between 100°C and 175°C using a rotating drum [96]. The resultant material is made into powder using a hammer mill; it is approximately 90% protein [97].

A protein's behaviour is assumed to be determined by its components. Therefore, the bloodmeal protein fractions (haemoglobin and plasma) can be useful in informing processing strategies. Certain amino acids found in haemoglobin and plasma have the propensity to form specific secondary structures such as α -helices, β -turns, β -sheets and random coils, which will influence mechanical properties and processing differently [98]. High ratios of α -helices to β -sheets were reported to contribute to the successful processing of zein protein into a product [99]. Bovine serum albumin has been reported [100] to fold into α -helices at about 50 – 60°C. however, above 60°C a reduction in α -helices with an increase in β -sheets was observed with FI-IR. Similar trends have been reported with regard to the effect of temperature on the secondary structure of porcine red blood cells above 40°C [101]. Bloodmeal has been reported by previous researchers to contain a high β -sheet content as a result of thermal aggregation during drying [98].

Bloodmeal has been successfully processed into a thermoplastic material that can be extruded and injection moulded in conventional polymer processing equipment [61; 71]. The processing of bloodmeal-based thermoplastics was registered and

patented as Novatein® thermoplastic protein [102]. Novatein® is an attractive alternative to petroleum-based polymers and offers a sustainable option over other raw materials that compete with food sources, as the meat industry in New Zealand alone processes a combined total of 25 million beef and sheep carcasses annually [103].

2.3.1 Novatein®

Novatein® (NTP) is produced using bloodmeal as a base material with additives such as sodium sulphite (SS) (reducing agent), sodium dodecyl sulphate (SDS) (surfactant), urea (denaturant) and tri-ethylene glycol (TEG) (plasticizer) in combination with water [61]. These additives are used to provide sufficient disruption to the inter- and intra-molecular interactions between polymer chains to ensure successful production of thermoplastic proteins [61].

Novatein® has an offensive odour, and it is reddish-brown in colour because of the haem chromophore in blood. These limit its use to some applications where these factors will be negligible, such as horticultural and agricultural products including biodegradable plant pots, seedling trays, vine and weasand clips, horticultural pegs, and abattoir rectal plugs (Figure 14) [104; 105]. Therefore, to enable wider acceptance and increased applications, decolouring of bloodmeal became imperative to eliminate its offensive odour and reddish-brown colour. Research has shown that the colour and odour of bloodmeal can be significantly removed by pre-treatment with peracetic acid (PAA) [11]. The treated bloodmeal is referred to as decoloured bloodmeal (DBM).

Peracetic acid (an equilibrium reaction of hydrogen peroxide, ethanoic acid (acetic acid or AA) and sulfuric acid as a catalyst) is not the only oxidizing agent used in previous studies to decolourize bloodmeal. Hydrogen peroxide and hypochloride have been used to degrade the haem in haemoglobin, which is responsible for the dark colour of bloodmeal [13; 106-109]. When using hydrogen peroxide and hypochloride, the haem needs to be freely soluble, easily accessible or in the form of oxyhaemoglobin [98]. The method used for processing blood into bloodmeal exposes the haemoglobin to thermal conditions causing significant structural changes to the protein. These changes include conversion of oxyhaemoglobin to

methaemoglobin and aggregation into antiparallel β -sheets, implying that hydrogen peroxide and hypochloride can no longer decolour bloodmeal effectively as they are either unable to access a portion of the haem in the bloodmeal or, upon accessing the haem, they are unable to degrade all of the haem species present. Therefore, the action of peracetic acid on methaemoglobin in bloodmeal's haem to ensure adequate decolourization is preferred [98].

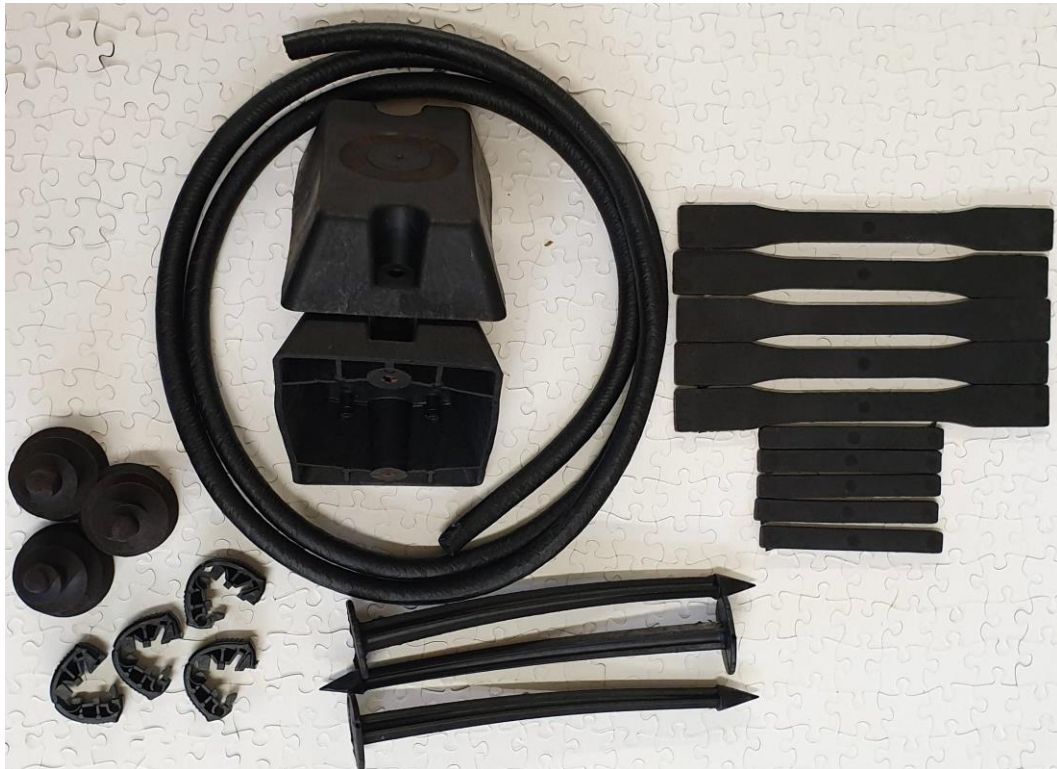


Figure 14: Image of produced Novatein® parts

2.3.2 Decoloured bloodmeal thermoplastic (DBT)

Decoloured bloodmeal (DBM) is a yellowish material containing 90% to 99% protein, derived from the pre-treatment of bloodmeal with 4% PAA [11]. Bloodmeal is decoloured through an oxidation reaction using PAA solution, sodium hydroxide, a neutralizing agent, and distilled water. The success of the decolouring of bloodmeal instigated a number of studies to investigate the role of PAA on the decolouring of bloodmeal, and the effect of oxidation on the composition,

physicochemical properties, protein structure and chain mobility of the final product [11; 110; 111].

Bloodmeal has a glass transition temperature, T_g , which is within the protein's thermal degradation temperature. However, upon oxidization with PAA, the T_g decreases to 50°C. Decoloured bloodmeal treated with PAA has a greater solubility in water and SDS solution compared to bloodmeal (solubility increases from 11% to 85% in 1% SDS) [11]. The increased solubility suggests that hydrophobic interactions are reduced after treatment with PAA. Oxidation causes changes in protein primary structure such as fragmentation, crosslinking and amino acid changes [112]. PAA acts as an electrophile in its molecular form to attack protein sites high in electron density [98]. Therefore, the amino acids most susceptible to oxidation with PAA are those commonly found in β -sheets, such as methionine and cysteine, due to their high reactivity with electrophiles, and the aromatic amino acids such as tyrosine and tryptophan, along with phenylalanine and histidine due to their high electron density. Dairy protein was reported [113] to contain an increased number of carbonyl groups, reduced thiol (SH) groups, aggregated protein and reduced solubility after oxidation with PAA solution.

Also, after oxidation with PAA, the DBM produced was found to have a greater proportion of charged and polar amino acids, with reductions in lysine, aromatic and heterocyclic amino acids, while cysteine was oxidized to cysteine sulfonate and cysteic acid [110; 111]. These amino acids are responsible for forming covalent bonds in proteins; therefore, their reduction implies no formation of disulphide crosslinks, so only TEG and SDS are required to successfully produce bioplastics using DBM. These changes in amino acids suggest changes to the protein structure, protein side groups and/or protein-protein interactions during oxidation. It is expected that changes in the primary structure of proteins would cause changes to the secondary structure as this is highly dependent on the physicochemical and stereo-chemical properties of amino acids. Aromatic or non-polar amino acids have been reported to have a higher propensity to form β -sheets, with the exception of threonine and cysteine, as they tend to form bends and sheets respectively while the other amino acids are more likely to form coils, bends and turns [64; 98; 114-116].

DBM has reduced crystallinity (from 35% to about 27 – 31%), and reduced thermal stability compared to Novatein®. DBM has improved colour and smell, increased enthalpy of relaxation, increased chain mobility and a change in its secondary structural composition, having less β -sheet aggregation and an increase in the number of disordered structures [13; 111].

The molecular mass of DBM increased from 139 kDa to 200 kDa [13]. This is assumed to be as a result of the oxidation reaction of PAA through the breaking of disulphide crosslinks and increasing solubility. Although there was an increase in the molecular weight of DBT, it was still within the molecular weight of Novatein® (130 kDa to 230 kDa), indicating that the protein chains were not interrupted during the decolouring process.

The reduction in thermal stability and T_g and an increase in solubility and molecular mass indicated that there is no formation of disulphide crosslinks. These changes in the properties and structural composition of DBM suggested that it remained suitable for processing into a thermoplastic.

DBM was successfully processed into thermoplastic protein using TEG, SDS, and water, then extruded and injection moulded on conventional processing equipment (Figure 15) [13]. The addition of TEG and SDS and heating facilitated chain mobility, leading to the transformation of random coils into α -helices and a more homogeneous distribution of secondary structures. The changes observed were reversible upon cooling [110]. These indicate ease of production during extrusion and/or sheet formation as these processes require rapid and homogeneous blending of crystalline and amorphous structures when heated to promote new interactions and prevent thermal degradation of the protein, as well as the strengthening of hydrogen bonds after processing to ensure optimal material properties.



Figure 15: Injection moulded sample of decoloured thermoplastic protein processed using TEG, SDS, and water.

Based on the known properties of DBM, it can be used in short lifespan applications such as packaging, coatings and agricultural products (Figure 16) like other biopolymers, because of its compostability, lack of odour and translucent colour.



Figure 16: Agricultural plant pots and injection moulded samples made from decoloured thermoplastic

2.4 Polymer Blends

2.4.1 The concept of polymer blends

Polymer blends make up nearly one-third of the total consumption of polymers today [117]. Polymer blends are mostly produced by mechanical mixing of two or more polymeric materials. The main purpose of polymer blending is to enhance the properties of individual components in the blend and increase the range of applications of both polymers [118]. Polymer blending is a widely used and convenient technique for modification of material properties because of its ability to use conventional technology at low cost and saves time compared to synthesizing new polymers. Specific blend properties can be achieved by changing the blend

composition [119]. The performance of polymer blends depends on the properties of the materials in the blend, their composition, and morphology.

Most common synthetic polymers have been blended to enhance their properties based on specific needs. The most commonly available synthetic polymer blends involve combinations of low-density polyethylene (LDPE), high-density polyethylene (HDPE), polyethylene terephthalate (PET), polystyrene (PS), polyamides (PA) polypropylene (PP) and polyvinyl chloride (PVC) [120-124].

In recent decades, the use of renewable resources to offset the high price of synthetic polymers and provide solutions to growing pollution problems has witnessed an increased demand for natural polymers. However, polymers from renewable resources are often expensive and have poor mechanical properties. Also, their hydrophilic nature and/or water solubility and high rates of degradation limit their applications [104]. To overcome these disadvantages, various blends have been developed to create materials with improved properties and performance. Polymers have been blended from three types of renewable resources: natural sources like starch, protein, and cellulose; synthetic sources from natural monomers like poly(lactic acid) (PLA), poly (butylene adipate-co-terephthalate (PBAT); and polymers from microbial fermentation, such as poly-hydroxybutyrate [125].

Polymer blending faces a major challenge as polymers are generally thermodynamically immiscible [126]. Therefore, achieving compatibilization of immiscible polymer blends is essential in the improvement of blend properties and performance. Polymer blends can be classified into four categories: immiscible, miscible, compatible and compatibilized polymer blends [127]. An immiscible polymer blend is a blended system with large size domains in the dispersed phase and poor adhesion between the polymer phases. A miscible polymer blend is a homogeneous blend system with a single-phase structure. A compatible polymer blend is an immiscible blend system that exhibits a visible uniform structure caused by sufficiently strong interfacial interactions between the polymers in the blend. A compatibilized polymer blend is a blended system where microstructure and physical properties are stabilized by the addition of surface-active monomers known as compatibilizers. However, these compatibilizers can influence

morphological processes such as deformation, coalescence of droplets and breakup [14; 128; 129].

2.4.1.1 POLYMER BLEND MISCIBILITY

When considering materials for polymer blends, materials with reactive groups capable of interacting with each other must be selected. Miscibility of polymeric materials is limited to a specific set of conditions. Therefore, most polymers form immiscible blends that require compatibilization [130] to ensure the development of a high-performance material with good adhesion between the matrix and dispersed phase.

Miscibility follows the same principles as thermodynamic solubility, where two or more components are miscible in each other if the free energy of mixing is less than zero [15; 131; 132]. However, most polymer blends have a major problem as they do not follow this principle, implying that polymer blends cannot mix thermodynamically.

The behaviour of dissimilar components in a blend is governed by the Gibbs change in free energy of mixing (ΔG_m), as shown in Equation (1),

$$\Delta G_m = \Delta H_m - T\Delta S_m \quad (1)$$

where ΔG_m is the free energy of mixing, ΔH_m is the enthalpy of mixing or heat of mixing, T is the absolute temperature, and ΔS_m is the entropy of mixing. ΔH_m is a measure of the extent of the interaction between the polymer molecules while ΔS_m is associated with the increase in the total entropy of the blend. A necessary criterion for miscibility to occur is that the Gibbs free energy must be negative. However, polymer blends give a positive ΔG_m as entropy increases in their blend system during mixing. Although ($\Delta G_m < 0$) is a necessary condition, it is not sufficient, as the phase stability of a binary mixture at a fixed temperature (T), and pressure (P) must also be satisfied for a stable one-phase system to be obtained. The expression that describes this criterion is given in equation (2)

$$\Delta G_m < 0, \left(\frac{\partial^2 \Delta G_m}{\partial \phi^2} \right)_{T,p} > 0 \quad (2)$$

The entropy of mixing ($T\Delta S_m$) is always positive because of the increase in entropy during mixing. Hence, the sign of ΔG_m always depends on the value of the enthalpy of mixing ΔH_m , which can be negative or positive. The number of possible arrangements for a polymer–solution blend system is much higher than for a two polymer blend system. The limited possible arrangements in a polymer-polymer blend system result in phase separation at high temperature and dissolution at a lower temperature. Therefore, the contribution of the volume of mixing to the free energy of mixing becomes substantial [15].

The Flory-Huggins model [133; 134] for the free energy of mixing of polymers in solution can be applied to polymer-polymer systems by introducing the concept of a reference segment (VR), which is approximated to the smallest polymer repeating unit, as shown in Equation (3)

$$\Delta G_{mix} = kTV \left[\frac{\phi_A \ln \phi_A}{V_A} + \frac{\phi_B \ln \phi_B}{V_B} \right] + \phi_A \phi_B X_{12} kTV / v_r \quad (3)$$

where k = Boltzmann's constant, T = absolute temperature, V = total volume, V_i = molar volume of each component, ϕ_i = volume fraction of each component, X_{12} = Flory-Huggins interaction parameter and v_r = interacting segment volume (repeat unit volume or reference). The polymer lattice is assumed to consist of N cells with a volume of V . Thus, each polymer molecule occupies volume V_A and V_B . Therefore, the volume fraction of component A and B is given by Equations (4) and (5)

$$\phi_A = \frac{V_A N_A}{V_A N_A + V_B N_B} \quad \text{and} \quad \phi_B = \frac{V_B N_B}{V_A N_A + V_B N_B} \quad (4)$$

Therefore:

$$V = V_A N_A + V_B N_B \quad (5)$$

Different phase behaviour (Figure 17) can be observed in a polymer blend as some blends may be miscible at a certain temperature and composition while across a range of temperatures and compositions, they become immiscible, resulting in phase separation. Phase separation occurs when a single-phase system encounters a change in pressure, composition or temperature, forcing it to enter either the metastable or the spinodal region. The composition range at which two polymer phases separate is not constant as it is temperature dependent.

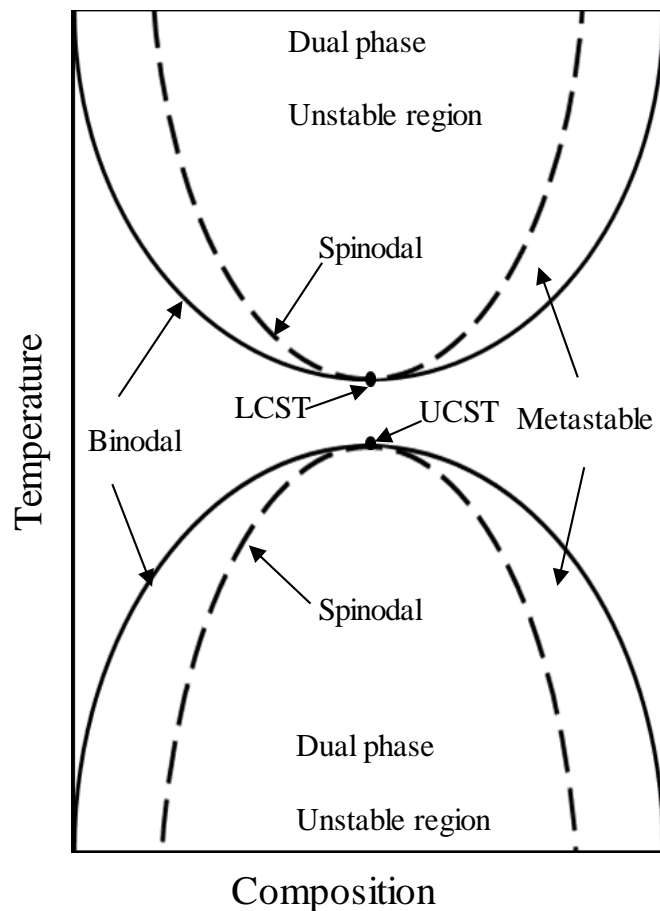


Figure 17: Phase diagram of a binary polymer blend indicating different phase regions, the lower critical solution temperature (LCST) and upper critical solution temperature (UCST)

The binodal curve is the region between the single-phase (miscible phase) and the metastable region where phase separation occurs by nucleation and growth, while the metastable region is the phase between the binodal and spinodal curves. Metastable region has a small concentration of fluctuation and spinodal decompositions (smaller disturbance). However, the fluctuations are too small to affect blend's stability. The spinodal curve is the region between the two-phase separated regions of immiscibility where phase separation is as a result of high concentration of fluctuation. As the temperature increases, the region of miscibility decreases. Blends with positive mixing entropic and enthalpic values such as polymer-solvent mixtures usually exhibit an upper critical solution temperature (UCST) while blends with negative values of entropies and enthalpies of mixing such as polymer-polymer mixtures generally exhibit lower critical solution temperatures (LCST). In other words, a polymer that exhibits as UCST will be immiscible at lower temperatures, mainly due to weak interactions between both components [15].

Binodal and spinodal decompositions are both present in UCST and LCST. Spinodal phase separation occurs by a spontaneous and continuous process attributed to a diffusional flux mechanism [127] while binodal phase separation occurs by a mechanism similar to crystallization, where slow nucleation occurs, followed by growth of the phase-separated domains through a conventional diffusion process [132].

2.4.1.2 POLYMER BLEND COMPATIBILITY

The objective of polymer blending is to produce a material with combined superior properties compared to the individual polymers in the blend. However, due to the thermodynamic instability of immiscible polymer blends, mixing processes such as moulding and annealing significantly affect the blend's properties, including its morphology. Therefore, to enhance miscibility between two polymers, the enthalpic value of the blend is forced to be negative by the addition of a compatibilizer, which improves the morphological stability through the introduction of specific interactions [135].

Compatibilization involves the reduction of interfacial tension, ensuring fine dispersion, and stability of structures of the blended material against thermal and

shear effects during processing, and the provision of interfacial adhesion in the solid state [136]. Compatibilization can be achieved through one or a combination of the following: [117; 127; 130].

- The addition of a new component (functional polymer) which is miscible with both material phases
- The addition of a copolymer whose different functional units are miscible or reactive with the different material phases
- The addition of nanoparticles, which influence the structure of the blend
- The addition of a core-shell copolymer (compatibilizer-cum-impact modifier)
- The modification of one or more macromolecular species through reactive compounding, resulting in the development of localized miscible regions with both material phases

The most studied compatibilization approach is the addition of a third component, such as a block or graft copolymer Figure 18, capable of mixing or reacting with both blend components to create a possible conformation as shown in Figure 18. The most frequently used copolymers are those containing segments that can chemically interact or are identical to both blend components, as they enhance the miscibility between the copolymer segment and the individual blend components. A block is formed when two monomers cluster together and form blocks of repeating units [137; 138], while a grafted copolymer has one or more blocks of homopolymers grafted as branches onto a main chain (i.e., a branched copolymer with one or more side chains of homopolymer attached to the backbone of the main chain [139]). Block polymers are widely preferred over graft copolymers. However, most block polymers are not commercially available and require modification for each blend system [127].

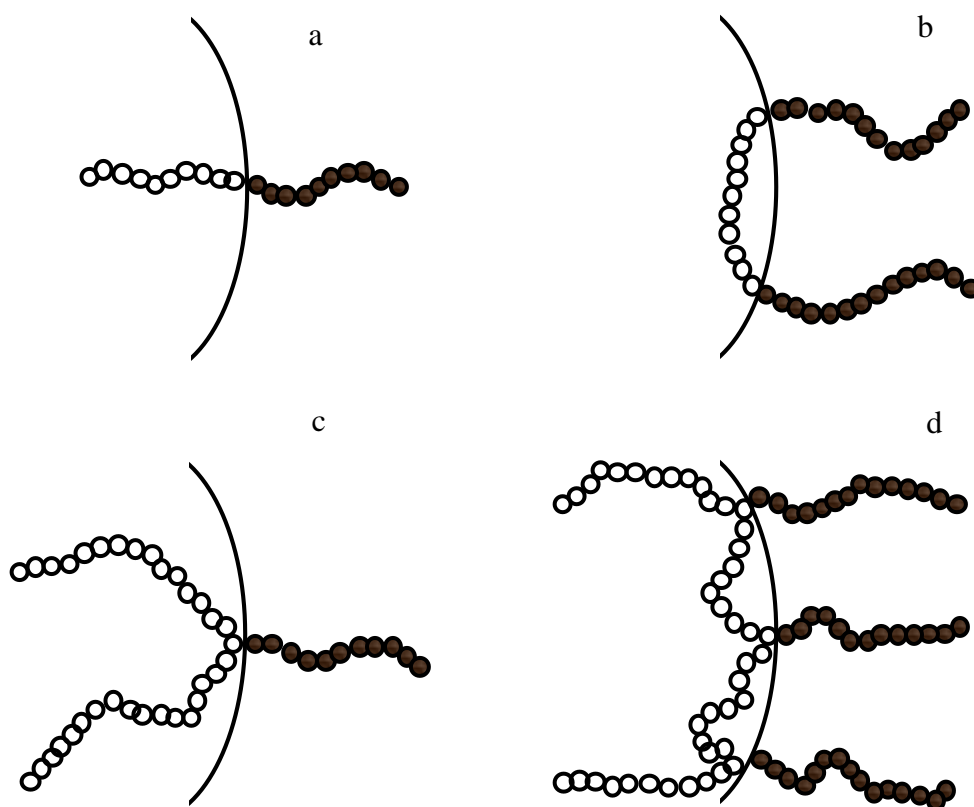


Figure 18: Structure of conformation of block (a; diblock and b; triblock) and grafted (c; single graft and d; multi-graft) copolymers at the interface of a heterogeneous polymer blend.

A heterogeneous polymer blend of A and B can be compatibilized with a diblock copolymer (C-d-D) (Figure 18a), provided that block C is miscible with polymer A and block D is miscible with polymer B. This implies specific interaction between (A and B) and (B and C). This is usually the most effective compatibilization approach for a heterogeneous polymer blend A/B system [135].

An alternative method of producing compatible blends is the in-situ formation of copolymers at the blend's interface during melting blending. This is done through reactive blending. This method has been widely used in commercial applications [140; 141]. Reactive regions are introduced in this compatibilization method through grafting, either as a component capable of mixing with one phase and reactive to the other phase, or as pendant or terminal groups in the blend.

Polymers may be grafted with functional and reactive groups through reactive extrusion. Polymers modified with itaconic anhydride or acids, maleic anhydride, acrylic acids or glycidyl methacrylate [127; 142-146] have been extensively used

as compatibilizers due to their ability to form either a chemical linkage or a polar or ionic interaction with polar polymers such as polyesters and polyamides.

A compatibilized blend shows a degree of mixing of polymer segments on a microscopic scale and a degree of thermodynamic compatibility which prevents immiscibility. However, it is important to note that reaching the highest degree of compatibility where miscibility is completely achieved ($\Delta G_m < 0$) does not always imply that the best possible final properties will be achieved. In order to achieve the desired final mechanical properties for most blends, a degree of phase separation is required [147]. The final properties of a blended system do not depend solely on the blend components properties; they are also determined by the blend phase morphology and interface adhesion as these determine the stress transfer within the blend and its end use applications [127].

2.4.1.3 BLEND MORPHOLOGY

Blend morphology depends on the processing conditions to which a blend has been subjected. Many factors determine the development and stability of morphology in multiphase polymer blends; the most important factors are blend composition, applied shear stress, and viscosity ratio [147].

Blend composition

Varying the composition and component of a polymer blend will result in different morphological structures. If the dispersed phase increases, then the particle size will increase as a result of coalescence. There is also the possibility of a significant increase in particle-particle interaction with an increase in the minor phase concentration, which will also promote coalescence.

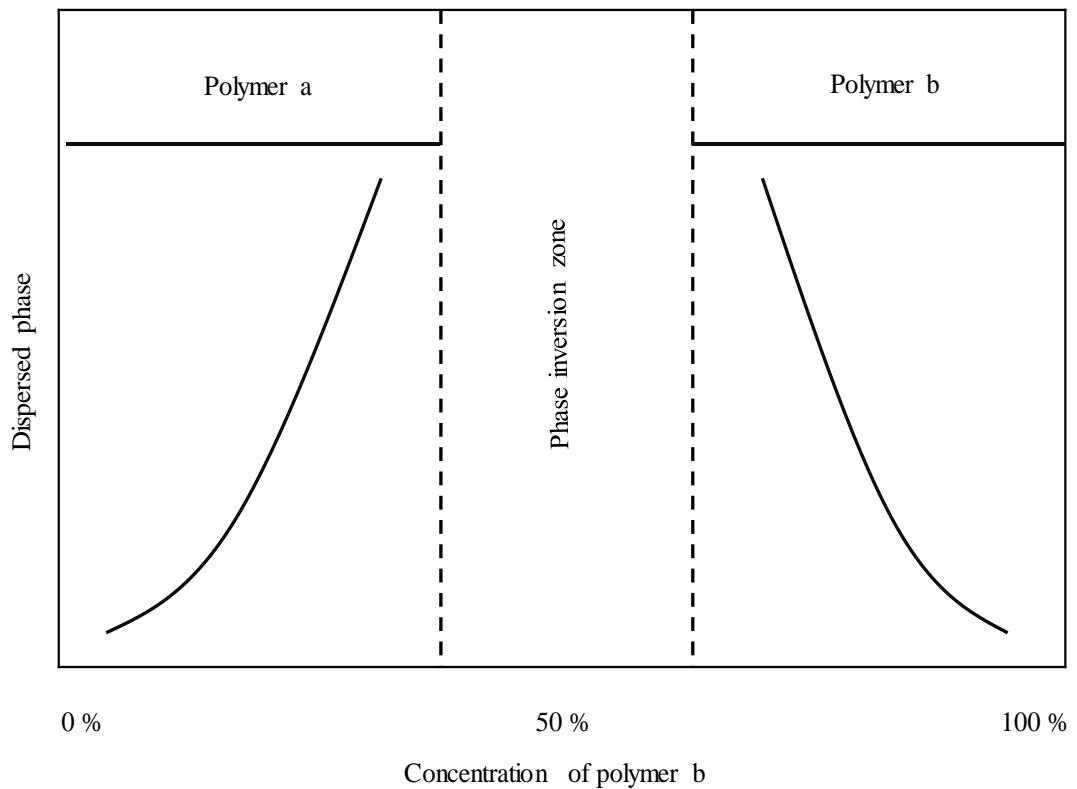


Figure 19: Dispersed phase size variation in a known polymer blend as a function of polymer b concentration [127]

For a known polymer blend (a/b), the composition of each component will define the region in the blend's matrix, as illustrated in Figure 19. A region where polymer a is dispersed in polymer b, a phase inversion region where both polymers a and polymer b are co-continuous and an inverted region where phase b is dispersed in polymer a matrix.

Viscosity ratio

This is the ratio between the viscosity of the dispersed phase and the viscosity of the matrix. This ratio is considered one of the most important factors for the control of blend morphology [15]. A minor blend component with a lower viscosity than the major blend component will produce a morphology where the minor component will be finely and homogeneously dispersed in the major component's matrix. However, if the minor component's viscosity is higher than the major component viscosity, then a morphology where the minor component is coarsely dispersed is obtained. A linear relationship between the average diameter of dispersed phase particles and viscosity ratio has been reported [147; 148]. These studies suggested

that a low viscosity of the minor blend component and a near unity viscosity ratio value can produce a fine dispersion of the minor phase in the matrix. However, as the viscosity ratio moves away from unity in either direction, the particles of the minor phase will become larger.

Shear stress

Phase size is inversely proportional to the applied shear stress. Shearing a polymer blend at high shear stress will result in finer and more dispersed morphologies. However, high shear rate may suppress capillary instability during flow, affecting the transient breakup process. S. Wu [149] reported that changing shear stress resulted in morphological changes. However, other researchers [150-152] suggested that a slight change in shear rate has little or no effect on the blend's morphology. It has been suggested that in an immiscible binary blend, shear stress is not continuous at the interface due to interlayer slippage. Favis Basil [148] argued that the apparent dispersion observed when the Weber number is plotted against torque ratio is a result of differences in the shear stress. It was concluded that the influence of shear stress in an immiscible polymer blend is less critical than had been assumed.

2.4.1.4 POLYMER BLENDING METHODS

Polymer blending involves different stages, including materials preparation, premixing of materials, melt mixing and forming. The most commonly used polymer blending methods are mixing using internal mixers such as a single shaft or multi-shaft mixer, and extrusion using single-screw and/or twin-screw extruders [3].

Mechanical blending method (mixing using melt process blending)

Mechanical mixing applies heat to the materials, causing them to flow readily and resulting in a blended material. This method is mostly used for materials that have a high melting temperature (above the processing temperature) and are miscible or compatibilized. Common technologies used are batch/continuous mixers, thermal pressing and extrusion processing.

Extruders

Both single-screw and twin-screw extruders have been widely used for blend preparations. However, twin-screw extruders offer a high level of stress, sufficient to obtain higher mixing levels in polymer blends. The main difference between a single-screw and a twin-screw extruder is in the conveying mechanism [153]. Single-screw extruders are made up of a single screw system while twin-screw extruders have two screws, which are either counter-rotating or co-rotating and intermeshing or non-intermeshing. Twin-screw extruders can be used for a wider range of raw materials, with varying moisture contents. Extruders are generally used for mixing, compounding and reacting polymeric materials. Compounder type, operating conditions (temperature, screw speed, and feed-rate) and the mixing elements of an extruder have a significant effect on the quality and morphology of the resulting polymer blend.

Mixers

Blends of powdered polymers are usually prepared using a single-shaft mixer such as a ribbon blender or a paddle mixer. However, viscous masses that require melting and mixing are mixed using an internal multi-shaft mixer. Internal multi-shaft mixers generate higher mechanical stresses than single-shaft mixers. For this reason, internal multi-shafts are generally preferred [148].

Non-mechanical blending methods

The most commonly used method for polymer blends is solvent/solution casting. Most natural polymers cannot be processed using a melt process because they either degrade below their melting temperature or cannot withstand high processing temperatures. Therefore, solution casting is the preferred technique. Solution casting has advantages over the melt process, including uniformity, the absence of pinholes and gel marks, purity and clarity, and lack of residual stresses, making it the preferred industrial technique for the production of thin layered films for a variety of applications [117]. Solvent casting is also preferred for biomedical applications [125].

Latex is another non-mechanical blending method that is being used in the industries today because of its potential for fine dispersion of blend components. However, it is a cost-intensive process [130] compared to solution casting.

2.4.2 Blends of bio-polymers

Most natural bio-polymers are hydrophilic, degrade very fast and have unsatisfactory mechanical properties, especially under humid environments [125]. These characteristics limit their application. To overcome the inherent hydrophilicity of bio-polymers and their poor mechanical properties, blending with conventional hydrophobic synthetic materials is often used. Bio-polymer blends are aimed at achieving improved material properties while maintaining biodegradability in composting and other biologically active environments [154]. Natural polymers such as starch, cellulose and aliphatic polyester have been successfully blended to improve their properties or to produce a new material with improved properties.

2.4.2.1 STARCH

Starch is one of the most researched natural polymers because of its abundance. Pure starch is mostly water-soluble, difficult to process and very brittle, with mechanical properties that are sensitive to moisture. Therefore, it is not a good alternative to petroleum-based polymers. Starch has been blended with more hydrophobic thermoplastic materials such as polycaprolactone, natural rubber, and polyhydroxybutyrate/valerate, as well as cellulose and cellulose acetate to reduce its water sensitivity [155-158]. Novamont Italy commercialized a biodegradable blend of starch/polycaprolactone under the trade name of Mater-Bi Z-class [159]. Narayan (USA) developed a process that uses reactive extrusion to process a plasticized starch and modified polycaprolactone blend in a twin-screw extruder [160].

2.4.2.2 CELLULOSE

Cellulose is one of the most abundant bio-polymers on earth. Cellulose and its derivatives have been blended with other natural polymers such as protein (silk fibroin, soy protein isolate, chitosan, and casein) to produce biodegradable materials with improved properties [125; 161-163].

2.4.2.3 ALIPHATIC POLYESTERS

Aliphatic polyesters like PLA and poly(hydroxyalkanoates) (PHAs) have also been widely studied for blends with other natural polymers. These polyesters are produced from renewable resources, are highly biodegradable and susceptible to hydrolytic degradation.

Poly(lactic acid) (PLA)

PLA's crystallinity and hydrophilicity can be controlled, which in turn controls its rate of degradation. PLA has low toxicity and high mechanical properties. However, its low thermal stability limits its ability to be used as an alternative to commercial polymer applications [164]. Blends of various stereocomplexes formed from PLA such as poly(L-lactic acid) (PLLA)/ poly(D-lactic acid) (PDLA) have been studied to improve their thermal properties and resistance to hydrolysis compared to the individual polymers [164-166]. Control of the hydrolytic degradability of PLA is essential in controlling its mechanical properties. The degradation of PLA was accelerated by blending PLA and poly(aspartic acid-co-lactide) (PAL) to study its effects on material properties [167]. Blends of starch and PLA [36; 168-170] have received broad attention because starch is cheap and abundant, while PLA has good mechanical properties but is expensive. Therefore, a blend can produce affordable materials with improved properties.

Poly(hydroxyalkanoates) (PHAs)

Some PHAs have similar behaviour to synthetic polymers such as polyethylene and polypropylene, while others are elastomeric [171]. The commonest type of PHA is poly(3-hydroxybutyrate) (PHB) because of its biodegradability and biocompatibility with most bio-polymers. Various blends of PHB with other PHAs have been investigated for suitability in biomedical applications [171-173]. Various PLA-based materials with improved processibility, miscibility and a broad range of physical properties have been produced using various combinations of PLA and PHAs [174; 175]. Poly(*cis*-1, 4- isoprene) (PIP) was reportedly blended with PHB to improve the mechanical properties of PHB [176]. PHB has been blended with starch acetate [177] and starch grafted with poly(glycidyl methacrylate) (starch-g-PGMA) [178] to investigate miscibility and improve the mechanical properties of starch. PHB has been blended with ethyl cellulose, cellulose propionate, and

cellulose acetate butyrate to investigate the miscibility, crystallization, phase morphology and melting behaviour of the blends [179-181]. These studies reported improved material properties for the blends produced.

2.4.3 Blends of protein-based polymers

The use of protein-based polymers has attracted an increasing amount of attention over the last decade for its potential in producing biodegradable plastics [5; 182]. Protein is one of the most promising natural polymers because of its inherent biodegradability and abundance in nature [183]. The use of pure protein is not a good substitute for synthetic polymers. Proteins are highly sensitive to water, which affects their mechanical properties [61]. Also, proteins are very difficult to process as they have a narrow window of processing temperature and are brittle when processed in the absence of a plasticizer [71; 104; 184]. However, recent investigations of protein-based polymers have revealed that proteins can be successfully blended with two or more different polymers to produce a material with the potential to overcome these difficulties; having good mechanical properties, film-forming ability and water/gas barrier properties suitable for use as packaging films, foams for the insulation of houses and coating on paperboards [104; 183; 185; 186].

Blends of soy meal and poly (butylene adipate-co-terephthalate) (PBAT) were investigated by Zhou et al., who reported an improved elongation after plasticization and denaturation, along with a smoother surface and better internal structure [187]. Guo et al. studied blends of soy protein isolate (SPI) and PBAT and reported an increase in thermal stability, tensile strength and elongation at lower SPI content [188]. Reddy et al. [69] investigated blends of plasticized corn meal and PBAT; they reported a network of formation showing long timescale elasticity. Also, tensile strength and elongation were reported to show a significant increase, indicating a strong interaction between the material phases in the blend matrix [69].

Aithani et al. studied the blends of plasticized corn gluten meal and poly (ϵ -caprolactone) (PCL), and reported better compatibility between the blended phases, improved elongation and impact strength [189]. Zhu et al. investigated the compatibilizing effects of maleated PLA on blends of soy protein concentrate (SPC)

and PLA [190], reporting a 19% increase in the tensile strength and storage modulus of the compatibilized blends, fine morphological structures and a lower damping peak, which suggested good interfacial adhesion between the phases [190].

Suyatma et al. investigated the water vapour barrier properties of a chitosan/PLA blend [191]. They reported an improvement in the water barrier properties and water sensitivity, and a decrease in tensile strength and elastic modulus. They suggested that the reduction in mechanical and thermal properties was evidence of incompatibility between chitosan and PLA. Blends of poly(3-hydroxybutyric acid) and α -chitin and/or chitosan were developed [192; 193]. The crystallization behaviour and environmental biodegradability of the blends were investigated. Chitosan was reported to have a stronger ability to suppress the crystallization of PHB than α -chitin. An increase in the biodegradation rate of the blends compared to the individual components was also reported.

Zhang et al. [194] studied the morphology and properties of soy protein and PLA blends. An improvement in the melt flowability, processibility, and reductions in water absorption properties of the blends were reported. Also, they reported that the addition of PEOX improved the compatibility and tensile strength of the blends. Liu et al. [195] investigated the synergetic effect of PEOX and polymeric methylene diphenyl diisocyanate (pMDI) in blends of soy protein concentrate and PLA. An improvement in processibility, interfacial adhesion between the blended phases, tensile strength, storage modulus even at a temperature above PLA glass transition temperature and reduced water uptake of the blended material was reported. Marsilla et al. [196] investigated the synergetic effect of PEOX and pMDI in blends of Novatein® thermoplastic protein (NTP) and polybutylene succinate (PBS). An improvement in tensile strength, dispersion of NTP particles and interfacial adhesion between both blend phases were reported. Marsilla et al. [197], studied blends of bloodmeal-based protein and low-density polyethylene (LDPE) compatibilized with maleic anhydride grafted polyethylene (PE-g-MA). They reported an improvement in compatibility between material phases, tensile strength, fine dispersion of NTP particles in the compatibilized blends and reduction in water absorption of NTP.

Most proteins are immiscible with other bio-polymers such as PLA, due to significant differences in their hydrophilicity and polarities. The interfacial bonding of these material blends is fairly weak. However, interfacial modifiers containing reactive functional groups such as maleic anhydride (MA), methylene diphenyl diisocyanate (MDI), itaconic anhydride (IA), polymeric diphenyl diisocyanate (pMDI) and poly (2-ethyl-2-oxazoline) (PEOX) are used to generate in-situ formed blocks or grafted copolymers at the material's interface to improve compatibilization [185; 190; 197-201].

2.4.4 Blend characterization

Mechanical, morphological and thermal properties are the most common method used to characterize blends [14].

2.4.4.1 MECHANICAL PROPERTIES

Blending two or more bio-polymers is aimed at producing a material with improved physical properties. For instance, soy protein concentrate (SPC) presented increased tensile strength and elongation at break when blended with PLA and a compatibilizer [80].

Achieving desired mechanical properties in blends is often considered evidence of compatibility from a practical point of view, making compatibilization essential. Depending on the proportion of each component in a polymer blend that is miscible at all levels, an average of their mechanical properties is obtained. Blends of two immiscible polymers without a compatibilizer produce mechanical properties worse than either individual polymer. However, blending two immiscible polymers with compatibilization is expected to produce a synergistic combination of properties from each polymer [131; 202].

Generally, blending two bio-polymers results in a weak and brittle material. This is as a result of the presence of stress concentrations and weak interfacial adhesion arising from poor mechanical coupling between the polymer phases. Previous reports have shown that compatibilization can improve interfacial adhesion between two bio-polymer phases in a blend, resulting in increased mechanical properties [104; 184; 203].

Blends of soy protein concentrate (SPC)/PLA and soy protein isolate (SPI)/PLA were compatibilized with poly(2-ethyl-2-oxazoline) (PEOX) [194]. Improvement in tensile strength, elongation at break and modulus with the addition of PEOX were reported. The authors suggested that the improvement reported was evidence of improved compatibility.

Zhu et al. investigated the effect of maleic anhydride grafted PLA (PLA-g-MA) compatibilizer on blends of SPC/PLA [190]. They reported an increase in tensile strength, elongation at break, modulus, finer domain sizes of SPC and a lower damping peak with the addition of compatibilizer.

Murali et al. [204] studied soy meal-based biodegradable blends. They investigated the effects of denaturant, plasticizer and polyester type on the tensile strength and elongation at break in the blends. They reported that polyester type had a significant effect on the tensile strength and elongation at break in the prepared blends.

Blends of Novatein® thermoplastic protein and PBS compatibilized with PEOX and pMDI were investigated by Marsilla et al. [196; 197]. Improvement in tensile strength was reported with the addition of both compatibilizers. Also, it was reported that the addition of PEOX during extrusion and pMDI during injection moulding showed further improvement in tensile strength. They concluded that using dual compatibilizers increased the blend's compatibility as PEOX improved dispersion of NTP while pMDI strengthened the adhesion between both material phases.

2.4.4.2 MORPHOLOGICAL PROPERTIES

Information on surface topography, size, and distribution of the dispersed phase and interfacial interaction between material phases in a blended matrix can be used to characterize a blend. A blend morphology with large and debonded phases suggests material immiscibility and inherently poor mechanical properties. Factors such as the viscosity of the blend's components, interfacial interaction, mixing conditions, blend composition and their relationship influences morphology and ultimately the blended material properties.

Blending involves melting, breaking of polymer chain structures and coalescence. Morphology development during extrusion has been extensively studied to control the final product morphology and design processing equipment [205; 206]. It is known that morphology development during extrusion has a significant influence on the final properties of the blended material.

Li. et al. [207] studied the morphology development of amorphous nylon (aPA)/polystyrene maleic anhydride (PSMA) and aPA/polystyrene (PS143). The effects of compatibilization and extruder rotation rate were investigated. Morphology development in compatibilized blends was reported to be faster than in uncompatibilized blends. It was suggested that dispersion was facilitated by reducing slip at phase interfaces with the addition of compatibilizer. This study also suggested that rotation rate influenced the morphology development of the polymer blends by changing the residence time of the polymer in the extruder.

The influence of morphology development during processing can be observed from the fracture surfaces or cross-sectional surfaces of the material samples. Zhong et al. [208] investigated the properties of soy protein isolate/polycaprolactone blends compatibilized with methylene diphenyl diisocyanate. They reported a rough and heterogeneous fractured surface with an increase in PCL content without compatibilizer. Plastic flow was observed at high PCL content, which showed an increase in toughness of the blends as PCL content increased. They concluded that compatibility and adhesion between SPI and PCL were improved with higher MDI content as no evidence of SPI particles was observed.

Marsilla et al. [185] reported finely dispersed particles of NTP in the fracture surface of NTP/linear low-density polyethylene (LLDPE) blends compatibilized with maleic anhydride grafted polyethylene (PE-g-MAH). Incompatibility between the NTP/LLDPE phases in the blend without compatibilizer was suggested to lead to a large NTP-rich domain suspended in a weak LLDPE matrix. The authors suggested this was supported by the rapid drop in tensile strength of the blend with NTP content between 20 and 30%. The blends of NTP and polybutylene (PBS) without compatibilizer [197] showed evenly distributed NTP particles in the PBS matrix. However, a clear separation was observed at higher magnification. They reported bridging between NTP and PBS phases as evidenced by elongated strands

of polymer observed in the blend's fracture surface. The addition of pMDI alone revealed fewer agglomerates of NTP particles compared to the uncompatibilized blend. However, a clear phase separation was visible. Using PEOX and pMDI as compatibilizers did not produce a significant change in morphology. However, improved adhesion compared to using pMDI alone was reported.

A distinct interface between PLA and SPI was observed on the fracture surface of a PLA/SPI blend without compatibilizer [79]. The dispersed SPI phase particles were large and non-uniform as a result of the inherent immiscibility. Blends containing 0.05% NaHSO₃ reportedly showed smaller SPI particles. A PLA/SPI blend containing 0.5% NaHSO₃ showed indistinct phase morphology. However, few agglomerates were observed. The agglomerates observed increased with an increase in NaHSO₃ content (3 wt.%). This was probably as a result of the breakage of SPI disulphide bonds, induced by the presence of NaHSO₃. Despite the presence of agglomerates of SPI, the interfaces of the blends containing both NaHSO₃ were barely distinguishable. It was concluded that the compatibility of PLA and SPI was improved by the use of NaHSO₃.

2.4.4.3 THERMAL PROPERTIES

Polymer blend miscibility can be determined by the presence of one or more glass transition temperatures (T_g) as measured by a variety of thermal techniques. The most popular techniques are dynamic mechanical analysis (DMA) and differential scanning calorimetry (DSC). T_g is the temperature range at which there is a gradual and reversible transition in amorphous materials or amorphous regions within semi-crystalline materials. The T_g of a material characterizes the range of temperatures over which the material will change from glassy to a viscous or rubbery phase. Below the T_g , polymers are in their glassy state, where chain movement is fixed by intermolecular interactions. Above the T_g , polymers are in a rubbery state, where they are soft and flexible [15].

A single T_g is observed for a miscible system, which is intermediate between the two phases. In this system, macromolecules are statistically distributed on a molecular level, presenting only one T_g . In partly miscible systems, a shift in T_g s of the material components towards each other is observed as a result of interactions between the polymer chains of both polymers in the blend. For an immiscible

system, distinctive T_g s for both material components are observed as the components are completely separated into different phases.

Another thermal transition that can be used to determine the miscibility of polymer blends is the crystalline phase structure of semi-crystalline or crystalline polymer blends. The rate of crystallization varies with temperature and will affect morphology as well as material properties. When a semi-crystalline blend cools from the melt, crystallization occurs. The interaction between the amorphous and crystalline phases determines the diffusion of the amorphous phase into the crystalline region. The properties of the semi-crystalline polymer blend can be determined by the degree of crystallinity as well as the size and orientation of the molecular chains.

2.5 Film/Sheet forming

Protein sheet formation generally involves the development of hydrophobic associations, hydrogen bonds and limited disulphide bonding between protein chains in the sheet matrix [25; 209; 210]. Polymer films are considered as stand-alone products, formed separately for an intended use [130]. Recent research in biopolymers for sheet forming has focused mostly on film formation of proteins and their blends [211-215]. The formation of sheets and films is similar, using the same technologies and techniques. However, a difference lies in their thickness. Sheets have a thickness exceeding 250 μm [118]. If the thickness is below 250 μm , the product is then known as a film. The literature covered in this area thus focuses primarily on film formation.

Most polymer films currently used in packaging and other applications are made from petroleum-based polymers. They have widespread uses in packaging applications as a result of their well-known advantages, which include large-scale availability, low production costs, light weight, and excellent mechanical and barrier properties [216; 217]. However, the drawback with petroleum-based polymers' is that they do not degrade, resulting in accumulation of residues as they are sent to landfill for incineration and dumping. This lack of degradability contributes to environmental pollution and waste hazards.

Presently, renewable bio-polymer films from agricultural, animal and microbial sources such as protein and polysaccharide have emerged as a promising substitute due to their ability to biodegrade into simple substances such as water, carbon dioxide, and biomass when exposed to optimum soil moisture, microorganisms and oxygen [211; 216]. Bio-polymers from these sources are associated with poor mechanical and barrier properties, and low thermal stability. Therefore, modification strategies are needed to improve the properties of bio-based polymer in the production of films or sheets.

2.5.1 Film or sheet formation

Film formation can be achieved using two main processes; dry and wet processing. The wet process involves dispersion and solubilization in a film-forming solution, followed by drying of the solvent. The dry process relies on the thermoplastic behaviour of the material at a low moisture content in compression moulding and extrusion [218; 219]. Polymer sheets and films can be processed using several methods, including casting, calendering (see section 2.5.1.2 below), compression moulding and sheet/film extrusion. The calendering process is the oldest method available for sheet or film processing. However, sheet extrusion is the most common and preferred method used [117].

2.5.1.1 FILM/SHEET EXTRUSION

Extrusion is one of the polymer processing techniques widely used today. Most synthetic polymer sheets or films are processed using extrusion. The application of extrusion technology in the production of protein sheets has been a challenge to researchers, and limited reports have been published.

Sheet extrusion involves the heating and kneading of the material in an extruder. The melted material is then extruded through a slit die to produce a film or sheet. The produced sheet is then passed through a system of rollers, which coil it onto a roll. Cooling rollers control the draw ratio and final film thickness [118; 220; 221]. The process can involve any or all of the following operations: feeding, conveying, heating, compressing, shearing, reacting, mixing, melting, homogenizing, shaping and cooling [222]. This method of sheet formation exhibits instabilities such as brittle fracture and draw resonances during sheet drawing. However, it is used

effectively in the manufacturing of thicker polymer sheets or films such as the multi-layer films used for meat packaging.

2.5.1.2 CALENDERING

Calendering involves the squeezing of polymer melt between pairs of co-rotating high precision rollers to produce films or sheets [31]. A typical calendering unit is composed of the plasticating unit, calendering unit, cooling unit, accumulator and wind-up station. The material to be processed is melted and mixed in the plasticating unit using an internal batch mixer or a roll-mill. The mixed material is then fed between the nip of the first pair of rollers through to the second pair of rollers. The sheet produced is then passed through a second calendering operation for embossing. The embossed sheet is then cooled by passing it through chilling rollers. When cooling is achieved, the film or sheet is wound up onto a roll. A typical calendering unit has four rollers; the first pair controls the feed rate while the others calibrate the sheet thickness and the surface finish [118; 223].

Calendering has the advantage of lower requirements for material stabilization compared to extrusion processes as a result of the shorter residence time. Also, this process is excellent for polymers that are heat sensitive, as it limits the chances of thermal degradation. It requires low temperatures for processing as it uses high pressures to work the material. Calendering requires precision in the dimension of the rollers in order to be able to produce a quality sheet with a uniform thickness distribution, with a tolerance as low as ± 0.005 mm [118; 223].

2.5.1.3 SOLUTION CASTING

In solution casting the polymer is dissolved in a solvent. pH adjustments or emulsifiers may be added if required to enhance film formation and/or properties. The mixture is heated above the emulsifier's melting point and then homogenized. The mixture is degassed to reduce bubble formation in the final product. The formulation is evenly spread on a non-stick surface to allow evaporation of the solvent. Solvent evaporation can also be accelerated by providing heated air at low humidity and high velocity [130; 224; 225]. This process has cost-related problems as it is very expensive to run and requires large drying spaces, making it unsuitable for industrial scale-up.

2.5.2 Films manufactured from proteins

Biodegradable films or sheets from natural sources such as protein, starch, cellulose, beeswax and fatty acids [226] are shown in Table 1. Bio-based films or sheets are classified based on their sources.

Table 1: Proteins used for biodegradable sheets/films and their sources

Protein type	Source	Reference
Collagen`	Animal	[169], [170; 180]
Gelatin	Animal	[169; 170; 180]
Fish myofibrillar	Marine	[180]
Keratin	Animal	[180; 181]
Egg white	Animal	[180]
Casein	Animal	[180]
Chitosan	Marine	[169; 180]
Whey	Animal	[169; 170; 180]
Corn zein	Plant	[169; 170; 180; 182; 183]
Sorghum kafirin	Plant	[180; 183]
Wheat gluten	Plant	[169; 170; 180; 183; 184]
Rice Bran	Plant	[180]
Soy	Plant	[169; 170; 180; 183]
Peanut	Plant	[170; 178; 180]
Cottonseed	Plant	[180]
Sunflower	Plant	[169; 170; 180]

Protein sheet formation requires the denaturation of the protein molecules using heat, acid, alkali and/or solvent, to form more extended structures. The sheet formed consists of interactions between protein chains, which produce the cohesive structure of the sheet. These interactions are determined by the degree of chain extension and the sequence of the amino acid residues [227].

Film or sheet formation of protein-based material requires the addition of low molecular weight hydrophilic plasticizers such as triethylene glycol, glycerol, polyethylene glycol, propylene glycol, sorbitol, ethylene glycol, polyol or water to

reduce brittleness and increase flexibility through the reduction of protein-protein interactions and lowering the T_g of the protein material [187]. Also, the addition of a surface-active (emulsifying) agent is required to aid film formation through the absorption of water and reduction of surface tension. The surface-active agent is mostly used for solution processing to provide adequate surface wetting and spreading. However, some proteins are sufficiently surface-active and do not require surface-active agents during processing. Antioxidants and antimicrobials may be added to enhance the sheet effectiveness. During film or sheet formation, proteins' secondary, tertiary and quaternary structures can be modified by various physical and chemical agents such as heat, mechanical treatment, pressure, irradiation, acids, alkalis, and lipid interfaces to optimize protein configuration, protein interactions and sheet properties.

Protein-based sheets and films can be used as covers, wraps, sachets, pouches, separation layers, disposable packaging material, trash bags, water soluble bags for fertilizer and pesticides, agricultural mulches, laminating coating, and loose-fill packaging [16; 216; 226].

Protein-based sheets/films, like other natural based sheets/films, still have some drawbacks that limit their general acceptance and wider use in large-scale industrial applications, such as difficulty in processing and non-competitive mechanical properties. However, approaches are being developed and investigated to control these drawbacks, such as blending with other polymers to produce sheets with improved properties.

2.5.3 Properties of protein-based sheets/films

2.5.3.1 MECHANICAL PROPERTIES

When considering sheet materials, mechanical properties are of utmost importance because the produced sheets must have adequate mechanical strength to maintain their integrity during handling and storage. To mechanically characterize sheets, the properties usually measured are tensile strength (TS), elongation (E) and elastic modulus (EM) [130; 226; 228]. However, tensile strength and elongation are the most measured mechanical properties [229].

The mechanical properties of protein-based sheets depend on both their composition and environmental conditions. Plasticizers have a significant effect on protein sheets' mechanical properties as they increase the protein chain mobility [226]. An increase in plasticizer content results in a decrease in tensile strength and elastic modulus while elongation increases [85; 230-232]. Control of the tensile strength of protein sheets through the reduction of plasticizer content results in a decrease in elongation values to below those of most synthetic polymers such as PE and PP sheets. Proteins are hydrophilic and thus absorb moisture more readily at higher humidity; this characteristic increases the plasticizing effect of water in produced sheets, which results in a decrease in tensile strength and increased elongation.

2.5.3.2 MICROSTRUCTURAL PROPERTIES

The microstructural properties of polymer sheets are closely related to their mechanical and barrier properties. Sheet formation processes greatly influence the microstructure of the sheets produced. The presence of large pores within a structure will result in increased water vapour permeability [233], and the presence of structural defects such as pinholes and cracks affect the barrier properties [234]. A smooth and uniform microstructure indicates homogeneity in the produced sheets and also suggests a more glassy and brittle material [226]. The microstructure of sheets is usually investigated using scanning electron microscopy (SEM).

2.5.3.3 SOLUBILITY

The solubility of a film or sheet material is an important property, which is very relevant to its intended use. A water-soluble film or sheet is desirable in some applications, such as vegetable pouches, where a water-soluble product is required, while insoluble film or sheet is required in some applications where resistance to water and improved product wholeness is desirable. The solubility of a protein sheet or film varies with the protein type, film formation conditions, and treatment used to process the sheet. Protein solubility increases with an increase in its level of hydrolysis because of the reduction in protein molecular weight, which results in an increase in polar groups.

2.5.4 Enhancement methods

In recent years attempts have been made to enhance protein sheet/film properties, including barrier properties, mechanical strength and solubility. Most approaches have involved the modification of protein structure and/or interactions of protein molecules [226]. Other approaches are the use of other polymeric materials to create blended or polymer composite sheets/films [130; 230; 235]. These can be added during pre-treatment, where the changes are achieved during the sheet forming process, or post-treatment, where other polymers are applied to the produced sheet/film [31].

2.5.4.1 PLASTICIZERS

Plasticizer types and amounts affect the interactions between protein molecules and thus strongly influence the properties of the sheet produced. The effect of plasticizers in proteins results from the ability of the plasticizer molecules to position themselves within a protein's three-dimensional network, increasing the free volume and facilitating protein chain mobility. Some plasticizers allow the achievement of desired mechanical properties with reduced effects on barrier properties. The problem of increases in the diffusion rate of water and gas vapour, as well as migration of plasticizer through the sheet caused by the use of low molecular weight hydrophilic plasticizers such as glycerol, can be addressed by replacing them with plasticizers with hydrophobic substituents [236; 237]. Amphiphilic substances such as palmitic acids, waxes, oils, oleic acid, and stearic acid have been effectively used as plasticizers to reduce water vapour permeability (WVP). The optimal selection of plasticizer can also improve the already excellent oxygen barrier properties of protein sheets.

2.5.4.2 PROTEIN STRUCTURE AND INTERACTION MODIFICATION

Another alternative for improving protein sheets or films is the modification of protein structure and interaction through crosslinking. Crosslinking of protein polypeptide chains is possible because of the reactive side groups present in proteins. Crosslinking of polypeptide chains can be achieved through chemical, enzymatic or physical treatment; for example, the addition of crosslinking agents [229; 238-242], the use of electromagnetic radiation [243-247], heat treatment of

film solutions [248-251], film drying and curing conditions [252-254] and enzymatic crosslinking [255-259].

Material structure and interactions modified using these treatment methods have produced materials with significant reductions in water vapour and oxygen permeability [130]. However, the reduction was not significant enough to produce a sheet that provided a good moisture barrier, although the reduction in oxygen permeability improved the oxygen barrier properties of protein sheets. Changes in protein structure and interaction have greater effects on mechanical properties and material solubility.

Bigi et al. investigated the mechanical and thermal properties of gelatin films with different degrees of glutaraldehyde (GTA) crosslinking [260]. They reported that at $\text{GTA} \geq 1 \text{ wt.}\%$, crosslinking of about 60% and possibly near 100% was obtained, with a decrease in film deformation and an increase in strain at break and Young's modulus. At 0.25% GTA, 85% crosslinking was obtained and gelatin release was prevented in buffer solution, with a significant reduction in swelling in physiological solution. Also, the use of low concentration of GTA allowed the modulation of the physicochemical properties of gelatin films, producing a stable material.

2.5.4.3 BLENDS

Blending is a widely used method in the enhancement of the barrier properties of protein sheets/films. The most commonly approach is the addition of hydrophobic compounds such as lipids, waxes or hydrophobic polymers to improve moisture barrier properties [130; 261-264].

Laminating proteins with a layer of lipid or wax to achieve a bilayer film has proven to produce films with better moisture barrier properties [130]. However, the reduction in water vapour permeability achieved by blending proteins with lipids or waxes is still not comparable to the water vapour permeability of pure lipids, pure waxes and synthetic polymers such as PE. Laminating biodegradable films between synthetic films produces multilayer films with good structural integrity and improved properties [31]. Gonzalez et al. [211] investigated bilayer blends of soy protein isolate and PLA. An increase in transparency and strong interfacial adhesion

between layered phases increased mechanical properties and produced significant decreases in water permeability, total soluble matter, and swelling index [211].

Monedero et al. [265] studied the effect of an oleic acid/beeswax mixture on the properties of soy protein isolate-based films. Oleic acid and oleic acid/beeswax had a plasticizing effect on the produced film. Reduced water vapour permeability was also reported [265]. Abugoch et al. [84] investigated blends of quinoa protein extract (PE) and chitosan (CH) edible films. They reported the blend yielded mechanically resistant films without the use of a plasticizer, showing good elongation. However, the water barrier properties were decreased compared to pure CH films. Also, the authors reported strong interfacial adhesion in the blended phase, forming a new material with enhanced mechanical properties [84]. Tian et al. [266] investigated the flexibility and water resistance of soy protein isolate blended with waterborne polyurethane (WPU). They reported good compatibility as a result of strong hydrogen bond interactions between both blended materials, significant improvement in film flexibility and water resistance, as well as enhanced mechanical properties of the film in water [266].

Blending with other polymers having good mechanical properties is an approach used to obtain biomaterials with improved mechanical properties for practical applications such as films and tissue engineering scaffolds. The use of compatible polysaccharides and proteins has proved effective, although their effect on water vapour permeability is insignificant [31; 130; 267; 268].

Xiong et al. investigated the blends of soluble eggshell membrane protein (SEP) and PLA films; the blended film was reported to have improved mechanical properties compared to pure SEP films and improved biocompatibility compared to pure PLA films [269]. Blends of chitosan and gelatine based films were investigated by Arvanitoyannis et al., and an increase in gas permeability of the blended films was reported [156]. Zhong et al. blended soy protein isolate (SPI) with polycaprolactone (PCL) and methylene diphenyl diisocyanate (MDI), and reported a significant increase in mechanical strength and water barrier properties in the blends [208]. Rhim et al. coated soy protein isolate film with polylactic acid, and reported an increase in tensile strength and water barrier properties as a result of the hydrophobic nature of PLA [270].

Natural fibres from sources such as grass and hemp have been used as reinforcement in polymeric films because of their excellent thermal, mechanical and sonic insulation properties as well as their low density, low cost, sustainability, environmental friendliness and biodegradable nature [271; 272]. Also, nanocomposites such as nano-clay, cellulose nano-whiskers, ultra-fine titanium dioxide, and carbon nano-tubes have emerged as new composite materials for the reinforcement of polymeric films [31].

2.5.5 Factors influencing sheet formability of polymer blend

Many factors can influence the sheet formability of polymer and polymer blends. However, the most important is rheological behaviour because this measures the ability of a material to flow.

2.5.5.1 POLYMER RHEOLOGY

Polymer rheology is the study of the flow/deformation behaviour of a polymer during flow-induced deformation and how it is affected by stress, strain and time [273]. Viscosity is the most important flow property [273], and it is a widely used material parameter when determining the flow behaviour of polymer during processing as it predicts the internal resistance of the melt to an externally applied stress [118]. It is important to understand the flow behaviour of any polymeric material and how its viscosity changes with temperature and processing rate for effective processing and design (machine, mould and die) [274; 275] as well as to ensure the production of a product with good mechanical performance. Viscosity can be defined, as shown in Equation (6), as the ratio of imposed shear stress τ (force F / area A) and the shear rate γ (velocity v / distance h).

$$\eta = \frac{\textit{shear stress}}{\textit{shear rate}} = \frac{\tau}{\gamma} \quad (6)$$

Basic rheological theories assume that a liquid structure is either stable (Newtonian behaviour) or it has a well-defined change (Non-Newtonian behaviour) [118]. Most polymers behave differently when subjected to different levels of stress. A material that displays constant viscosity (η) when exposed to any shear rate (γ) is known as

a Newtonian fluid while non-Newtonian fluids are those with viscosities (η) that vary according to the rate of shear (γ) applied. As the shear rate applied is varied, the viscosity of dilatant (or shear thickening) fluids, Newtonian fluids and pseudoplastic fluids (power fluids, also known as shear thinning fluids) behave differently, as shown in Figure 20.

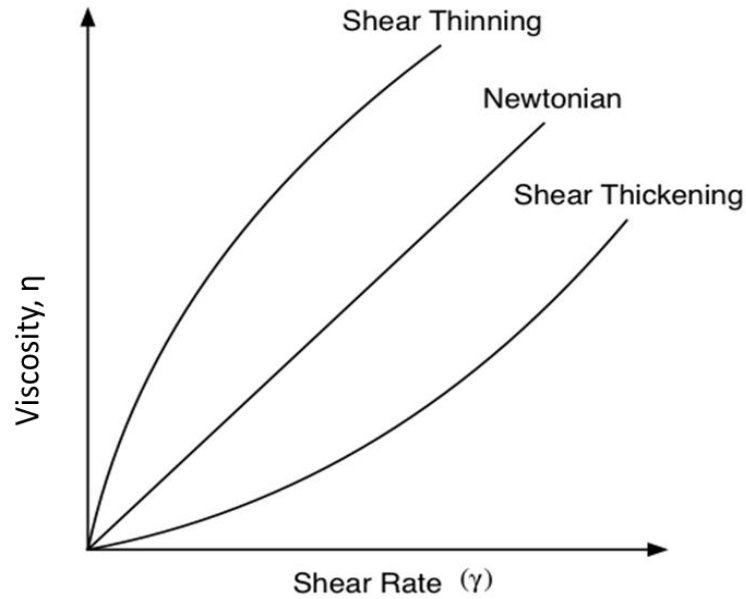


Figure 20: Viscosity behaviour of different fluids as the applied shear rate varies.

A dilatant fluid is a shear thickening fluid and as the shear rate increases, it shows an increase in viscosity. In contrast, a pseudoplastic fluid is a shear thinning fluid, which exhibits decreased viscosity as the shear rate increases. Newtonian fluids show a linear relationship to the shear rate. The viscosity of a Newtonian fluid is defined in Equation (7), where η is the proportionality between shear stress and shear rate.

$$\tau = \gamma\eta \quad (7)$$

Polymer melts are shear thinning [273]. Protein polymers such as whey, soybean, sunflower, oat, and gluten-based plastics have shown shear thinning [276-278].

The most commonly used equipment for the measurement of polymer melt is the capillary viscometer, in which the pressure applied by the piston determines the shear stress while the flow rate determines the shear rate. The shear stress and shear rate in a capillary viscometer are calculated using Equations (8) and (9) below,

$$\tau = \frac{\Delta PR}{2L} \text{ (N/m)}^2 \text{ Shear stress} \quad (8)$$

where ΔP (Pa) is the pressure drop across the capillary tube, and it is calculated as $\Delta P = P_2 - P_1$ (exit pressure corresponds to atmospheric pressure), L is the length of the capillary, and R is the radius of the capillary,

$$\gamma = \frac{4Q}{\pi R^3} \text{ (S}^{-1}\text{)} \text{ Shear rate} \quad (9)$$

And where Q ($\text{mm}^3 \cdot \text{sec}^{-1}$) is volumetric flow rate.

The Bagley correction corresponding to the adjustment for excess pressure at the die entrance can be calculated using the equation below.

$$\tau_{\omega} = \frac{\Delta P - \Delta P_e}{2L/R} \quad (10)$$

Where ΔP is the pressure in capillary P_2 and ΔP_e is the pressure at the orifice.

The Rabinowitsch-Weissenberg correction is used to account for the influence of shear thinning in the calculation of shear rate and corresponding viscosity. As shown in equation 11.

$$\gamma_{\omega} = \frac{(3n+1)}{4n} \gamma_{\alpha} \quad (11)$$

The apparent shear rate of a Non-Newtonian fluid (shear thinning behaviour) can be expressed by the power law model in terms of shear rate as in Equation (12),

$$\eta = m\dot{\gamma}^{n-1} \quad (12)$$

where m is the flow consistency index, $\dot{\gamma}$ is the shear rate, η is the viscosity, and n is the power law index. If $n = 1$ constant viscosity is obtained (Newtonian model) and the smaller the n value, the more shear thinning the polymer exhibits (i.e. $n < 1$, for non-Newtonian fluids) [273; 275].

Good understanding of the elongational flow properties of polymer melts is an essential and important aspect of material rheology in the processing of polymers as most difficulties encountered during the processing of polymer melts are associated with their elongational flow properties [279]. Elongational viscosity is the polymer melt's resistance to extension [273]. Elongational viscosity is a function of stretch rate ($\dot{\epsilon}$) while shear viscosity is a function of shear rate ($\dot{\gamma}$). Elongational viscosity has an advantage over shear viscosity, as measurement of elongational viscosity does not involve interference with the walls of the equipment. However, measurement of elongational viscosity is more difficult than the measurement of shear viscosity, making its use very rare in the measurement of elongational properties [280]. Slight changes in molecular structure as a result of factors such as branching and the presence of high molecular weight tails in the chain distribution of a polymer material are readily detected in the processing performance of the material. These changes are not detected by shear flow properties. However, elongational flow properties can easily detect these changes in molecular structure. Therefore, for a better understanding of a material's

suitability for sheet processing, it is important to understand its elongational viscosity.

Extrusion processes, film drawing, and blow filming involve elongation/extension. Materials with high elongational viscosity exhibit more stability during film or sheet processing [273]. The flow of a polymer melt from the extruder barrel (large reservoir) into a smaller diameter capillary encounters excess pressure due to elongational viscosity. The elongational viscosity η_e from excess pressure drop ΔP can be measured using the Cogswell method as shown Equation (13) below.

$$\eta^e = \frac{(n+1)^2(\Delta Pe)^2}{32n\gamma^2} \quad (13)$$

Elongational stress can be measured using Equation (14)

$$\gamma^e = \frac{3}{8} (n + 1)pe \quad (14)$$

2.5.5.2 RHEOLOGY OF POLYMER BLENDS

The rheological behaviour of polymer blends differs from that of simple liquids because of the viscoelastic nature of polymers and their blends. The determination of flow behaviour of multiphase materials such as polymer blends should be conducted at constant stress and a constant deformation rate because such materials exhibit a large shear dependence. Multiphase materials rarely exhibit Newtonian or non-Newtonian behaviour as the sheared layer orientation may account for either dilatant or pseudoplastic behaviour and strong inter-particle interaction may lead to yield stress or transient behaviour [117].

Polymer blends are considered to be dispersions of deformable, liquid-like particles. Their rheological behaviour is governed by the state of dispersion, shape, and orientation of the dispersed phase as well as particle-particle interactions [281]. The rheological behaviour of amorphous and semi-crystalline polymer blends will reflect features of either deformable (liquid-like) or rigid (solid-like) dispersion [15],

because of the unclarified distinction between deformable and rigid dispersion; the crystallization of the dispersed semi-crystalline phase inflow will change the dispersed phase from fluid to solid.

Van Oene [281] studied the mode of dispersion of a co-extruded finely divided mixture of two incompatible polymers. Two type of dispersion were reported; ribbon and droplet type dispersion. Van Oene suggested that the mode of dispersion observed is independent of the magnitude of the shear stress and temperature applied.

There are two levels of study of the rheology of dispersions: the macro-rheological level and the micro-rheological level. Macro-rheological examinations involve measurement of the rheological properties of the dispersion itself, such as the viscosity and stresses applied, while micro-rheological assessment focuses on the motion of the individual particles themselves. However, it is believed that macro-rheological properties can be predicted from the observed micro-rheological behaviour.

Chapter 3

Preparation and Properties of Decoloured Blood-meal/ Poly(lactic) Acid Blends modified with Itaconic Anhydride

Preparation and Properties of Decoloured Blood-meal/Poly (lactic) Acid Blends modified with Itaconic Anhydride

3.1 Abstract

Blends of semi-crystalline poly(lactic) acid (PLA), and decoloured blood-meal thermoplastic (DBT) were prepared using reactive extrusion to produce a bio-based polymer. The blend had improved mechanical properties compared to neat DBT. Free radical grafting was used to graft itaconic anhydride onto PLA to create reactive side groups. Varying formulations of DBT and different ratios of DBT to PLA blends with and without compatibilizer were prepared. The compatibility between the material blends was investigated by mechanical testing, scanning electron microscopy (SEM), differential scanning calorimetry (DSC), dynamic mechanical analysis (DMA) and wide-angle X-ray scattering (WAXS). Blending DBT with PLA increased the tensile strength and modulus of DBT, whereas the strain at break decreased. The glass transition temperature increased when compared to neat DBT. Scanning electron microscopy revealed enhanced interfacial adhesion between the two phases in the blends with PLA-g-IA evident from the more homogenous microstructure obtained. WAXS revealed an insignificant decrease in the crystallinity of the blends compared to neat DBT, indicating that blending with PLA caused no structural effects in DBT. The results presented in this study show the feasibility of improving the properties of DBT with PLA-g-IA for use in agricultural and packaging applications.

3.2 Introduction

Bio-polymers have been considered an attractive alternative to petroleum-based polymers because they are abundant, inexpensive, biodegradable, renewable and environmentally friendly. Bio-polymers such as protein, starch, cellulose, PLA and gluten are very attractive as replacements due to their availability and properties [83; 282; 283]. PLA's unique properties, such as glossy optical appearance, biodegradability, composability, high tensile strength and excellent barrier properties with regard to carbon dioxide, oxygen and water [142; 197; 284] have encouraged substantial growth in its application. PLA is a biodegradable thermoplastic polyester synthesized from lactic acid, which is derived from cornstarch and sugar beets, with several applications in biomedical and pharmaceutical fields as a material used in surgical operations, tissue regeneration, and drug delivery systems [285; 286]. PLA is also considered suitable for high-volume packaging applications [284; 287] because of its excellent barrier properties to aromas and permeability to carbon dioxide, oxygen, and water. However, PLA is expensive and has low heat deflection temperature, which remain limitations to its wider application. This has led to PLA often being blended with other polymers to reduce cost and improve blend properties [191; 194; 284; 288].

Decoloured blood-meal thermoplastic (DBT) is a newly developed bio-polymer using bloodmeal as a starting material [289; 290]. Blood-meal is one of the animal sources of protein, containing 90 to 95% dry weight of protein [10; 11; 291] and it is a by-product of animal slaughterhouses. Bloodmeal can potentially be used as an alternative resource for bioplastics in agricultural and horticultural applications such as weasand clips, weed mat and pegs, and biodegradable plant pots [292-294]. There are some limitations to the wider application of bloodmeal-based polymers due to their offensive odour and colour. However, the colour and odour were successfully eliminated by pre-treatment with peracetic acid (PAA) [11], resulting in a bio-feedstock referred to as decoloured blood-meal (DBM). Decoloured blood-meal has been processed into a thermoplastic protein known as decoloured blood-meal thermoplastic (DBT), using triethylene glycol (TEG), water and sodium dodecyl sulphate (SDS) [12]. However, its properties are relatively poor compared to other polymers used in sheet production [289]. DBT consists of complex molecules with strong intra- and inter-molecular interactions. These strong interactions make melt processing of DBT very difficult unless an adequate amount

of plasticizer is added to promote mobility and flexibility of the protein chains, enabling flow and consolidation during processing. Low molecular weight polyols such as glycerol, propylene glycol, ethylene glycol and their derivatives [16; 222; 289; 291; 295] are used as plasticizers for proteins to reduce intermolecular interactions and glass transition temperatures (T_g). However, the amount of plasticizer used affects the material's mechanical properties and leads to phase separation [194; 197].

Previous research has shown that DBT can be successfully processed using extrusion and injection moulding [184]. However, like every other protein polymer, moisture evaporates during processing, leading to highly brittle material and loss of functionality. Studies have concentrated on improvement of the properties of protein-based polymers through association with other hydrophobic thermoplastics with desirable properties, to increase processibility and moisture resistance [185; 194; 197; 201; 296; 297]. Association with other polymers can be achieved through blending, coating or lamination. Blending is the most effective and easiest way of modifying polymer properties. Therefore, DBT was blended with PLA. Most polyesters are immiscible with proteins because of their different polarities [79; 190; 197; 297], resulting in weak interfacial adhesion and poor material properties [298]. However, this can be addressed by using compatibilizers to create reactive functional groups capable of reacting with both polymer phases, resulting in improved properties [185; 190; 194; 197; 296]. Interfacial modification plays an important role in manipulating solid-state adhesion between the components of two incompatible materials [284], making compatibilization of DBT and PLA essential.

Compatibilizers such as poly-2-ethyl-2-oxazoline (PEOX) [9, 19], polymeric methylene diphenyl diisocyanate (pMDI) [5, 20], methylene diphenyl diisocyanate (MDI) [23, 24], interfacial modification of PLA by grafting a reactive moiety such as maleic anhydride [190; 200; 284; 294; 299-301], and itaconic anhydride [142; 293] have been used to enhance the interfacial interaction between PLA and other polymers. Research on compatibilized blends of protein thermoplastics and polybutylene succinate reported an improvement in water resistance and tensile strength [5]. Using maleic anhydride (MA) grafted on low-density polyethylene (LLDPE), an improvement was observed in the compatibility of Novatein® thermoplastic protein (NTP) and LLDPE, as well as improved tensile strength and

reduced water absorption [20]. Itaconic anhydride (IA) is a highly reactive monomer in free radical grafting, as it can produce tertiary radicals [27]. Although IA has not been extensively studied, it has been used as a renewable monomer for synthesizing bio-based copolymers through conventional copolymerization [28], and can be used for acetylating lysine, tyrosine, and cysteine [29]. IA is extremely stable when reacted with proteins, compared to MA.

In this study, blends of DBT and PLA compatibilized with itaconic anhydride were investigated. DBT refers to either decoloured blood-meal powder (DBTP) or decoloured blood-meal granules (DBTG). The main objective of this chapter was to demonstrate that DBT can be blended with PLA, as other proteins and starch have already been blended with PLA. This investigation also aimed to find the best processing conditions, formulation of DBT and blend composition. The morphology and the thermal, mechanical and structural properties of DBT/PLA blends were investigated.

3.3 Materials and Methods

3.3.1 Materials

Blood-meal (BM) was obtained from Wallace Corporation Limited, New Zealand and used as received. One batch of blood-meal was used for this chapter and for the majority of the thesis studies. The purchased bloodmeal was stored under appropriate conditions (in an airtight container at room temperature). Therefore, it was reasonable to assume that there were no significant variations in properties. Analytical grade itaconic anhydride (IA), dicumyl peroxide (DCP), acetone, 50 wt.% hydrogen peroxide, and technical grade sodium dodecyl sulphate (SDS) and triethylene glycol (TEG) were purchased from Sigma Aldrich NSW, Australia. Peracetic acid (Peraclean 5) was purchased from Evonik Industries, Morrinsville, New Zealand. Poly (lactic acid) (PLA) grade 3052D was purchased from NatureWorks LLC, Minnetonka, MN (supplied locally by Clariant NZ Ltd, Auckland) in pellet form.

3.3.2 Sample preparation

3.3.2.1 ITACONIC ANHYDRIDE GRAFTING ON PLA

Itaconic anhydride was grafted onto PLA using free radical grafting to create reactive side groups as described by Marsilla and Verbeek [142]. PLA was dried at 80 °C for 4 h to control moisture. 4.2 g itaconic anhydride and 0.8 g dicumyl peroxide were dissolved in 30 mL acetone. The solution was poured over the oven dried PLA and the mix was kept in the fume-hood for about 2 h. The solution was decanted before oven drying the PLA for 3 h at 50 °C. The material was extruded using a LabTech twin screw co-rotating extruder with a screw diameter of 20 mm and L/D of 44:1, a temperature profile of 145 (feed zone), 145, 165, 165, 180, 180, 180, 180, 160, 160, 155 °C (die zone). Constant screw speed was maintained at 150 rpm. A vacuum pump was attached on the 7th heating zone of the extruder to remove vapour generated during extrusion. To avoid the crystallization of the extruded PLA-g-IA, it was collected in a water bath upon exiting the die and subsequently pelletized. The pelletized PLA-g-IA was oven dried for 12 h prior to blending with decoloured blood-meal protein (DBP) to minimize PLA hydrolysis during melt processing.

3.3.2.2 BLOOD-MEAL DECOLOURING

Blood-meal was decoloured using the standard method with a solution of peracetic acid (PAA) [11; 111]. A 4 wt.% PAA solution was prepared by diluting a 5 wt.% stock solution with distilled water with a constant percentage ratio of 80:20 respectively. 150 g blood-meal was decoloured by adding 450 g of 4 wt.% PAA in a high-speed mixer and mixing continuously for 5 mins to ensure homogenous decolouring of the blood-meal. Following this, 450 g of distilled water was added and the combination was mixed for another 5 mins to ensure complete dilution of the slurry. The slurry was neutralized by adjusting to pH7 with sodium hydroxide solution. The neutralized slurry was filtered using a wire mesh sieve (aperture size 60) and subsequently washed by adding another 450 g of distilled water. The decoloured blood-meal (DBM) produced was dried for approximately 15 h in a 70 °C oven.

3.3.2.3 DECOLOURED BLOODMEAL THERMOPLASTIC PREPARATION

Decoloured blood-meal thermoplastic powder (DBTP)

Decoloured blood-meal thermoplastic (DBTP) was formulated by dissolving SDS in water heated to 60 °C while stirring. The solution was added to decoloured blood-meal powder in a high-speed mixer and mixed for 5 min. TEG was added to the mixture and mixed for another 5 min to ensure a homogeneous mixture was obtained. The mixed material was stored in an airtight bag overnight at 2 °C in a fridge to equilibrate. Different formulations of DBT with a variety of additives were prepared as shown in Table 2.

Decoloured blood-meal thermoplastic granules (DBTG)

Following the same method used for DBTP preparation, the prepared formulation of DBTP was stored in an airtight bag overnight in a fridge at 2 °C to equilibrate. Then the equilibrated DBTP was compounded using a twin screw co-rotating extruder (LabTech). The extruder barrel had eleven heating zones, and the screw speed was maintained at 150 rpm. The compounding extrusion temperatures were 100 (feed zone), 100, 100, 100, 100, 100, 100, 100, 100, 115 and 120 °C (die zone). The extrudate was granulated using a tri-blade granulator from Castin Manufacturing Limited to produce decoloured bloodmeal granules (DBTG).

Table 2: DBT formulations and additive contents

Sample name	DBM (g)	Water (pph_D)	SDS (pph_D)	TEG (pph_D)
Formulation 1 (F1)	100	0	0	20
Formulation 2 (F2)	100	40	3	20
Formulation 3 (F3)	100	30	6	30
Formulation 4 (F4)	100	40	6	30
DBM	100	0	0	0

pph_D = parts per hundred grams decoloured blood-meal

3.3.2.4 BLEND PREPARATION

Two blend approaches were used, as shown in Figure 21, to determine the best starting DBT material for blending with PLA based on processability. The first approach involved blending decoloured blood-meal

thermoplastic granules (DBTG) with PLA while the second blended decoloured blood-meal thermoplastic powder (DBTP) with PLA. DBTP is a homogenized mixture of decoloured blood-meal powder and additives while DBTG is compounded and granulated decoloured blood-meal and additives. Different formulations of DBT (DBTP or DBTG) and different blend ratios, with and without compatibilizer were prepared. The prepared blends were compounded using a twin screw co-rotating extruder (LabTech). The extruder screw speed was maintained at 150 rpm. The extruder has 11 heating zones, which includes one melting zone and three mixing zones. The extrusion temperature increased along the barrel, from 100 °C (feed zone) to 140 °C (die zone). The extrusion temperature was decreased by 10 °C along the barrel for blends with higher DBT content (Table 3). The extrudate produced was granulated using a tri-blade granulator from Castin Manufacturing Limited.

When either DBTP or DBTG is compounded with PLA and/or PLA-g-IA, it is referred to as a DBT/PLA blend (i.e., decoloured blood-meal thermoplastic/poly(lactic) acid blend).

Table 3: Blend composition

Sample Name	Formulations (Table 2)	Blending Composition		
		DBT (pph)	PLA (pph)	PLA-g-IA (pph)
DP37	4	30	70	0
DgP37	4	30	0	70
DP55	4	50	50	0
DgP55	4	50	0	50
DP73	4	70	30	0
DgP73	4	70	0	30
DP91	4	90	10	0
DgP91	4	90	0	10
F1P	1	50	50	0
F1gP	1	50	0	50
F2P	2	50	50	0
F2gP	2	50	0	50
F3P	3	50	50	0
F3gP	3	50	0	50
F4P	4	50	50	0
F4gP	4	50	0	50
DBMP	DBM	50	50	0
DBMgP	DBM	50	0	50

pph = parts per hundred-gram sample

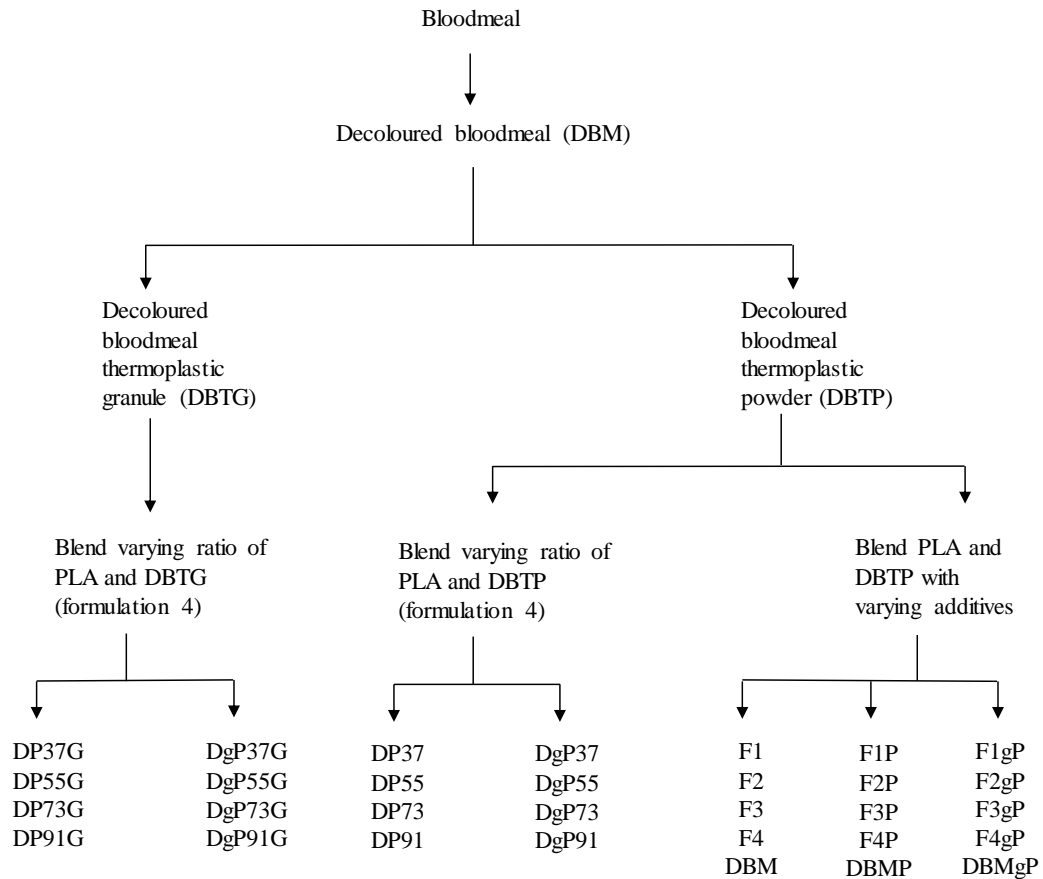


Figure 21: Flowchart of the experimental plan showing different blend approach, varying blend ratio and content (Table 3).

3.3.2.5 TEST SPECIMEN PREPARATION

ASTM D638-14 standard tensile test samples [302] and ISO 179-1:2010 impact test samples [303] of the blends were injection moulded using a BOY 35A injection moulding machine. The samples were injected through a cold runner into a 60 °C water-heated mould. The injection moulder has five heating zones including the feed and the die zone. The temperature profile used is shown in Table 4. The selected temperatures for injection moulding of the DBT/PLA blends were based on an initial temperature trial run to determine the best processing temperature window for each blend ratio (result not included). The screw speed was constant at 150 rpm. The sample specimens produced were also used for mechanical, thermal and morphological testing.

Table 4: Injection moulding temperatures determined during trial runs.

Sample name	Heating Zones (°C)				
	Feed				Die
DBT	100	100	120	120	120
PLA	150	175	175	175	180
Blends DP37, DP55	100	130	140	140	140
Blends DP72, DP91	100	120	120	120	120

Note: similar temperature was used for DgP having corresponding DP contents.

3.3.3 Sample testing

All samples were conditioned for 7 days at 23°C and 50% relative humidity in a Binder humidity chamber before testing, except where otherwise stated.

3.3.3.1 MECHANICAL PROPERTIES

The mechanical testing was performed according to ASTM D638 using an Instron Universal Testing machine (model 33R4204) at a crosshead speed of 5 mm/min and an extensometer gauge length of 50 mm. A total of 5 repeats were conducted for each sample type to obtain an average value.

Charpy edgewise impact strength was performed according to ISO 179-1:2010 standard using a RAY-RAN Pendulum Impact System. The pendulum impact system has an impact energy of 4 J, a hammer weight of 0.95kg and a hammer speed of 2.9 m/s. Bars tested were notched according to standard. Five bars were tested to obtain the average impact strength of the material.

3.3.3.2 THERMAL ANALYSIS

Dynamic mechanical analysis (DMA) was conducted using a Perkin Elmer DMA 8000 fitted with a high-temperature furnace and cooled with liquid nitrogen. Rectangular samples (30 x 9 x 4 mm) were cut from injection moulded samples and tested in a single cantilever fixture using a free length of 12.5 mm and scanning temperatures ranging from -80 to 150°C at 2°C/min. Data were collected at multiple oscillation frequencies (0.1 – 30 Hz). Tan δ peak values were recorded as glass transition temperatures.

Differential scanning calorimetry (DSC) was conducted using a Perkin Elmer DSC 8500. About 5 mg of sample was crimp sealed in a 30 μ L DSC aluminum pan. All

samples were heated from 25 to 200°C at 10°C/min and kept isothermal for 5 min before cooling to 25°C at 10°C/min. The data collected were analyzed using Pyris software version 11.1.1.0492. The reported values are averages of three replicates.

3.3.3.3 WIDE ANGLE X-RAY SCATTERING MEASUREMENT (WAXS)

WAXS was used to measure the x-ray diffraction patterns of the blends. WAXS was performed with a PANalytical Empyrean X-ray diffractometer operating at 45 Kv and 40 mA using CuK α radiation. The diffraction data were collected from 2 θ values of 4° to 40° with a step size of 0.013°. A fixed 7.5 mm anti-scatter slit, fixed incidence beam mask of 10 mm and a Soller slit of 0.04 rad were used. The data collected were baseline corrected from 5 - 40° and amorphous haloes were fitted to this region to determine the crystallinity of the blends.

3.3.3.4 PHASE MORPHOLOGY

The phase structure of the blends was investigated using a Hitachi S-4700 field emission scanning electron microscope (SEM). The injection moulded specimens were cryo-fractured using liquid nitrogen. The specimens were sputter coated with platinum using a Hitachi E-1030 Ion sputter coater before scanning. For the digested surface, the samples were extracted with chloroform and then rinsed with hot water to remove the PLA phase, as DBP is not soluble in chloroform. The extracted surface was dried, and sputter coated prior to the examination. The SEM images presented in this chapter are representative of multiple images taken from different points across each sample piece.

3.4 Results and Discussion

3.4.1 Decoloured blood-meal thermoplastic processing

Plasticized decoloured blood-meal formulations (F2, F3, and F4) were within the acceptable processing window as defined by Verbeek et al. [184], having adequate tensile strength and strain at break.

Formulation 1 was not extrudable as it produced mostly compressed powder, which was evidence of poor consolidation. This was suggested by Low et al. [289] to be due to insufficient protein chain unfolding caused by the absence of SDS during heating, thus restricting consolidation (in other words, a low contact area between

protein chains resulting in few intermolecular interactions and limited entanglement). Mo et al. [203] also suggested that when protein chains unfold, the surface area available for new stabilizing interactions and entanglements increases. SDS is required to promote β -sheet transformation to α -helices and random coils. Therefore, in the absence of SDS, protein chains did not unfold sufficiently, resulting in fewer intermolecular interactions and limited entanglement leading to poor consolidation. No sample was produced for testing for formulation 1.

Formulations 2, 3 and 4 were easier to process and were easily reproducible. They were easy to pull out of the mould and most self-injected from the mould. They showed moderate injection time and barrel refill time. Looking at the visible clarity of the samples as shown in

Figure 22, the browning of injection moulded material has been reported [184] to be due to the action of water and TEG. However, insufficient SDS even in the presence of water and TEG can also result in sample browning. SDS is required to unfold the protein chain, which promotes the interaction between the plasticizer molecules (water & TEG) and the proteins. Browning is a result of lack of thermal stability due to insufficient or low plasticization; therefore, F4 with a higher plasticizer content (water) was better coloured than F2 and F3. The higher water content provided more thermal stability and prevented the browning reaction by diluting the protein and pigments, and also improved the processing.

A ductile material with high toughness is favourable for sheet processing. Formulation 4 had the highest impact strength and strain at break. Therefore, it was considered the best formulation for blending with PLA.

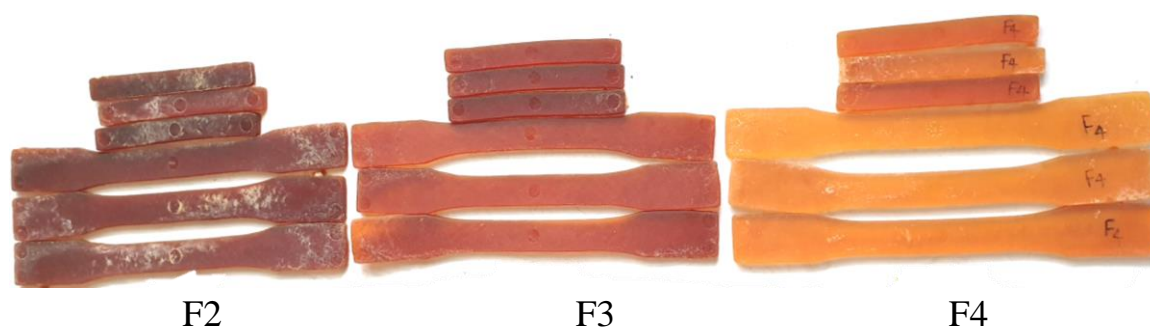


Figure 22: Injection moulded samples produced from the different DBT formulations

DBT FORMULATIONS

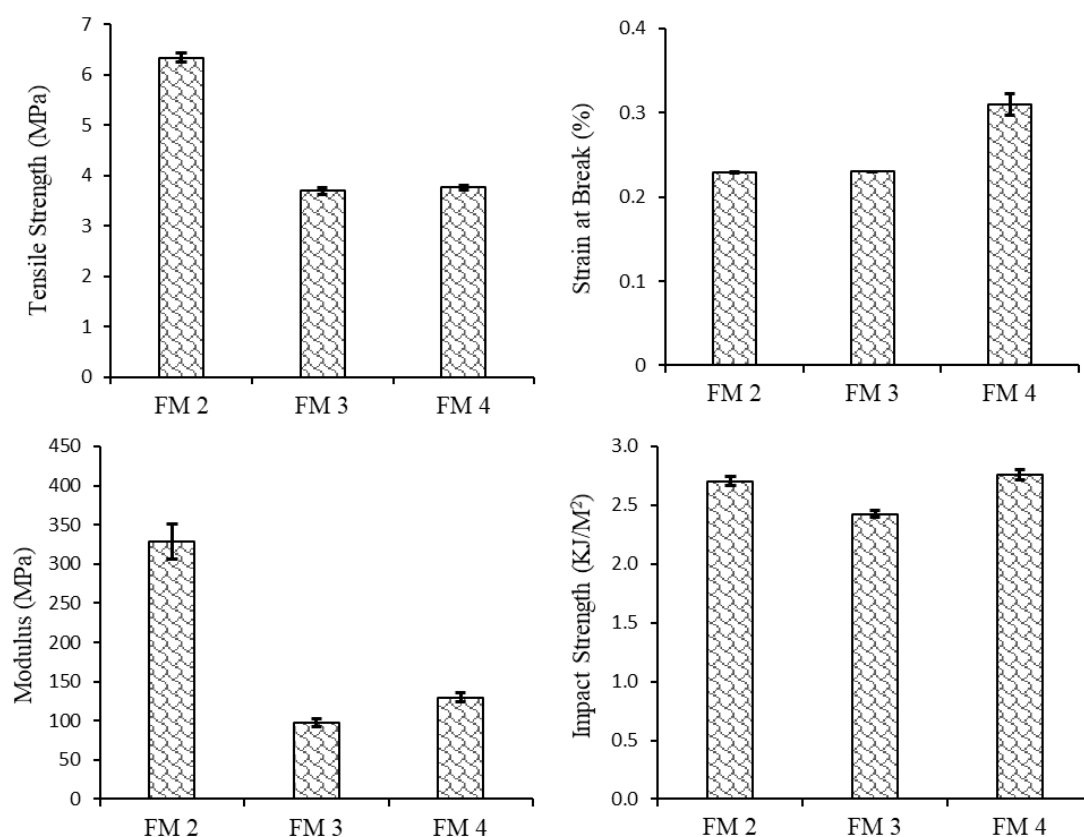


Figure 23: Mechanical properties of DBT formulations with different ratios of additives (Table 2).

3.4.2 Blending and processing

Two different blending methods (DBTG and DBTP), as shown in Figure 21, were used to determine the best approach for blending DBP/PLA. DBTP is a homogenized mixture of decoloured blood-meal powder and additives while DBTG is compounded and granulated decoloured blood-meal and additives.

3.4.2.1 EXTRUSION PROCESSING OF THE BLENDED MATERIAL

Extruding blends of DBTG or DBTP and PLA with and without compatibilizer produced consolidated extrudates with reasonably smooth surfaces, under moderate torque and pressure. The extrudates were flexible and rubbery prior to cooling. Small surface defects such as shark-skinning (Figure 24) were observed in the blends with a high ratio of DBT to PLA.

It can be seen that the higher the DBP content, the brighter the extrudate (see Figure 24). This supports the idea that a higher moisture or plasticizer content in the blend prevents browning of the extrudate during heat processing. However, this may affect the properties of the blend as PLA is best processed in the absence of moisture/water.

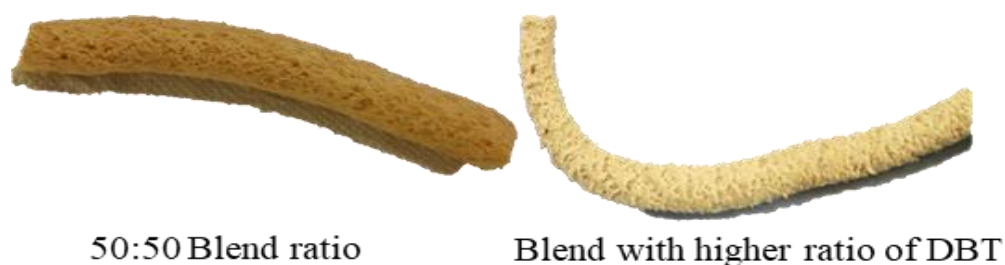


Figure 24: DBT/PLA blend extrudates produced using DBTP as a starting material.

3.4.2.2 INJECTION MOULDING OF THE BLENDED MATERIAL

Injection moulding of DBTG (granules) and PLA

DBTG/PLA blends could not be injection moulded due to excessive blockage of the injection moulder feed throat and protein degradation. Addition of Struktol processing aid did not affect blend processing as it became more difficult to feed through the barrel, resulting in feed throat blockage. This was considered to be an effect of the lack of plasticizer in the blends. It was probably a result of the loss of plasticizers through evaporation during extrusion. Similar behaviour has been reported by other researchers [184; 289] for DBM material with lower plasticizer levels, as a result of low initial water content in addition to some plasticizer evaporation during extrusion. In an attempt to reduce excessive heat treatment during processing, DBTP was blended with PLA instead. This meant that the protein was extruded once, together with PLA, compared to producing DBT prior to blending.

Injection moulding of DBTP and PLA blended

Injection moulding of DBTP and PLA blends worked well without a processing aid and produced flexible, consolidated samples using the optimal injection moulding temperature (Table 4). The injection moulding of blends produced three types of sample bar as shown in Table 5.

Table 5: Description of injection moulding of sampled blends

Injection type	Description
1	Did not self-eject out of the mould, longer injection time and barrel refill time, very difficult to pull out of the mould due to spur block
2	Did not self-eject out of the mould; reduced injection time and barrel refill time, easy to pull out of the mould unit and spur section.
3	Mostly self-ejected out of the mould and easy to remove from the mould unit manually; reduced injection time and barrel filling time.

Injection type 1 was observed mainly for blends with a high amount of DBTP (over 70%), while for blends with DBTP levels below 50%, injection types 2 and 3 were observed. Injection type 3 was observed only for the 50:50 blend. Based on the observations here, this approach was chosen as the optimal method for blending.

DBTG was discontinued due to the inability to injection mould it, and DBTP was adopted as the starting decoloured bloodmeal material for blends with PLA and for further investigations. Therefore, DBT/PLA refers to the compounded blend of DBTP and PLA or PLA-g-IA.

3.4.3 Blend composition ratio determination

Blend composition plays an important role in polymer blend systems as different material properties can be generated via varying blend compositions. Willemse et al. suggested that material composition has a strong influence on the tensile modulus of polymer blends [304]. Muller-Buschbaum et al. suggested that changes in the surface morphology of deuterated polystyrene (dPS) and poly(p-

methylstyrene) (PpMS) blend depended on the material blend composition [305]. Therefore, it is crucial to determine the best blend composition for DBT/PLA blending systems. Varying compositions of DBTP to PLA, as shown in Figure 21 were prepared for the assessment of optimal blend compositions.

3.4.3.1 PHASE MORPHOLOGY

The study of polymer blend morphology is important as it is related to the mechanical and barrier properties of the blend [222; 306] and it is essential in understanding the property–structure relationships of the material. Most polymer blends are immiscible and therefore produce a heterogeneous morphology [306]. Compatibilizers are used to reduce the interfacial tension in polymer blends, thereby stabilizing the morphology, and often resulting in a co-continuous structure [197]. Co-continuous morphology exhibits a combination of both polymer components' characteristics [307], and is formed mainly around the point of phase inversions such that the matrix is indistinguishable from the dispersed phase.

Figure 25 shows the cryo-fractured phase structure of DBT/PLA with and without compatibilizer and with blend compositions varying from 30:70 to 90:10 (w/w). A dispersed phase morphology was observed with blends without itaconic anhydride, showing one phase that was rich in DBT and another that was rich in PLA. Interstices were observed between the DBT phase and PLA matrix for the uncompatibilized blends, indicating poor interfacial adhesion. This was expected, as DBT contains 90% protein, which is highly polar and hydrophilic, while PLA is hydrophobic; this leads to poor interfacial interaction between the two phases. A blend of Novatein® and polybutylene succinate (PBS) without compatibilizer was reported to have poor interfacial adhesion [197].

As the DBT content increased, the size of the DBT-rich phase increased for blends without itaconic anhydride. This is attributed to the poor interfacial adhesion between DBT and PLA phases. However, the addition of itaconic anhydride (compatibilized) showed an improved and even dispersion of the DBT phase within the matrix. Although some interstices were still observed in the compatibilized sample, they were fewer and smaller compared to the uncompatibilized blends. The improved dispersion observed with blends compatibilized with itaconic anhydride is probably a result of the formation of branched and cross-linked macromolecules

initiated by the reaction of the anhydride group of PLA-g-IA with the amino groups of the DBT. The same phenomena have been reported for compatibilized PLA blends with protein and starch [190; 288]. It has also been reported that the addition of poly (2-ethyl-2-oxazoline) (PEOX) improved interfacial adhesions in SPC/PLA blends, resulting in a finer and more homogeneous phase structure [194].

Compatibilization showed no clear effect on the 30:70 blend ratio (Figure 25, b and b'); this is probably due to the overwhelming effect of high PLA content in the matrix. This was further explored through mechanical properties testing, thermal analysis and wide-angle X-ray scattering (WAXS).

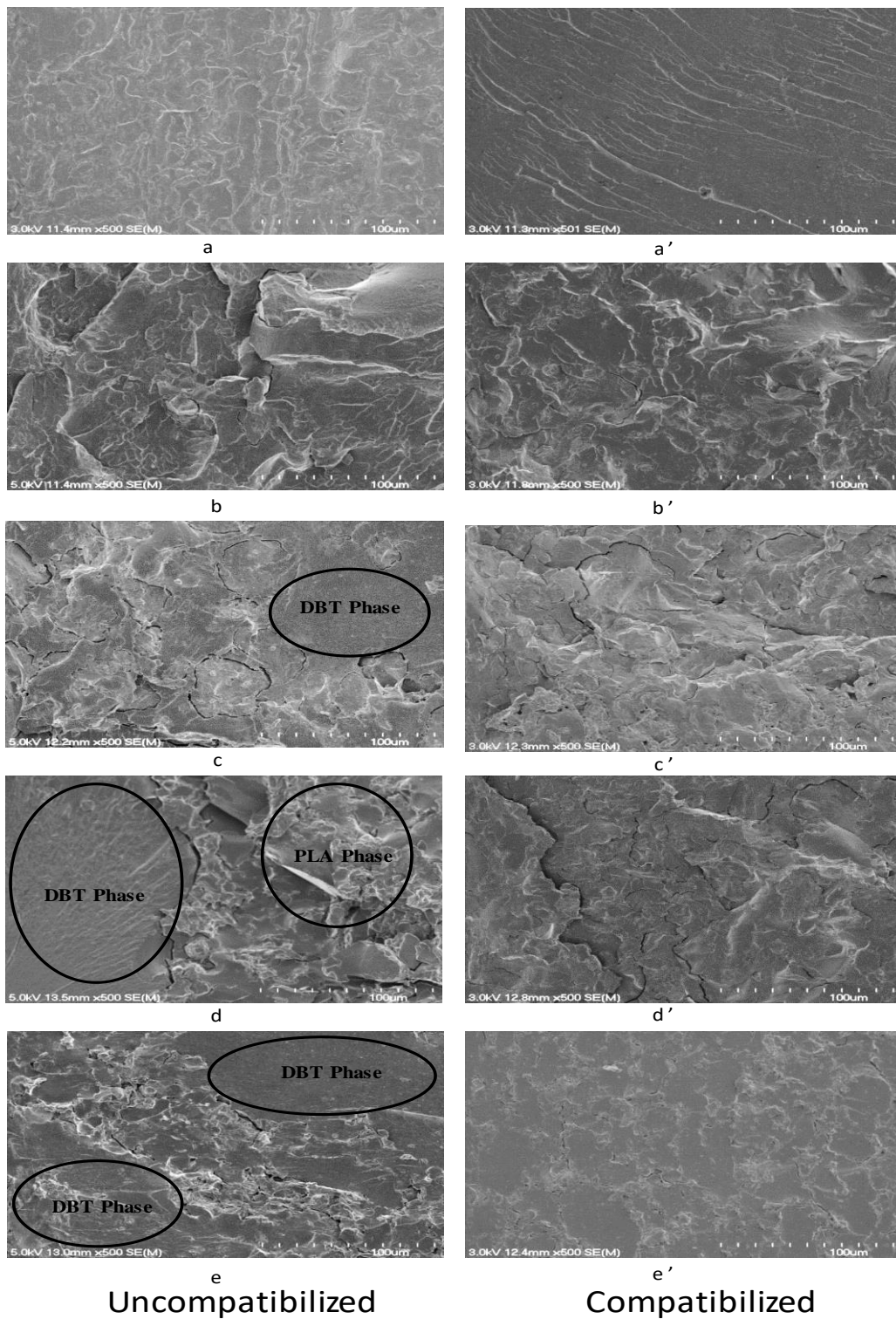


Figure 25: SEM micrographs of the cryo-fractured surface of DBTP/ PLA blends with and without compatibilizer. a and a': PLA and DBT; b and b': DP37 and DgP37; c and c': DP55 and DgP55; d and d': DP73 and DgP73; e and e': DP91 and DgP91

3.4.3.2 MECHANICAL PROPERTIES

The mechanical properties of PLA, DBT and DBT/PLA blends with varying blend compositions are shown in Figure 26. PLA has been reported to have high tensile strength, impact strength, modulus and low elongation [36] while DBT has low tensile strength, impact strength, modulus and high elongation [184].

All blend compositions, with and without compatibilizer, showed rigid and brittle behaviour. The modulus of the blends was higher than that of neat DBT due to the incorporation of rigid PLA.

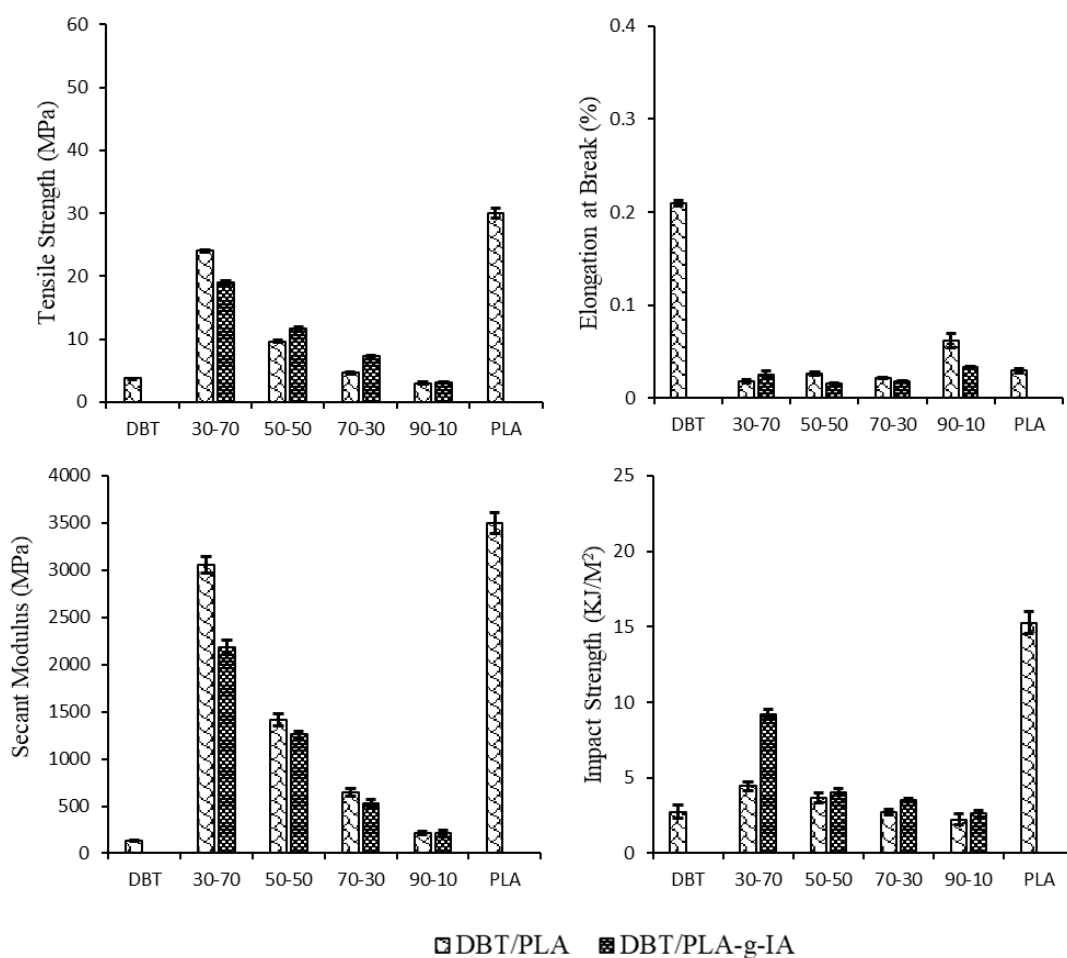


Figure 26: Mechanical properties of DBT, PLA and varying compositions of DBT/PLA blends with (DBT/PLA-g-IA) and without compatibilizer (DBT/PLA)

Tensile strengths observed for all blends with and without compatibilizer were inferior compared to neat PLA, although an improvement was observed when compared to neat DBT except for 90:10 blends (DP91 and DgP91), which showed

a decrease. The decrease observed in tensile strength for 90:10 blends was probably due to the overwhelming effect of DBT in the blends, restricting PLA chain movement and resulting in a much lower tensile strength.

The inferior tensile strength observed for blends compared to PLA is probably a result of weak interfacial adhesion between the two phases, or DBT restricting the chain movement of PLA in the blend, as observed by an increase in tensile strength of the blends with a decrease in DBT content. Previous studies have reported inferior tensile strength for blends of PLA/Novatein® [308] and PLA/Soy protein [190] compared to pure PLA. The addition of itaconic anhydride showed a slight improvement for 50-50 (DgP55) and 70-30 (DgP73) blends. The tensile strength of 30-70 compatibilized (DgP37) blend was very poor compared to the uncompatibilized blend (DP37) while the 90-10 blend showed no effect. It is assumed that below 50% and above 70% DBT content, either DBT or PLA overwhelms the compatibilizing effect of itaconic anhydride, resulting in poor tensile strength.

Secant modulus increased with a decrease in the DBT content for both compatibilized and uncompatibilized blends. This is probably due to the restriction of the protein chains' movement by the rigid PLA in the blend, resulting in a more brittle material.

DBT has a good strain at break compared to PLA. However, blending DBT with PLA showed a drastic decrease compared to DBT. The strain at break of the blends was similar to that of PLA, which is consistent with the blend morphology observed in Figure 25. This confirms DBT to be the dispersed phase while PLA is the continuous phase.

The anhydride groups of itaconic anhydride were likely to react with the amino groups of DBP protein, thus enhancing the interfacial adhesion, as observed in the SEM micrograph Figure 25, which played a role in reducing the size of the DBP phase in the compatibilized blends. However, this interfacial adhesion is considered to be very weak, and thus wasn't strong enough to effect significant improvement in the mechanical properties. This is probably due to an insufficient amount of compatibilizer (i.e., a low degree of grafting) or an indication that itaconic

anhydride is not a suitable compatibilizer for the DBP/PLA blend system. Zhu et al. reported an increase in both tensile strength and elongation of PLA/Soy protein composite with an increase in compatibilizer content [190].

3.4.3.3 DYNAMIC MECHANICAL PROPERTIES

Understanding the thermal transition of polymer materials is very important in the prediction of a material's performance under different end-use conditions. Figure 27 shows the $\tan \delta$ and storage modulus (E') of neat PLA, PLA-g-IA, and DBT. PLA and DBT showed broad and low damping peaks, also known as glass transition temperatures (T_g), while PLA-g-IA exhibited a sharp and high damping peak. The high damping peaks observed are probably due to low crystallization of PLA induced by itaconic anhydride, which makes it very soft when the temperature is above its α -transition. Similar observations have been reported for PLA used in blends with soy protein composites [190; 194].

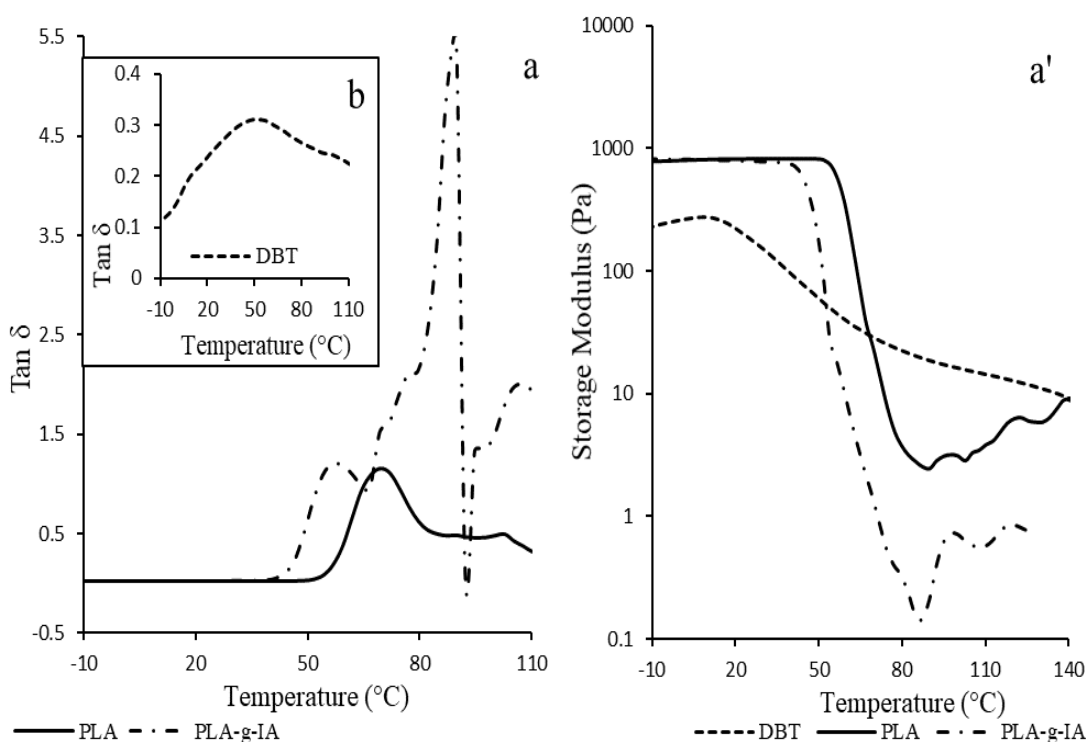


Figure 27: $\tan \delta$ (a) PLA and PLA-g-IA, (b) DBT, and storage modulus (a') of PLA, PLA-g-IA, and DBT

The damping peaks of PLA and PLA-g-IA in the blends were observed to be lower than those of the neat PLA and PLA-g-IA. This suggests that DBT in the blends

was still in the glassy state in the α -transition range of PLA and PLA-g-IA. The damping peak height decreased with increasing DBT content for both compatibilized and uncompatibilized blends; this is probably attributed to the effective contribution of the DBT phase to the storage modulus in the rubbery region of PLA [190; 194; 309]. A decrease was observed with the damping peak height of compatibilized blends compared to uncompatibilized blends. This suggests an interactive effect of itaconic anhydride within the material phase.

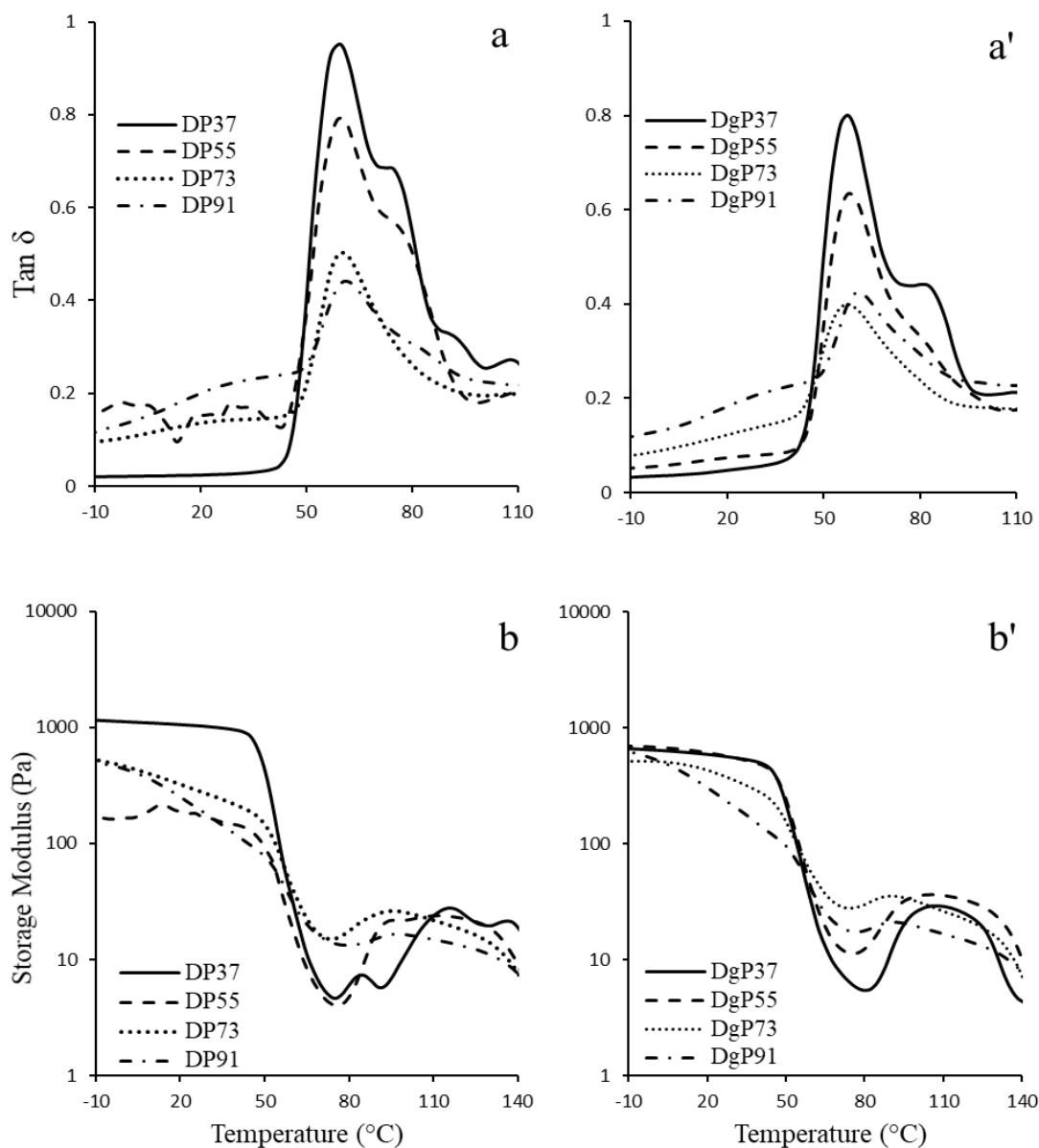


Figure 28: $\text{Tan } \delta$ (a and a') and storage modulus (b and b') of blends. DP: uncompatibilized and DgP: Compatibilized with itaconic anhydride

The glass transition temperature (T_g) of DBT was observed at 50°C while that for PLA was observed at 72°C. The T_g s of both compatibilized and uncompatibilized blends were observed to be below the T_g of PLA at approximately 59 to 62°C. The decrease in T_g observed with the blends compared to that of PLA is probably due to the migration of small molecules of plasticizers from the DBT phase to the PLA matrix during compounding. No significant difference was observed in the T_g of the compatibilizer and the uncompatibilized blends. This suggests that compatibilization has no significant effect on the melting of PLA in the blends.

A peak and a shoulder were observed in the $\tan \delta$ of 30:70 (DP37) and 50:50 (DP55) blends without compatibilizer (Figure 28a). The peak corresponds to the α -transition of the DBT region, and the shoulder could be associated with the α -transition of the PLA region in the blends. The distance between the observed peak and shoulder increased with the addition of compatibilizer for DP37. Both the peak and shoulder became broader compared to the uncompatibilized blend. This suggests a degree of incompatibility between DBT and PLA phases at this blend composition with the addition of itaconic anhydride. This confirms PLA's overwhelming effect on itaconic anhydride at higher PLA content, as suggested by the mechanical properties.

On the other hand, the shoulder observed for DP55 (uncompatibilized) decreased (becoming nearly invisible) with the addition of compatibilizer, suggesting an improved compatibility between the DBT and PLA phases. This was also reflected in the increase observed in the tensile strength of the blend and the improved even dispersion of DBT in the PLA matrix with the addition of compatibilizer. Zhang et al. observed the same trend with soy protein isolate/PLA compatibilizer with PEOX [194]

Only one peak was observed for both 70:30 and 90:10 blends with and without compatibilizer and no significant shift in peak temperature was observed. This confirms the overwhelming effect of DBT in the blend, restricting PLA chain movement at higher DBT content as suggested by the tensile strength.

The storage moduli of DBT and PLA showed PLA is stiffer than DBT. The blends showed storage modulus values closer to that of PLA, indicating a stiffer material

compared to DBT. This suggests that PLA was restricting the chain movement of DBT, making DBT stiffer in the blend. This can also be confirmed by the increase observed in the secant modulus of the blends when compared to DBT. The storage moduli of both compatibilized and uncompatibilized blends dropped when the T_g of DBT (≈ 50 °C) was reached, and then recovered to a significant degree between 90 and 95 °C due to the cold crystallization of PLA. A similar observation was also reported by previous researchers [190; 194; 310].

The loss moduli of PLA, DBT, PLA-g-IA and their blends are shown in Figure 29. It is expected that the continuous phase in the blend will dominate the shape of the loss modulus curve observed. All blends' loss modulus curves were similar to the loss modulus curve of PLA. At low PLA content, the similarity is not pronounced; however, as PLA content increased the loss modulus curve of the blend looked more like that of PLA. These results confirmed the observations regarding the blends' morphology, suggesting a co-continuous phase with PLA as the blend matrix.

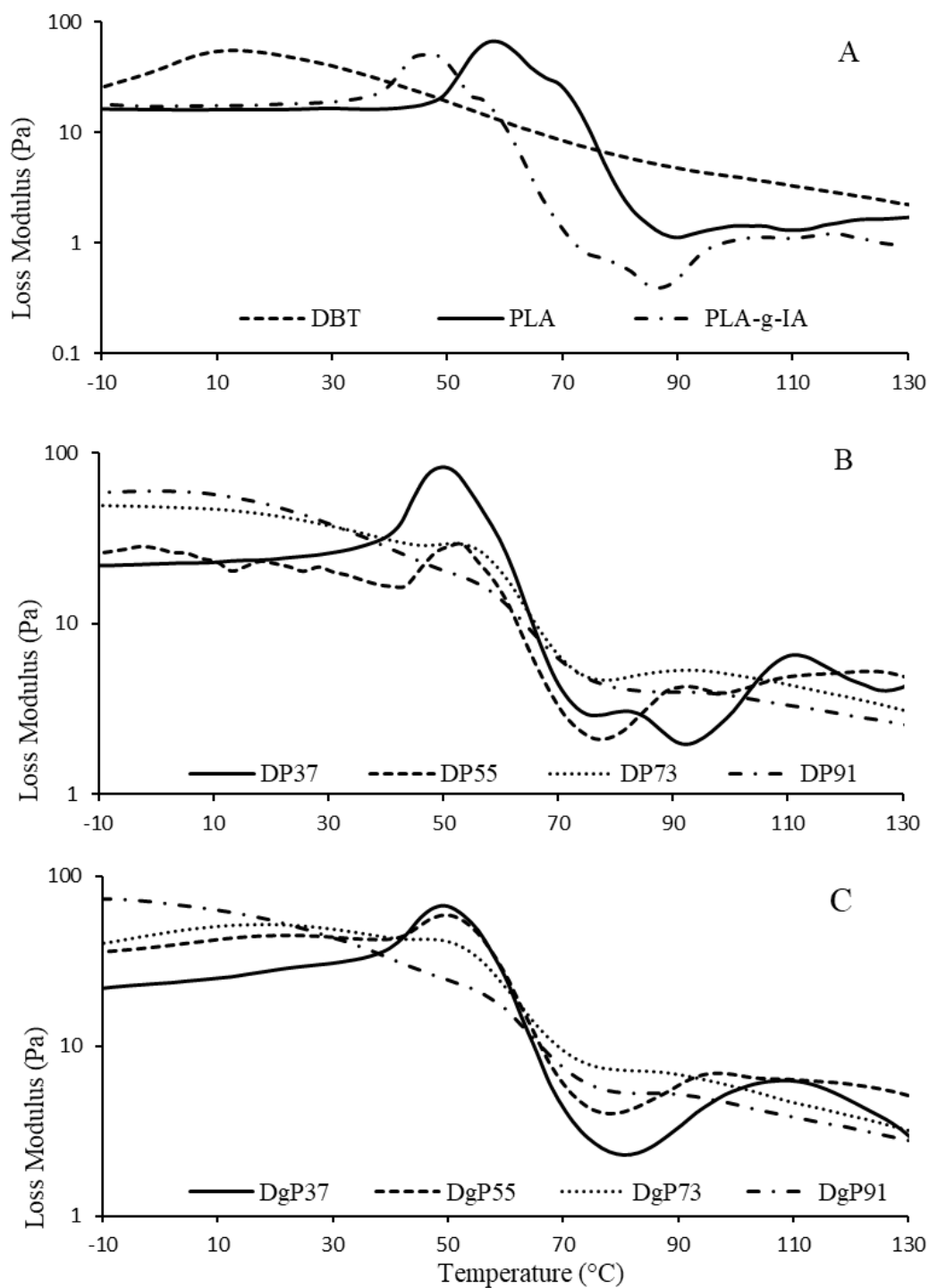


Figure 29: Loss modulus of pure material (A) and blends without (B) and with (C) compatibilizer

3.4.3.4 WIDE ANGLE X-RAY SCATTERING (WAXS) MEASUREMENT

The WAXS diffractograms of PLA, DBT and their blends with and without compatibilizer and their summation are shown in Figure 30. An amorphous peak at

$16^\circ 2\theta$ was observed for PLA. DBT is semi-crystalline with less aggregated β -sheets and a high number of disordered structures [289]. The peak at $2\theta = 9^\circ$ corresponds to helical spacing and inter- β -sheet while the peak at $2\theta = 22^\circ$ corresponds to a repeated distance within each structure. There was no change in the WAXS diffractogram of PLA and PLA-g-IA. Therefore, only the PLA diffractogram is presented.

The summation of the DBT and PLA diffractograms looks similar to the diffractogram of DBT/PLA blends both with and without compatibilizer, although without the presence of the sharp peak at 16° . This suggests contributions from both DBT and PLA to the blend's structure and implies that DBT and PLA in the blends did not influence each other's structure.

No change was observed in 2θ for the two peaks at 16° and 22° with the addition of compatibilizer for all blends. This suggests that itaconic anhydride had no structural effect within the crystal region of the blend, and therefore may be a good compatibilizer for DBT/PLA blend systems.

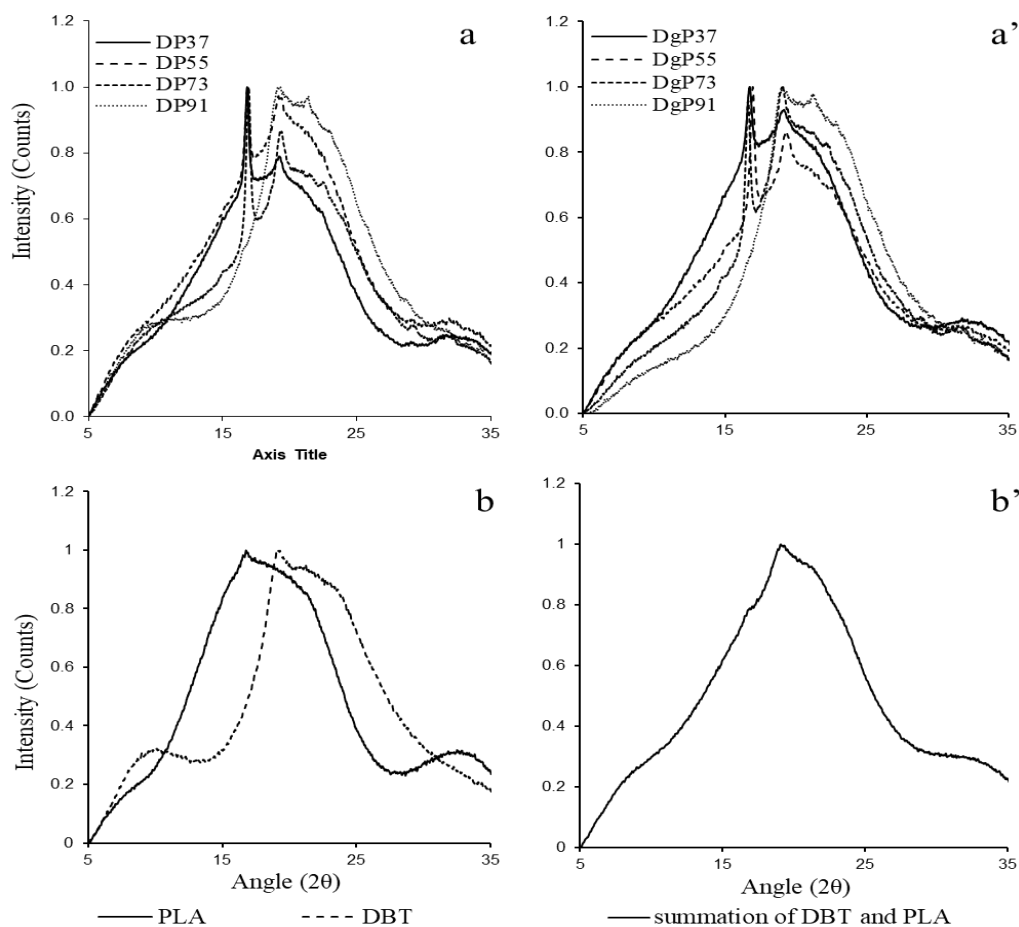


Figure 30: WAXS diffractograms of DBT/PLA blends without (a) and with compatibilizer (a'), PLA and DBT (b), and summation of DBT and PLA (b').

3.4.3.5 CONCLUSION

SEM of DBT/PLA blends showed a dispersed phase morphology with agglomerates of DBT in the PLA matrix and the presence of interstices. However, the agglomerates of DBT and interstices observed reduced with the addition of itaconic anhydride. This suggests that compatibilization is essential for DBT/PLA blends to enhance the interfacial adhesion between both material phases.

Blending DBT and PLA improved the tensile property of DBT except for the 90:10 blend (DP91). The addition of compatibilizers produced a slight improvement for 50:50 (DP55) and 70:30 (DP73) blends. However, 30:70 (DP37) showed a decrease in tensile strength with the addition of compatibilizer while 90:10 (DP91) showed no change. Possibly higher levels of either PLA or DBT overwhelm the compatibilization effect of itaconic anhydride, resulting in the observed decrease in tensile strength with the addition of itaconic anhydride. The strain at break observed

for the blends was similar to that of PLA, confirming the observation with blend morphology, and suggests DBT is the dispersed phase while PLA is the continuous phase. This is also consistent with the blends' loss modulus curves, as they closely resemble that of PLA.

The DMA data obtained showed that the shoulder observed for the compatibilized 50:50 blend decreased significantly, suggesting improved compatibility of DBT/PLA phase in this blend composition. This also was reflected in the increase in tensile strength and improved dispersion of the DBT phase with the addition of itaconic anhydride for this blend ratio.

The diffractogram of the blends looked similar to the summation of DBT and PLA diffractograms. Also, no change was observed in the 2θ for peaks observed at 16° and 22° with the addition of compatibilizer for all blends. This suggested that DBT, PLA and itaconic anhydride had no structural effect within the crystal region of the blends.

From the data obtained, 50 wt.% of DBT was considered the best composition for the blend system as it showed a more even dispersion of DBT and better distribution of both material phases in the blend matrix with fewer interstices, and having acceptable mechanical properties compared to the other compositions trialed.

3.4.4 DBT formulation determination

From the previous section, 50 wt.% of DBT was considered the best ratio for DBT/PLA blends. However, it was important to determine the optimal DBT formulation for the blend system. Therefore, blends of PLA and different DBT formulations, with and without compatibilizer, were produced to determine the optimal DBT formulation for blending (see Figure 21).

3.4.4.1 PHASE MORPHOLOGY

The cryo-fractured and digested surface micrographs of the DBT/PLA blends (with and without compatibilizer) with different DBT formulations are shown in Figure 32 and Figure 33 respectively. The cryo-fractured surface of blends without itaconic anhydride (IA) showed relatively large and unevenly distributed DBT agglomerates because of the inherent immiscibility. However, the addition of PLA-g-IA produced

a much finer and more homogeneously dispersed matrix, indicating improved mixing and improved interfacial adhesion, as the DBT agglomerates observed in the blends without itaconic anhydride were not distinct. Interstices were observed in the blends without itaconic anhydride, indicating poor interfacial adhesion. Some interstices were still visible in the blends with PLA-g-IA, but they were much smaller and fewer compared to the blends without itaconic anhydride.

The clear phase separation observed in the blends without IA is an indication of poor blend compatibility. Blending different formulations of DBT with PLA-g-IA improved the morphology of the blend significantly as reduction of the DBT-rich phase size was observed. There were no visible clear differences between the SEM surface structures of the different formulations trialed, except for F1gP, which showed more interstices than the other formulations.

The blend morphology of different DBT formulations trialed was further investigated through SEM of digested surfaces. Larger voids were observed in blends without itaconic anhydride (Figure 33, uncompatibilized) indicating a poor dispersion of PLA in the blends, corresponding to the agglomerates observed in Figure 32 for blends without itaconic anhydride.

Blends with PLA-g-IA exhibited a much finer phase structure with relatively uniform voids of small dimensions. This fine structure confirms an improved interfacial interaction between the two phases, as suggested in Figure 32 with PLA-g-IA. This shows that blending the two immiscible polymers without compatibilization will result in a material with undesirable properties due to the high interfacial tension between both material phases.

F3P, DBMP, and DBMgP disintegrated in chloroform (Figure 31) suggesting that DBT was the dispersed phase while PLA formed the continuous phase in the blend matrix. F2gP, F3gP, and F4gP were considered the best formulations for a blend with PLA as their digested surface micrographs showed a smaller void with relatively uniform diameter, suggesting co-continuous phase structure and improved dispersion of both polymer phases.

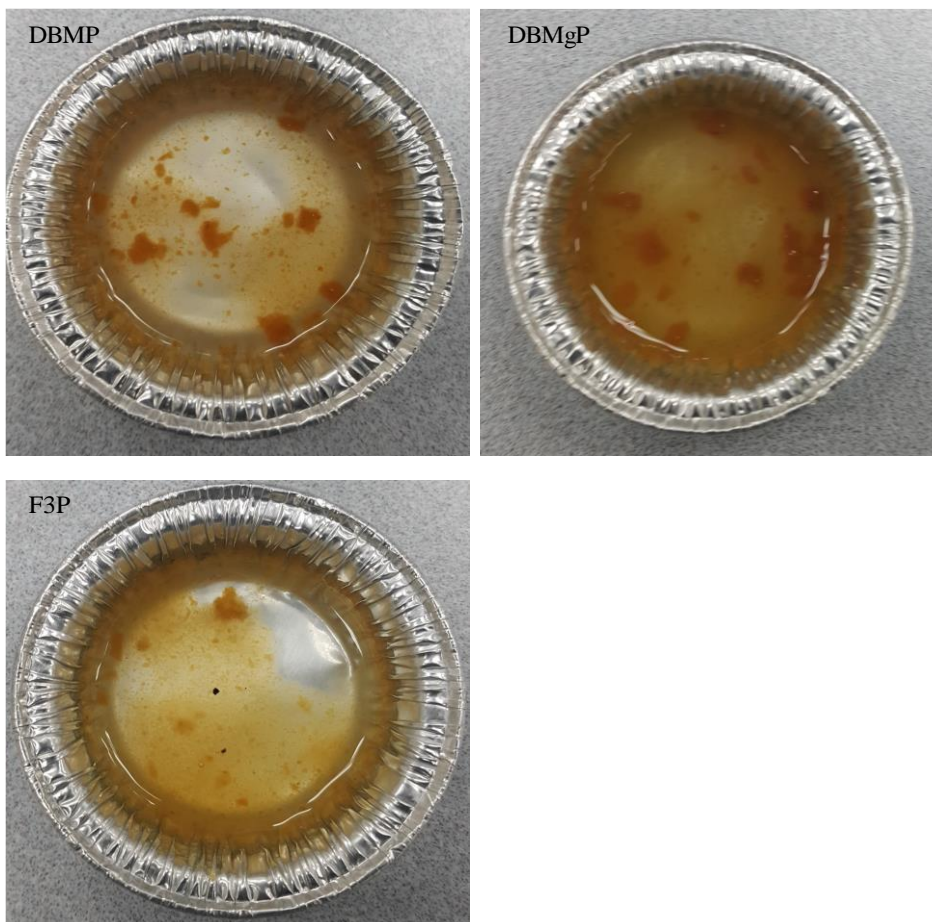


Figure 31: Unsuccessful washed surface of F3P, DP and DgP blend in chloroform.

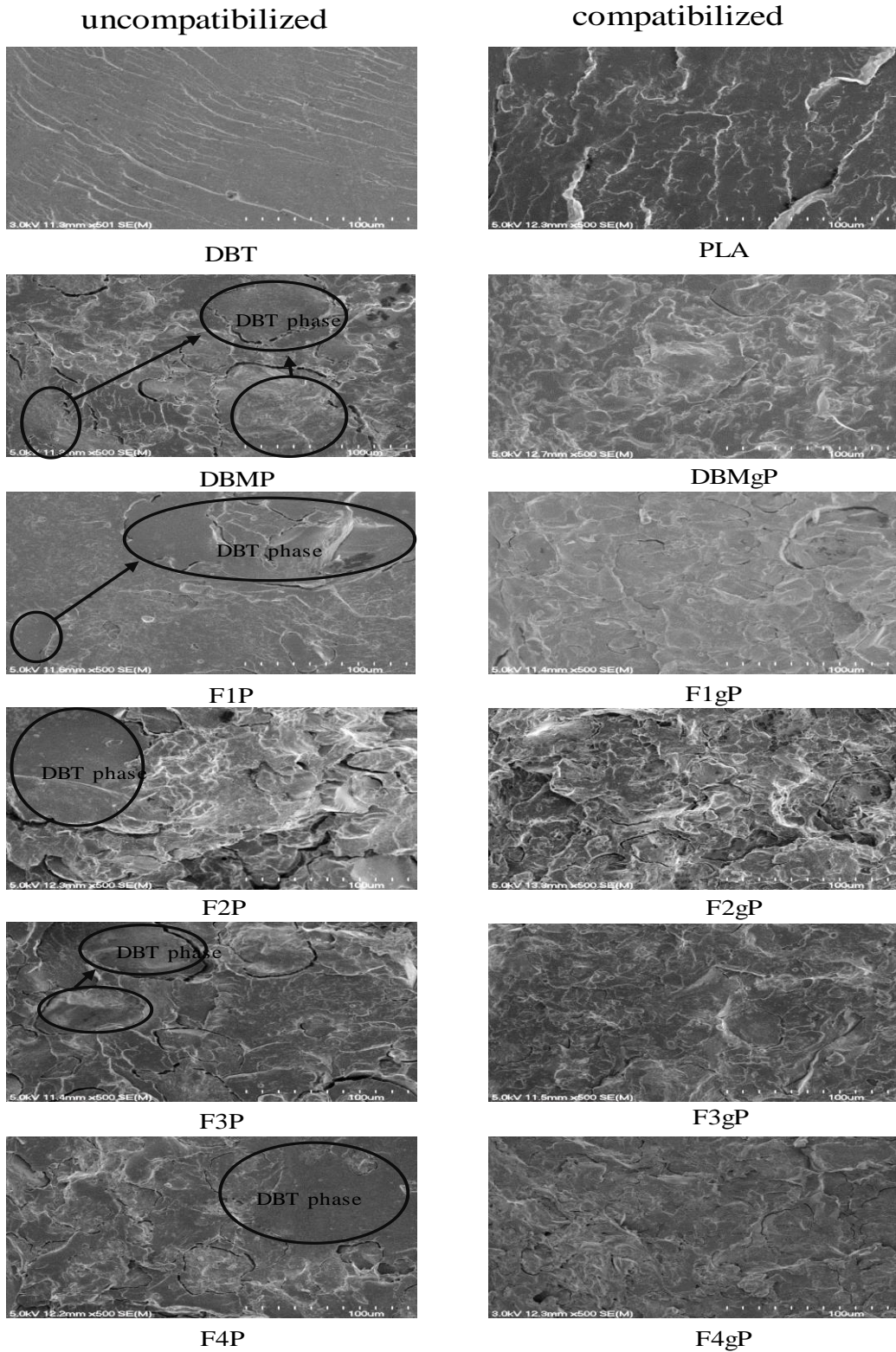


Figure 32: SEM cryo-fracture surfaces of DBTP/PLA blends with and without itaconic anhydride.

Key:

DBMP, F1P, F2P, F3P, F4P are blends without itaconic anhydride, DBMgP, F1gP, F2gP, F3gP, F4gP are blends with itaconic anhydride, DBM have no additive (dried decoloured bloodmeal blend) while F1, F2, F3 and F4 have varying water (30 – 40_{pph}), SDS (3 – 6_{pph}) and TEG (20 – 30_{pph}) content (see Table 2).

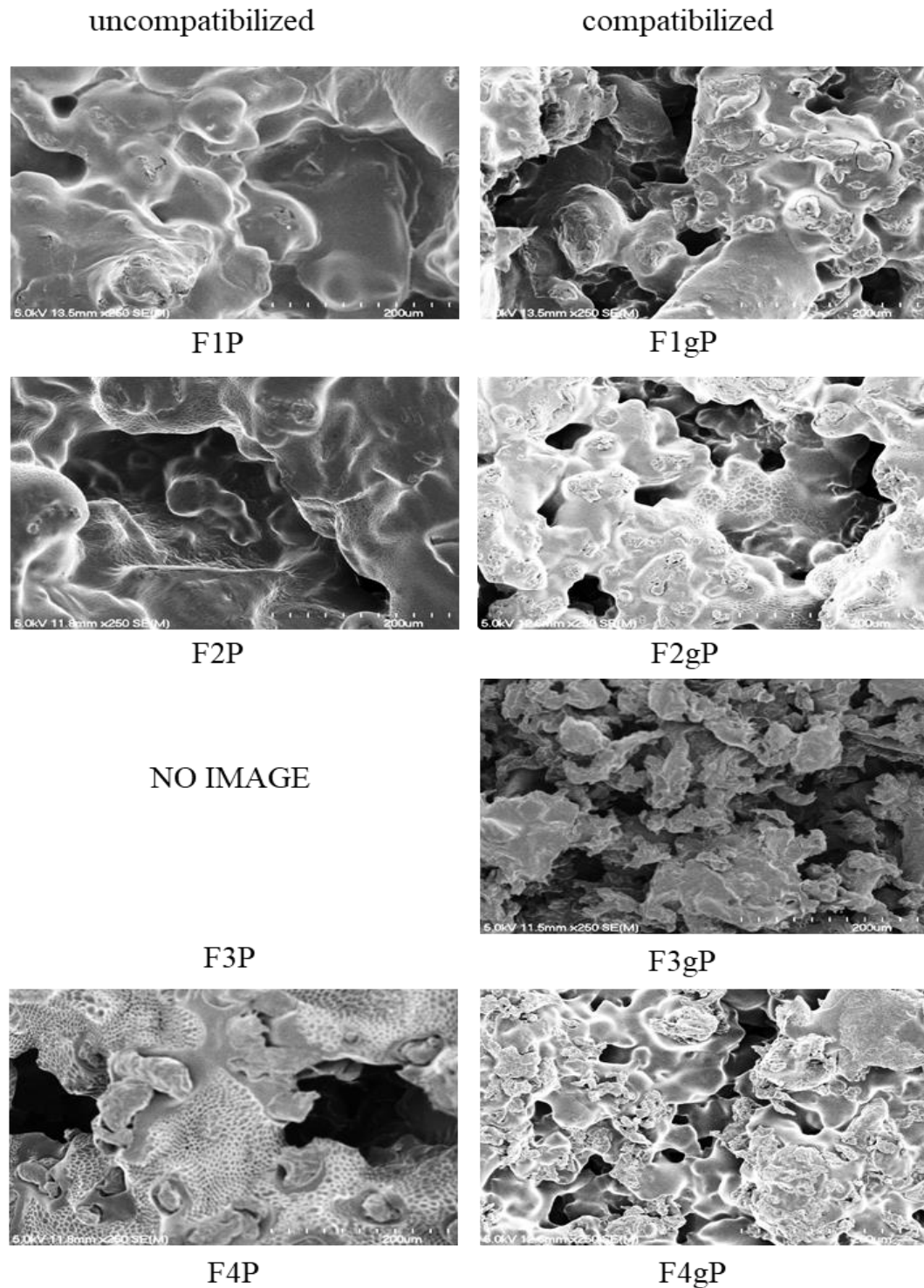


Figure 33: SEM Digested surface micrographs of DBP/PLA blends with and without Itaconic anhydride.

Key:

DBMP, F1P, F2P, F3P, F4P are blends without itaconic anhydride, DBMgP, F1gP, F2gP, F3gP, F4gP are blends with itaconic anhydride, DBM have no additive (dried decoloured bloodmeal blend) while F1, F2, F3 and F4 have varying water (30 – 40_{pph}), SDS (3 – 6_{pph}) and TEG (20 – 30_{pph}) content (see Table 2).

3.4.4.2 MECHANICAL PROPERTIES

A material's performance during processing, storage and handling can be predicted from its mechanical properties as a function of flexibility, toughness, and elongation. Mechanical properties may be used to assess a polymer blend's miscibility, as miscibility depends on the intermolecular interaction, chain stiffness and molecular symmetry of the individual polymers in the blend matrix [311]. Willemse et al. suggested that the tensile modulus of polymer blends depends strongly on the composition and morphology of the blends [304].

Figure 34 shows the mechanical properties of different DBT formulations and PLA blends (with and without compatibilizer). DBT and PLA are known to be rigid polymers and to show brittle behaviour, which was reflected in the blends' elongation and moduli. The mechanical properties of blends were compared with that of neat DBT.

The tensile strength of blends without (DBT/PLA) and with (DBT/PLA-g-IA) compatibilizer increased while the elongation decreased compared to neat DBP. No significant difference was observed in the tensile properties of compatibilized blends compared to the uncompatibilized blends except for the DBMP blend, which showed a drastic decrease in the tensile strength of the compatibilized blend. Therefore, it is thought that itaconic anhydride improved the phase dispersion and interfacial adhesion between both phases as observed in Figure 32 (compatibilized). However, the interaction between both phases was weak, resulting in slightly low or insignificant increases in tensile strength compared to uncompatibilized blends. However, the DBMP blend showed a homogeneously mixed and finer phase structure with the addition of compatibilizer. It is believed that DBT was encapsulated in the PLA matrix, resulting in a homogeneously mixed structure with no visible DBM phases. However, the encapsulated DBT acted as a stress concentrator, promoting cracks, which resulted in the poor tensile strength observed. This is also supported by the washed surface morphology (Figure 31) as DBT disintegrated when the PLA phase was washed off, indicating that DBT is encapsulated by PLA.

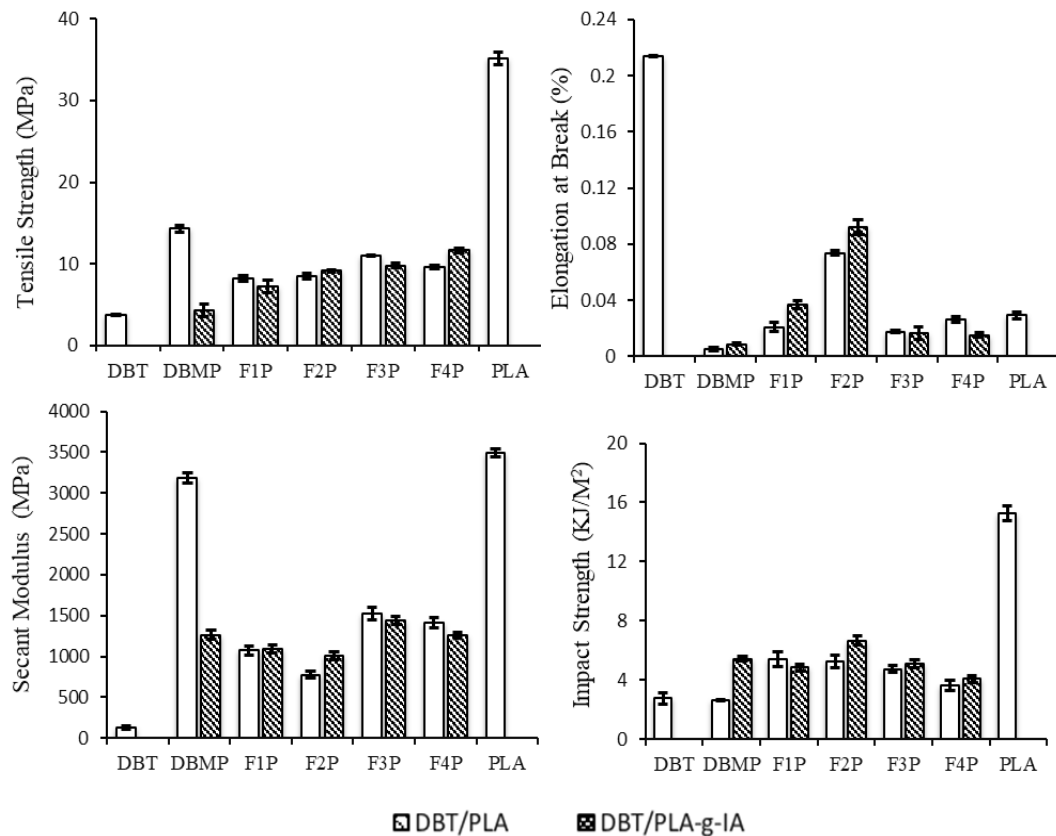


Figure 34: The mechanical properties of DBT/PLA blends with and without itaconic anhydride.

Key:

DBMP, F1P, F2P, F3P, F4P are blends without itaconic anhydride, DBMgP, F1gP, F2gP, F3gP, F4gP are blends with itaconic anhydride, DBM have no additive (dried decoloured bloodmeal blend) while F1, F2, F3 and F4 have varying water (30 – 40_{pph}), SDS (3 – 6_{pph}) and TEG (20 – 30_{pph}) content (see Table 2)

Blending decoloured bloodmeal (DBMP) and PLA without compatibilizer revealed an increase in tensile strength compared to all blends. However, with the addition of compatibilizer (PLA-g-IA), it gave the lowest tensile strength. Therefore, it is thought that decoloured bloodmeal (without additives) acted as a filler in the blend. However, blending PLA with plasticized bloodmeal (F1P) or thermoplastic processed decoloured bloodmeal (F2P) showed a decrease in tensile strength compared to the decoloured bloodmeal (DBMP) blend. The addition of compatibilizer revealed an increase in F1gP and F2gP compared to DBMgP. The drastic decrease observed in the tensile strength of DBMP with the addition of compatibilizer suggests that for a compatibilized DBT/PLA blend, plasticization is important for DBT formulations to ensure the re-arrangement of the protein, which will in turn improve the blend's material interaction.

Comparing F1P to F2P, no significant change was observed in the tensile strength of the blends. However, a slight improvement was observed with the addition of compatibilizer. Apparently, using either plasticized DBM or decoloured bloodmeal thermoplastic did not affect the tensile strength of the blend. However, elongation at break improved significantly for the F2P blend compared to F1P, suggesting an improvement in plasticization with the addition of SDS and water compared to TEG alone.

Increasing the water content (F3P to F4P) showed a slight decrease in tensile strength for the uncompatibilized blend. However, compatibilization revealed an increase in tensile strength for F4P compared to F3P. No changes were observed in their elongation at break or secant modulus, suggesting that increasing water content alone is not sufficient to effect change in the blend's elongation and flexibility.

All blends revealed a reduction in elongation compared to DBT. This is due to the addition of the rigid PLA, which restricted the movement of polymer chains, thereby decreasing the elongation at break. The interactions between the phases may also have caused a reduction in elongation. Marsilla et al. reported similar findings with protein thermoplastic and polybutylene succinate blends [197].

The secant modulus showed an increase for all blends compared to neat DBT. The addition of compatibilizer produced no significant difference except for the decoloured bloodmeal/PLA blend, which showed a decrease. This is probably due to the restriction of the protein chains' movement by the rigid PLA in the blend, resulting in a more brittle material.

An increase was observed in the impact strength of all blends without compatibilizer compared to DBT. A further slight increase was observed with the addition of compatibilizer, except for the F1P blend, which showed a slight decrease with the addition of compatibilizer. Blending decoloured bloodmeal without additives produced a decrease in impact strength. However, a significant increase was observed with the incorporation of a compatibilizer.

The compatibilized F2P (F2gP) blend showed a considerable increase in elongation at break, exceeding that of all other blends, an increase in tensile strength and an impact strength more than double that of neat DBT. This suggests better compatibility between PLA and this DBT formulation. Compromising elongation at break, the tensile strength and impact strength of compatibilized F4P (F4gP) showed an acceptable increase. Therefore, the optimal formulation was considered to be between F2gP and F4gP, depending on the desired properties and functionalities of the material produced.

3.4.4.3 DIFFERENTIAL SCANNING CALORIMETRY (DSC)

DSC thermograms of PLA, DBT and their blends are shown in Figure 35 and Figure 36, and the results are listed in Table 6. Glass transition, cold crystallization, and melting endotherm can be seen in the DSC curve of PLA and all blends. However, protein do not show cold crystallization; therefore, none was observed for DBT.

The DBT curve showed only one glass transition temperature. Other researchers suggested that small water molecules act as plasticizers in protein systems, reducing proteins' exothermic temperature [79; 312]. A single T_g peak was observed for all blends, suggesting a degree of miscibility. The presence of two distinct glass transition temperatures has been reported as evidence of immiscibility by other researchers [310; 313]. Cold crystallization peaks and double-melting peaks were observed for all blends (excluding DBMP) at temperatures below that of PLA. This suggested that DBT acted as a heterogeneous nucleating agent for the PLA matrix, inducing and accelerating PLA crystallization.

A glass transition temperature of 49.8°C and a cold crystallization temperature of 102.86°C, which are higher than the T_g and cold crystallization temperature of PLA, were observed for the DBMP blend (decoloured bloodmeal/PLA blend). Similar T_g and cold crystallization temperatures have been observed for soy protein isolate/PLA blends [79]. However, with the addition of itaconic anhydride, both T_g and cold crystallization shifted to lower temperatures of 47.94°C and 95.81°C respectively. The increase in T_g and cold crystallization temperatures of DBMP compared to PLA is probably a result of DBT restricting the mobility of the PLA chain in the blend.

The blends of DBT/PLA (excluding DBMP) showed a slight increase in both T_g and cold crystallization temperatures with the addition of itaconic anhydride. The increase observed is attributed to the restricted slippage of the PLA macromolecular segment due to increased interaction between the PLA and DBT phases. This confirms the suggested increase in interaction observed in the surface morphology of the blends with compatibilization.

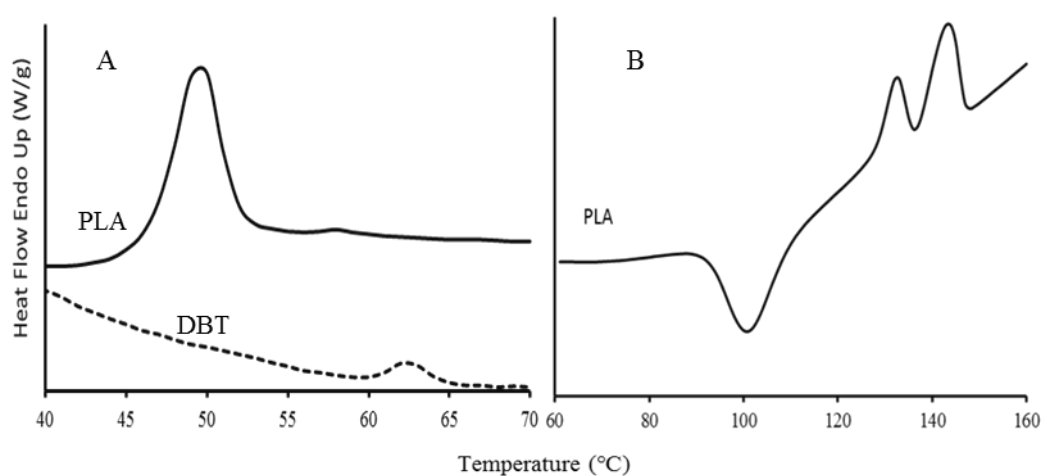


Figure 35: Glass transition temperature (T_g), crystallization peak (T_{cc}) and melting endotherms (T_m) of PLA and DBT

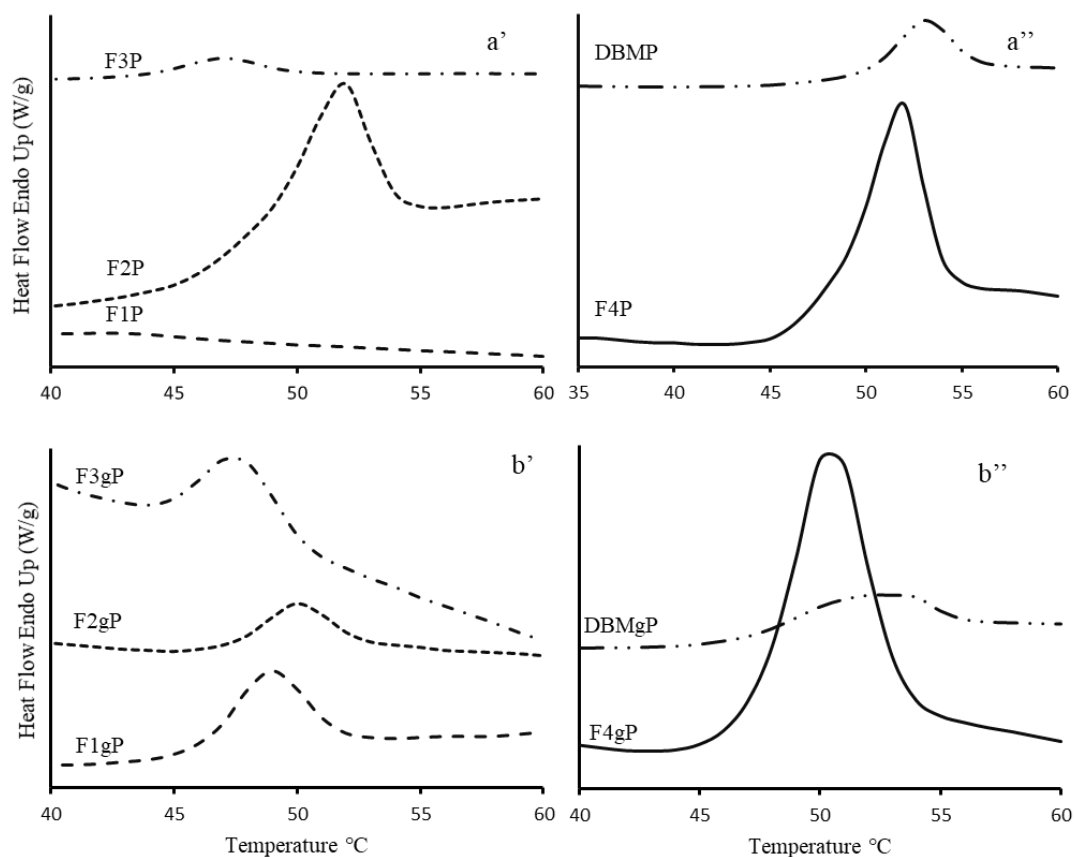


Figure 36: Glass transition temperature (T_g) of different formulations of DBT/PLA blends (DSC first heat scan thermograms).

Key:

a' and a'' are blends without itaconic anhydride, b' and b'' are blends with itaconic anhydride, DBM have no additive (dried decoloured bloodmeal blend) while F1, F2, F3 and F4 have varying water (30 – 40_{pph}), SDS (3 – 6_{pph}) and TEG (20 – 30_{pph}) content (see Table 2).

The PLA in the blends (both compatibilized and uncompatibilized blends) exhibited cold crystallization at a lower temperature than PLA. This suggested that DBT accelerated the crystallization of PLA and substantially increased the crystallinity of PLA in the blends.

The melting of PLA in the blend was reflected by the bimodal endotherm transition observed at ~ 120 – 145°C. The peak at the lower temperature reflects the melting of crystals with less perfection in the boundary regions followed by the melting of recrystallized PLA at a higher temperature [194; 310].

Crystallization and melting temperatures of all blends showed a decrease compared to PLA. This can be attributed to the residual moisture in the blends, which plasticizes the PLA molecules and increases their flexibility, resulting in lower

crystallization and melting temperatures. Zhang et al. observed a continuous decrease in T_g , T_{cc} , and T_m with an increase in moisture content of SPI/PLA containing 3 phr PEOX conditioned at different relative humidities [194].

The ΔH_m values observed (Table 6) are larger than the ΔH_{cc} values. This is also an indication that the addition of DBT promoted a certain degree of PLA crystallinity.

The DSC result obtained (Figure 37) indicated that T_g , T_{cc} , and T_m of PLA in the blends were not affected by the different DBT formulations trialed.

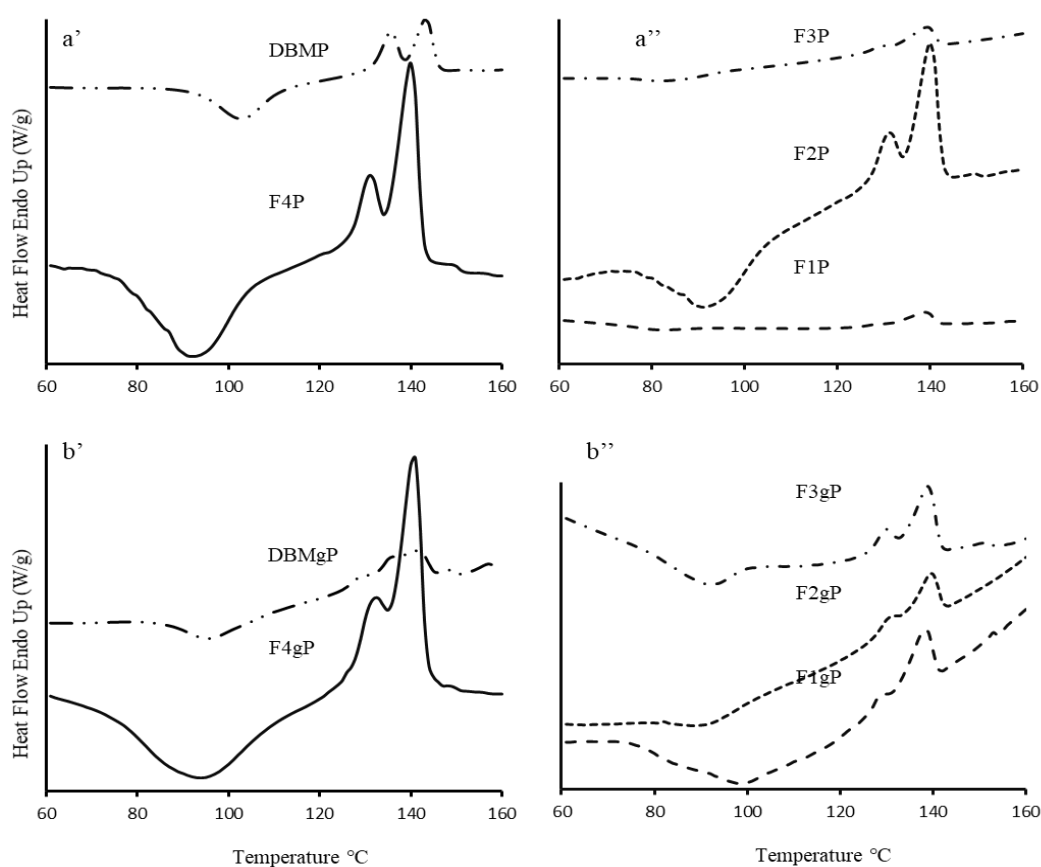


Figure 37: DSC first heat scan thermograms of different formulations of DBT/PLA blends showing crystallization peak (T_{cc}) and melting endotherm (T_m).

Key:

a' and a'' are blends without itaconic anhydride, b' and b'' are blends with itaconic anhydride, DBM have no additive (dried decoloured bloodmeal blend) while F1, F2, F3 and F4 have varying water ($30 - 40_{pph}$), SDS ($3 - 6_{pph}$) and TEG ($20 - 30_{pph}$) content (Table 2).

Table 6: Glass transition temperatures, cold crystallization peaks and melting endotherms of blends, PLA and DBT

Sample	T_g (°C)	cold crystallization		melting T_m (°C)		ΔH_m (J/g)
		T_{cc} (°C)	ΔH_{cc} ^a (J/g)	1	2	
PLA ^a	53.67	99.48	-2.736	131.81	142.89	2.4303
DBT	60.5			nd	nd	
DBMP	49.8	102.86	-3.122	135.6	142.27	3.4074
DBMgP	47.94	95.81	-2.456	135.55	140.62	1.6384
F1P	39.53	81.32	-0.6967	124	138.78	1.0073
F1gP	45.51	98.38	-3.09	128.49	138.19	0.8297
F2P	47.37	92.08	-10.133	130.97	140.06	10.8316
F2gP	47.43	92.2	-0.6146	130.18	139.32	0.7878
F3P	43.59	83.98	-0.9813	129.29	139.21	1.601
F3gP	44.14	91.42	-0.6898	129.79	138.92	1.1314
F4P	47.51	91.58	-11.068	130.97	140.06	11.0577
F4gP	47.67	91.75	-5.3824	130.8	141.19	10.4048

^a Data collected on the second heat scan of samples, T_g : glass transition temperature, T_{cc} : cold crystallization temperature, T_m : melting endotherm, ΔH_m : enthalpy of melt and ΔH_{cc} : enthalpy of cold crystallization

3.4.4.4 WIDE ANGLE X-RAY SCATTERING (WAXS) MEASUREMENT

WAXS analysis was performed on the blends for better insight into the blend morphology. Data obtained from the XRD of a material can be used for phase identification of a crystalline material and to characterize the composition of a polymer blend. It can also provide information on unit cell dimensions.

Figure 38 presents the wide-angle X-ray diffractogram for PLA and DBT, PLA-g-IA and blends of DBT/PLA with and without compatibilizer. PLA shows only an amorphous halo while DBT shows both an amorphous and a crystalline region.

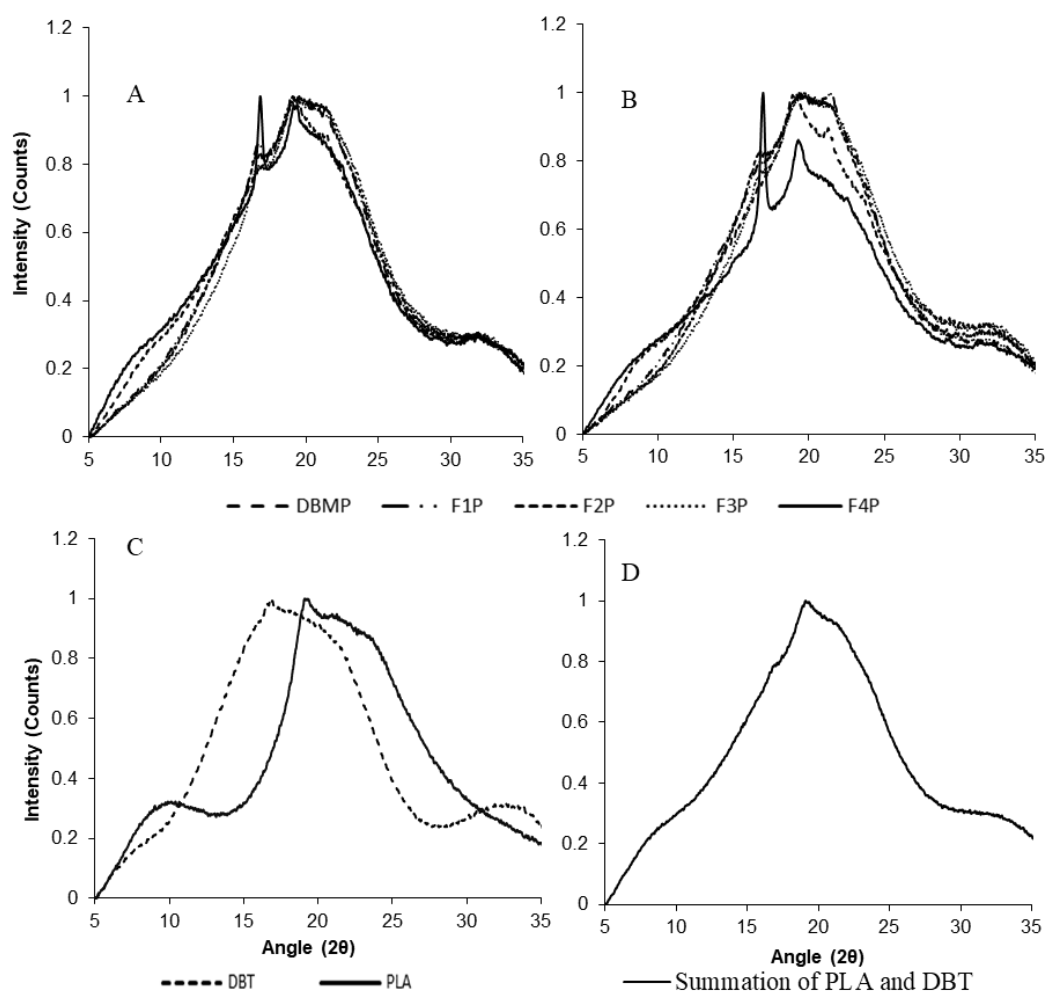


Figure 38: WAXS diffraction patterns for DBT/PLA blends without (A) and with (B) itaconic anhydride, pure PLA, DBP (C), and summation of PLA and DBT (D)

Key:

DBM have no additive (dried decoloured bloodmeal blend) while F1, F2, F3 and F4 have varying water (30 – 40_{pph}), SDS (3 – 6_{pph}) and TEG (20 – 30_{pph}) content. (see Table 2).

The blends of DBT/PLA looked more like the summation of PLA and DBT except for the F4P blends (both compatibilized and uncompatibilized). Crystalline peaks were observed at $2\theta = 16^\circ$ and 20° for both compatibilized and uncompatibilized F4P while a shoulder was observed at $2\theta = 16^\circ$ for F1P, F2P, and F3P for both the compatibilized and uncompatibilized blends. However, this was not observed for DBMP blends. This is probably due to the residual moisture in the blends resulting in the crystallization of PLA in the blend.

The appearance of peaks at $2\theta = 16^\circ$ and 20° for PLA has been reported by other researchers, who identified the peak at $2\theta = 16^\circ$ as a reflection of α -form homo-

crystal structure and that at $2\theta = 22^\circ$ as a reflection of stereo-complex crystals [286; 314-318]. The presence of a stable crystal structure has been suggested to be evidence of some degree of PLA hydrolytic degradation [286; 313].

The formation of stereo-complex crystals, as well as the α -form homo-crystal structure observed in the WAXS diffractogram of both compatibilized and uncompatibilized blends, suggests that significant chain orientations occurred during the blend processing, possibly due to hydrolytic degradation of PLA. The hydrolysis of the PLA in the blend is probably a result of moisture immigration from the DBT phase to PLA phases during processing. Also, it is thought that the significant presence of these peaks in F4P is due to the large amounts of added water and plasticizer used in this formulation.

The peaks at $2\theta = 9^\circ$ observed in the diffractogram of DBT corresponds to helical spacing and inter β -sheet, while the peak at $2\theta = 20^\circ$ corresponds to the repeated distance within each structure. The amorphous regions of the compatibilized blends showed a slight reduction, which may be due to the integration of both PLA and DBT amorphous regions as confirmed by the reduction of DBT agglomerates with the addition of compatibilizer in SEM thermograms, as shown in Figure 32.

The WAXS diffractogram suggested the possibility of PLA hydrolysis during processing, thus suggesting the manipulation of processing and blend conditions to control the hydrolysis of PLA. The addition of itaconic anhydride showed a slight reduction in the blends' amorphous regions, confirming improved compatibility of both material phases.

3.4.4.5 CONCLUSION

The digested surface SEM of blends revealed a much finer phase structure with relatively uniform voids for F2P, F3P and F4P blends with compatibilizer, suggesting co-continuous phase structure and improved dispersion of both polymer phases.

Mechanical property data obtained suggested that compatibilized F2P and F4P blends are the optimal formulations for DBT/PLA blends, considering the desired material properties and functionalities of the end product.

WAXS data obtained suggested the hydrolytic degradation of PLA during processing; therefore, manipulation of processing and blend conditions to control for this event is imperative. The improved compatibility of DBT and PLA phases with the addition of itaconic anhydride was also confirmed from the WAXS data obtained.

3.5 Conclusion

Decoloured bloodmeal thermoplastic and PLA blends were successfully prepared through reactive extrusion and injection moulding using decoloured bloodmeal thermoplastic powder. The processability and flowability of DBT increased after blending with PLA enabling processing without processing aids.

The mechanical properties of DBT were enhanced by the addition of PLA. Data obtained from the SEM and WAXS indicated the compatibility of DBT and PLA using itaconic anhydride. The addition of itaconic anhydride led to improved mixing of the two phases, which resulted in a finer phase structure. However, no significant effect was observed in the blend's mechanical properties with the addition of itaconic anhydride. This was attributed to itaconic anhydride improving the dispersion of DBT as observed in SEM thermogram, thereby enhancing the interfacial adhesion. However, the interfacial adhesion is probably weak resulting in an insignificant increase or low mechanical properties compared to the uncompatibilized blends. All blends showed low elongation at break and brittle fracture failure in tensile testing, suggesting a gap for toughening and plasticization in future investigation.

WAXS of DBT/PLA blends revealed peaks at $2\theta = 16^\circ$ and 20° on the PLA in the blends, suggesting the occurrence of significant chain orientations due to PLA hydrolysis. With the addition of itaconic anhydride, the presence of this crystal structure became clearer, which is probably responsible for the insignificant effect of itaconic anhydride on the mechanical properties of DBT/PLA blends. This suggests the manipulation of processing and blends conditions to better control for hydrolysis of PLA in the blends.

The data obtained from the mechanical properties of the F2P/PLA blend compatibilized with itaconic anhydride suggest that F2P is the preferred DBTP formulation for a blend with PLA as it showed better tensile strength, elongation at break, impact strength and flexibility. However, the balance could be between compatibilized F2P and F4P blends if elongation at break is compromised, depending on the desired material properties.

Compatibilized 50:50 and 70:30 blends were considered acceptable blend compositions, as the evidence suggests that below 50% and above 70% DBT content, either DBT or PLA overwhelms the compatibilizing effect of itaconic anhydride, resulting in poor mechanical properties.

In conclusion, the data presented in this chapter demonstrates that DBT and PLA can be blended like other protein polymers and PLA blends. It shows that blending DBT and PLA can be achieved using decoloured bloodmeal thermoplastic powder and a compatibilizer in the absence of a processing aid. It also supports the suggestion that 50 wt.% of DBT is a trade-off for this blend system. However, the mechanical properties of the blends produced were poor even with the addition of itaconic anhydride as a compatibilizer. WAXS data obtained suggested that a degree of PLA hydrolysis occurs during processing as a result of moisture immigration from the DBT phase to the PLA phase, resulting in the poor mechanical properties observed. Therefore, it is imperative to explore the manipulation of processing and blend conditions to control this process.

Chapter 4

Mechanical Properties of Decoloured Bloodmeal Protein and Poly (lactic) Acid Blends

Mechanical Properties of Decoloured Bloodmeal Thermoplastic Protein and Poly(lactic) acid Blends

4.1 Abstract

Blends of decoloured blood-meal thermoplastic (DBT), a thermoplastic protein material from slaughterhouse by-products, and poly(lactic acid) (PLA), a thermoplastic polyester, were prepared using reactive extrusion. Itaconic anhydride grafted PLA (PLA-g-IA), poly (2-ethyl-2-oxazoline) (PEOX) and poly (phenyl isocyanate)-co-formaldehyde (pMDI) were used as compatibilizers. The interactions between DBT and PLA blends, compatibilizer approach and plasticizer type were investigated using mechanical testing, scanning electron microscopy (SEM) and dynamic mechanical analysis (DMA). SEM revealed PLA to be the continuous phase while DBT is the dispersed phase. The addition of compatibilizers improved the dispersion of DBT in the PLA matrix, indicating improved interfacial adhesion between both material phases. Tensile strength and impact strength exceeding that of DBT were observed for the blends, excluding the impact strength for the PEOX systems. Blends with PLA-g-IA showed better tensile strength, improved impact strength and interfacial adhesion compared to PEOX/pMDI and PEOX-only systems, indicating that PLA-g-IA was the best compatibilizer for DBT and PLA blend systems. TEG was considered the best plasticizer for this blend system.

4.2 Introduction

Recent increases in environmental awareness and the known effects of petroleum resources on the environment have attracted more attention to the development of biodegradable, environmentally friendly and renewable materials [47; 54; 319].

Blood-meal is a protein by-product of the meat processing industry and consists of complex macromolecules containing 20 different amino acids with strong intra- and inter-molecular interactions.[5]. Based on the New Zealand industry alone,

350,000 tonnes of lamb, 341,000 tonnes of beef and 165,000 tonnes of other meat sources and their products (such as cheese) are exported yearly [96]. Blood-meal has been successfully processed into a thermoplastic known as Novatein® [291] and used to produce end-use products in agriculture and horticulture [105; 308]. Blood-meal has been treated with peracetic acid to eliminate its odour and dark colour and subsequently processed into thermoplastics using conventional methods. However, the mechanical properties of the produced thermoplastic, known as decoloured blood-meal thermoplastic (DBT), are very poor compared to conventional polymers. Efforts have been made to blend protein material and other polymers to produce fully biodegradable materials with improved mechanical properties from renewable resources [79; 80; 183; 190; 194; 208; 270; 296; 320]. PLA is one of the polymers that have been used for blending with proteins [79; 80; 195; 321].

PLA is an aliphatic polyester derived from lactic acid, obtained from fermentation of renewable resources such as corn and sugarcane [322]. PLA has been shown to be a good alternative to petroleum-based polymers due to its attractive properties, including high strength, good permeability, high transparency, high modulus, biodegradability and renewable origin [323-325]. PLA has found applications in the biomedical, disposable and food packaging industries [323]. Although blending is an effective way of improving polymer properties [296], blending two polymers results in an incompatible and inferior material because of poor interfacial adhesion between both distinct polymer phases [15].

Polymer blend compatibility can be improved by either the addition of a third component or by grafting a reactive group onto one of the blend's components capable of interacting with each polymer phase. Previous research reported a significant improvement in the mechanical properties of PLA and wheat blend with 0.5 wt.% methylene diphenyl diisocyanate (MDI) compared to the blend without MDI [326]. An increase in tensile strength, finer domain size of SPC and lower damping peak were reported for a soy protein concentrate (SPC)/PLA blend with maleic anhydride grafted PLA (PLA-g-MA), compared to the uncompatibilized blend. Zhu et al. suggested that the observations were evidence of good interfacial adhesion between the blend components [190]. Li et al. reported a finer phase structure with good dispersion of poly(butylene succinate) (PBS) in the blend

matrix, improved tensile strength and modulus of soy protein isolate (SPI)/poly(butylene succinate) (PBS) blends with pretreated PBS (pretreated with urethane and isocyanate group) compared to blends without pretreated PBS [296]. Zhang et al. used poly(2-ethyl-2-oxazoline) (PEOX) as a compatibilizer to improve compatibility of soy protein and PLA [194].

It is best practice to process PLA in the absence of water to avoid hydrolysis, which will result in poor material properties. When blending with DBT there is a strong possibility of PLA hydrolysis, which is probably one of the main reasons for the poor mechanical properties observed in the previous chapter. An approach to fully eliminate water from DBTP prior to blending with PLA was used. The optimal formulations: F2 (432) and F4 (463) from the previous chapter were used in this chapter. Different blend ratios and compatibilization approaches were used.

The objective of this chapter was to evaluate the effects of different compatibilizers and compatibilization approaches on the mechanical and structural properties of DBT and PLA blends for the optimization of DBT-based plastics.

4.3 Material and Methods

4.3.1 Materials

Blood-meal was obtained from Wallace Corporation Limited, New Zealand and used as received. Analytical grade itaconic anhydride (IA), dicumyl peroxide (DCP), acetone, 50 wt.% hydrogen peroxide, and technical grade sodium dodecyl sulphate (SDS), triethylene glycol (TEG), glycerol, PEOX, and pMDI were all acquired from Sigma Aldrich, Auckland, New Zealand. Peracetic acid (Peraclean 5) was purchased from Evonik Industries, Morrinsville, New Zealand. Poly (lactic acid) (PLA) grade 3052D was purchased from NatureWorks LLC, Minnetonka, MN, sourced from Clariant New Zealand Ltd, Auckland, New Zealand in pellet form. Distilled water was produced on site.

4.3.2 Sample Preparation

4.3.2.1 PLA GRAFTING

PLA was modified with itaconic anhydride via free radical grafting [142] to create reactive side-groups. PLA was dried at 80 °C for 4 h to control moisture. 4.2 g itaconic anhydride and 0.8 g dicumyl peroxide were dissolved in 30 mL acetone. The preformed solution was poured over the oven dried PLA and was kept in the fume hood for about 2 h. The solution was decanted before oven drying the PLA for 3 h at 50 °C. The material was reactively extruded to produce PLA-g-IA using a LabTech twin screw co-rotating extruder with a screw diameter of 20 mm and L/D of 44:1. The temperature profile increased along the barrel from 145 (feed zone) to 180 °C, with the highest temperature at the midzone and 155 °C at the die zone. A constant screw speed was maintained at 150 rpm. A vacuum pump was attached on the 7th heating zone of the extruder to remove vapour generated during extrusion. The pelletized PLA-g-IA was oven dried for 12 h prior to blending to minimize hydrolysis during melt processing. A level of 0.5% grafting was achieved, as reported by previous researchers [142].

4.3.2.2 BLOOD-MEAL DECOLOURING

Blood-meal was decoloured using a solution of peracetic acid (PAA) according to previous methods [11; 111] and as described in Chapter 3. A 4 wt.% PAA solution was prepared by diluting a 5 wt.% PAA stock solution with distilled water at a constant ratio of 80:20 respectively. Then, 150 g blood-meal was decoloured by adding 450 g of 4 wt.% PAA in a high-speed mixer. The mixture was allowed to mix continuously for 5 min to ensure homogenous decolouring of blood-meal. Then, 450 g of distilled water was added, and mixing was continued for another 5 min to ensure complete dilution of the slurry. The slurry was neutralized by adjusting to pH7 with sodium hydroxide solution. The neutralized slurry was filtered using a wire mesh sieve (aperture size 60) and subsequently washed by adding another 450 g of distilled water. The decoloured blood-meal (DBM) was dried for approximately 15 h in a 75 °C oven.

4.3.2.3 DECOLOURED BLOODMEAL THERMOPLASTIC POWDER PREPARATION

The decolouring method described in Chapter 3 was used to produce decoloured blood-meal. Decoloured blood-meal thermoplastic powder (DBTP) was formulated by dissolving SDS in water heated to 60 °C while stirring. The solution was added to decoloured blood-meal in a high-speed mixer and mixed for 5 min. Plasticizer was added to the mixture and mixed for another 5 min to ensure a homogeneous mixture was obtained. The prepared DBTP was stored in an airtight bag overnight at 2 °C in a fridge to equilibrate.

4.3.2.4 BLEND PREPARATION

DBTP and PLA grafting were performed prior to blending. All blends contained 50 wt.% DBTP, 40 wt.% PLA and 10 wt.% compatibilizer (PLA-g-IA, PEOX and PEOX/pMDI) as presented in Table 7. DBTP formulations were oven dried prior to blending at 70 °C until equilibrium content was obtained, to control the effect of inbound water content on PLA hydrolysis during blend processing. DBTP was dried over a range of temperatures and times to determine the optimal drying window. Blends were compounded using the same extruder profile used for grafting PLA. The extrusion temperature varied from 70 to 145 °C (having the lowest temperature at the feed zone and the highest at the die zone). The extrudates were granulated using a tri-blade granulator from Castin Manufacturing Limited. The compounded blend of DBTP, PLA and PLA-g-IA is referred to as DBT/PLA blend.

Table 7: Composition of the blends sampled

Sample Name	Composition						
	DBT	PLA	Compatibilizer			Plasticizers	
			PLA-g-IA	PEOX	pMDI	TEG(pph _D)	Glycerol (pph _D)
DBT	100	0	0	0	0	30	0
PLA	0	100	0	0	0	0	0
432.PLA	50	50	0	0	0	20	0
463.PLA	50	50	0	0	0	30	0
D432.IA	50	40	10	0	0	20	0
D432.PEOX	50	40	0	10	0	20	0
D432.PP	50	40	0	3	7	20	0
D463.IA	50	40	10	0	0	30	0
D463.PEOX	50	40	0	10	0	30	0
D463.PP	50	40	0	3	7	30	0
Dg432.IA	50	40	10	0	0	0	20
Dg432.PEOX	50	40	0	10	0	0	20
Dg432.PP	50	40	0	3	7	0	20
Dg463.IA	50	40	10	0	0	0	30
Dg463.PEOX	50	40	0	10	0	0	30
Dg463.PP	50	40	0	3	7	0	30
D432.5	50	0	50	0	0	20	0
D463.5	50	0	50	0	0	30	0
D432.4.1	50	40	10	0	0	20	0
D463.4.1	50	40	10	0	0	30	0

pph_D: parts per hundred decoloured bloodmeal

4.3.2.5 TEST SPECIMEN PREPARATION

ASTM D638-14 standard tensile test samples [302] and ISO 179-1:2010 impact test specimens [303] were injection moulded using a BOY 35A injection moulding machine. The samples were injected through a cold runner into a 60 °C water-heated mould. The injection moulder had five heating zones including the feed and the die zone. The temperature profile increased along the barrel, from 100 °C at the feed zone to 140 °C at the injection nozzle. The screw speed was constant at 150 rpm. The sample specimens produced were also used for morphology testing.

4.3.3 Sample Analysis

All samples were conditioned for 7 days at 23 °C and 50% relative humidity before testing.

4.3.3.1 MECHANICAL PROPERTIES

Mechanical testing was performed according to ASTM D638 using an Instron Universal Testing machine (model 33R4204) at a crosshead speed of 5 mm/min and with an extensometer gauge length of 50 mm. Five repeats were tested for each sample type to obtain an average value.

Impact testing bars measuring 80 x 10 x 4 mm were produced using the injection moulder. Charpy edgewise impact strength was measured according to ISO 179-1:2010 using a RAY-RAN Pendulum Impact System. The bar tested was notched according to standard. Five bars were tested to obtain the average impact strength of the material.

4.3.3.2 MORPHOLOGY

The phase structure of the blends was investigated using a Hitachi S-4700 field emission scanning electron microscope (SEM). The injection moulded specimens were cryo-fractured using liquid nitrogen. The specimens were sputter coated with platinum using a Hitachi E-1030 ion sputter coater before scanning. Samples for the digested surface were extracted with chloroform and then rinsed with hot water

to remove the PLA phase as DBT is not soluble in chloroform. The extracted surface was dried, and sputter coated prior to examination.

4.3.3.3 DYNAMIC MECHANICAL ANALYSIS (DMA)

Dynamic mechanical analysis (DMA) was conducted using an Elmer DMA 8000 fitted with a high-temperature furnace and cooled with liquid nitrogen. Rectangular samples (30 x 9 x 4 mm) were cut from injection-moulded samples and tested in a single cantilever fixture using a free length of 12.5 mm and scanning temperatures ranging from -80 to 150 °C at 2 °C/min. Data were collected at a single oscillation frequency of 1 Hz. Tan δ peak values were recorded as glass transition temperatures.

4.3.3.4 INTRINSIC VISCOSITY

The intrinsic viscosities of extruded PLA, dried PLA, PLA-g-IA, and PLA extracted from different blends of DBTP and PLA were measured by dissolving the polymer in chloroform to concentrations of 0.44, 0.88 and 1.20 g/dL. An Ubbelohde viscometer partially submerged in a temperature-controlled water bath at a constant temperature of 20 °C was used. The efflux time of the solvent and solution were determined and used to calculate the relative viscosity of each sample for each sampled concentration. Intrinsic viscosity was determined by extrapolating a plot of concentration vs. ln relative viscosity to zero concentration.

4.4 Results and Discussion

This chapter considered the effect of the processing water content of DBT on PLA hydrolysis. It is very important to understand the effect of DBT processing water content on the PLA in the blend (that is if the PLA in the blend was been hydrolysed, as suggested by WAXS) to determine possible control strategies. Techniques such as Fourier transform infrared spectroscopy (FTIR) and nuclear magnetic resonance spectroscopy (NMR) were trialled to determine the hydrolysis of PLA in the blend through its functional groups. An increase in the peak intensity of PLA's hydroxy (OH) and carboxyl (COOH) groups implies the hydrolysis of PLA. However, proteins have lots of functional groups (amine (NH), OH, carbon-carbon double and carbon-carbon bonds) and extraction of DBT from the blend using Soxhlet extraction was probably not sufficient to extract all protein and compatibilizer molecules from the blends. In this case the increase in OH and COOH intensities observed could be from either overlapping of bonds in proteins or compatibilizer bonds at the same frequency of light where an increase in OH and COOH from PLA should be observed. Therefore, these investigations were considered unsuccessful/unreliable and not a true representation of PLA hydrolysis.

It was assumed that inbound moisture immigration from DBTP to PLA was connected to the poor material properties observed in Chapter 3. However, in the absence of a more direct method to confirm this, drying of DBTP to equilibrium content prior to blending with the PLA was accepted as the best way to control the effect of processing water (if any) on PLA hydrolysis.

DBT was dried to equilibrium content. To determine the optimal drying window for DBT, it was oven dried over a range of temperatures (between 65 °C and 100 °C) and times (8 to 12 h). It was observed that 70 °C was sufficient to dry about 5 kg of DBT to equilibrium content over a period of 10 h. It was found that drying at high temperatures (above 70 °C) resulted in material caking and browning. Therefore, DBT requires drying at low heat over a given period of time (it is time dependent based on the quantity of DBT) to avoid this problem. Also, the moisture contents of DBTP, dried DBTP and blends containing either DBTP or dried DBTP were measured (results not included) to ensure that equilibrium moisture content was achieved before blend compounding.

4.4.1 Morphological properties

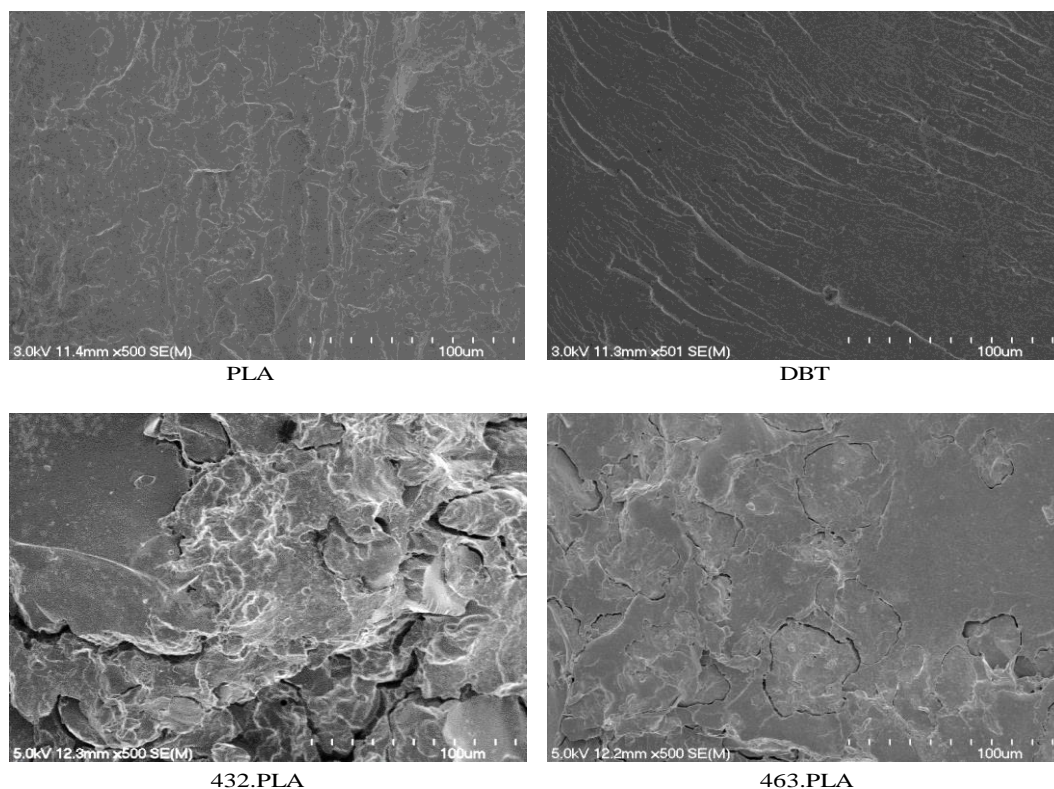


Figure 39: Scanning electron micrographs of cryo-fractured surfaces of pure DBT, pure PLA and their blends without compatibilizer. 432 represents 40 parts water, 3 parts SDS and 20 parts plasticiser and 463 represents 40 parts water, 6 parts SDS and 30 parts plasticisers.

The microstructure of blends is generally associated with their mechanical properties. Blends of almost equal proportions of immiscible polymer often lead to a co-continuous morphology [197]. Normally compatibilizers are used to stabilize the blend's morphology through reduction of the interfacial tension between both immiscible polymer phases. Compatibilization can be achieved using a variety of approaches, either through the grafting of a reactive group into one component of the blend which is capable of reacting with both blend components, or by introducing a third component capable of reacting with both blend components as compatibilized.

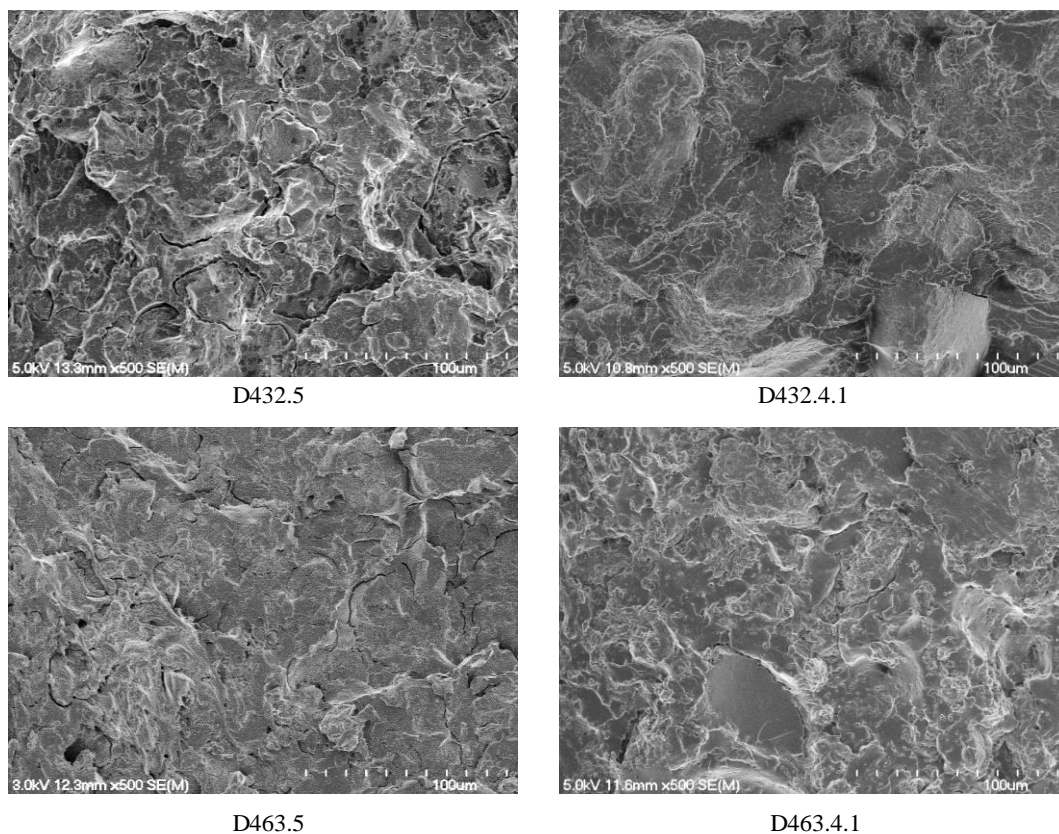


Figure 40: Blends of DBT/PLA with different compatibilization approaches. (D432.5 and D463.5 had itaconic anhydride grafted onto the PLA in the blend while D432.4.1 and D463.4.1 had PLA-g-IA added as a third component in the blend).

Figure 40 shows the fracture surface of DBT/PLA blends using different compatibilization approaches. Introducing PLA-g-IA as a third component produced a more homogeneously mixed and finer morphology with evenly dispersed DBT particles in the PLA matrix. Less or no visible DBT agglomerates and reduced interstices were observed compared to the blends where itaconic anhydride was grafted onto the PLA in the blend (i.e., D432.5 and D463.5). These observations indicate that introducing PLA-g-IA into the blends as a third component, rather than grafting itaconic anhydride onto the PLA in the blend, is the best compatibilization approach for this system.

4.4.1.1 FRACTURED SURFACE

The cryo-fractured surfaces of DBT/PLA blends with different compatibilizers and plasticizers are shown in Figure 41 and Figure 42 respectively. The presence of interstices and clear agglomerates of DBT particles embedded in the PLA matrix

were more visible for blends containing PEOX alone, and higher magnifications (not included) revealed elongated strand-like structures between phases rich in DBT and PLA. This is indicative of poor interfacial adhesion. However, it showed an improvement compared to the uncompatibilized blend (Figure 39, 432.PLA and 463.PLA).

The blends with both PEOX and pMDI showed an improved morphology, although voids were also seen for this blend. At higher magnification (not included), fewer elongated strand-like structures were observed. This is evidence of an improvement in the interfacial interaction between DBT and PLA, compared to using PEOX alone. The blends of Novatein® thermoplastic protein and polybutylene succinate showed an improved compatibility using both PEOX and pMDI as reported by Marsilla. et al. [327], suggesting that PEOX improved the dispersion of NTP and pMDI strengthened the adhesion between both material phases.

Using PLA-g-IA showed an improved morphology compared to PEOX alone and pMDI/PEOX, with much finer and more evenly dispersed DBT particles in the blend matrix. Few agglomerates of DBT were observed. It is possible that the DBT-rich phase was encapsulated in the PLA-rich phase, resulting in a finer phase structure and improved adhesion compared to using pMDI and PEOX, or PEOX alone. Walallavita et al. [328] reported improved tensile strength, impact strength and improved interfacial adhesion between PLA and Novatein compatibilized with itaconic anhydride grafted poly (lactic acid) (PLA-g-IA).

Comparing blends plasticized with triethylene glycol (TEG) (Figure 41) and blends plasticized with glycerol (Figure 42), DBT agglomerates were observed to be encapsulated rather than dispersed in the PLA matrix, with few interstices, for blend plasticized with TEG. Blends plasticized with glycerol showed more interstices and larger DBT domain sizes compared to TEG plasticized blends. This suggests a degree of phase separation with glycerol plasticised blends compared to TEG plasticized blends. pMDI and PEOX compatibilized blends (D432.pp and D463.pp) revealed higher DBT domain sizes, clear voids and visibly clear interstices when plasticized with TEG compared to glycerol. Clear voids and stretched bridge-like structures were also observed for these blends. This suggests a degree of incompatibility within the blends.

4.4.1.2 DIGESTED SURFACES

Scanning electron micrographs of PLA digested surfaces of DBT/PLA blends plasticized with either TEG or glycerol are shown in Figure 43 and Figure 44 respectively. Spherical, evenly distributed pores with small DBT domain sizes were observed for blends plasticized with TEG, while blends plasticized with glycerol showed slightly elongated DBT domains with uneven DBT domain sizes. This suggests better dispersion of DBT for blends plasticized with TEG compared to glycerol.

Using PEOX alone revealed a more phase-separated structure and increased domain sizes, regardless of the plasticizer used. There was no improvement observed for glycerol plasticized blends compatibilized with pMDI and PEOX compared to PEOX alone. However, TEG plasticizer blends with pMDI and PEOX showed an improvement compared to using PEOX alone. Plasticizing itaconic anhydride compatibilized blends with TEG revealed more evenly distributed and relatively small pores.

Comparing the digested surfaces of both compatibilization approaches, more evenly distributed pores, small DBT domain sizes and finer phase structure were observed for the approach where PLA-g-IA was added as a third component. This suggests improvement of interfacial adhesion between the phases in the blends using this approach, as a result of the better dispersion of DBT observed.

From the fracture and digested surface morphology, glycerol plasticized blends showed more interstices, larger DBT domain sizes, clear voids, and unevenly distributed and elongated DBT pore sizes compared to TEG plasticized blends. This suggested a degree of phase separation and poor dispersion of DBT particles within the PLA matrix and consequently poor interfacial interaction between DBT and PLA for blends plasticized with glycerol. Therefore, TEG was probably a better plasticizer for this blend system.

Comparing the SEM images of digested surfaces presented in Chapter 3 (Figure 33) with this chapter (Figure 43 and Figure 44), Figure 43 and Figure 44 presented

spherical or slightly elongated, even distribution of pores with small DBT domain sizes compared to Figure 33. This confirms that the processing and blending approach used in this chapter accounted for the improvement observed for this blend system.

The cryo-fractured morphology of the blends suggests that PLA-g-IA as a third component is a better compatibilization approach for DBT/PLA blend systems. This is due to the observed homogeneous and finer morphology with evenly dispersed DBT domains for this compatibilization approach, and the fracture and digested surface morphologies obtained. Better dispersion with small DBT domain sizes and evenly distributed small size pores observed for blends compatibilized with PLA-g-IA suggest that it is a better compatibilizer for the blend system.

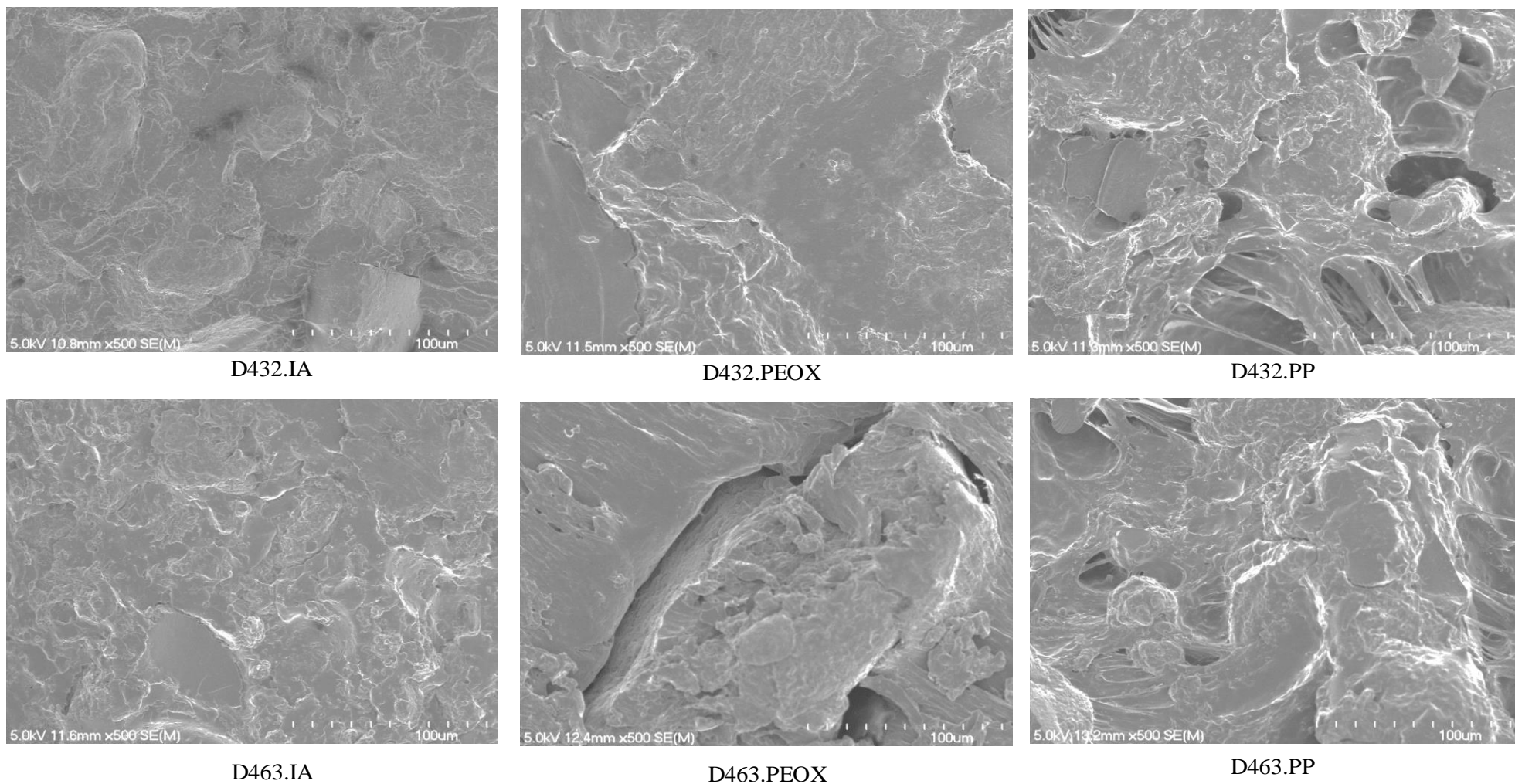


Figure 41: The fractured surfaces of DBTP and PLA blends plasticized with tri-ethylene glycol and having different compatibilizers. D432.IA and D463.IA were compatibilized with PLA-g-IA, D432.PEOX and D463.PEOX were compatibilized with PEOX alone, and D432.PP and D463.PP were compatibilized with pMDI and PEOX.

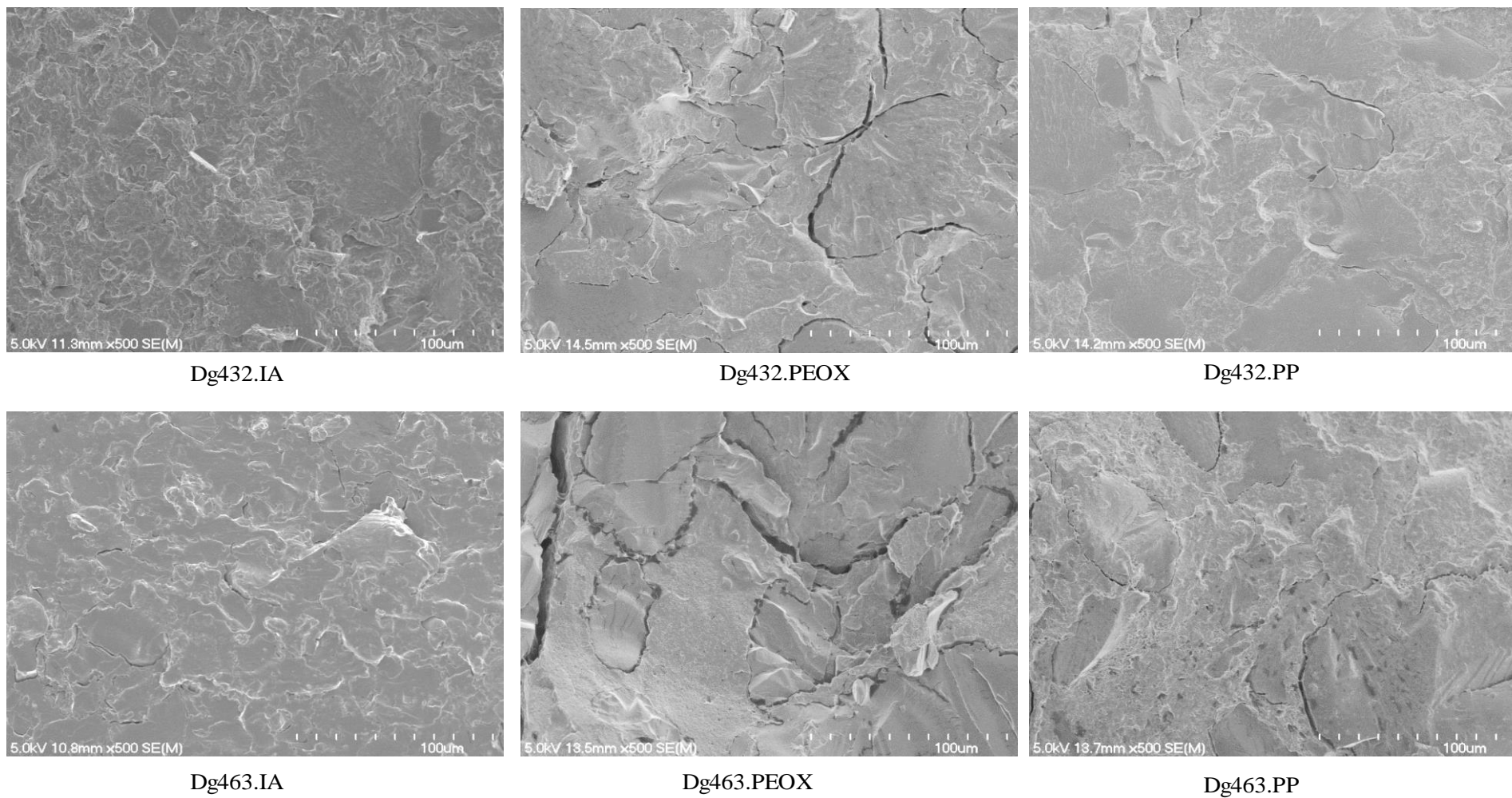


Figure 42: The fractured surfaces of DBTP and PLA blends plasticized with glycerol having different compatibilizers. Dg432.IA and Dg463.IA were compatibilized with PLA-g-IA, Dg432.PEOX and Dg463.PEOX were compatibilized with PEOX alone, and Dg432.PP and Dg463.PP were compatibilized with pMDI and PEOX.

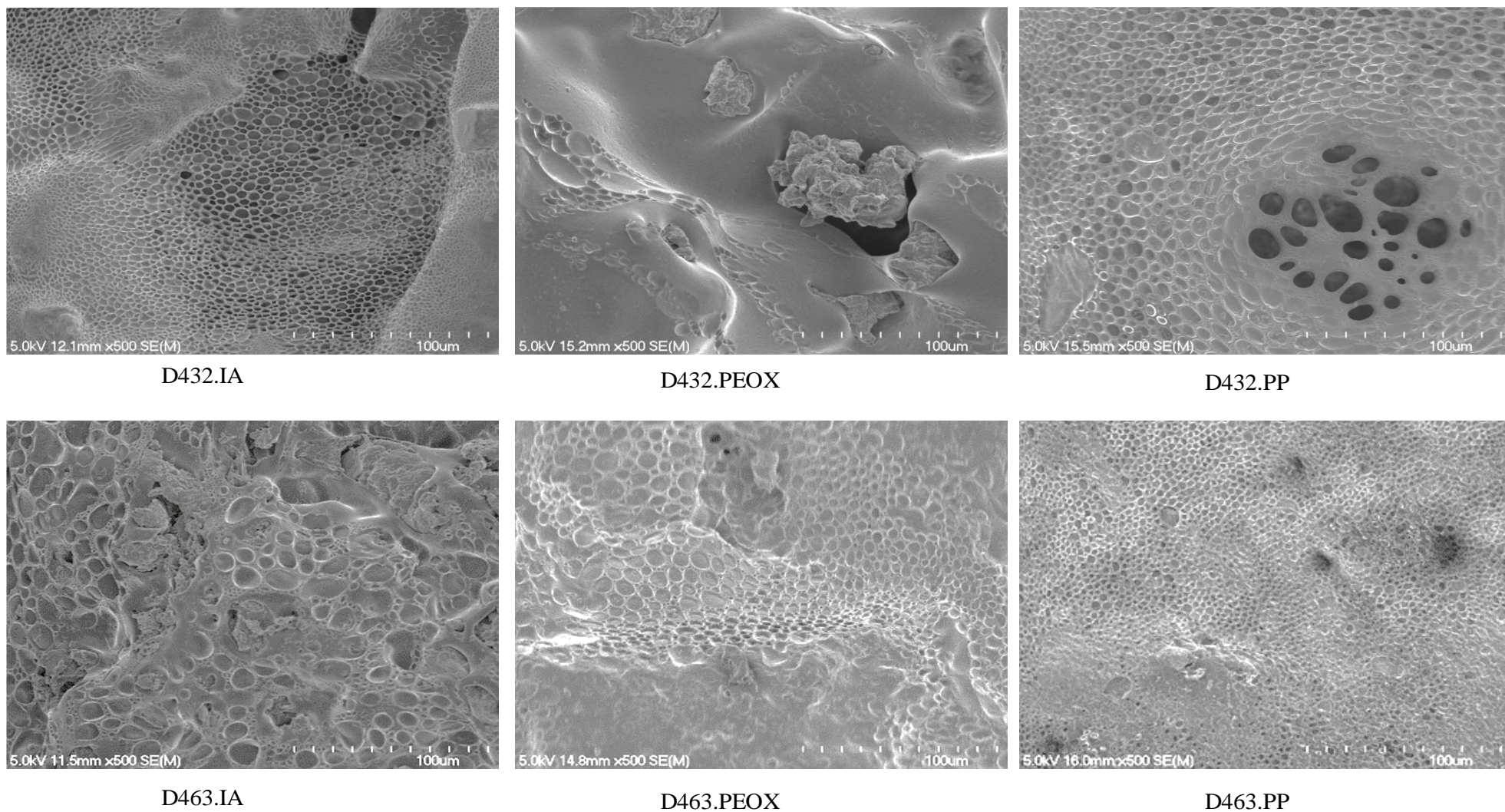
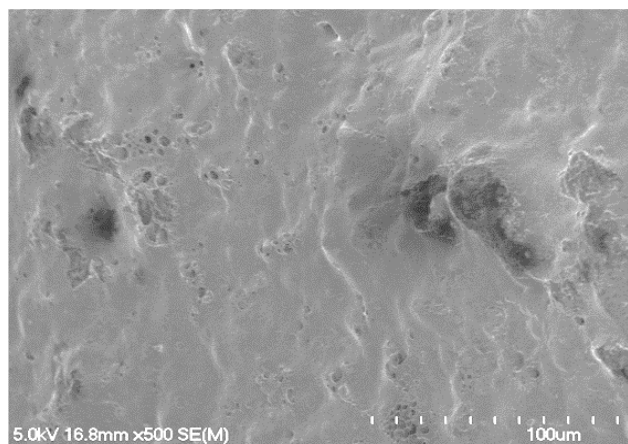
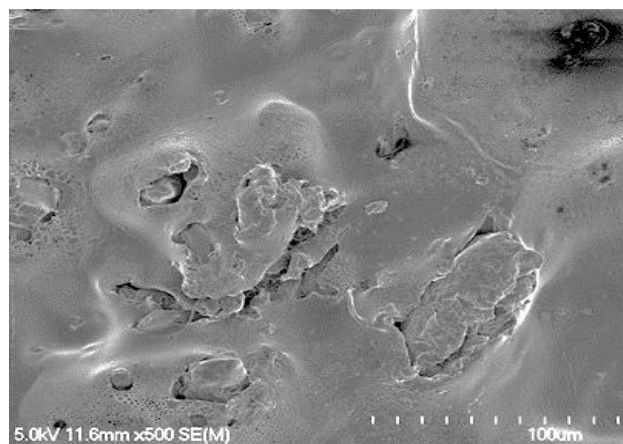


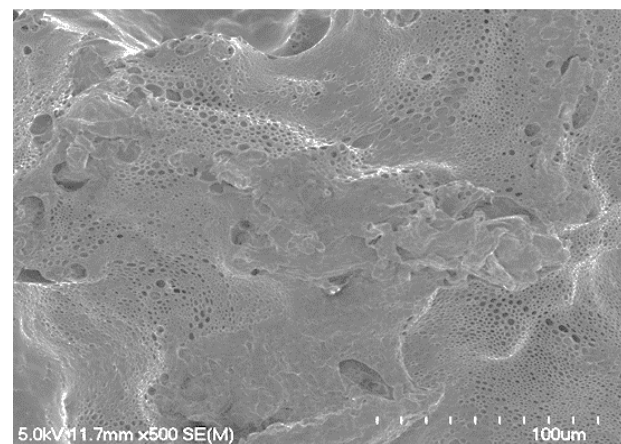
Figure 43: The digested surfaces of DBTP and PLA blends plasticized with tri-ethylene glycol having different compatibilizers. D432.IA and D463.IA were compatibilized with PLA-g-IA, D432.PEOX and D463.PEOX were compatibilized with PEOX alone, and D432.PP and D463.PP were compatibilized with pMDI and PEOX.



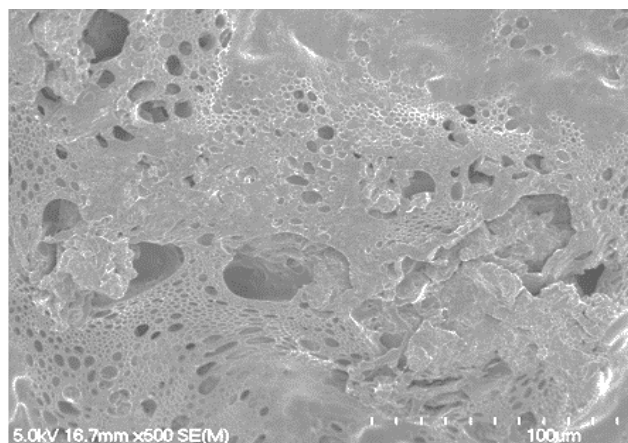
Dg432.IA



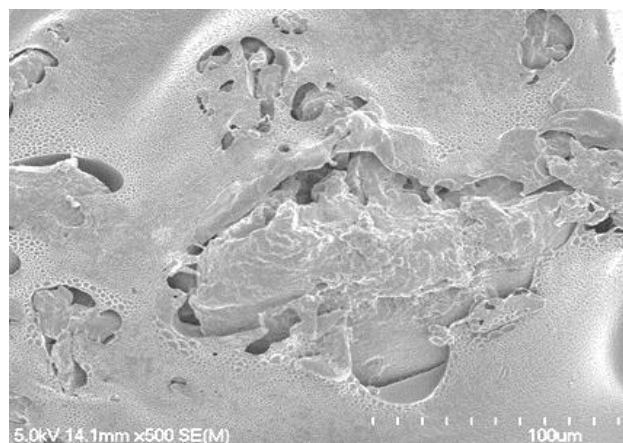
Dg432.PEOX



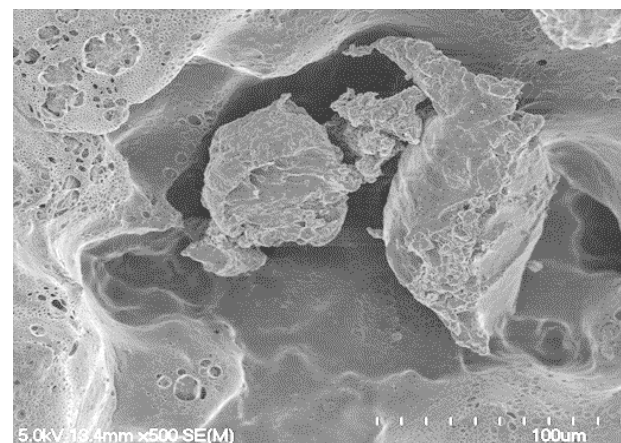
Dg432.PEOX



Dg463.IA



Dg463.PEOX



Dg463.PP

Figure 44: The digested surfaces of DBTP and PLA blends plasticized with glycerol having different compatibilizers. Dg432.IA and Dg463.IA were compatibilized with PLA-g-IA, Dg432.PEOX and Dg463.PEOX were compatibilized with PEOX alone, and Dg432.PP and Dg463.PP were compatibilized with pMDI and PEOX.

4.4.2 Mechanical properties

The mechanical properties of the blends and the pure materials confirmed that the morphology of individual polymers influenced the mechanical properties of the blends significantly.

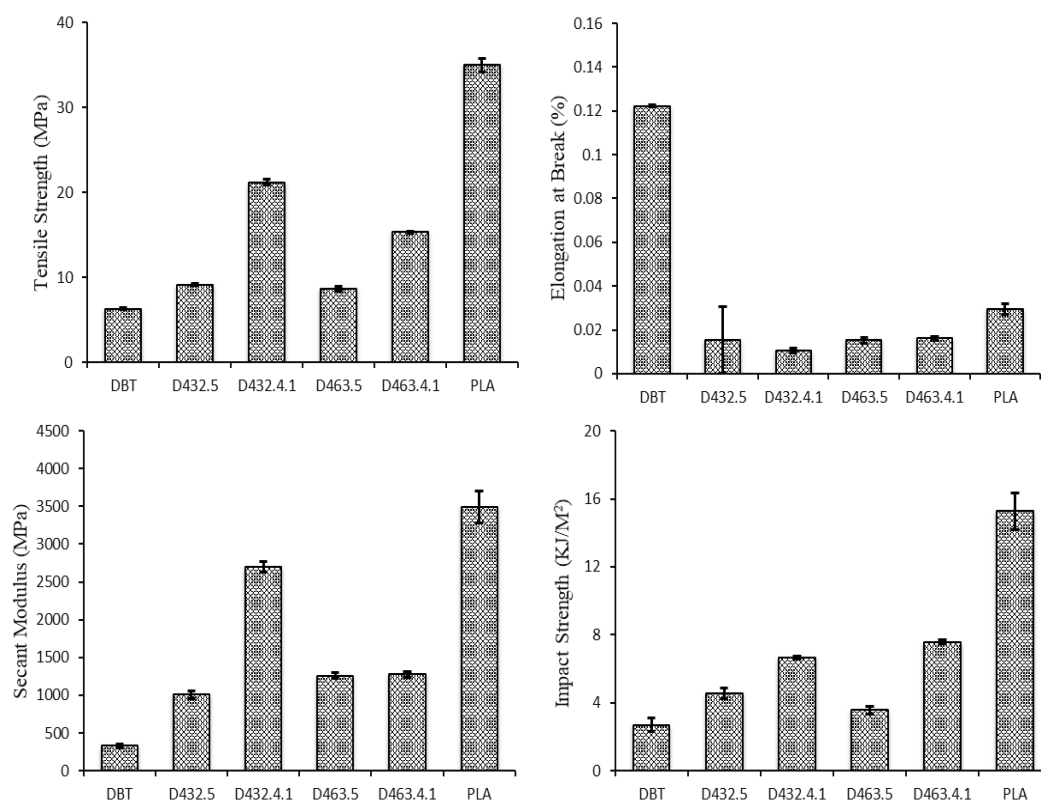


Figure 45: Mechanical properties of DBT/PLA blends with different compatibilization approaches. (D432.5 and D463.5 had itaconic anhydride grafted onto the PLA in the blend while D432.4.1 and D463.4.1 had PLA-g-IA added as a third component in the blend)

Blending DBT/PLA without compatibilizer showed a decrease in the tensile strength of the blend compared to both pure PLA and DBT (Figure 45). Previous research [36; 104; 329-331] suggests this is a result of poor interfacial interaction due to incompatibility between the two polymer phases. DBT/PLA blends without compatibilizer showed clear interstices between the PLA matrix and the DBT domain (Figure 39: 432.PLA and 463.PLA). As suggested by previous researchers [324; 332], DBT and the interstices observed appear to act as stress concentrations in the blend, inducing cracks and subsequently resulting in lower tensile strength.

The mechanical properties of DBT/PLA blends with different compatibilization approaches are shown in Figure 45. Approaches in which itaconic anhydride was

grafted directly onto the PLA in the blend (D432.5 and D463.5) and where PLA-g-IA was introduced as a third component (D432.4.1 and D463.4.1) were used.

D432.4.1 and D463.4.1 showed a significant increase in tensile strength and impact strength compared to D432.5 and D463.5. This supports the observations on their morphology (Figure 40). It is possible that the increase in tensile properties observed for the blends where PLA-g-IA was incorporated as a third component is as a result of the improved dispersion of DBT particles in the PLA matrix and reduced interstices as a result of improved interfacial interaction between both phases in the blends.

An increase in secant modulus was observed for these blends, suggesting the blends were more brittle due to the increased interaction between the DBT and PLA phases. Elongation at break showed no significant difference regardless of the approach used.

Comparing the mechanical properties presented in Chapter 3 (Figure 34) with those presented in this chapter (Figure 45), there is an improvement in the mechanical properties presented in Figure 45. This supports the observations and conclusions drawn from the samples' surface morphologies that the blending and processing method used in this chapter accounted for the improvement observed in the material properties.

Table 8: Mechanical properties of other thermoplastic proteins and polyester blends

Sample	Tensile strength (MPa)	Elongation at break (%)	Modulus (MPa)	Reference
NTP/PBS	13.8	4.91	1289	[104]
NTP/PBAT	12.8	1.2	1500	[332]
PLA/SPC	48.6	1.68	4300	[190]
SPI/PLA	20.1	1.9	3750	[194]
SPC/PLA	22.5	2.1	4250	[194]
SPI/PBS	18.2	51.5	176	[296]

NTP is Novatein® thermoplastic protein, PBS is polybutylene succinate, PBAT is poly(butylene adipate-co-terephthalate), SPC is soy protein composites, SPI is soy protein isolate and PLA is poly(lactic acid).

The tensile strength of blends processed using the second blend approach where PLA-g-IA was added as a third component in the blend (D432.4.1 and D463.4.1) (Figure 45) are comparable to the mechanical properties of other thermoplastic proteins and polyester blends (Table 8) reported by other researchers. D432.4.1 and D463.4.1 also, presented modulus which is comparable to the modulus of other proteins and polyester blends. This supports the conclusion drawn from the morphologies and tensile properties that the blending and processing used in this chapter accounted for the improvement observed in that material properties. Also, that incorporating PLA-g-IA as a third blend component accounted for the highest improvement observed for this blend system.

The mechanical properties of pure PLA, DBT and blends incorporating different compatibilizers and plasticizers are presented in Figure 46. The blends with PLA-g-IA had the highest tensile strength while blends with PEOX alone had the lowest strength. This supports the observed differences in their morphologies. Blends with PLA-g-IA had more homogeneously dispersed DBT particles with reduced DBT agglomerates and finer morphology. This suggests improved interaction between DBT and PLA in the blend, which resulted in an improved tensile strength, while blends with PEOX alone revealed more interstices and higher DBT domain sizes that resulted in lower tensile strength as a result of DBT acting as a stress concentrator in the blends.

Elongation at break showed no significant change in the blends compared to pure PLA for all compatibilizers. The blend with PLA-g-IA had higher toughness than blends with PEOX alone or PEOX and pMDI.

Previous research by Ku-Marsilla et al. [197] suggested that PEOX interacts with NTP through the arrangement of hydrogen-bonded water molecules and the addition of pMDI, further strengthening the interactions between PBS and NTP. It is possible that the lowest tensile and impact strengths observed for blends compatibilized with PEOX alone interacted in a similar manner with DBT and PLA, which was further strengthened with pMDI (blends with pMDI and PEOX).

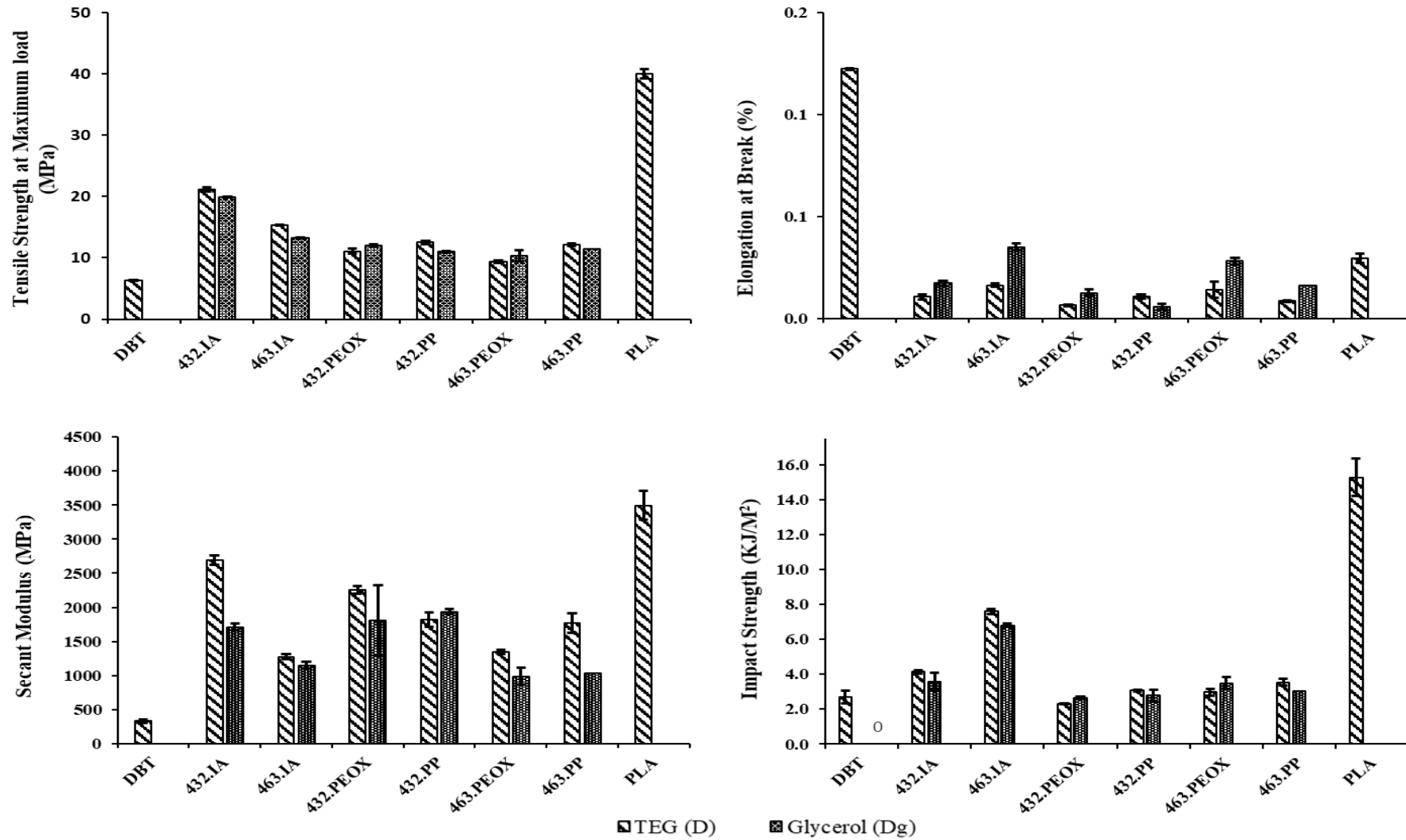


Figure 46: Mechanical properties of DBT and PLA blends with different compatibilizers and plasticizers. 432.IA and 463.IA were compatibilized with PLA-g-IA, 432.PEOX and 463.PEOX were compatibilized with PEOX alone, and 432.PP and 463.PP were compatibilized with pMDI and PEOX.

Secant modulus increased for all blends compared to DBT. However, a decrease was observed in the secant modulus of the blends plasticized with glycerol compared to TEG, except for the 432.PP blend plasticized with glycerol. This suggests that TEG made this blend more rigid, although it showed better dispersion in the blend's morphology and increased tensile strength compared to using only PEOX as a compatibilizer.

The mechanical properties of PLA-g-IA compatibilized blends showed an increase in the tensile and impact strength of TEG plasticized blends compared to glycerol plasticized blends. This confirmed the observations and conclusions drawn from their morphology; TEG is the best plasticizer for PLA-g-IA compatibilized blends.

4.4.3 Dynamic mechanical properties

Glass transition temperature (T_g), molecular mobility and material stiffness in dynamic mode can be evaluated using DMA measurements [333]. The movement and broadening of damping peaks help to predict the degree of miscibility in a polymer blend.

Tan delta ($\tan \delta$), storage modulus and loss modulus as a function of temperature for PLA, DBT and DBT/PLA blends with different compatibilizers and plasticizers are shown in Figure 47 and Figure 48 respectively. PLA showed a sharp and high T_g at approximately 70 °C while DBT exhibited a broad and low T_g at approximately 50 °C. The high damping peak observed for PLA is probably associated with PLA's low crystallinity; PLA becomes very soft when temperatures are above its α -transition of approximately 70 °C, thereby presenting a high damping peak within the transition zone [190]. In contrast, DBT is in its glassy state and has many protein chain interactions, thus presenting a low damping temperature compared to PLA. The damping peak of the blends is lower than the damping peak of PLA. However, it is high compared to the damping peak of DBT. This suggests

that DBT behaved like a rigid material in the blends, reducing the damping peak of PLA in the blends compared to pure PLA.

Good interaction and compatibility between two polymer phases in a blend is usually determined by the movement of their damping temperatures towards each other [197; 199; 296]. A peak and a shoulder were observed on the $\tan \delta$ of the blends. The peak is consistent with the DBT damping temperature while the shoulder observed is consistent with the PLA phase. This confirms that DBT restricted the movement of the PLA chain, thereby reducing the T_g of PLA and leading to broadening of the peak. The shoulder decreased in intensity with the addition of compatibilizers. This may be due to the more effective contribution of the DBT phase to the storage modulus in the rubbery region of PLA with the addition of compatibilizer.

No change was observed in the T_g of PLA in the blend for all compatibilizer types. However, a slight shift was observed in the T_g of DBT in the blend toward the T_g of PLA for blends compatibilized with PLA-g-IA, except for Dg463.4.1. This indicates a degree of miscibility between DBT and PLA with the addition of PLA-g-IA.

The blends plasticized with glycerol showed an increase in their $\tan \delta$ peak height compared to TEG plasticized blends. However, the shoulder observed in the blends was broader for TEG plasticized blends compared to glycerol plasticized blends. This suggests better interaction in these blends, as suggested from the mechanical and morphological properties. Also, the peaks and shoulders observed in the $\tan \delta$ graph of the blends plasticized with TEG appeared at temperatures closer to each other than in blends plasticized with glycerol. This also supports the interaction and miscibility suggested for blends plasticized with TEG.

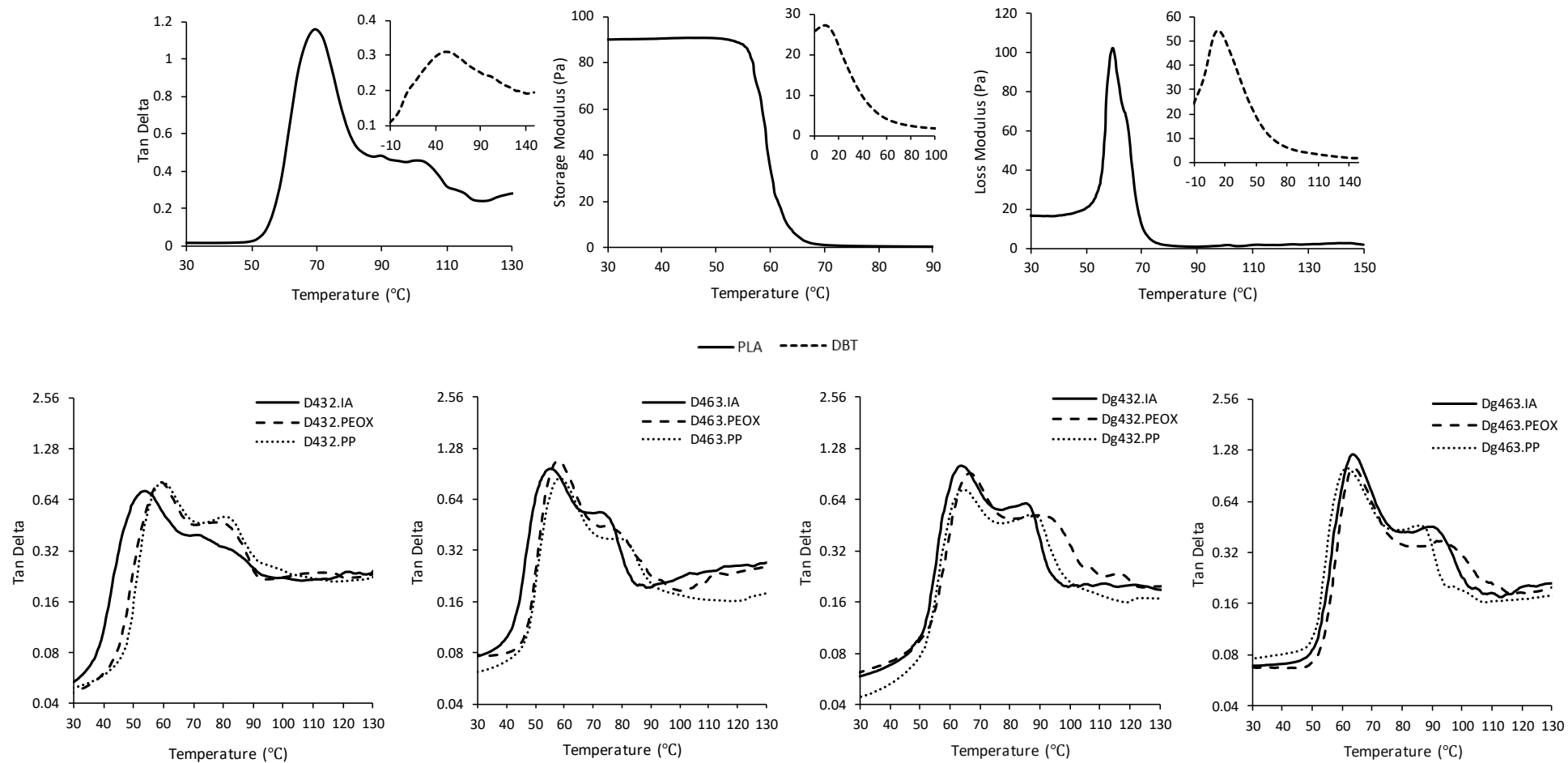


Figure 47: Tan δ of DBT, PLA and DBTP/PLA blends with different plasticizers and different compatibilizers. Sample names starting with D were plasticized with TEG while those with Dg were plasticized with glycerol. 432.IA and 463.IA were compatibilized with PLA-g-IA, 432.PEOX and 463.PEOX were compatibilized with PEOX alone, and 432.PP and 463.PP were compatibilized with pMDI and PEOX.

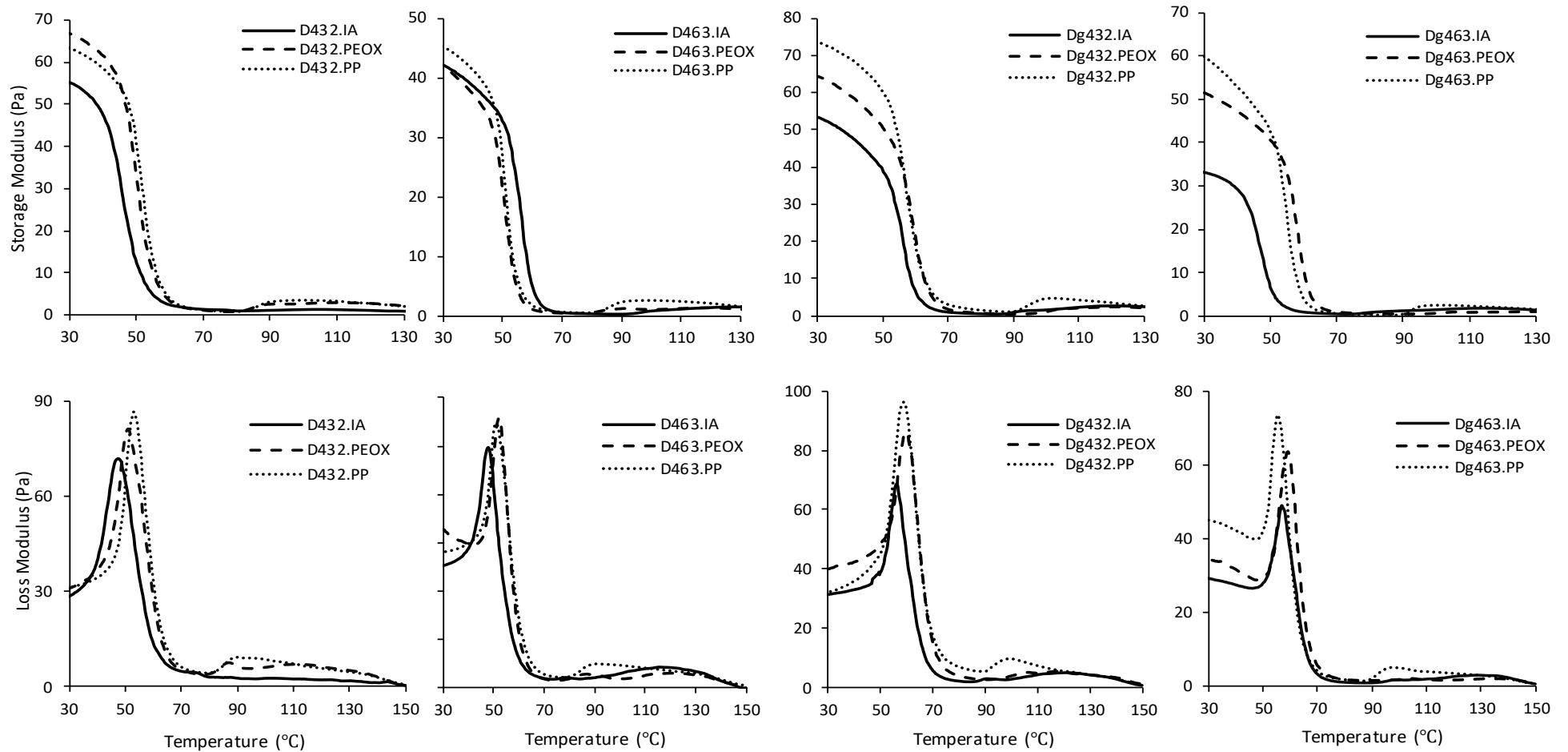


Figure 48: Storage and loss moduli of DBTP/PLA blends with different plasticizers and different compatibilizers. Sample names starting with D were plasticized with TEG while those with Dg were plasticized with glycerol. 432.IA and 463.IA were compatibilized with PLA-g-IA, 432.PEOX and 463.PEOX were compatibilized with PEOX alone, and 432.PP and 463.PP were compatibilized with pMDI and PEOX.

High storage modulus was observed for TEG plasticized blends compared to glycerol plasticized blends, indicating an improvement in the interaction between DBT and PLA phases in blends plasticized with TEG. The blend's storage modulus suggests that PLA-g-IA is less rigid than PEOX alone or PEOX and pMDI.

The loss modulus curve of PLA showed a sharp peak at 60 °C while DBT showed a broader peak at approximately 20 °C. The blends of DBT and PLA showed peaks at approximately 50 °C with a drop when the T_g of PLA was reached, followed by recovery to a significant degree between 90 and 130 °C.

It is expected that the loss modulus curve of a polymer blend will be similar to the loss modulus curve of the continuous phase, as it provides a greater contribution to the loss modulus of the blend. The loss modulus curves of the blends resembled that of PLA, although there was a decrease in the peak's intensity and an apparent recovery between 100 and 120 °C. This recovery was probably due to the cold crystallization of PLA. The similarities in the curves of PLA and the blends support the idea that PLA coalesces and encapsulates DBT, making PLA the continuous phase and DBT the dispersed phase, as observed in their morphologies.

The peak intensities of blends compatibilized with PEOX alone and PEOX/pMDI increased significantly compared to the blends compatibilized with PLA-g-IA. However, for PLA-g-IA compatibilized blends, the peak intensity of glycerol plasticized blends decreased compared to TEG plasticized blends, while for the dual compatibilized blends (PEOX/pMDI), the glycerol blends peak intensities increased compared to the TEG plasticized blends. However, a slight decrease and no change were observed in the peak intensities of blends compatibilized with PEOX alone. This suggests that TEG is a better compatibilizer for PLA-g-IA compatibilized blends, while for dual compatibilized blends, glycerol is preferable. Blends compatibilized with PEOX alone showed no effect on the peak intensities for glycerol and TEG plasticized blends.

4.4.4 Intrinsic viscosity

The effects of different compatibilizers and different plasticizers on the intrinsic viscosity of the PLA in the blends are shown in Figure 49. PLA's intrinsic viscosity was 0.2134 dL/g. All blends displayed a higher intrinsic viscosity. This is probably either as a result of the bulky functional groups of the compatibilizers (i.e., IA, PEOX/pMDI) in the blends, altering chain mobility, or of increased crosslinking in the blend due to plasticization, as both TEG and glycerol are soluble in chloroform. These would increase the end-to-end length of the dissolved molecule, reflecting in an increase in the intrinsic viscosity compared to pure PLA.

The intrinsic viscosity of PLA in the blends compatibilized with PEOX/pMDI increased in comparison to PLA-g-IA compatibilized blends. This would suggest that chain scission did not occur with PEOX/pMDI compared to blends with PLA-g-IA.

The PLA-g-IA compatibilized blend showed no change in intrinsic viscosity between the TEG plasticized and glycerol plasticized blends. This suggests that the plasticizers (TEG and glycerol) did not contribute to the increase in intrinsic viscosity observed for the PLA in this blend system. It is possible that the bulky functional group of IA altered the chain mobility, which is reflected in an increase in intrinsic viscosity. Marsilla and Verbeek [142] suggested a similar effect on PLA with the addition of itaconic anhydride. For PEOX/pMDI compatibilized blends, an increase was observed for blends plasticized with glycerol compared to TEG, suggesting that the bulky functional group, as well as glycerol, contributed to the chain mobility observed, resulting in an increased intrinsic viscosity.

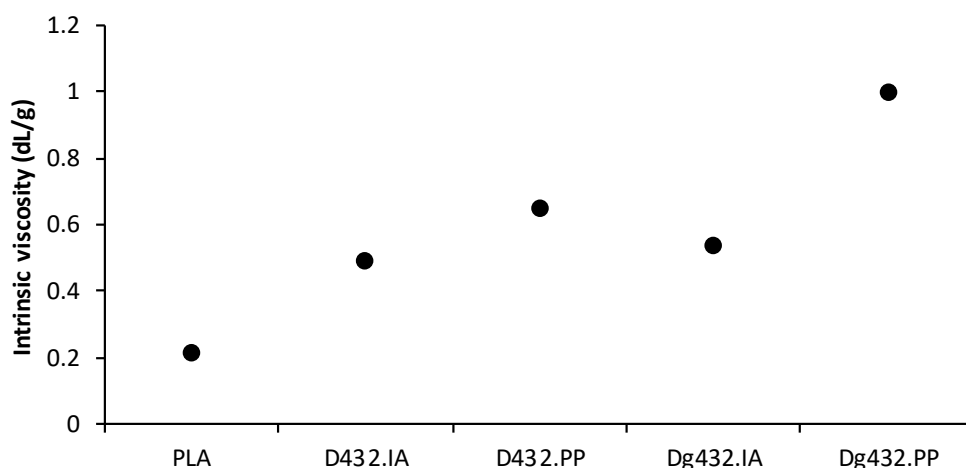


Figure 49: Intrinsic viscosity of PLA (dried, grafted and extruded) and different blends of PLA and DBTP. Sample names starting with D were plasticized with TEG while those with Dg were plasticized with glycerol. 432.IA were compatibilized with PLA-g-IA, and 432.PP were compatibilized with pMDI and PEOX.

4.5 Conclusion

The morphology of DBT/PLA blends without compatibilizer revealed the presence of interstices and clear agglomerates of DBT embedded in the PLA matrix, indicating the presence of interfacial tension and leading to poor mechanical properties. However, with the addition of compatibilizer, an even distribution of the DBT particles and reduced interstices was observed. The morphology also suggested that PLA is the continuous phase while DBT is the dispersed phase. This is supported by the similarities in the loss modulus curves of PLA and the blends. Comparing the different compatibilizers, PLA-g-IA showed a better morphological structure compared to all other compatibilizers used (pMDI and PEOX or PEOX alone), producing much finer and more evenly dispersed DBT particles in the blend matrix. It is thought that the DBT-rich phase was encapsulated in the PLA-rich phase, which resulted in the finer phase structure and improved adhesion observed in the SEM studies.

The mechanical properties of DBT/PLA showed that PLA-g-IA and TEG are the best compatibilizer and plasticizer, respectively, for DBT/PLA blend systems. Comparing the different compatibilizers sampled, PEOX alone and PEOX/pMDI showed a decrease in tensile and impact strength compared to the PLA-g-IA

compatibilized blend. Also, the addition of PLA-g-IA as a third blend component was accepted as the best compatibilizer approach because of the increase observed in the tensile and impact strength of D432.4.1 and D463.4.1 compared to D432.4 and D463.5 respectively. More evenly dispersed DBT particles within the PLA matrix and finer morphology were also observed for D432.4.1 and D463.4.1.

The peak and the shoulder observed in the $\text{Tan } \delta$ of DBT/PLA blends shifted towards each other compared to the $\text{Tan } \delta$ of pure PLA and DBT. The blends with PLA-g-IA had the highest shifts towards each other, suggesting that better interfacial adhesion was achieved in the presence of PLA-g-IA.

Comparing the data obtained in Chapter 3 to the data obtained in this chapter, the blending and processing method used in this chapter accounted for the improvement observed for this blend system.

This study successfully demonstrated that PLA-g-IA was the most effective compatibilizer for DBT/PLA blends. Using PLA-g-IA produced a significant effect on the morphology and properties of DBT/PLA blends compared to PEOX alone and PEOX/pMDI. This study also demonstrated that adding PLA-g-IA as a third component in the blends is an effective compatibilization approach, and TEG was considered the best plasticizer for PLA-g-IA blend systems.

Chapter 5

Sheet Extrusion of DBT/PLA Blends

Sheet Extrusion of DBT/PLA Blends

5.1 Abstract

The feasibility of processing DBT/PLA blends to form continuous sheets was demonstrated with twin-screw extrusion using different processing methods and different processing steps. The effect of using either amorphous or semi-crystalline PLA, decoloured bloodmeal thermoplastic powder (DBTP) or decoloured bloodmeal thermoplastic granules (DBTG), and 2-step (sheet extrusion of the combined blend components) or 3-step processing (pre-compounding of the blend components before sheet extrusion) methods was assessed using SEM, water absorption and mechanical properties, as well as rheology characterization. The collective effect of reduced heat processes and processing steps (i.e., a 2-step process, elimination of pre-compounding of DBTP into DBTG and blending with amorphous PLA, which requires low processing heat to soften) was observed to have the greatest effect on the properties of the produced sheets, and this was evident from the observed properties of the blend processing using M₄ method (blend with amorphous PLA and . M₄ produced a sheet with the highest tensile properties and the lowest water absorption percentage of about 8% within the first 24 h of immersion, and a relatively smooth surface without the presence of surface defects compared to other methods. Therefore, M₄ was accepted as the preferred processing method for DBT/PLA based sheets.

5.2 Introduction

The use of bio-based polymers has received considerable attention in recent years because of their potential role as industrial polymer materials [334]. This is due to growing environmental awareness and the imminent petroleum crisis. Bio-polymers such as proteins, starch, and their blends have been investigated for the preparation of films [182; 211-213; 222; 229; 335-337]. Bio-polymers have been used to produce packaging materials to solve the end-of-life issues of plastic packaging. Proteins, cellulose, starch, and polymers synthesized chemically from monomers such as lactic acid have been used for commercial packaging materials [338].

Bloodmeal, a by-product of meat processing with a high protein content, has been processed using peracetic acid (PAA) to remove odour and pigmentation [11]. The processed bloodmeal, known as decoloured bloodmeal (DBM), has been subsequently processed into bioplastics using thermo-mechanical processing techniques such as extrusion, compression, and injection moulding [184]. The bioplastic is referred to as decoloured bloodmeal thermoplastic (DBT).

Recent research into bio-polymers for sheet extrusion processing has mainly focused on film extrusion processing of starches, proteins and their blends [211-215]. The limited data available on sheet processing of starch, and protein film extrusion processing, are mainly based on plasticization to improve material properties. However, sheet and film extrusion use the same principles and processing techniques. Their differences lie in the material thickness: sheets have a thickness exceeding 250 μm , and below this thickness, materials are referred to as films [118].

For most proteins and their blends, their films are produced by solution casting, where protein, plasticizers and other agent are dissolved in an appropriate solvent, and the solution is then cast on a non-stick flat surface to allow the solvent to evaporate. The film is then peeled off. Solution casting is very expensive and difficult to upscale, which limits its uses in the industry. Melt processing of films such as film/sheet extrusion is a promising technique for preparing packaging film because of its ease of processing and versatility.

Extrusion is commonly used to produce plastics on a commercial scale [338]. Therefore, processing DBT/PLA using extrusion will increase its potential for commercialization. The application of extrusion technology for the production of protein films/sheets has been a challenge, and there is limited literature available. Ha and Padua [339] extruded zein sheets plasticized with fatty acids. The mixture of zein and fatty acid dissolved in aqueous ethanol and mixed with cold water to form a resin was dried and fed into an extruder with aqueous ethanol to aid processing. They produced extrudates that were collected and rolled into a sheet. The effect of oleic acid content on the tensile properties of rolled zein sheets was investigated by Santosa and Padua [340], who reported a decrease in the tensile

strength of the produced sheet from 9.4 MPa to 2.2 MPa with an increase in oleic acid content, while elongation at break reached a maximum of 46.9% for sheets containing 0.7 g oleic acid.

The previous chapters have demonstrated the possibility of blending DBT/PLA to produce an improved material compared to DBT. Decoloured bloodmeal, SDS and TEG were blended to produce decoloured bloodmeal powder, which was successfully compounded with PLA and compatibilizer using reactive extrusion to produce a decoloured bloodmeal thermoplastic (DBT)/PLA blend. However, for value-added end products, it is advantageous to sheet process the produced material. The technologies used to convert most polymer resins into sheets and other useful products require an understanding of the material's flow properties (rheology). Therefore, the measurement of DBT/PLA blends' rheological properties, as well as sheet processibility, is important.

The objective of this chapter was to determine the feasibility of extruding DBT/PLA blends to form a continuous sheet. It aimed at determining the effect of processing methods on the sheets' mechanical and structural properties. Moisture absorption properties were also analyzed, along with measurement of the blends' rheology to support sheet processing.

5.3 Material and Methods

5.3.1 Materials

Bloodmeal (BM) was obtained from Wallace Corporation Limited, New Zealand and used as received. Analytical grade itaconic anhydride (IA), dicumyl peroxide (DCP), acetone, 50 wt. % hydrogen peroxide, and technical grade sodium dodecyl sulphate (SDS) and triethylene glycol (TEG) were all acquired from Sigma Aldrich Auckland, New Zealand. Peracetic acid (Peraclean 5) was acquired from Evonik Industries, Morrinsville, New Zealand. Poly (lactic acid) (PLA) grade 3052D was purchased from NatureWorks LLC, Minnetonka, MN, sourced from Clariant New Zealand Ltd, Auckland, New Zealand in pellet form. Distilled water was produced on site at the University of Waikato.

5.3.2 Sample Preparation

5.3.2.1 PLA GRAFTING

PLA was modified with itaconic anhydride using free radical grafting [142] to create reactive side-groups, as described in Chapters 3 and 4 respectively. PLA was dried at 80 °C for 4 h to control moisture. 4.2 g itaconic anhydride and 0.8 g dicumyl peroxide were dissolved in 30 mL acetone. The preformed solution was poured over the oven dried PLA and was kept in the fume hood for about 2 h. The solution was decanted before oven drying the PLA for 3 h at 50 °C. The material was reactively extruded to produce PLA-g-IA using a LabTech twin screw co-rotating extruder with a screw diameter of 20 mm and L/D of 44:1. The temperature profile increased along the barrel from 145 (feed zone) to 180 °C, with the highest temperature occurring at the mid-zone and 155 °C at the die zone. A constant screw speed was maintained at 150 rpm. A vacuum pump was attached on the 7th heating zone of the extruder to remove vapour generated during extrusion. The pelletized PLA-g-IA was oven dried for 12 h prior to blending to minimize hydrolysis during melt processing.

5.3.2.2 BLOODMEAL DECOLOURING

Bloodmeal was decoloured using a solution of peracetic acid (PAA) according to previous methods [11; 111] as used in Chapters 3 and 4. A 4 wt.% PAA solution was prepared by diluting 5 wt.% PAA stock solution with distilled water at a constant ratio of 80:20 respectively. 150 g bloodmeal was decoloured by adding 450 g of 4 wt.% PAA in a high-speed mixer. The mixture was allowed to mix continuously for 5 min to ensure homogenous decolouring of the bloodmeal. Then 450 g of distilled water was added and the slurry was mixed for another 5 min to ensure complete dilution. The slurry was neutralized by adjusting to pH7 with sodium hydroxide solution. The neutralized slurry was filtered using a wire mesh sieve (aperture size 60) and subsequently washed by adding another 450 g of distilled water. The decoloured bloodmeal (DBM) was dried for approximately 15 h in a 75 °C oven.

5.3.2.3 DECOLOURED BLOODMEAL THERMOPLASTIC PREPARATION

Decoloured blood-meal thermoplastic powder (DBTP)

A D463 formulation of decoloured bloodmeal thermoplastic powder (DBTP) was formulated by dissolving 6 pph_D SDS in 40 pph_D water heated to 60 °C while stirring. The solution was added to decoloured bloodmeal in a high-speed mixer and mixed for 5 min, 30 pph_D TEG was added to the mixture and mixed for another 5 min to ensure a homogeneous mixture was obtained. The prepared DBTP was stored in an airtight bag overnight at 2 °C in a fridge to equilibrate. The produced DBTP was dried to equilibrium moisture content in a 75 °C oven prior to blending with PLA.

Decoloured blood-meal thermoplastic granules (DBTG)

Following the same method used for DBTP preparation, the prepared D463 formulation of DBTP was stored in an airtight bag overnight in a fridge at 2 °C to equilibrate. Then the equilibrated DBTP was compounded using a twin screw co-rotating extruder (LabTech). The extruder barrel had eleven heating zones, and the screw speed was maintained at 150 rpm. The compounding extrusion temperatures were 100 (feed zone), 100, 100, 100, 100, 100, 100, 100, 100, 115 and 120 °C (die zone). The extrudate was granulated using a tri-blade granulator from Castin Manufacturing Limited to produce decoloured bloodmeal granules (DBTG). The produced DBTG were dried to equilibrium moisture content in a 75 °C oven prior to blending with PLA.

5.3.2.4 BLEND PREPARATION

DBTP, DBTG and PLA grafting was performed before blending. All blends contained 50 wt.% DBTP, 40 wt.% PLA and 10 wt.% PLA-g-IA. DBTP and DBTG formulations were completely dried, prior to blending, in a 75 °C oven to equilibrium weight to eliminate inbound and processing water and thus control PLA hydrolysis during blending. Blends were compounded using the same extruder profile used for grafting PLA. The extrusion temperatures varied from 70 to 145 °C (with the lowest temperature at the feed zone and the highest at the die zone). The extrudate was granulated using a tri-blade granulator from Castin Manufacturing Limited. Once DBTP or DBTG is compounded with PLA and PLA-g-IA, it is referred to as a DBT/PLA blend.

5.3.2.5 SHEET PROCESSING

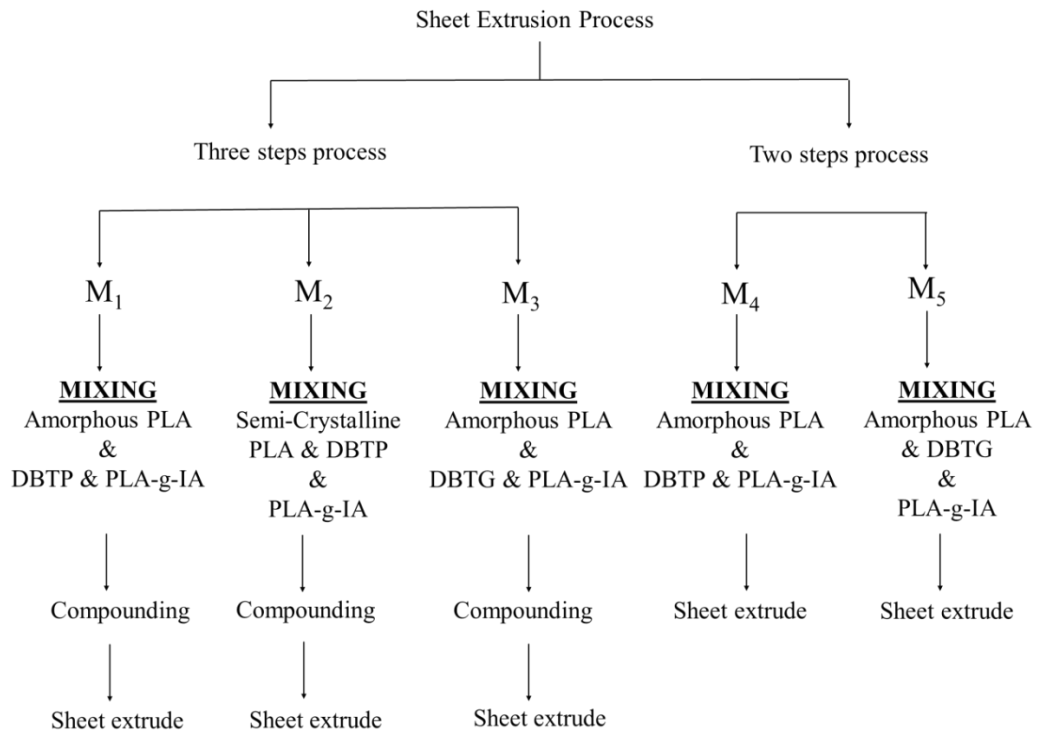


Figure 50: Summary of sheet extrusion methods trialled

Different sheet processing methods, as shown in Figure 50, were trialled. DBT/PLA blends were extruded in a LabTech twin screw co-rotating extruder with a screw diameter of 20 mm and L/D of 44:1, where D and L are the diameter and length of the screw, respectively. Constant screw speed and the feed rate were maintained at 30 rpm and 150 rpm respectively. The blends were formed into a sheet by passing them through a slit die. The extruder heating zones were operated at 100, 100, 100, 130, 130, 150, 150, 140, 140, 140 °C and the slit die was operated at 120 °C for amorphous PLA blends and 130°C for semi-crystalline PLA. However, to ensure the melting of the crystal region of semi-crystalline PLA during blending, barrel temperatures of 100, 100, 130, 130, 150, 150, 150, 140, 140, 140 °C were used for compounding. The sheet coming out of the slit die was pulled with a manual roller. The thickness of the sheets ranged from 2.5 to 3.0 mm. Pure PLA was extruded as a control to account for the effect of the extruder and die profile.

The rationale for sheet extrusion methods

In the previous chapters, it has been shown that blending DBT with PLA is possible. However, it is not a straightforward process due to the temperature requirements of both materials. PLA can be amorphous or semi-crystalline, which are different grades. For this research work, semi-crystalline grade PLA was used. To obtain an amorphous PLA, the semi-crystalline PLA was extruded to ensure that we had comparable data, as different grades of PLA have varying properties and may affect blends' properties differently.

Semi-crystalline PLA requires processing at a high temperature, above its melt temperature, to ensure melting of the crystalline region during blending with DBT. This implies that DBT has to be processed at a temperature above its degradation temperature, which will degrade the DBT protein structure. However, blending DBT with amorphous PLA involves processing at a much lower temperature, which allows softening of the PLA molecules, enabling the compounding of PLA and DBT at a much lower temperature. This informed the decision to investigate the effect of using either amorphous PLA (M₁) or semi-crystalline (M₂) on blend properties.

Favouring amorphous PLA, investigation into the best DBT starting material – either DBTP (M₁) or DBTG (M₃) – was conducted. DBTP is the mixture of decoloured bloodmeal and additives (water, SDS, TEG) before they are compounded into a polymer and DBTG is an already compounded polymer. It was assumed that if the starting material is already a thermoplastic, it will behave like any other thermoplastic polymer during the mixing process. However, it seemed likely that blending with DBTP would be more favourable as it reduces excessive heat treatment of DBT, ensuring that protein crosslinks are not destroyed. Also, it was likely that during blend compounding or sheet extrusion, DBTP would also be compounded into a thermoplastic polymer while interacting with added compatibilizer and PLA. Therefore, it was expected that blends with DBTP would have better properties than those prepared with DBTG.

The previous chapters have shown that the choice of starting material affects the blend's morphology. Blend morphology is dependent on the viscosity ratio, interfacial tension, and shearing in the extruder [15; 132]. Therefore, it is important

to study the morphology of the blends as morphology is also directly linked to the mechanical properties and permeability of the sheet.

For wider acceptance of any material, it is important to consider the commercial aspects of its processing. Cheaper and shorter processes are always desirable. Considering this, extrusion of the sheet after mixing (a two-step process) was considered. During sheet processing, material compounding still occurs, so we used a twin-screw extruder, which is preferable for material compounding in the sheet extrusion process.

In order to assess the different methods used, several variables were investigated. The effect of using semi-crystalline or amorphous PLA on the final sheet was investigated by comparing M₁ to M₂ (Figure 50). The effects of processing using DBTP or DBTG as a DBT starting material for the blends were investigated by comparing M₁ to M₃ (Figure 50). This considered the effect of multiple heat treatments of DBT on the sheet properties (i.e., pre-compounding prior to compounding with PLA and PLA-g-IA). The third variable considered the commercial aspects of DBT/PLA sheet processing as reduced processing is always desirable when upscaling production processes. Therefore, the possibility and effects of reduced processing step sizes were considered by using a two-step process. M₄ was compared to M₁ and M₅ to M₃ for this purpose.

5.3.3 Sample Analysis

5.3.3.1 SURFACE MORPHOLOGY

The phase structure of the blends was investigated using a Hitachi S-4700 field emission Scanning Electron Microscope (SEM). The extruded sheet specimens were cut using a Hafco Woodmaster BP-480 band saw. The specimens were sputter coated with platinum using a Hitachi E-1030 Ion sputter coater before scanning.

5.3.3.2 MECHANICAL PROPERTIES

The mechanical testing was performed according to ASTM D638 using an Instron Universal Testing machine (model 33R4204) at a crosshead speed of 5 mm/min and an extensometer gauge length of 50 mm. Five samples were tested for each sample

type to obtain an average value. The samples tested were cut from the extruded sheets with a Hafco Woodmaster BP-480 band saw.

5.3.3.3 WATER ABSORPTION

All samples were oven dried at 70 °C to equilibrium weight. Water absorption testing was performed according to ASTM D570-98 (ISO 10350). Dried samples were immersed in distilled water at room temperature for 24 h or until equilibrium (until water absorption essentially ceased). Samples were removed from the water as desired, patted dry with tissue paper to remove excess water and weighed. The absorption was calculated on a dry sample weight basis.

5.3.3.4 RHEOLOGY MEASUREMENTS

The flow behaviour of DBT/PLA blends was measured using a Gottfert high-pressure capillary rheometer. The rheometer was equipped with two capillaries: an orifice (P1) and a 180 °C entrance 30 mm capillary (P2). The rheological measurements of PLA and the blends were carried out at 150 °C and 200 °C respectively. The temperature used was the highest used in the sheet extruder for the respective materials. This was to ensure that similar conditions to those used in the sheet extruder were achieved in the rheometer. Piston speeds used were 6.60, 3.33 5.00 and 1.66 mm/s, corresponding to apparent shear rates of 373.5, 749.25, 1125 and 1498.5 S⁻¹ respectively. The WinRheo® application was used to extract time and pressure data for both capillary and orifice. Apparent viscosity was determined by calculating the ratio between apparent shear stress [341] as shown in Equation (15) and apparent shear rate, as in Equation [342] (16).

$$\gamma_{\alpha} = \frac{4Q}{\pi R^3} \quad (15)$$

$$\tau_{\alpha} = \frac{\Delta P}{2(L/R)} \quad (16)$$

Bagley correction [342], corresponding to adjustment for excess pressure at the die entrance, was calculated using Equation (17),

$$\tau_{\omega} = \frac{\Delta P - \Delta P_e}{2L/R} \quad (17)$$

where ΔP is the pressure in capillary P_2 and ΔP_e is the pressure at the orifice.

The Rabinowitsch-Weissenberg correction [343] was used to account for the influence of shear thinning in the calculation of shear rate (see Equation (18)) and corresponding viscosity.

$$\gamma_{\omega} = \frac{(3n+1)}{4n} \gamma_{\alpha} \quad (18)$$

5.4 Results and Discussion

Successful sheet processing of DBT/PLA blends will increase their potential for broader use and acceptance. PLA can be extruded into sheets because of its good melt properties and low elongational viscosity, and it has been used to fabricate biaxially oriented films [344]. On the other hand, DBT is not sheet extrudable due to its high elongational viscosity, which will limit its flowability and the ability to fill the sheet die. It is expected that blending PLA will enhance the sheet processability of the DBT.

The feasibility of extruding DBT/PLA blends into a continuous sheet using a twin-screw extruder was demonstrated in this chapter. Figure 51 illustrates twin-screw extrusion formation of DBT/PLA sheet with a slit die. Extruded sheets were flexible upon exiting the dies but hardened upon cooling.



Figure 51: Twin-screw extrusion of DBT/PLA sheet using a LabTech twin screw co-rotating extruder.

5.4.1 Sheet formation

Sheet processing of DBT based material was carried out using several methods referred to as M₁ to M₅, and different numbers of processing steps (2- or 3-step processes) (see Figure 50). The 3-step process includes mixing of the blend components, and compounding using an extruder before sheet extrusion, while the

2-step process involves the mixing of blend components and sheet extrusion of the mixed blend components without prior compounding of the blends.

M₁ contained blends of amorphous PLA, DBTP, and PLA-g-IA; M₂ contained semi-crystalline PLA, DBTP, and PLA-g-IA; M₃ contained amorphous PLA, DBTG, and PLA-g-IA; M₄ contained amorphous PLA, DBTP, and PLA-g-IA; and M₅ contained amorphous PLA, DBPG, and PLA-g-IA. M₁ and M₂ investigated the effect of using either amorphous or semi-crystalline PLA on sheet properties while M₁ and M₃ investigated the effect of using either DBTP or DBTG as a decoloured bloodmeal thermoplastic material on the sheet properties. M₄ and M₅ considered the possibility of reducing the processing steps and the effects of this on sheet properties.

Blends with semi-crystalline PLA were processed at a die temperature of 130 °C. However, in order to ensure the melting of the crystalline region of PLA, barrel temperatures of 100, 100, 130, 130, 150, 150, 150, 140, 140, 140 °C were used. Other blends were produced at a 120 °C die temperature. Processing sheets using different methods at die temperatures above 140 °C proved problematic as shown in Figure 52. Material flowed evenly but lacked sheet forming ability (poor cohesion). This was probably due to the degradation of DBT at high temperature, as suggested by another study, which indicated that high processing temperature leads to protein degradation and consequent difficulty in sheet formability [345].



Figure 52: Image of poorly formed DBT/PLA sheets processed at die temperatures above 140 °C

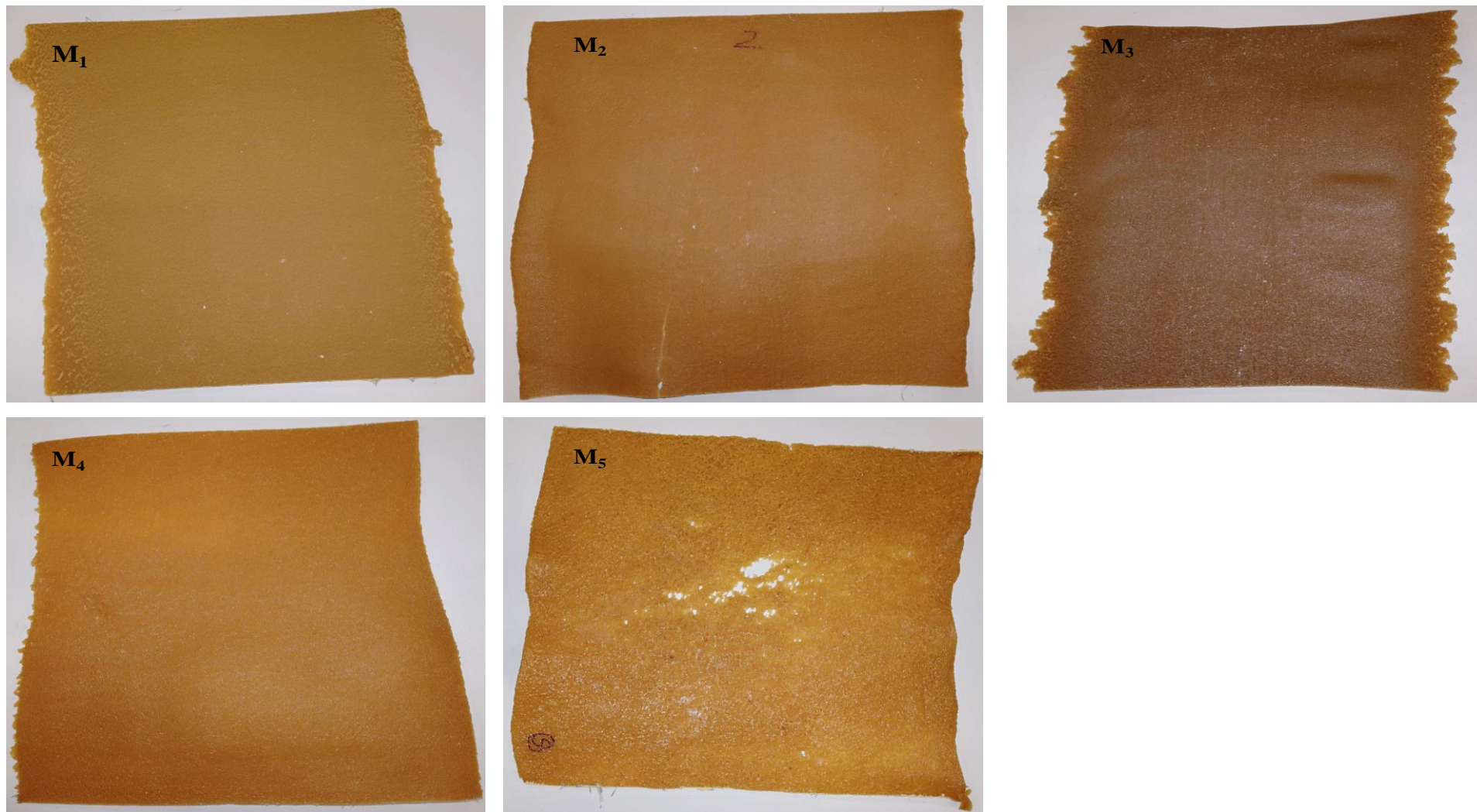


Figure 53: Photograph of DBT/PLA sheets produced using different processing methods ($M_1 - M_5$) and different processing steps (two or three steps). (see Figure 50)

Figure 53 shows general photographs of DBT/PLA blend sheets. Each sample (using different processing methods) produced a sheet with dimensions exceeding 100 cm x 25 cm (Figure 54), which was large enough for characterization of the material's properties. The sheets illustrated were processed using the methods described in figure 50. The surface of sheet M₁ was slightly rough, and there were no cracks or micro-holes, and while the surface of sheet M₂ was smooth, there was a crack, induced during test sample cutting, which is probably evidence of material brittleness. M₃ produced a sheet with a semi-smooth surface with no cracks. However, there were slight small ripples present. The produced sheet was darker than the other sheets produced. This suggests a degree of DBT degradation, possibly as a result of high processing temperature or excessive exposure of DBT to heat due to the extra heat treatment applied to compound the decoloured bloodmeal powder and additives into DBTG. M₄ produced a sheet with a relatively smooth surface compared to the other produced sheets. M₅ produced a substandard sheet with a relatively rough surface, displaying cracks and micro-holes. The most promising sheet was M₄, as it produced the best consolidated sheet with the smoothest surface.

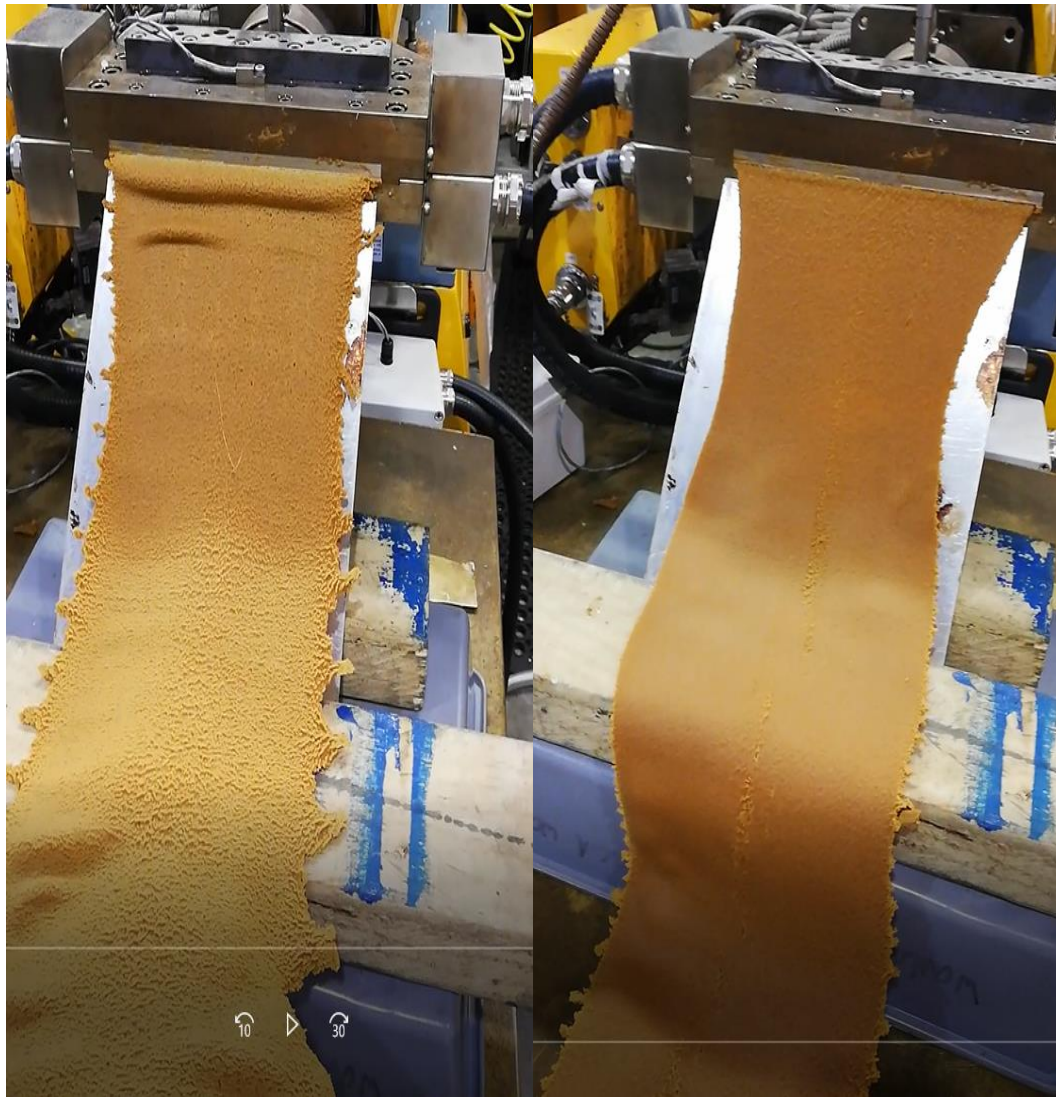


Figure 54: Image of produced DBT/PLA blend sheets produced using different methods (M_1 and M_4 respectively).

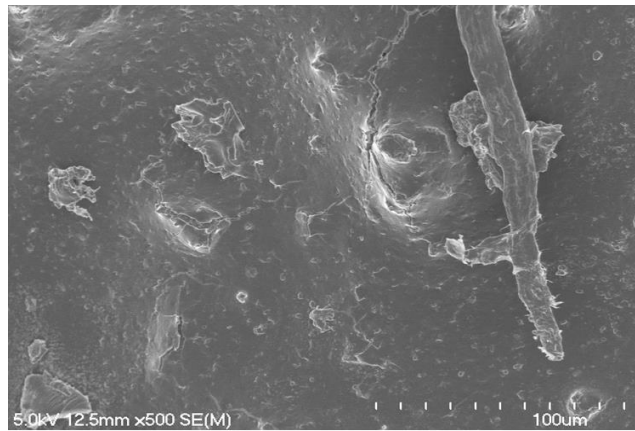
5.4.2 Surface morphology

Surface morphology can provide information on the interfacial interaction and dispersion of material components in a blend. The interaction of protein with other components in a blend for a material considered for sheet processing is very important as the properties of the produced sheets depend mainly on these interactions. The interaction of protein with other components in a blend determines the cohesion of protein-based material components. For example, Farnum et al. [346] suggested that hydrophobic interaction between proteins and lipids played a vital role in the structural stability of soy films.

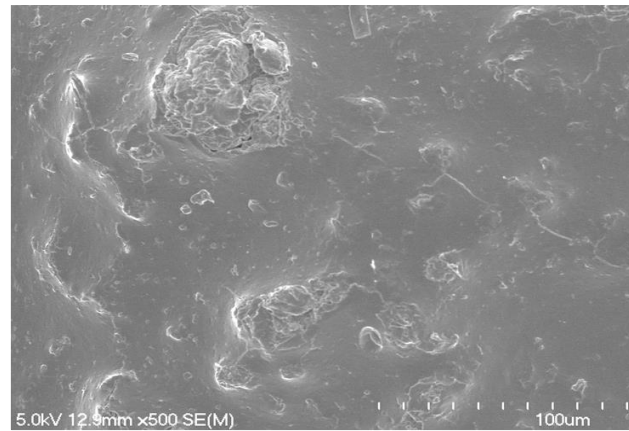
SEM was used to examine the surface morphologies of DBT/PLA blends processed using different methods and processing steps (see figure 50 for the methods used). The resulting micrographs are shown in figure 55. The blends' sheet structures showed a homogeneous blend at a microscopic level, suggesting properly dispersed and evenly distributed material phases. Rough and coarse surface structures were observed for all blend methods. However, M₄ showed relatively smooth surface topographies compared to the other processing methods. This is also supported by the observation in figure 53, and is probably due to either the reduction of heat treatment on DBTP by eliminating the heat applied during pre-compounding of DBTP into DBTG, and reducing the heat applied during blend compounding with PLA and PLA-g-IA before sheet extrusion, or better dispersion of DBT particles due to the reduced particle sizes of DBTP (powder) compared to granules. This observation may also be as a result of PLA encapsulating DBT particles to produce a relatively smooth surface. This was further investigated through the sheet mechanical properties.

The surface structure showed a well-consolidated material with no voids. However, DBT domains were observed in the sheet surface micro-structure. M₄ showed few DBT domains (smaller sizes) compared to the other methods. It is expected that the DBT phase should be smaller in size and produce continuous domains in the sheet surface structure as high shear rates facilitate the dispersion and distribution of the minor phase.

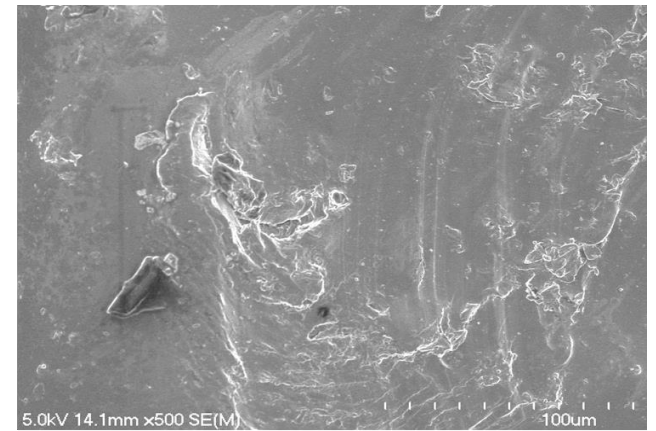
No difference was observed in the surface structure of M₁ compared to M₂. Comparing M₁ to M₃, there was again no difference observed in the surface structure of the blends. Comparing both processing steps trialled, no significant change was observed in the blends with DBTG. However, M₅ showed more surface cracks compared to M₃, while blends with DBTP displayed a smoother surface for the 2-step process compared to the 3-step process. Therefore, it appears that no single variable trialled had a significant effect on the surface structure of the blends; rather the collective effect of the variables trialled (i.e., a 2-step process using amorphous PLA and DBTP) produced a better surface structure (M₄).



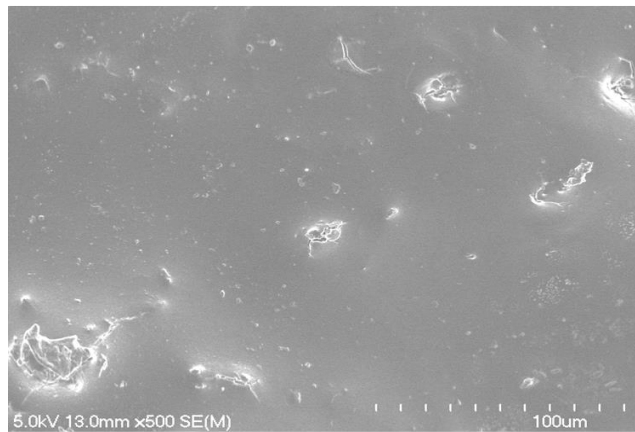
M₁



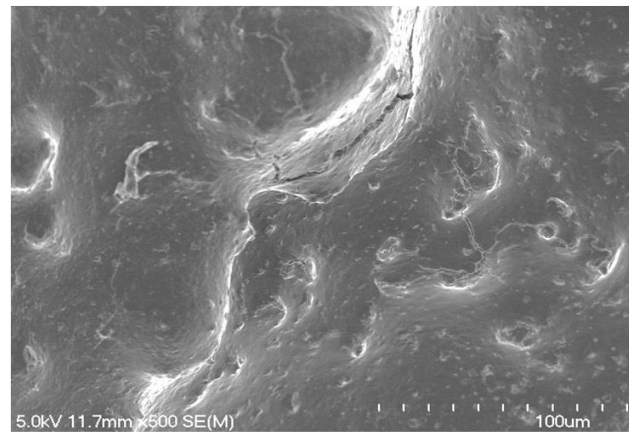
M₂



M₃



M₄



M₅

Figure 55: Surface morphology of DBT/PLA sheets processed using different methods (M1 - M₅) and different processing steps (two or three step process). (see Figure 50).

5.4.3 Mechanical properties

The tensile properties of DBT/PLA sheets are presented in figure 56. M₄ showed higher tensile strength and greater elongation than the other blends and showed a higher modulus compared to M₂, M₃, and M₅. The increase in tensile properties observed is probably a result of reduced heat treatment of DBTP due to the elimination of the pre-compounding of DBTP into DBTG before blending, and the reduction of processing steps before sheet extrusion. This was also suggested by the surface morphology observed (Figure 55).

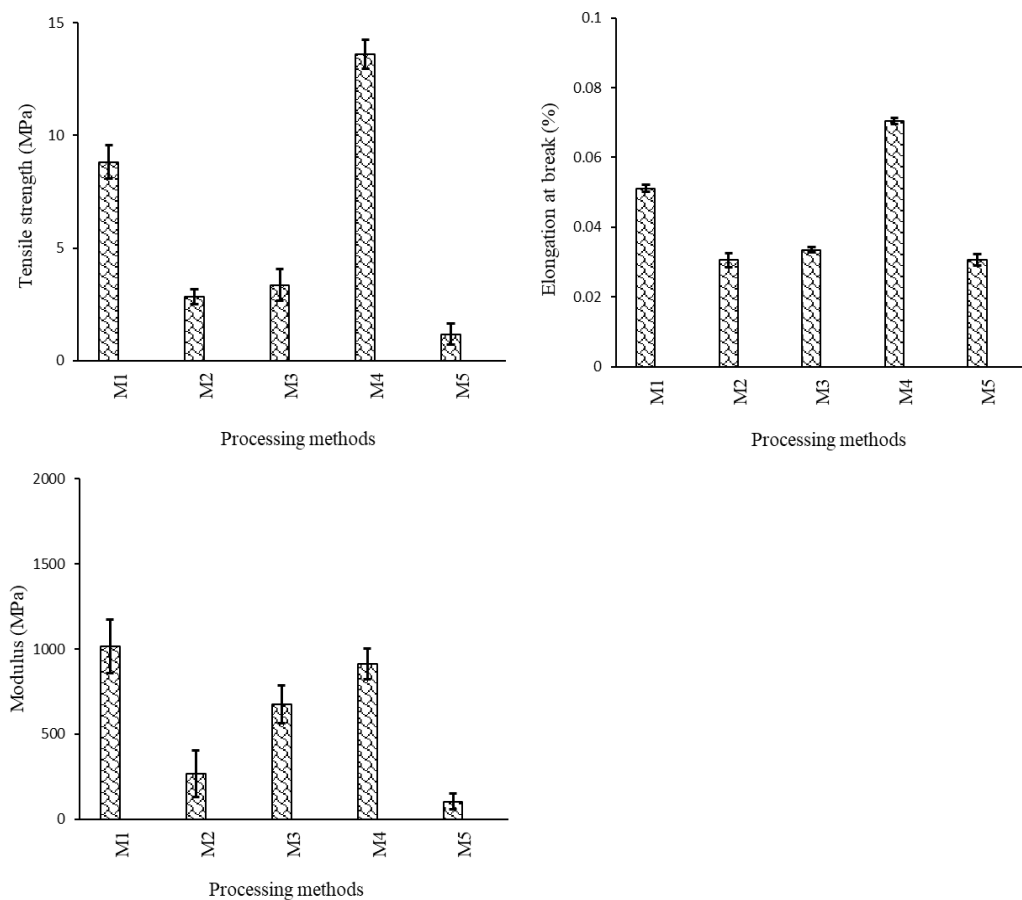


Figure 56: Mechanical properties of DBT/PLA sheets processed using different methods (M₁ – M₅) and different processing steps (two or three steps). (see Figure 50).

M₁, which was blended with amorphous PLA, showed an increase in tensile strength compared to M₂ (blended with semi-crystalline PLA). This supports the expectation expressed in the literature that processing with semi-crystalline PLA

will lead to reduced blend properties as a result of DBT degradation caused by the high processing heat required to melt the crystal region of PLA [286]. Considering the effect of starting with DBT powder (DBTP) or pre-compounded DBT (DBTG), M₁ showed improved tensile strength compared to M₃, suggesting a better interaction between the PLA phase and the DBT phase for blends with DBTP (powder) compared to DBTG (granules). Reducing the number of steps alone was considered not sufficient to effect the observed change in mechanical properties as M₅ revealed a poor tensile strength and showed no changes in elongation at break compared to M₃, while M₄ displayed better tensile strength and elongation at break compared with M₁. However, it was probably the collective effect of reduced heat and fewer processing steps (using a 2-step process and the elimination of pre-compounding of DBTP into DBTG) on DBT as well as blending with amorphous PLA (requiring a lower temperature to soften compared to the melting point of the crystal region of semi-crystalline PLA) that influenced the mechanical properties of the produced sheet, resulting in the better tensile strength and elongation at break observed for the M₄ blend.

5.4.4 Water absorption

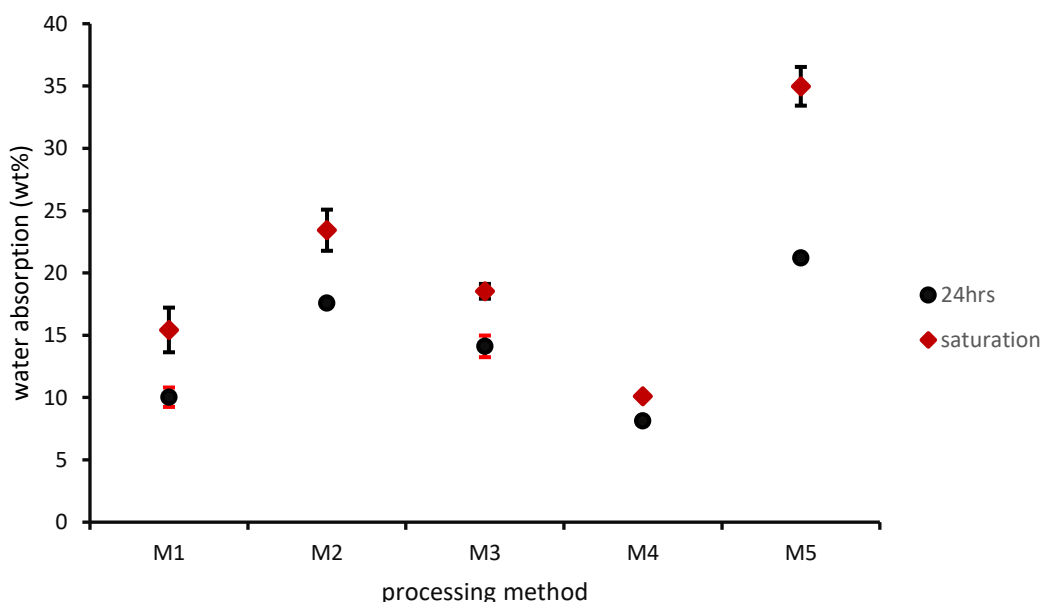


Figure 57: Water absorption (wt.%) of DBT/PLA sheets produced using different processing methods (M1 - M5) and steps (two or three step process). (Figure 50).

The water absorption of DBT/PLA sheets produced using different methods and processing steps is shown in Figure 57. The water absorption of the blend sheets after 24 h ranged from 8 to 21% and ranged from 10 to 34% upon saturation. M₄ have the lowest water absorption percentage of 8% within 24 h and 10% upon saturation. Most of the water uptake occurred rapidly within 24 h and slowed until saturation was reached, regardless of the method used. M₅ showed the highest water absorption percentage. Blending with amorphous PLA (M₁) showed a reduction in water absorption in the produced sheet compared to the blends using semi-crystalline PLA (M₂). Processing DBT/PLA sheets using DBTP (M₁) revealed a reduction in water absorption of the produced sheet compared to DBTG (M₃). Also, considering the processing steps used, blends with DBTG (M₃ and M₅) showed the highest absorption percentages for both 24 h and saturation immersion time compared to DBTP (M₁ and M₄). Blending DBT/PLA for sheet extrusion appears to favour DBTP as a DBT-based starting material regardless of the processing steps used.

The water absorption properties of the sheets followed similar patterns to the tensile properties of the blends. This confirms that the collective effect of reduced heat processes and processing steps was responsible for the improvements observed in the sheet properties,

M₄ showed the lowest water absorption percentage, and had the highest tensile strength, highest elongation and a relatively smooth surface imaging and morphology compared to other processing methods. This confirms the suggestion that using the M₄ processing method produced a sheet with improved interfacial interaction and immiscibility between the DBT and PLA phases. Therefore, M₄ was considered the optimal method for processing DBT/PLA sheets.

5.4.5 Rheology characterization

Materials' rheology is important in determining their suitability for sheet or film processing. Materials with low melt viscosity flow more readily in directions that allow sheet die fill; therefore, a low melt viscosity material is preferred for sheet or film processing. To better understand the effect of processing heat treatment and

processing steps on sheet properties, it is important to understand a blend's flow properties. Therefore, the materials' flow behaviour was measured. Figure 58 and Table 9 show the shear viscosity as a function of shear rate, and the power law indices for PLA and the blend sheets. The material used for the rheology calculation was processed according to the methods and processing steps described in Figure 50. M₁, M₂, and M₃ were processed as compounded blends while M₄ and M₅ were processed as mixtures in the rheometer. It can be seen that the sheets trialed displayed non-Newtonian behaviour and exhibited shear thinning behaviour. The rheology of the materials processed using different processing methods was similar to other thermoplastic proteins blends such as soy protein/chemically modified poly(butylene succinate and soy protein concentrate/ poly(butylene adipate-co-terephthalate) [82; 347].

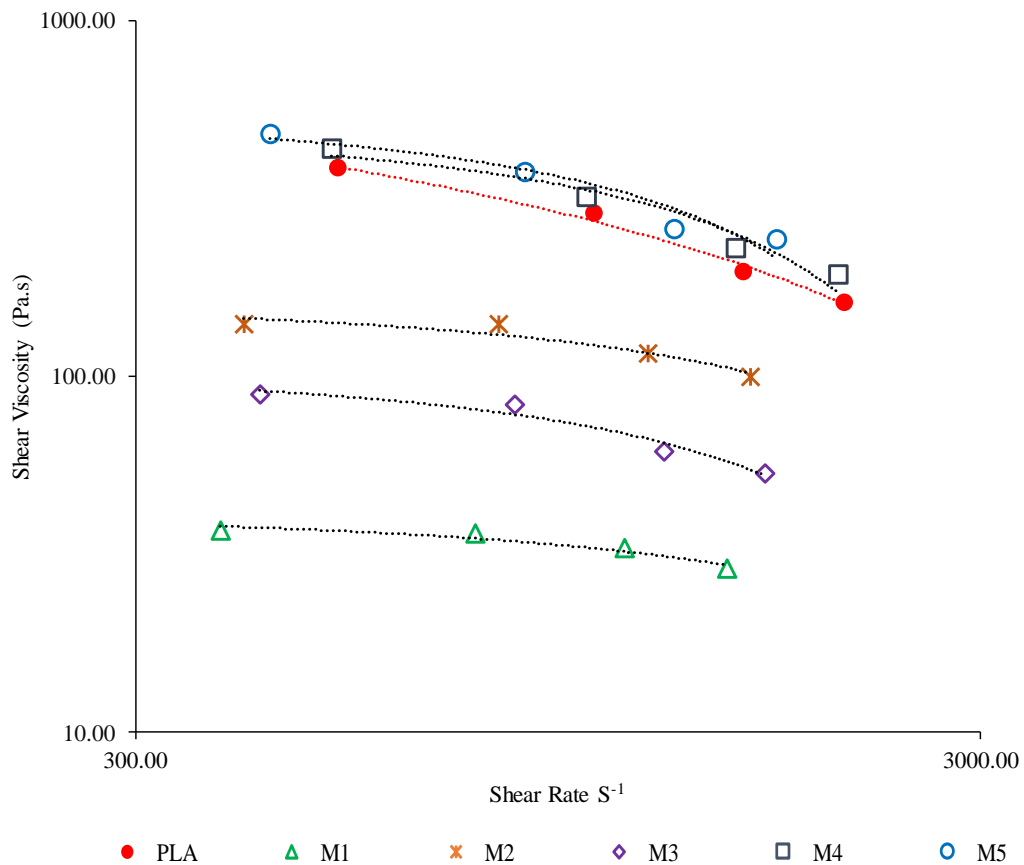


Figure 58: Shear viscosity of DBT/PLA sheets material using different processing steps (two or three step process) and different methods (M₁ - M₅) (see Figure 50).

Table 9: Power law indices of DBT/PLA sheet material using different processing methods (M₁ - M₅) and processing steps (two or three step process) (see Figure 50).

Processing methods	K	R²	n
M ₁	704.58	0.7792	0.95
M ₂	618.46	0.7652	0.76
M ₃	922.59	0.8601	0.67
M ₄	18492	0.9811	0.40
M ₅	12024	0.9574	0.61
PLA	5996.4	0.9953	0.50

As a control experiment, the viscosity of amorphous PLA was measured, and it was found to be within the viscosity of the M₄ and M₅ processing steps. PLA showed a shear viscosity higher than the materials processed using the 3-step process (M₁, M₂, and M₃). This implies that M₁, M₂, and M₃ required low processing temperatures and flowed readily compared to PLA, M₄, and M₅. This is desirable as materials processed using 3 steps had already been exposed to multiple heat treatments compared to materials processed using the 2-step process. Therefore, they may require low temperatures to achieve softening and thinning of the material during sheet extrusion.

An increase in the shear viscosity of a blend's melt suggests that more entangled points exist in the blend melt [284], due to stronger interactions between blend molecules as the molecular weight increases. Therefore, blends with relatively lower molecular weights are expected to have lower viscosity. M₄ and M₅ showed an increase in shear viscosity compared to other processing methods. It is safe to say that processing using a 3-step process reduced the molecular weight of the material due to the excessive heat treatment that caused degradation of DBT and resulted in reduced tensile properties. This confirms processing heat treatment as the major cause of the poor mechanical properties observed for materials processed using the 3-step process (M₁) compared to those processed using the 2-step process (M₄).

Shear viscosity measurements showed that the blend made from DBTP (using M₁) flowed readily compared to that with DBTG (M₂). Also, blends with amorphous PLA (M₁, M₃) showed increased ease of processing compared to semi-crystalline PLA (M₂), with a decrease observed in the shear viscosity of M₁ and M₃ compared to the M₂ material melt.

Polymer processing, such as sheet extrusion, requires a high shear rate. Therefore, a material that exhibits shear thinning is desirable because as the shear rate increases, viscosity decreases. M₄ and M₅ had shear viscosities similar to PLA, suggesting that they behaved more like a thermoplastic. M₁, M₂, and M₃ viscosities, which were below PLA's shear viscosity, were probably a result of protein aggregation or degradation. This is probably due to the excessive heat treatment used to compound these blends before processing in the rheometer. This protein aggregation or degradation prevents the material from forming a thermoplastic and might also be the reason for the poor tensile and water absorption properties observed for the materials processed using these methods.

The processing methods trialled have power-law indices (Table 9), which are comparable to the power-law indices reported for bio-polymers and bio-polymer blends such as cellulose, soy protein, and wheat gluten [345; 347-349]. The power-law index (n) derived from the experimental data demonstrates that M₄ is shear thinning, with a lower n value compared to other methods trialled.

5.4.6 Conclusion

A DBT/PLA blend was successfully formed into continuous sheets using twin-screw extrusion. Different sheet processing methods and steps were trialled. Above die temperatures of 140°C, sheet processing was impossible and proved problematic. This was probably due to the degradation of DBT at higher processing temperatures. Method M₄ was found to produce the most promising sheets, with better consolidation and relatively smooth surfaces.

SEM revealed a relatively smooth surface topography with smaller DBT domains for material processed using the M₄ approach compared to the other methods. It

appears that no single variable trialled had an effect on the surface structure of the blends; rather the collective effect of the variables trialled (i.e., a 2-step process using amorphous PLA and DBTP) produced a better surface structure (M₄).

The SEM, tensile properties and water absorption of the sheets produced suggest that the collective effects of reduced heat processing and fewer processing steps (i.e., a 2-step process, elimination of pre-compounding of DBTP into DBTG, and blending with amorphous PLA, which requires a low processing heat to soften) improved the sheet properties.

The rheological measurements obtained revealed M₄ to be shear thinning, with a lower n value lower than the other methods trialled.

The data obtained from the experimental work demonstrated the possibility of modifying processing conditions for the optimization of production of DBT/PLA-based sheets.

Chapter 6

Conclusion and Recommendations

Conclusion and Recommendations

The increasing economic and environmental issues surrounding petroleum-based polymers have drawn attention to more sustainable material alternatives from the agricultural sector. Biomass-based polymers such as decoloured bloodmeal thermoplastic (DBT) are one such alternative, being sustainable and renewable.

DBT, like most other protein polymers, is brittle, with low mechanical strength, and is more difficult to process using the conventional technology applied in the current plastic industry. These problems led to this study of the feasibility of blending DBT with PLA in order to improve its mechanical properties and processability, and the possibility of developing sheet extrusion methods for DBT/PLA blends.

Decoloured bloodmeal thermoplastic was blended with PLA with and without compatibilizers, using extrusion. Different compatibilizers such as PLA-g-IA, pMDI, and PEOX were used to improve the compatibility between the DBT phase and the PLA phase in the blend. Different plasticizers such as triethylene glycol and glycerol were used to plasticize the DBT formulations used for blends with PLA. The DBT/PLA blends produced were processed using sheet extrusion. The resulting blends and sheets were examined to characterize their mechanical, thermal, morphological and rheological properties.

As expected, blending DBT with PLA without compatibilizers resulted in an immiscible blend displaying a coarse morphology and poor interfacial interaction between the DBT and PLA phases. This was supported by the two different T_g values observed in the blends' DMA. The addition of compatibilizers led to an improvement in the interfacial adhesion of DBT and PLA in the blend and consequently a stabilized morphology. The improvement of interfacial adhesion and morphology stability led to significant improvements in the mechanical, thermal and rheological properties of DBT.

The objective of blending DBT and PLA was met by applying a variety of blend processing conditions, DBT formulations, and blend composition ratios. Two blend processing approaches were used: the first was to blend with decoloured bloodmeal

thermoplastic powder (DBTP), while the second was to blend with decoloured bloodmeal thermoplastic granules (DBTG). DBTP contains decoloured bloodmeal and additive which is equilibrated at 2°C overnight, while DBTG is a compounded and granulated decoloured bloodmeal thermoplastic which has been powered. Both approaches produced consolidated extrudates with reasonably smooth surfaces. The extrudates were flexible and rubbery before cooling. Small surface defects such as shark-skin were observed for blends with a high ratio of DBT to PLA, above a 50:50 blend ratio. Injection moulding of blends with DBTP was successful; consolidated samples were produced without processing aids, using optimal injection moulding temperatures. However, blends with DBTG were not injection mouldable due to excessive blockage of the injection moulder feed throat and protein degradation. No improvement was observed with the addition of processing aids. Therefore, blending using DBTG was discontinued and DBTP was used for further investigations. Hence, DBT/PLA blends refer to a compounded blend of DBTP and PLA or PLA-g-IA (i.e. a compounded blend of DBTP, PLA and compatibilizer).

Four blend composition ratios: 30:70 (DP37), 50:50 (DP55), 70:30 (DP73) and 90:10 (DP91), with and without compatibilizer (PLA-g-IA), were used to determine the optimal blend ratio for a DBT/PLA blend. DP55 and DP73 were considered the optimal blend composition ratios from the data obtained. It seems that below 50% and above 70% DBT, either DBT or PLA overwhelms the compatibilizing effect of itaconic anhydride, resulting in poor mechanical properties, as observed from the mechanical properties obtained.

Different formulations of DBT: formulation 1 (F1); formulation 2 (F2); formulation 3 (F3); and formulation 4 (F4) were blended with PLA and PLA-g-IA to determine the best DBT formulation for a DBT/PLA blend system. Formulation 1 was plasticized dried decoloured bloodmeal (DBM); formulation 2 contained 100 parts DBM, 40 parts water, 3 parts sodium dodecyl sulphate (SDS), 20 parts tri-ethylene glycol (TEG); formulation 3 contained 100 parts DBM, 30 parts water, 6 parts SDS, 30 parts TEG; and formulation 4 contained 100 parts DBM, 40 parts water, 6 parts SDS and 30 parts TEG. The data obtained for the mechanical properties and digested surfaces suggested F2 was the preferable DBT formulation for DBT/PLA blends. This was due to the observed improvement in tensile strength, elongation at break, impact strength and interfacial interaction between the DBT and PLA phases

of the compatibilized blend. However, balance can be achieved between the compatibilized F2 and F4 blends, if elongation at break is compromised depending on the desired material properties and functionality of the end product.

Assessment of different methods to improve the mechanical properties of DBT/PLA blends led to the biggest improvement in the blend properties. From the knowledge obtained from the PLA literature, DBTP was fully dried prior to blending with PLA to control for PLA hydrolysis during processing. Optimization of the DBT/PLA blend properties was achieved through the assessment of different compatibilizers, the compatibilization approach and plasticizer type. PLA-g-IA produced the greatest improvement in tensile strength, impact strength and morphological structure compared to pMDI and PEOX or PEOX alone. Introducing PLA-g-IA as a third blend component allowed the greatest interaction between phases, which was reflected in the increase observed in the tensile and impact strengths of D432.4.1 and D463.4.1 (adding PLA-g-IA as a third blend component) compared to the grafting of itaconic anhydride onto PLA in the blend (D432.5 and D463.5). The washed surface morphology of blends plasticized with TEG showed evenly distributed pores with small DBT domain sizes, compared to plasticizing with glycerol.

From the data obtained, PLA-g-IA was the most effective compatibilizer for DBT/PLA blends. Adding PLA-g-IA as a third component in the blend rather than grafting itaconic anhydride onto the PLA in the blend was an effective compatibilization approach and TEG was considered the best plasticizer for DBT/PLA blends compatibilized with PLA-g-IA. This provided the basis of the blending method used for subsequent assessment of blends using a DBT/PLA-based system.

With an understanding of a suitable DBT/PLA blending method, DBT/PLA was successfully processed into sheets using the sheet processing methods previously described as M₁, M₂, M₃, M₄, M₅ (see figure 50) and processing steps referred to as two and three step processes. Amorphous PLA, semi-crystalline PLA, DBTP, DBTG, mixing and compounding of blends before sheet extrusion and mixing then sheet extrusion were variably used to create the different processing methods and steps trialled. It was not possible to sheet extrude DBT. This was probably due to

the protein's high extensional viscosity compared to PLA. It was found that above die temperatures of 140°C, sheet extrusion of the blends was impossible. This was probably due to the degradation of DBT at higher temperatures.

The data obtained for surface morphology, tensile properties, rheology and water absorption of the sheets produced suggest that the collective effect of reduced heat processes and fewer processing steps (i.e., a 2-step process, elimination of pre-compounding of DBTP into DBTG, and blending with amorphous PLA, which requires a low processing heat to soften) improved the sheet properties. M₄ produced the most promising sheet, with better consolidation, a relatively smooth surface and better properties as revealed by SEM topography, water absorption and tensile properties.

Overall, it was found that blending DBT with PLA is a complicated process. This is because both materials are quite sensitive to processing conditions detrimental to each other (i.e., DBT and PLA have a very narrow processing window). For example, successful processing of DBT requires effective plasticization and water is the best plasticizer. In contrast, processing PLA in the presence of moisture, even as a result of moisture immigration from the DBT phase, results in PLA hydrolysis and poor material properties. The processing temperature is another important variable. Processing DBT at high temperatures (above 140°C) will result in protein degradation, while a high temperature is required to process PLA to ensure the melting of the PLA crystalline region and full development of PLA melt flow, as PLA has a high T_m, above 140°C. However, a balance was achieved in this research through the modification of processing conditions, such as complete elimination of processing and inbound water in DBT prior to blending with PLA. Also, semi-crystalline PLA was pre-extruded prior to blending to transform it into an amorphous polymer, thereby reducing its melt temperature.

Blending 50 wt.% DBT and PLA in the presence of compatibilizer successfully produced a material with better properties than pure DBT, which was sheet extrudable. The results obtained from this study have created a platform from which further advances can be made to optimize the sheet processability of DBT based polymers, and to produce new blends of DBT with other polymers that can achieve a degree of miscibility with compatibilization, having high affinity between both

material phases. This may enable expansion of production of a value-added product incorporating DBT.

The main aims of this study, of blending and improving DBT's properties and processibility with PLA, and achieving sheet processing of the blended material, are considered to have been fulfilled.

For future work, there are still limitations in the processing of bloodmeal into decoloured bloodmeal. The processes used in this study were time and energy consuming, as they only produced a small amount of decoloured bloodmeal per cycle, and required technical accuracy and precision to ensure that pH7 was achieved. Building a pilot-scale or semi-automatic plant to produce decoloured bloodmeal will be an exciting prospect.

Much remains unknown about DBT. The blend processed at die temperatures above 140 °C flowed evenly but lacked sheet-forming ability (poor cohesion). This is probably a result of DBT degradation due to the high processing temperature. Measurement of blends' extensional viscosity was not possible in this research work due to time limitations. The blending of DBT/PLA was cumbersome and the conditions for Cogwell's equation was not met; hence extensional viscosity was not calculated. Understanding the relationship between shear and extensional flow with regard to processing temperature and molecular weight will allow significant improvements in process design and optimization of blends' sheet processing, and is thus recommended.

Blends of DBT/PLA are brittle because of the brittleness of both PLA and DBT. It is therefore recommended that blends of DBT with other synthesized biodegradable polymers with wider processing windows and higher ductility such as poly(butylene succinate-co-adipate), poly caprolactone, poly(hydroxyl ester ether) and poly(butylene adipate-co-terephthalate) should be considered. Other researchers have demonstrated the possibility of blending these polymers with proteins [197; 332; 347].

References

- [1] Varshney, P. K., & Gupta, S. (2011). Natural polymer-based electrolytes for electrochemical devices: a review. *Ionics*, 17(6), 479-483.
- [2] Bouyer, E., Mekhloufi, G., Rosilio, V., Grossiord, J.-L., & Agnely, F. (2012). Proteins, polysaccharides, and their complexes used as stabilizers for emulsions: alternatives to synthetic surfactants in the pharmaceutical field? *International journal of pharmaceutics*, 436(1-2), 359-378.
- [3] Wang, Y. (2004). *Processing and Characterization of Extruded Zein-Based Biodegradable Films*. thesis, University of Illinois at Urbana-Champaign.
- [4] Verbeek, C. J., & Berg, L. E. (2009). Recent developments in thermo-mechanical processing of proteinous bioplastics. *Recent Patents on Materials Science*, 2(3), 171-189.
- [5] Van den Berg, L. E. (2009). *Development of 2nd generation proteinous bioplastics*. thesis, The University of Waikato.
- [6] Swan, J. (1992). Animal by-product processing. *Encyclopedia food science technology*, 4, 42-49.
- [7] Chen, G.-Q. (2003). Production and applications of microbial polyhydroxyalkanoates. In *Biodegradable polymers and plastics* (pp. 155-166). Springer.
- [8] Chiellini, E., Chiellini, F., Cinelli, P., & Ilieva, V. I. (2003). Biobased polymeric materials for agriculture applications. In *Biodegradable polymers and plastics* (pp. 185-210). Springer.
- [9] Song, J., Murphy, R., Narayan, R., & Davies, G. (2009). Biodegradable and compostable alternatives to conventional plastics. *Philosophical transactions of the royal society B: Biological sciences*, 364(1526), 2127-2139.
- [10] Grant, R. (1980). *Applied protein chemistry*. Applied Science Publishers.
- [11] Low, A., Verbeek, C. J. R., & Lay, M. C. (2014). Treating Bloodmeal with Peracetic Acid to Produce a Bioplastic Feedstock. *Macromolecular Materials and Engineering*, 299(1), 75-84.
- [12] Low, A., Verbeek, C. J. R., & Lay, M. C. (2012). Processing peracetic acid treated bloodmeal into bioplastic. *Chemeca 2012: Quality of life through chemical engineering: 23-26 September 2012, Wellington, New Zealand*, 1433.
- [13] Low, A. (2012). *Decoloured Bloodmeal Based Bioplastic*. thesis, University of Waikato.

- [14] Marsilla, K. (2015). *Development of Bloodmeal Protein Thermoplastic Blends*. thesis, University of Waikato.
- [15] Blends, P. (Compiler) (2000). *Paul, DR, Bucknall, CB, Eds*: Wiley: New York.
- [16] Gennadios, A. (2002). *Protein-based films and coatings*. CRC Press.
- [17] Rouilly, A., & Rigal, L. (2002). Agro-materials: a bibliographic review. *Journal of Macromolecular Science, Part C: Polymer Reviews*, 42(4), 441-479.
- [18] Selling, G. W. (2010). The effect of extrusion processing on Zein. *Polymer degradation and stability*, 95(12), 2241-2249.
- [19] Rouilly, A., Mériaux, A., Geneau, C., Silvestre, F., & Rigal, L. (2006). Film extrusion of sunflower protein isolate. *Polymer Engineering & Science*, 46(11), 1635-1640.
- [20] Conca, K. (2002). Protein-based films and coating for military packaging applications. *Protein-based films and coatings*. CRC, Boca Raton, FL, 551-577.
- [21] Naga, M., Kirihara, S., Tokugawa, Y., Tsuda, F., Saito, T., & Hirotsuka, M. (Compiler) (1996). *Process for producing edible proteinaceous film*: Google Patents. <http://www.google.com/patents/US5569482>.
- [22] Powell, P. C., & Housz, A. J. I. (1998). *Engineering with Polymers, 2nd Edition*. Taylor & Francis.
- [23] Bier, J. M., Verbeek, C. J. R., & Lay, M. C. (2012). An eco-profile of thermoplastic protein derived from blood meal Part 1: allocation issues. *International Journal of Life Cycle Assessment*, 17(2), 208-219.
- [24] Vroman, I., & Tighzert, L. (2009). Biodegradable polymers. *Materials*, 2(2), 307-344.
- [25] Albertsson, A., & Karlsson, S. (1994). Chemistry and biochemistry of polymer biodegradation.
- [26] Rudin, A., & Choi, P. (2012). *The elements of polymer science and engineering*. Academic press.
- [27] Shivam, P. (2016). Recent developments on biodegradable polymers and their future trends. *International Research Journal of Science and Engineering*, 4, 17-26.
- [28] Basnett, P., & Roy, I. (2010). Microbial production of biodegradable polymers and their role in cardiac stent development. *Current Res Technol Educat Topics Applied Microbiol Microbial Biotechnol*, 405-1415.
- [29] Verma, S., Bhatia, Y., Valappil, S. P., & Roy, I. (2002). A possible role of poly-3-hydroxybutyric acid in antibiotic production in *Streptomyces*. *Archives of microbiology*, 179(1), 66-69.

- [30] Madison, L. L., & Huisman, G. W. (1999). Metabolic engineering of poly (3-hydroxyalkanoates): from DNA to plastic. *Microbiology and molecular biology reviews*, 63(1), 21-53.
- [31] Lal, S. (2012). *Biodegradable Packaging from Whey Protein*. thesis, ResearchSpace@ Auckland.
- [32] Zinn, M., Witholt, B., & Egli, T. (2001). Occurrence, synthesis and medical application of bacterial polyhydroxyalkanoate. *Advanced drug delivery reviews*, 53(1), 5-21.
- [33] Nayak, P. L. (1999). Biodegradable polymers: opportunities and challenges.
- [34] Fliieger, M., Kantorova, M., Prell, A., Řezanka, T., & Votruba, J. (2003). Biodegradable plastics from renewable sources. *Folia microbiologica*, 48(1), 27.
- [35] Södergård, A., & Stolt, M. (2002). Properties of lactic acid based polymers and their correlation with composition. *Progress in polymer science*, 27(6), 1123-1163.
- [36] Martin, O., & Averous, L. (2001). Poly (lactic acid): plasticization and properties of biodegradable multiphase systems. *Polymer*, 42(14), 6209-6219.
- [37] Haywood, G., Anderson, A., & Dawes, E. (1989). A survey of the accumulation of novel polyhydroxyalkanoates by bacteria. *Biotechnology letters*, 11(7), 471-476.
- [38] Nampoothiri, K. M., Nair, N. R., & John, R. P. (2010). An overview of the recent developments in polylactide (PLA) research. *Bioresource technology*, 101(22), 8493-8501.
- [39] Siparsky, G. L., Voorhees, K. J., & Miao, F. (1998). Hydrolysis of polylactic acid (PLA) and polycaprolactone (PCL) in aqueous acetonitrile solutions: autocatalysis. *Journal of environmental polymer degradation*, 6(1), 31-41.
- [40] García, M. C. (2018). Drug delivery systems based on nonimmunogenic biopolymers. In *Engineering of Biomaterials for Drug Delivery Systems* (pp. 317-344). Elsevier.
- [41] Barrett, A. D., & Stanberry, L. R. (2009). *Vaccines for biodefense and emerging and neglected diseases*. Academic Press.
- [42] Abdel-Akher, M., Hamilton, J. K., Montgomery, R., & Smith, F. (1952). A new procedure for the determination of the fine structure of polysaccharides. *Journal of the American Chemical Society*, 74(19), 4970-4971.
- [43] Heinze, T., Liebert, T., & Koschella, A. (Compiler) (2006). *Structure of polysaccharides*: Springer.
- [44] Aspinall, G. O. (2014). *The polysaccharides*. Academic Press.

- [45] Liu, J., Willför, S., & Xu, C. (2015). A review of bioactive plant polysaccharides: Biological activities, functionalization, and biomedical applications. *Bioactive Carbohydrates and Dietary Fibre*, 5(1), 31-61.
- [46] Liu, Z., Jiao, Y., Wang, Y., Zhou, C., & Zhang, Z. (2008). Polysaccharides-based nanoparticles as drug delivery systems. *Advanced drug delivery reviews*, 60(15), 1650-1662.
- [47] Bosworth, L., & Downes, S. (2011). *Electrospinning for tissue regeneration*. Elsevier.
- [48] Edgar, K. J., Buchanan, C. M., Debenham, J. S., Rundquist, P. A., Seiler, B. D., Shelton, M. C., & Tindall, D. (2001). Advances in cellulose ester performance and application. *Progress in Polymer Science*, 26(9), 1605-1688.
- [49] Simon, J., Müller, H., Koch, R., & Müller, V. (1998). Thermoplastic and biodegradable polymers of cellulose. *Polymer degradation and stability*, 59(1-3), 107-115.
- [50] Herrmann, A., Nickel, J., & Riedel, U. (1998). Construction materials based upon biologically renewable resources—from components to finished parts. *Polymer Degradation and Stability*, 59(1-3), 251-261.
- [51] Nickel, J., & Riedel, U. (2001). Structural Materials Made Of Renewable Resources (Biocomposites). In *Biorelated Polymers* (pp. 27-40). Springer.
- [52] Mohanty, A. K., Misra, M. a., & Hinrichsen, G. (2000). Biofibres, biodegradable polymers and biocomposites: An overview. *Macromolecular materials and Engineering*, 276(1), 1-24.
- [53] Bastioli, C. (2001). Global status of the production of biobased packaging materials. *Starch - Stärke*, 53(8), 351-355.
- [54] Wurzburg, O. B. (1986). *Modified starches: properties and uses*.
- [55] Hudson, S., & Smith, C. (1998). Polysaccharides: chitin and chitosan: chemistry and technology of their use as structural materials. In *Biopolymers from renewable resources* (pp. 96-118). Springer.
- [56] Kumar, M. N. R. (2000). A review of chitin and chitosan applications. *Reactive and functional polymers*, 46(1), 1-27.
- [57] Goosen, M. F. (1996). *Applications of Chitan and Chitosan*. CRC Press.
- [58] Jeon, Y.-J., Shahidi, F., & KIM, S.-K. (2000). Preparation of chitin and chitosan oligomers and their applications in physiological functional foods. *Food Reviews International*, 16(2), 159-176.
- [59] Singla, A., & Chawla, M. (2001). Chitosan: Some pharmaceutical and biological aspects - an update. *Journal of Pharmacy and Pharmacology*, 53(8), 1047-1067.

- [60] Nakai, S., & Modler, H. W. (1996). *Food proteins: properties and characterization*. John Wiley & Sons.
- [61] Verbeek, C. J., & Van den Berg, L. E. (2011). Development of proteinous bioplastics using bloodmeal. *Journal of Polymers and the Environment*, 19(1), 1-10.
- [62] Adapted by University of Massachusetts Amherst from Protein Structure in Wikipedia. *Primary, Secondary, Tertiary and Quaternary Protein Structure*. Retrieved march, 26th, 2015. <https://www.umass.edu/molvis/workshop/prot1234.htm>.
- [63] Guerrero Manso, P. M. (2013). *Processing and characterization of soy protein-based materials*.
- [64] Yu, P., Mckinnon, J. J., Christensen, C. R., & Christensen, D. A. (2004). Using synchrotron-based FTIR microspectroscopy to reveal chemical features of feather protein secondary structure: comparison with other feed protein sources. *Journal of agricultural and food chemistry*, 52(24), 7353-7361.
- [65] contributors, W. (2019). *Structural Biochemistry/Proteins/Fibrous Proteins*. Retrieved July 27 13:27 UTC, 2019. [https://en.wikibooks.org/w/index.php?title=Structural Biochemistry/Proteins/Fibrous Proteins&oldid=3550883](https://en.wikibooks.org/w/index.php?title=Structural_Biochemistry/Proteins/Fibrous_Proteins&oldid=3550883).
- [66] Whitford, D. (2013). *Proteins: structure and function*. John Wiley & Sons.
- [67] Silva, N. H., Vilela, C., Marrucho, I. M., Freire, C. S., Neto, C. P., & Silvestre, A. J. (2014). Protein-based materials: from sources to innovative sustainable materials for biomedical applications. *Journal of Materials Chemistry B*, 2(24), 3715-3740.
- [68] Van Beilen, J. B., & Poirier, Y. (2008). Production of renewable polymers from crop plants. *The Plant Journal*, 54(4), 684-701.
- [69] Reddy, M. M., Misra, M., & Mohanty, A. K. (2014). Biodegradable Blends from Corn Gluten Meal and Poly (butylene adipate-co-terephthalate)(PBAT): Studies on the Influence of Plasticization and Destructurization on Rheology, Tensile Properties and Interfacial Interactions. *Journal of Polymers and the Environment*, 22(2), 167-175.
- [70] Pickering, K. L., Verbeek, C. J., & Viljoen, C. (2012). The effect of aqueous urea on the processing, structure and properties of CGM. *Journal of Polymers and the Environment*, 20(2), 335-343.
- [71] Verbeek, C. J., & van den Berg, L. E. (2010). Extrusion Processing and Properties of Protein - Based Thermoplastics. *Macromolecular materials and engineering*, 295(1), 10-21.
- [72] Jain, S., Reddy, M. M., Mohanty, A. K., Misra, M., & Ghosh, A. K. (2010). A new biodegradable flexible composite sheet from poly (lactic acid)/poly (ϵ - caprolactone) blends and Micro - Talc. *Macromolecular materials and engineering*, 295(8), 750-762.

- [73] Samarasinghe, S., Easteal, A. J., & Edmonds, N. R. (2008). Biodegradable plastic composites from corn gluten meal. *Polymer International*, 57(2), 359-364.
- [74] Ly, Y.-P., Johnson, L., & Jane, J. (1998). Soy protein as biopolymer. In *Biopolymers from renewable resources* (pp. 144-176). Springer.
- [75] Berk, A., Zipursky, S., & Lodish, H. (Compiler) (2000). *Molecular Cell Biology 4th edition*: National Center for Biotechnology Information's Bookshelf.
- [76] Silvipriya, K., Kumar, K. K., Bhat, A., Kumar, B. D., John, A., & Lakshmanan, P. (2015). Collagen: Animal sources and biomedical application. *J App Pharm Sci*, 5(3), 123-127.
- [77] Hoffman, J. R., & Falvo, M. J. (2004). Protein—which is best? *Journal of sports science & medicine*, 3(3), 118.
- [78] De Graaf, L. A., & Kolster, P. (1998). Industrial proteins as a green alternative for 'petro'polymers: potentials and limitations. In *Macromolecular Symposia* (Vol. 127, pp. 51-58): Wiley Online Library.
- [79] Fang, K., Wang, B., Sheng, K., & Sun, X. S. (2009). Properties and morphology of poly (lactic acid)/soy protein isolate blends. *Journal of applied polymer science*, 114(2), 754-759.
- [80] Graiver, D., Waikul, L., Berger, C., & Narayan, R. (2004). Biodegradable soy protein–polyester blends by reactive extrusion process. *Journal of applied polymer science*, 92(5), 3231-3239.
- [81] Huang, J., Zhang, L., Wei, H., & Cao, X. (2004). Soy protein isolate/kraft lignin composites compatibilized with methylene diphenyl diisocyanate. *Journal of applied polymer science*, 93(2), 624-629.
- [82] Li, Y.-D., Zeng, J.-B., Li, W.-D., Yang, K.-K., Wang, X.-L., & Wang, Y.-Z. (2009). Rheology, crystallization, and biodegradability of blends based on soy protein and chemically modified poly (butylene succinate). *Industrial & Engineering Chemistry Research*, 48(10), 4817-4825.
- [83] Mohamed, A. A., Gordon, S. H., Carriere, C. J., & Kim, S. (2006). Thermal characteristics of polylactic acid/wheat gluten blends. *Journal of food quality*, 29(3), 266-281.
- [84] Abugoch, L. E., Tapia, C., Villamán, M. C., Yazdani-Pedram, M., & Díaz-Dosque, M. (2011). Characterization of quinoa protein–chitosan blend edible films. *Food Hydrocolloids*, 25(5), 879-886.
- [85] Anker, M., Stading, M., & Hermansson, A.-M. (1998). Mechanical properties, water vapor permeability, and moisture contents of β -lactoglobulin and whey protein films using multivariate analysis. *Journal of Agricultural and Food Chemistry*, 46(5), 1820-1829.
- [86] Brandenburg, A., Weller, C., & Testin, R. (1993). Edible films and coatings from soy protein. *Journal of food Science*, 58(5), 1086-1089.

- [87] Bowman, B. j. O., C M. (2002). *Protein-based films and coatings*. CRC Press.
- [88] Piot, J., Guillochon, D., & Thomas, D. (1986). Preparation of decolorized peptides from slaughter-house blood. *MIRCEN journal of applied microbiology and biotechnology*, 2(3), 359-364.
- [89] Ockerman, H., & Hansen, C. (Compiler). *Animal By-Product Processing and Utilization. 2000*: Boca Raton, USA: CRC Press.
- [90] Duarte, R. T., Carvalho Simões, M. C., & Sgarbieri, V. C. (1999). Bovine blood components: fractionation, composition, and nutritive value. *Journal of Agricultural and Food Chemistry*, 47(1), 231-236.
- [91] Bah, C. S., Bekhit, A. E. D. A., Carne, A., & McConnell, M. A. (2013). Slaughterhouse blood: an emerging source of bioactive compounds. *Comprehensive Reviews in Food Science and Food Safety*, 12(3), 314-331.
- [92] Adje, E. Y., Balti, R., Kouach, M., Dhulster, P., Guillochon, D., & Nedjar-Arroume, N. (2011). Obtaining antimicrobial peptides by controlled peptic hydrolysis of bovine hemoglobin. *International Journal of Biological Macromolecules*, 49(2), 143-153.
- [93] Adler-Nissen, J. (1986). *Enzymic hydrolysis of food proteins*. Elsevier applied science publishers.
- [94] Wismer-Pedersen, J. (1988). Use of haemoglobin in foods—a review. *Meat Science*, 24(1), 31-45.
- [95] HOWELL, N. K., & Lawrie, R. (1983). Functional aspects of blood plasma proteins. I. Separation and characterization. *International Journal of Food Science & Technology*, 18(6), 747-762.
- [96] Izuchukwu, S. C. P. (2015). *The Effect of Moisture Content and Extrusion Temperature on the Processing, Thermal and Mechanical Properties of Novatein®*. Masters thesis, University of Waikato, Hamilton, New Zealand.
- [97] Verbeek, C. J., & van den Berg, L. E. (2011). Mechanical properties and water absorption of thermoplastic bloodmeal. *Macromolecular Materials and Engineering*, 296(6), 524-534.
- [98] Hicks, T., Verbeek, C. J., Lay, M. C., & Bier, J. M. (2014). Effect of oxidative treatment on the secondary structure of decoloured bloodmeal. *RSC Advances*, 4(59), 31201-31209.
- [99] Gavin, C., Verbeek, C. J., Lay, M. C., Bier, J. M., & Hicks, T. M. (2019). Thermal analysis and secondary structure of protein fractions in a highly aggregated protein material. *Polymer Testing*.
- [100] Murayama, K., & Tomida, M. (2004). Heat-induced secondary structure and conformation change of bovine serum albumin investigated by Fourier transform infrared spectroscopy. *Biochemistry*, 43(36), 11526-11532.
- [101] Wolkers, W. F., & Oldenhof, H. (2010). In situ FTIR studies on mammalian cells. *Journal of Spectroscopy*, 24(5), 525-534.

- [102] Verbeek, C., Viljoen, C., Pickering, K., & van den Berg, L. (2009). Plastics material. *NZ Patent NZ551531. Waikatolink Limited, Hamilton.*
- [103] Zealand(PIANZ), P. I. A. o. N. (Compiler). *New Zealand Poultry Meat Production Statistics 1997-2011.* 2011.
- [104] Ku Marsilla, K., & Verbeek, C. J. (2014). Mechanical Properties of Thermoplastic Protein From Bloodmeal and Polyester Blends. *Macromolecular Materials and Engineering*, 299(7), 885-895.
- [105] Van Der Merwe, D. W. (2014). *The environmental and economic impact for producing the port jackson from novatein.* thesis, University of Waikato.
- [106] Low, A., Lay, M., Verbeek, J., & Swan, J. (2012). Decoloring hemoglobin as a feedstock for second-generation bioplastics. *Preparative Biochemistry and Biotechnology*, 42(1), 29-43.
- [107] Florence, T. (1985). The degradation of cytochrome c by hydrogen peroxide. *Journal of inorganic biochemistry*, 23(2), 131-141.
- [108] Nagababu, E., & Rifkind, J. M. (2000). Heme degradation during autoxidation of oxyhemoglobin. *Biochemical and biophysical research communications*, 273(3), 839-845.
- [109] Nagababu, E., & Rifkind, J. M. (1998). Formation of fluorescent heme degradation products during the oxidation of hemoglobin by hydrogen peroxide. *Biochemical and biophysical research communications*, 247(3), 592-596.
- [110] Hicks, T. M., Verbeek, C. J., Lay, M. C., & Bier, J. M. (2014). The Effect of SDS and TEG on Chain Mobility and Secondary Structure of Decolored Bloodmeal. *Macromolecular Materials and Engineering*.
- [111] Hicks, T. M., Verbeek, C. J. R., Lay, M. C., & Manley-Harris, M. (2013). The role of peracetic acid in bloodmeal decoloring. *Journal of the American Oil Chemists' Society*, 90(10), 1577-1587.
- [112] Zhang, W., Xiao, S., & Ahn, D. U. (2013). Protein oxidation: basic principles and implications for meat quality. *Critical reviews in food science and nutrition*, 53(11), 1191-1201.
- [113] Kerkaert, B., Mestdagh, F., Cucu, T., Aedo, P. R., Ling, S. Y., & De Meulenaer, B. (2011). Hypochlorous and peracetic acid induced oxidation of dairy proteins. *Journal of agricultural and food chemistry*, 59(3), 907-914.
- [114] Yu, P. (2004). Application of advanced synchrotron radiation-based Fourier transform infrared (SR-FTIR) microspectroscopy to animal nutrition and feed science: a novel approach. *British journal of nutrition*, 92(6), 869-885.
- [115] Malkov, S. N., Živković, M. V., Beljanski, M. V., Hall, M. B., & Zarić, S. D. (2008). A reexamination of the propensities of amino acids towards a particular secondary structure: classification of amino acids based on their chemical structure. *Journal of molecular modeling*, 14(8), 769-775.

- [116] Davies, K., Delsignore, M., & Lin, S. (1987). Protein damage and degradation by oxygen radicals. II. Modification of amino acids. *Journal of Biological Chemistry*, 262(20), 9902-9907.
- [117] Utracki, L. A., Mukhopadhyay, P., & Gupta, R. (2014). Polymer Blends: Introduction. In *Polymer Blends Handbook* (pp. 3-170). Springer.
- [118] Osswald, T. A. (2011). *Understanding polymer processing: processes and governing equations*. Hanser.
- [119] Wang, D., Li, Y., Xie, X.-M., & Guo, B.-H. (2011). Compatibilization and morphology development of immiscible ternary polymer blends. *Polymer*, 52(1), 191-200.
- [120] Khan, I., Chohan, M., & Mazumder, M. (2018). Polymer Blends. In (pp. 1-38).
- [121] Stein, R. S. (1994). Polymer Science and Engineering-The Shifting Research Frontiers. *Journal of Polymer Science Part A: Polymer Chemistry*, 32(16), 3215-3221.
- [122] Visakh, P., Markovic, G., & Pasquini, D. (2016). *Recent Developments in Polymer Macro, Micro and Nano Blends: Preparation and Characterisation*. Woodhead Publishing.
- [123] Sperling, L. (2000). History and Development of Polymer Blends and IPNs. *Applied Polymer Science: 21st Century*, 345.
- [124] Cheng, S. Z. (2002). *Handbook of thermal analysis and calorimetry: applications to polymers and plastics*. (Vol. 3). Elsevier.
- [125] Yu, L., Dean, K., & Li, L. (2006). Polymer blends and composites from renewable resources. *Progress in polymer science*, 31(6), 576-602.
- [126] Sperling, L. H. (2005). *Introduction to physical polymer science*. John Wiley & Sons.
- [127] Saldivar-Guerra, E., & Vivaldo-Lima, E. (2013). *Handbook of polymer synthesis, characterization, and processing*. John Wiley & Sons.
- [128] Van Hemelrijck, E., Van Puyvelde, P., Velankar, S., Macosko, C. W., & Moldenaers, P. (2004). Interfacial elasticity and coalescence suppression in compatibilized polymer blends. *Journal of Rheology*, 48(1), 143-158.
- [129] Velankar, S., Van Puyvelde, P., Mewis, J., & Moldenaers, P. (2004). Steady-shear rheological properties of model compatibilized blends. *Journal of Rheology*, 48(4), 725-744.
- [130] Duryodhan, M. (Revised 21th June, 2002). *Elastomer blends* (Vol. 75). Rubber chemistry and technology.
- [131] Kulshreshtha, A. K., & Vasile, C. (2003). *Handbook of polymer blends and composites*. (Vol. 3). Rapra Technology Limited.

- [132] Folkes, M., & Hope, P. (1993). *Polymer blends and alloys*. Springer.
- [133] Hill, T. L. (1960). *An Introduction to Statistical Thermodynamics*.
- [134] Flory, P. J. (1942). Thermodynamics of high polymer solutions. *The Journal of chemical physics*, *10*(1), 51-61.
- [135] Rigby, D., Lin, J., & Roe, R. (1985). Compatibilizing effect of random or block copolymer added to binary mixture of homopolymers. *Macromolecules*, *18*(11), 2269-2273.
- [136] Datta, S., & Lohse, D. (Compiler) (1996). *Polymeric compatibilizers*: New York: Hanser Publishers.
- [137] Mayo, F. R., & Lewis, F. M. (1944). Copolymerization. I. A basis for comparing the behavior of monomers in copolymerization; the copolymerization of styrene and methyl methacrylate. *Journal of the American Chemical Society*, *66*(9), 1594-1601.
- [138] Chanda, M. (2006). *Introduction to polymer science and chemistry: a problem-solving approach*. CRC Press.
- [139] Feng, C., Li, Y., Yang, D., Hu, J., Zhang, X., & Huang, X. (2011). Well-defined graft copolymers: from controlled synthesis to multipurpose applications. *Chemical Society Reviews*, *40*(3), 1282-1295.
- [140] Chu, P. K., & Liu, X. (2008). *Biomaterials fabrication and processing handbook*. CRC press.
- [141] VIVALDO-LIMA, E., Guerrero Sánchez, C., Hornung, C., Quintero - Ortega, I., & Luna - Bárcenas, G. (2013). *Handbook of polymer synthesis, characterization, and processing*.
- [142] Marsilla, K. K., & Verbeek, C. (2015). Modification of poly (lactic acid) using itaconic anhydride by reactive extrusion. *European Polymer Journal*, *67*, 213-223.
- [143] De Vito, G., Lanzetta, N., Maglio, G., Malinconico, M., Musto, P., & Palumbo, R. (1984). Functionalization of an amorphous ethylene - propylene copolymer by free radical initiated grafting of unsaturated molecules. *Journal of Polymer Science: Polymer Chemistry Edition*, *22*(6), 1335-1347.
- [144] Machado, A., Covas, J., & Van Duin, M. (2001). Effect of polyolefin structure on maleic anhydride grafting. *Polymer*, *42*(8), 3649-3655.
- [145] Hwang, S. W., Lee, S. B., Lee, C. K., Lee, J. Y., Shim, J. K., Selke, S. E., Soto-Valdez, H., Matuana, L., Rubino, M., & Auras, R. (2012). Grafting of maleic anhydride on poly (L-lactic acid). Effects on physical and mechanical properties. *Polymer Testing*, *31*(2), 333-344.
- [146] Mani, R., Bhattacharya, M., & Tang, J. (1999). Functionalization of polyesters with maleic anhydride by reactive extrusion. *Journal of Polymer Science Part A: Polymer Chemistry*, *37*(11), 1693-1702.

- [147] Paul, D., & Newman, S. (1978). *Polymer blends*, vol. 2. *Academic, New York*.
- [148] Favis, B. D. (1992). Processing/morphology/rheology relationships in polymer blends. In *Makromolekulare Chemie. Macromolecular Symposia* (Vol. 56, pp. 143-150): Wiley Online Library.
- [149] Wu, S. (1987). Formation of dispersed phase in incompatible polymer blends: Interfacial and rheological effects. *Polymer Engineering & Science*, 27(5), 335-343.
- [150] Favis, B. D., & Chalifoux, J.-P. (1987). The effect of viscosity ratio on the morphology of polypropylene/polycarbonate blends during processing. *Polymer Engineering & Science*, 27(21), 1591-1600.
- [151] Favis, B. D. (1990). The effect of processing parameters on the morphology of an immiscible binary blend. *Journal of applied polymer science*, 39(2), 285-300.
- [152] Walczak, Z. K. (1973). Influence of shearing history on the properties of polymer melt. II. *Journal of Applied Polymer Science*, 17(1), 169-176.
- [153] Ha, T. T. (1999). *Extrusion processing of zein-based biodegradable plastics*. thesis, University of Illinois at Urbana-Champaign.
- [154] Fang, J., & Fowler, P. (2003). The use of starch and its derivatives as biopolymer sources of packaging materials. *Journal of Food Agriculture and Environment*, 1, 82-84.
- [155] Yu, L. (2009). *Biodegradable polymer blends and composites from renewable resources*. John Wiley & Sons.
- [156] Arvanitoyannis, I. S., Nakayama, A., & Aiba, S.-i. (1998). Chitosan and gelatin based edible films: state diagrams, mechanical and permeation properties. *Carbohydrate polymers*, 37(4), 371-382.
- [157] Carvalho, A., Job, A., Alves, N., Curvelo, A., & Gandini, A. (2003). Thermoplastic starch/natural rubber blends. *Carbohydrate Polymers*, 53(1), 95-99.
- [158] Warth, H., Mülhaupt, R., & Schätzle, J. (1997). Thermoplastic cellulose acetate and cellulose acetate compounds prepared by reactive processing. *Journal of applied polymer science*, 64(2), 231-242.
- [159] Bastioli, C. (1998). Properties and applications of Mater-Bi starch-based materials. *Polymer Degradation and Stability*, 59(1-3), 263-272.
- [160] Bloembergen, S., & Narayan, R. (Compiler) (1995). *Biodegradable moldable products and films comprising blends of starch esters and polyesters*: Google Patents.
- [161] Jayaraju, J., Raviprakash, S., Keshavayya, J., & Rai, S. (2006). Miscibility studies on chitosan/hydroxypropylmethyl cellulose blend in solution by viscosity, ultrasonic velocity, density, and refractive index methods. *Journal of applied polymer science*, 102(3), 2738-2742.

- [162] Wali, A., Naidu, B. V. K., Mallikarjuna, N., Sainkar, S., Halligudi, S., & Aminabhavi, T. (2005). Miscibility of chitosan–hydroxyethylcellulose blends in aqueous acetic acid solutions at 35° C. *Journal of applied polymer science*, 96(5), 1996-1998.
- [163] Yin, J., Luo, K., Chen, X., & Khutoryanskiy, V. V. (2006). Miscibility studies of the blends of chitosan with some cellulose ethers. *Carbohydrate polymers*, 63(2), 238-244.
- [164] Tsuji, H., & Fukui, I. (2003). Enhanced thermal stability of poly (lactide) s in the melt by enantiomeric polymer blending. *Polymer*, 44(10), 2891-2896.
- [165] Ikada, Y., Jamshidi, K., Tsuji, H., & Hyon, S. H. (1987). Stereocomplex formation between enantiomeric poly (lactides). *Macromolecules*, 20(4), 904-906.
- [166] Tsuji, H. (2002). Autocatalytic hydrolysis of amorphous-made polylactides: effects of L-lactide content, tacticity, and enantiomeric polymer blending. *Polymer*, 43(6), 1789-1796.
- [167] Shinoda, H., Asou, Y., Kashima, T., Kato, T., Tseng, Y., & Yagi, T. (2003). Amphiphilic biodegradable copolymer, poly (aspartic acid-co-lactide): acceleration of degradation rate and improvement of thermal stability for poly (lactic acid), poly (butylene succinate) and poly (ϵ -caprolactone). *Polymer degradation and stability*, 80(2), 241-250.
- [168] Park, J. W., Im, S. S., Kim, S. H., & Kim, Y. H. (2000). Biodegradable polymer blends of poly (l - lactic acid) and gelatinized starch. *Polymer Engineering & Science*, 40(12), 2539-2550.
- [169] Willett, J., & Shogren, R. (2002). Processing and properties of extruded starch/polymer foams. *Polymer*, 43(22), 5935-5947.
- [170] Ke, T., & Sun, X. (2003). Melting behavior and crystallization kinetics of starch and poly (lactic acid) composites. *Journal of Applied Polymer Science*, 89(5), 1203-1210.
- [171] Yang, X., Zhao, K., & Chen, G.-Q. (2002). Effect of surface treatment on the biocompatibility of microbial polyhydroxyalkanoates. *Biomaterials*, 23(5), 1391-1397.
- [172] Deng, Y., Zhao, K., Zhang, X.-f., Hu, P., & Chen, G.-Q. (2002). Study on the three-dimensional proliferation of rabbit articular cartilage-derived chondrocytes on polyhydroxyalkanoate scaffolds. *Biomaterials*, 23(20), 4049-4056.
- [173] Zhao, K., Deng, Y., Chen, J. C., & Chen, G.-Q. (2003). Polyhydroxyalkanoate (PHA) scaffolds with good mechanical properties and biocompatibility. *Biomaterials*, 24(6), 1041-1045.
- [174] Koyama, N., & Doi, Y. (1997). Miscibility of binary blends of poly [(R)-3-hydroxybutyric acid] and poly [(S)-lactic acid]. *Polymer*, 38(7), 1589-1593.

- [175] Ohkoshi, I., Abe, H., & Doi, Y. (2000). Miscibility and solid-state structures for blends of poly [(S)-lactide] with atactic poly [(R, S)-3-hydroxybutyrate]. *Polymer*, 41(15), 5985-5992.
- [176] Yoon, J.-S., Lee, W.-S., Jin, H.-J., Chin, I.-J., Kim, M.-N., & Go, J.-H. (1999). Toughening of poly (3-hydroxybutyrate) with poly (cis-1, 4-isoprene). *European Polymer Journal*, 35(5), 781-788.
- [177] Zhang, L., Deng, X., Zhao, S., & Huang, Z. (1997). Biodegradable polymer blends of poly (3 - hydroxybutyrate) and starch acetate. *Polymer international*, 44(1), 104-110.
- [178] Willett, J., Kotnis, M., O'brien, G., Fanta, G., & Gordon, S. (1998). Properties of starch - graft - poly (glycidyl methacrylate) - PHBV composites. *Journal of applied polymer science*, 70(6), 1121-1127.
- [179] El-Shafee, E., Saad, G. R., & Fahmy, S. M. (2001). Miscibility, crystallization and phase structure of poly (3-hydroxybutyrate)/cellulose acetate butyrate blends. *European Polymer Journal*, 37(10), 2091-2104.
- [180] Zhang, L., Deng, X., & Huang, Z. (1997). Miscibility, thermal behaviour and morphological structure of poly (3-hydroxybutyrate) and ethyl cellulose binary blends. *Polymer*, 38(21), 5379-5387.
- [181] Maekawa, M., Pearce, R., Marchessault, R., & Manley, R. (1999). Miscibility and tensile properties of poly (β -hydroxybutyrate)-cellulose propionate blends. *Polymer*, 40(6), 1501-1505.
- [182] Cuq, B., Gontard, N., & Guilbert, S. (1998). Proteins as agricultural polymers for packaging production. *Cereal chemistry*, 75(1), 1-9.
- [183] John, J., & Bhattacharya, M. (1999). Properties of reactively blended soy protein and modified polyesters. *Polymer international*, 48(11), 1165-1172.
- [184] Verbeek, C. J. R., Low, A., Lay, M. C., & Hicks, T. M. (2017). Processability and mechanical properties of bioplastics produced from decoloured bloodmeal. *Advances in Polymer Technology*.
- [185] Marsilla, K., & Verbeek, C. J. R. (2013). Properties of Bloodmeal/Linear Low - density Polyethylene Blends Compatibilized with Maleic Anhydride Grafted Polyethylene. *Journal of Applied Polymer Science*, 130(3), 1890-1897.
- [186] Otaigbe, J., & Jane, J. (1997). Pressure-volume-temperature relationships of soy protein isolate/starch plastic. *Journal of environmental polymer degradation*, 5(2), 75-80.
- [187] Zhou, X., Mohanty, A., & Misra, M. (2013). A new biodegradable injection moulded bioplastic from modified soy meal and poly (butylene adipate-co-terephthalate): Effect of plasticizer and denaturant. *Journal of Polymers and the Environment*, 21(3), 615-622.

- [188] Guo, G., Zhang, C., Du, Z., Zou, W., Tian, H., Xiang, A., & Li, H. (2015). Structure and property of biodegradable soy protein isolate/PBAT blends. *Industrial Crops and Products*, 74, 731-736.
- [189] Aithani, D., & Mohanty, A. K. (2006). Value-added new materials from byproduct of corn based ethanol industries: Blends of plasticized corn gluten meal and poly (ϵ -caprolactone). *Industrial & engineering chemistry research*, 45(18), 6147-6152.
- [190] Zhu, R., Liu, H., & Zhang, J. (2012). Compatibilizing effects of maleated poly (lactic acid)(PLA) on properties of PLA/Soy protein composites. *Industrial & Engineering Chemistry Research*, 51(22), 7786-7792.
- [191] Suyatma, N. E., Copinet, A., Tighzert, L., & Coma, V. (2004). Mechanical and barrier properties of biodegradable films made from chitosan and poly (lactic acid) blends. *Journal of Polymers and the Environment*, 12(1), 1-6.
- [192] Ikejima, T., Yagi, K., & Inoue, Y. (1999). Thermal properties and crystallization behavior of poly (3 - hydroxybutyric acid) in blends with chitin and chitosan. *Macromolecular Chemistry and Physics*, 200(2), 413-421.
- [193] Ikejima, T., & Inoue, Y. (2000). Crystallization behavior and environmental biodegradability of the blend films of poly (3-hydroxybutyric acid) with chitin and chitosan. *Carbohydrate Polymers*, 41(4), 351-356.
- [194] Zhang, J., Jiang, L., Zhu, L., Jane, J.-l., & Mungara, P. (2006). Morphology and properties of soy protein and polylactide blends. *Biomacromolecules*, 7(5), 1551-1561.
- [195] Liu, B., Jiang, L., Liu, H., & Zhang, J. (2010). Synergetic effect of dual compatibilizers on in situ formed poly (lactic acid)/soy protein composites. *Industrial & Engineering Chemistry Research*, 49(14), 6399-6406.
- [196] Marsilla, K. K., & Verbeek, C. (2013). Properties of Blends of Novatein Thermoplastic Protein from Bloodmeal and Polybutylene Succinate Using Two Compatibilizers. *International Journal of Chemical Engineering and Applications*, 4(3), 106.
- [197] Ku - Marsilla, K., & Verbeek, C. (2015). Compatibilization of Protein Thermoplastics and Polybutylene Succinate Blends. *Macromolecular Materials and Engineering*, 300(2), 161-171.
- [198] Walallavita, A. S., Verbeek, C. J. R., & Lay, M. C. (2017). Biopolymer foams from Novatein thermoplastic protein and poly (lactic acid). *Journal of Applied Polymer Science*, 134(48), 45561.
- [199] Mohamed, A., Finkenstadt, V. L., Gordon, S. H., & Palmquist, D. E. (2010). Thermal and mechanical properties of compression - molded pMDI - reinforced PCL/gluten composites. *Journal of applied polymer science*, 118(5), 2778-2790.

- [200] Orozco, V. H., Brostow, W., Chonkaew, W., & Lopez, B. L. (2009). Preparation and characterization of poly (Lactic acid) - g - maleic anhydride+ starch blends. In *Macromolecular symposia* (Vol. 277, pp. 69-80): Wiley Online Library.
- [201] Zhong, Z., & Sun, S. X. (2003). Properties of soy protein isolate/poly (ethylene - co - ethyl acrylate - co - maleic anhydride) blends. *Journal of applied polymer science*, 88(2), 407-413.
- [202] Robeson, L. M. (2007). Polymer blends. *A Comprehensive Review*.
- [203] Mo, X., & Sun, X. (2000). Thermal and mechanical properties of plastics molded from sodium dodecyl sulfate-modified soy protein isolates. *Journal of Polymers and the Environment*, 8(4), 161-166.
- [204] Reddy, M. M., Mohanty, A. K., & Misra, M. (2012). Optimization of tensile properties thermoplastic blends from soy and biodegradable polyesters: Taguchi design of experiments approach. *Journal of Materials Science*, 47(6), 2591-2599.
- [205] Scott, C. E., & Macosko, C. W. (1995). Morphology development during the initial stages of polymer-polymer blending. *Polymer*, 36(3), 461-470.
- [206] Chen, X., Xu, J., & Guo, B. H. (2006). Development of dispersed phase size and its dependence on processing parameters. *Journal of applied polymer science*, 102(4), 3201-3211.
- [207] Li, H., & Sundararaj, U. (2009). Morphology development of polymer blends in extruder: the effects of compatibilization and rotation rate. *Macromolecular Chemistry and Physics*, 210(10), 852-863.
- [208] Zhong, Z., & Sun, X. S. (2001). Properties of soy protein isolate/polycaprolactone blends compatibilized by methylene diphenyl diisocyanate. *Polymer*, 42(16), 6961-6969.
- [209] Gennadios, A., McHugh, T., & Weller, C. (Compiler) (1994). *Edible coatings and films based on proteins*. In "Edible Coatings and Films to Improve Food Quality". JM Krochta, EA Baldwin and MO Nisperos-Carriedo: Technomic Publishing Company, Inc. Lancaster (PA).
- [210] Damodaran, S. (2017). *Food proteins and their applications*. Routledge.
- [211] González, A., & Igarzabal, C. I. A. (2013). Soy protein–Poly (lactic acid) bilayer films as biodegradable material for active food packaging. *Food Hydrocolloids*, 33(2), 289-296.
- [212] Muller, J., González-Martínez, C., & Chiralt, A. (2017). Poly (lactic) acid (PLA) and starch bilayer films, containing cinnamaldehyde, obtained by compression moulding. *European Polymer Journal*, 95, 56-70.
- [213] Otoni, C. G., Avena-Bustillos, R. J., Olsen, C. W., Bilbao-Sáinz, C., & McHugh, T. H. (2016). Mechanical and water barrier properties of isolated soy protein composite edible films as affected by carvacrol and cinnamaldehyde micro and nanoemulsions. *Food Hydrocolloids*, 57, 72-79.

- [214] Guerrero, P., Retegi, A., Gabilondo, N., & De la Caba, K. (2010). Mechanical and thermal properties of soy protein films processed by casting and compression. *Journal of Food Engineering*, 100(1), 145-151.
- [215] Li, M., Liu, P., Zou, W., Yu, L., Xie, F., Pu, H., Liu, H., & Chen, L. (2011). Extrusion processing and characterization of edible starch films with different amylose contents. *Journal of Food Engineering*, 106(1), 95-101.
- [216] Tharanathan, R. (2003). Biodegradable films and composite coatings: past, present and future. *Trends in Food Science & Technology*, 14(3), 71-78.
- [217] Hanani, Z. N., Roos, Y., & Kerry, J. (2014). Use and application of gelatin as potential biodegradable packaging materials for food products. *International journal of biological macromolecules*, 71, 94-102.
- [218] Cuq, B., Gontard, N., & Guilbert, S. (1997). Thermoplastic properties of fish myofibrillar proteins: application to biopackaging fabrication. *Polymer*, 38(16), 4071-4078.
- [219] Liu, L., Kerry, J. F., & Kerry, J. P. (2006). Effect of food ingredients and selected lipids on the physical properties of extruded edible films/casings. *International journal of food science & technology*, 41(3), 295-302.
- [220] Guerrero, P., Beatty, E., Kerry, J., & De La Caba, K. (2012). Extrusion of soy protein with gelatin and sugars at low moisture content. *Journal of Food Engineering*, 110(1), 53-59.
- [221] Barone, J. R., Schmidt, W. F., & Gregoire, N. (2006). Extrusion of feather keratin. *Journal of applied polymer science*, 100(2), 1432-1442.
- [222] Hernandez - Izquierdo, V., & Krochta, J. (2008). Thermoplastic processing of proteins for film formation—a review. *Journal of food science*, 73(2), R30-R39.
- [223] Chanda, M., & Roy, S. K. (2006). *Plastics technology handbook*. (Vol. 72). CRC press.
- [224] Ishizuka, K., & Nishimi, T. (Compiler) (2012). *Method of manufacturing polymer film*: Google Patents.
- [225] Reddy, N., Chen, L., & Yang, Y. (2013). Thermoplastic films from peanut proteins extracted from peanut meal. *Industrial Crops and Products*, 43, 159-164.
- [226] Wihodo, M., & Moraru, C. I. (2013). Physical and chemical methods used to enhance the structure and mechanical properties of protein films: A review. *Journal of Food Engineering*, 114(3), 292-302.
- [227] Bourtoom, T. (2008). Edible films and coatings: characteristics and properties. *International Food Research Journal*, 15(3), 237-248.
- [228] Landel, R. F., & Nielsen, L. E. (1993). *Mechanical properties of polymers and composites*. CRC Press.

- [229] Mchugh, T. H., Weller, C. L., & Krochta, J. M. (1994). Edible coatings and films based on proteins. *Edible coatings and films to improve food quality*, 201.
- [230] Krochta, J. M., & De Mulder-Johnston, C. (1997). Edible and biodegradable polymer films: challenges and opportunities. *Food technology (USA)*.
- [231] McHugh, T. H., & Krochta, J. M. (1994). Sorbitol-vs glycerol-plasticized whey protein edible films: integrated oxygen permeability and tensile property evaluation. *Journal of Agricultural and Food Chemistry*, 42(4), 841-845.
- [232] Sothornvit, R., & Krochta, J. (2000). Oxygen permeability and mechanical properties of films from hydrolyzed whey protein. *Journal of agricultural and food chemistry*, 48(9), 3913-3916.
- [233] KROCHTA, J. M., Baldwin, E., & Nisperos-Carriedo, M. (1994). Permeability properties of edible films. *Edible Coatings and Films to Improve Food Quality*, 139.
- [234] Debeaufort, F., Quezada-Gallo, J.-A., & Voilley, A. (1998). Edible films and coatings: tomorrow's packagings: a review. *Critical Reviews in Food Science*, 38(4), 299-313.
- [235] Ku - Marsilla, K., & Verbeek, C. (2014). Compatibilization of Protein Thermoplastics and Polybutylene Succinate Blends. *Macromolecular Materials and Engineering*.
- [236] Mangavel, C., Barbot, J., Gueguen, J., & Popineau, Y. (2003). Molecular determinants of the influence of hydrophilic plasticizers on the mechanical properties of cast wheat gluten films. *Journal of agricultural and food chemistry*, 51(5), 1447-1452.
- [237] Pommet, M., Redl, A., Morel, M.-H., & Guilbert, S. (2003). Study of wheat gluten plasticization with fatty acids. *Polymer*, 44(1), 115-122.
- [238] Avena - Bustillos, R., & Krochta, J. (1993). Water Vapor Permeability of Caseinate - Based Edible Films as Affected by pH, Calcium Crosslinking and Lipid Content. *Journal of food science*, 58(4), 904-907.
- [239] Gennadios, A., WELLER, C., & Testin, R. (1993). Temperature effect on oxygen permeability of edible protein - based films. *Journal of food science*, 58(1), 212-214.
- [240] Marquie, C., Aymard, C., Cuq, J. L., & Guilbert, S. (1995). Biodegradable packaging made from cottonseed flour: formation and improvement by chemical treatments with gossypol, formaldehyde, and glutaraldehyde. *Journal of Agricultural and Food Chemistry*, 43(10), 2762-2767.
- [241] Parris, N., Coffin, D. R., Dickey, L. C., & Craig, J. C. (1998). Composition factors affecting the physical properties of hydrophilic zein films. *Paradigm for Successful Utilization of Renewable Resources. AOCS Press, Champaign, IL*, 255-265.

- [242] Were, L., Hettiarachchy, N., & Coleman, M. (1999). Properties of cysteine - added soy protein - wheat gluten films. *Journal of food science*, 64(3), 514-518.
- [243] Gennadios, A., Rhim, J., Handa, A., Weller, C., & Hanna, M. (1998). Ultraviolet radiation affects physical and molecular properties of soy protein films. *Journal of food science*, 63(2), 225-228.
- [244] Rhim, J. W., Gennadios, A., Fu, D., Weller, C. L., & Hanna, M. A. (1999). Properties of ultraviolet irradiated protein films. *LWT-Food Science and Technology*, 32(3), 129-133.
- [245] Cieśla, K., Salmieri, S., Lacroix, M., & Le Tien, C. (2004). Gamma irradiation influence on physical properties of milk proteins. *Radiation Physics and Chemistry*, 71(1), 95-99.
- [246] Lacroix, M., Le, T., Ouattara, B., Yu, H., Letendre, M., Sabato, S., Mateescu, M., & Patterson, G. (2002). Use of γ -irradiation to produce films from whey, casein and soya proteins: structure and functionals characteristics. *Radiation Physics and Chemistry*, 63(3), 827-832.
- [247] Sabato, S., Ouattara, B., Yu, H., D'aprano, G., Le Tien, C., Mateescu, M., & Lacroix, M. (2001). Mechanical and barrier properties of cross-linked soy and whey protein based films. *Journal of Agricultural and Food Chemistry*, 49(3), 1397-1403.
- [248] Miller, K., & Krochta, J. (1997). Oxygen and aroma barrier properties of edible films: A review. *Trends in Food Science & Technology*, 8(7), 228-237.
- [249] Ali, Y., Ghorpade, V. M., & Hanna, M. A. (1997). Properties of thermally-treated wheat gluten films. *Industrial Crops and Products*, 6(2), 177-184.
- [250] Roy, S., Weller, C., Gennadios, A., Zeece, M., & Testin, R. (1999). Physical and molecular properties of wheat gluten films cast from heated film - forming solutions. *Journal of Food Science*, 64(1), 57-60.
- [251] Fischer, H. (2003). Polymer nanocomposites: from fundamental research to specific applications. *Materials Science and Engineering: C*, 23(6), 763-772.
- [252] Gennadios, A., Ghorpade, V., Weller, C. L., & Hanna, M. (1996). Heat curing of soy protein films. *Biological Systems Engineering: Papers and Publications*, 94.
- [253] Alcantara, C., Rumsey, T., & Krochta, J. (1998). Drying rate effect on the properties of whey protein films. *Journal of Food Process Engineering*, 21(5), 387-405.
- [254] Jangchud, A., & Chinnan, M. (1999). Peanut protein film as affected by drying temperature and pH of film forming solution. *Journal of Food Science*, 64(1), 153-157.

- [255] Stuchell, Y. M., & Krochta, J. M. (1994). Enzymatic treatments and thermal effects on edible soy protein films. *Journal of Food Science*, 59(6), 1332-1337.
- [256] Lim, L.-T., Mine, Y., & Tung, M. A. (1998). Transglutaminase cross-linked egg white protein films: tensile properties and oxygen permeability. *Journal of Agricultural and Food Chemistry*, 46(10), 4022-4029.
- [257] Mahmoud, R., & Savello, P. A. (1992). Mechanical properties of and water vapor transferability through whey protein films. *Journal of Dairy Science*, 75(4), 942-946.
- [258] Mahmoud, R., & Savello, P. A. (1993). Solubility and hydrolyzability of films produced by transglutaminase catalytic crosslinking of whey protein. *Journal of Dairy Science*, 76(1), 29-35.
- [259] Larre, C., Desserme, C., Barbot, J., & Gueguen, J. (2000). Properties of deamidated gluten films enzymatically cross-linked. *Journal of agricultural and food chemistry*, 48(11), 5444-5449.
- [260] Bigi, A., Bracci, B., Cojazzi, G., Panzavolta, S., & Roveri, N. (1998). Drawn gelatin films with improved mechanical properties. *Biomaterials*, 19(24), 2335-2340.
- [261] Wong, D. W., Gastineau, F. A., Gregorski, K. S., Tillin, S. J., & Pavlath, A. E. (1992). Chitosan-lipid films: microstructure and surface energy. *Journal of Agricultural and Food Chemistry*, 40(4), 540-544.
- [262] Fairley, P., Monahan, F. J., German, J. B., & Krochta, J. M. (1996). Mechanical properties and water vapor permeability of edible films from whey protein isolate and N-ethylmaleimide or cysteine. *Journal of Agricultural and Food Chemistry*, 44(12), 3789-3792.
- [263] McHugh, T. (2000). Protein - lipid interactions in edible films and coatings. *Food/Nahrung*, 44(3), 148-151.
- [264] Gontard, N., Duchez, C., CUQ, J. L., & GUILBERT, S. (1994). Edible composite films of wheat gluten and lipids: water vapour permeability and other physical properties. *International journal of food science & technology*, 29(1), 39-50.
- [265] Monedero, F. M., Fabra, M. J., Talens, P., & Chiralt, A. (2009). Effect of oleic acid-beeswax mixtures on mechanical, optical and water barrier properties of soy protein isolate based films. *Journal of Food Engineering*, 91(4), 509-515.
- [266] Tian, H., Wang, Y., Zhang, L., Quan, C., & Zhang, X. (2010). Improved flexibility and water resistance of soy protein thermoplastics containing waterborne polyurethane. *Industrial Crops and Products*, 32(1), 13-20.
- [267] Arvanitoyannis, I., Psomiadou, E., Nakayama, A., Aiba, S., & Yamamoto, N. (1997). Edible films made from gelatin, soluble starch and polyols, Part 3. *Food Chemistry*, 60(4), 593-604.

- [268] Arvanitoyannis, I., Nakayama, A., & Aiba, S.-i. (1998). Edible films made from hydroxypropyl starch and gelatin and plasticized by polyols and water. *Carbohydrate Polymers*, 36(2), 105-119.
- [269] Xiong, X., Li, Q., Lu, J. W., Guo, Z. X., & Yu, J. (2010). Poly (lactic acid)/soluble eggshell membrane protein blend films: Preparation and characterization. *Journal of applied polymer science*, 117(4), 1955-1959.
- [270] Rhim, J.-W., Lee, J. H., & Ng, P. K. (2007). Mechanical and barrier properties of biodegradable soy protein isolate-based films coated with polylactic acid. *LWT-Food Science and Technology*, 40(2), 232-238.
- [271] Kalia, S., Kaith, B., & Kaur, I. (2009). Pretreatments of natural fibers and their application as reinforcing material in polymer composites—a review. *Polymer Engineering & Science*, 49(7), 1253-1272.
- [272] Kunanopparat, T., Menut, P., Morel, M.-H., & Guilbert, S. (2008). Reinforcement of plasticized wheat gluten with natural fibers: From mechanical improvement to deplasticizing effect. *Composites part A: Applied science and manufacturing*, 39(5), 777-785.
- [273] Vlachopoulos, J., & Strutt, D. (2003). The role of rheology in polymer extrusion. In *New Technology for Extrusion Conference. Milan, Italy. Nov* (pp. 20-21).
- [274] Grellmann, W., & Seidler, S. (2007). *Polymer testing*. Hanser Munich.
- [275] Mohan, V. B., & Verbeek, C. J. (2015). Rheology and processing of bloodmeal-based thermoplastics.
- [276] Mohamed, A., Biresaw, G., Xu, J., Hojilla-Evangelista, M. P., & Rayas-Duarte, P. (2009). Oats protein isolate: thermal, rheological, surface and functional properties. *Food research international*, 42(1), 107-114.
- [277] Ralston, B., & Osswald, T. (2008). Viscosity of soy protein plastics determined by screw-driven capillary rheometry. *Journal of Polymers and the Environment*, 16(3), 169.
- [278] Gómez-Martínez, D., Partal, P., Martínez, I., & Gallegos, C. (2009). Rheological behaviour and physical properties of controlled-release gluten-based bioplastics. *Bioresource technology*, 100(5), 1828-1832.
- [279] Baird, D. (1999). The role of extensional rheology in polymer processing. *Korea-Australia Rheology Journal*, 11(4), 305-311.
- [280] Cogswell, F. N. (1981). *Polymer melt rheology: a guide for industrial practice*. Elsevier.
- [281] Van Oene, H. (1978). Rheology of polymer blends and dispersions. In *Polymer Blends, Volume 1* (pp. 295-352). Elsevier.
- [282] Sue, H.-J., Wang, S., & Jane, J.-L. (1997). Morphology and mechanical behaviour of engineering soy plastics. *Polymer*, 38(20), 5035-5040.

- [283] Vaidya, U. R., & Bhattacharya, M. (1994). Properties of blends of starch and synthetic polymers containing anhydride groups. *Journal of applied polymer science*, 52(5), 617-628.
- [284] Huneault, M. A., & Li, H. (2007). Morphology and properties of compatibilized polylactide/thermoplastic starch blends. *Polymer*, 48(1), 270-280.
- [285] Garlotta, D. (2001). A literature review of poly (lactic acid). *Journal of Polymers and the Environment*, 9(2), 63-84.
- [286] Gorrasi, G., & Pantani, R. (2013). Effect of PLA grades and morphologies on hydrolytic degradation at composting temperature: assessment of structural modification and kinetic parameters. *Polymer degradation and stability*, 98(5), 1006-1014.
- [287] Auras, R., Harte, B., & Selke, S. (2004). An overview of polylactides as packaging materials. *Macromolecular bioscience*, 4(9), 835-864.
- [288] Wang, N., Yu, J., & Ma, X. (2007). Preparation and characterization of thermoplastic starch/PLA blends by one - step reactive extrusion. *Polymer International*, 56(11), 1440-1447.
- [289] Low, A. (2012). *Decoloured bloodmeal based bioplastic*. PhD thesis, University of Waikato, Hamilton, New Zealand.
- [290] Verbeek, C. J. R., Lay, M. C., & Low, A. W. K. (Compiler) (2013). *Methods of manufacturing plastic materials from decolorized blood protein*: Google Patents.
- [291] Pickering, K. L., Verbeek, C. J. R., Viljoen, C., & Van Den Berg, L. E. (Compiler) (2012). *Plastics material*: Google Patents.
- [292] van der Merwe, D. W. (2014). *The Environmental and Economic Impacts for Producing the Port Jackson from Novatein®*. thesis, University of Waikato.
- [293] Walallavita, A. S., Verbeek, C. J. R., & Lay, M. C. Biopolymer foams from Novatein thermoplastic protein and poly (lactic acid). *Journal of Applied Polymer Science*.
- [294] Gavin, C., Lay, M. C., & Verbeek, C. J. (2016). Extrusion foaming of protein-based thermoplastic and polyethylene blends. In *AIP Conference Proceedings* (Vol. 1713, pp. 100003): AIP Publishing.
- [295] Zhang, J., Mungara, P., & Jane, J.-I. (2001). Mechanical and thermal properties of extruded soy protein sheets. *Polymer*, 42(6), 2569-2578.
- [296] Li, Y.-D., Zeng, J.-B., Wang, X.-L., Yang, K.-K., & Wang, Y.-Z. (2008). Structure and properties of soy protein/poly (butylene succinate) blends with improved compatibility. *Biomacromolecules*, 9(11), 3157-3164.

- [297] Mungara, P., Chang, T., Zhu, J., & Jane, J. (2002). Processing and physical properties of plastics made from soy protein polyester blends. *Journal of Polymers and the Environment*, 10(1), 31-37.
- [298] Wang, L., Shogren, R., & Carriere, C. (2000). Preparation and properties of thermoplastic starch - polyester laminate sheets by coextrusion. *Polymer Engineering & Science*, 40(2), 499-506.
- [299] Carlson, D., Nie, L., Narayan, R., & Dubois, P. (1999). Maleation of polylactide (PLA) by reactive extrusion. *Journal of applied polymer science*, 72(4), 477-485.
- [300] Nyambo, C., Mohanty, A. K., & Misra, M. (2011). Effect of maleated compatibilizer on performance of PLA/wheat Straw - Based green composites. *Macromolecular Materials and Engineering*, 296(8), 710-718.
- [301] Zhang, J.-F., & Sun, X. (2004). Mechanical properties of poly (lactic acid)/starch composites compatibilized by maleic anhydride. *Biomacromolecules*, 5(4), 1446-1451.
- [302] Properties, A. S. D. o. M. (1996). Standard test method for tensile properties of plastics. In: American Society for Testing and Materials.
- [303] ISO, E. 179-1 (2010).". *Plastics. Determination of Charpy impact properties. Part, 1.*
- [304] Willemse, R., Speijer, A., Langeraar, A., & De Boer, A. P. (1999). Tensile moduli of co-continuous polymer blends. *Polymer*, 40(24), 6645-6650.
- [305] Müller-Buschbaum, P., Gutmann, J. S., & Stamm, M. (2000). Influence of blend composition on phase separation and dewetting of thin polymer blend films. *Macromolecules*, 33(13), 4886-4895.
- [306] Willemse, R., De Boer, A. P., Van Dam, J., & Gotsis, A. (1998). Co-continuous morphologies in polymer blends: a new model. *Polymer*, 39(24), 5879-5887.
- [307] Xie, H.-Q., Xu, J., & Zhou, S. (1991). Polymer blends with two kinds of elastomeric ionomers. *Polymer*, 32(1), 95-102.
- [308] Walallavita, A., Verbeek, C. J., & Lay, M. (2016). Blending Novatein® thermoplastic protein with PLA for carbon dioxide assisted batch foaming. In *AIP Conference Proceedings* (Vol. 1713, pp. 100006): AIP Publishing.
- [309] Sumita, M., Tsukihi, H., Miyasaka, K., & Ishikawa, K. (1984). Dynamic mechanical properties of polypropylene composites filled with ultrafine particles. *Journal of applied polymer science*, 29(5), 1523-1530.
- [310] Jiang, L., Wolcott, M. P., & Zhang, J. (2006). Study of biodegradable polylactide/poly (butylene adipate-co-terephthalate) blends. *Biomacromolecules*, 7(1), 199-207.

- [311] Joseph, S., & Thomas, S. (2002). Modeling of tensile moduli in polystyrene/polybutadiene blends. *Journal of Polymer Science Part B: Polymer Physics*, 40(8), 755-764.
- [312] Mo, X., Sun, X. S., & Wang, Y. (1999). Effects of molding temperature and pressure on properties of soy protein polymers. *Journal of applied polymer science*, 73(13), 2595-2602.
- [313] Signori, F., Coltelli, M.-B., & Bronco, S. (2009). Thermal degradation of poly (lactic acid)(PLA) and poly (butylene adipate-co-terephthalate)(PBAT) and their blends upon melt processing. *Polymer degradation and stability*, 94(1), 74-82.
- [314] Mihai, M., Huneault, M. A., Favis, B. D., & Li, H. (2007). Extrusion Foaming of Semi - Crystalline PLA and PLA/Thermoplastic Starch Blends. *Macromolecular bioscience*, 7(7), 907-920.
- [315] Zhang, X., Espiritu, M., Bilyk, A., & Kurniawan, L. (2008). Morphological behaviour of poly (lactic acid) during hydrolytic degradation. *Polymer Degradation and Stability*, 93(10), 1964-1970.
- [316] Furuhashi, Y., Kimura, Y., & Yamane, H. (2007). Higher order structural analysis of stereocomplex - type poly (lactic acid) melt - spun fibers. *Journal of Polymer Science Part B: Polymer Physics*, 45(2), 218-228.
- [317] Tsuji, H., Takai, H., & Saha, S. K. (2006). Isothermal and non-isothermal crystallization behavior of poly (l-lactic acid): effects of stereocomplex as nucleating agent. *Polymer*, 47(11), 3826-3837.
- [318] Mittal, V., Akhtar, T., Luckachan, G., & Matsko, N. (2015). PLA, TPS and PCL binary and ternary blends: structural characterization and time-dependent morphological changes. *Colloid and Polymer Science*, 293(2), 573-585.
- [319] Powell, P. C., & Housz, A. I. (1998). *Engineering with polymers*. CRC Press.
- [320] Marsilla, K., & Verbeek, C. J. R. (2012). Blends of linear-low-density polyethylene and thermoplastic bloodmeal using maleic anhydride grafted polyethylene as compatibilizer.
- [321] Rhim, J.-W., Mohanty, K. A., Singh, S. P., & Ng, P. K. (2006). Preparation and properties of biodegradable multilayer films based on soy protein isolate and poly (lactide). *Industrial & engineering chemistry research*, 45(9), 3059-3066.
- [322] Yang, S.-l., Wu, Z.-H., Yang, W., & Yang, M.-B. (2008). Thermal and mechanical properties of chemical crosslinked polylactide (PLA). *Polymer Testing*, 27(8), 957-963.
- [323] Ali, F., Chang, Y.-W., Kang, S. C., & Yoon, J. Y. (2009). Thermal, mechanical and rheological properties of poly (lactic acid)/epoxidized soybean oil blends. *Polymer Bulletin*, 62(1), 91-98.

- [324] Wang, H., Sun, X., & Seib, P. (2002). Mechanical properties of poly (lactic acid) and wheat starch blends with methylenediphenyl diisocyanate. *Journal of applied polymer science*, 84(6), 1257-1262.
- [325] Noori, F. T. M., & Ali, N. A. (2014). Study the mechanical and thermal properties of biodegradable polylactic acid/poly ethylene glycol nanocomposites. *Int J Appl Innov Eng Manag*, 3(1), 459-464.
- [326] Wang, H., Sun, X., & Seib, P. (2003). Properties of poly (lactic acid) blends with various starches as affected by physical aging. *Journal of applied polymer science*, 90(13), 3683-3689.
- [327] Marsilla, K. K., & Verbeek, C. Properties of Blends of Novatein Thermoplastic Protein from Bloodmeal and Polybutylene Succinate Using Two Compatibilizers.
- [328] Walallavita, A., Verbeek, C., & Lay, M. (2018). Morphology and Mechanical Properties of Itaconic Anhydride Grafted Poly (lactic acid) and Thermoplastic Protein Blends. *International Polymer Processing*, 33(2), 153-163.
- [329] George, S., Joseph, R., Thomas, S., & Varughese, K. (1995). Blends of isotactic polypropylene and nitrile rubber: morphology, mechanical properties and compatibilization. *Polymer*, 36(23), 4405-4416.
- [330] Ibrahim, B. A., & Kadum, K. M. (2010). Influence of polymer blending on mechanical and thermal properties. *Modern Applied Science*, 4(9), 157.
- [331] Jose, S., Nair, S., Thomas, S., & Karger - Kocsis, J. (2006). Effect of reactive compatibilisation on the phase morphology and tensile properties of PA12/PP blends. *Journal of applied polymer science*, 99(5), 2640-2660.
- [332] Smith, M. J., & Verbeek, C. J. (2018). Compatibilization effects in thermoplastic protein/polyester blends. *Journal of Applied Polymer Science*, 135(6).
- [333] Menczel, J. D., & Prime, R. B. (2014). *Thermal analysis of polymers: fundamentals and applications*. John Wiley & Sons.
- [334] Tian, H., Guo, G., Fu, X., Yao, Y., Yuan, L., & Xiang, A. (2018). Fabrication, properties and applications of soy-protein-based materials: A review. *International journal of biological macromolecules*.
- [335] Pérez-Gago, M. B. (2012). Protein-based films and coatings. *Edible coatings and films to improve food quality*. CRC Press, Taylor & Francis Group, Boca Raton, Philadelphia, USA, 13-77.
- [336] Kester, J. J., & Fennema, O. (1986). Edible films and coatings: a review. *Food technology (USA)*.
- [337] Han, J. H. (2014). Edible films and coatings: a review. In *Innovations in Food Packaging (Second Edition)* (pp. 213-255). Elsevier.

- [338] Kumar, P., Sandeep, K., Alavi, S., Truong, V., & Gorga, R. (2010). Preparation and characterization of bio-nanocomposite films based on soy protein isolate and montmorillonite using melt extrusion. *Journal of Food Engineering*, 100(3), 480-489.
- [339] Ha, T., & Padua, G. (2001). Effect of extrusion processing on properties of zein-fatty acids sheets. *Transactions of the ASAE*, 44(5), 1223.
- [340] Budi Santosa, F., & Padua, G. W. (1999). Tensile properties and water absorption of zein sheets plasticized with oleic and linoleic acids. *Journal of agricultural and food chemistry*, 47(5), 2070-2074.
- [341] Sarkar, D., & Gupta, M. (2000). Estimation of elongational viscosity using entrance flow simulation. *CAE and Related Innovations for Polymer Processing, ASME, MD*, 90, 309-318.
- [342] Osswald, T., & Rudolph, N. (2015). Polymer rheology. *Carl Hanser, München*.
- [343] Kalambur, S., & Rizvi, S. S. (2006). Rheological behavior of starch-polycaprolactone (PCL) nanocomposite melts synthesized by reactive extrusion. *Polymer Engineering & Science*, 46(5), 650-658.
- [344] Li, H., & Huneault, M. A. (2011). Comparison of sorbitol and glycerol as plasticizers for thermoplastic starch in TPS/PLA blends. *Journal of Applied Polymer Science*, 119(4), 2439-2448.
- [345] Klüver, E., & Meyer, M. (2015). Thermoplastic processing, rheology, and extrudate properties of wheat, soy, and pea proteins. *Polymer Engineering & Science*, 55(8), 1912-1919.
- [346] Farnum, C., Stanley, D., & Gray, J. (1976). Protein-lipid interactions in soy films. *Canadian Institute of Food Science and Technology Journal*, 9(4), 201-206.
- [347] Chen, F., & Zhang, J. (2010). Effects of plasticization and shear stress on phase structure development and properties of soy protein blends. *ACS applied materials & interfaces*, 2(11), 3324-3332.
- [348] Paradkar, A., Kelly, A., Coates, P., & York, P. (2009). Shear and extensional rheology of hydroxypropyl cellulose melt using capillary rheometry. *Journal of pharmaceutical and biomedical analysis*, 49(2), 304-310.
- [349] Hayashi, N., Hayakawa, I., & Fujio, Y. (1991). Entrance effect correction on the flow of moisturized soy protein isolate melt in an extrusion viscometer. *International journal of food science & technology*, 26(6), 567-574.

Appendices

Appendix 1

Preparation and Characterisation of Decoloured Novatein® and modified PLA blends

Sandra C. P. Izuchukwu^{a*}, Casparus J. R. Verbeek^a, and James Michael Bier^b

*Corresponding author; sciokoro@gmail.com, scpi1@students.waikato.ac.nz

^a School of Engineering, University of Waikato, Private bag 3105, Hamilton 3240, New Zealand

^b Aduro Biopolymers LP, Private Bag 3105, Hamilton 3240, New Zealand

Abstract

Modified Poly (lactic acid) (PLA) was blended with Decoloured Novatein® (DNTP), a thermoplastic protein material using reactive extrusion to produce a degradable material with improved properties compared to neat Decoloured Novatein®. PLA was modified through free radical grafting of itaconic anhydride to create reactive side-chain groups. Varying ratios of DNTP/ PLA-g-IA or PLA were prepared. Blending DNTP with PLA was found to increase tensile strength between 22% to 538% and modulus between 201 GPa to 3193 GPa, whereas the strain at break decreased between 80% to 94% depending on the blend ratio. The glass transition temperature of the blends which was measured as the $\tan \delta$ peak, also revealed an increase when compared to neat DNTP. Scanning electron microscope revealed an enhanced interfacial adhesion between the two phases in the blends with PLA-g-IA suggesting a more homogenous microstructure. WAXS result revealed an insignificant decrease in the crystallinity of the blends compared to neat DNTP, indicating that blending with PLA had no structural effect on DNTP. The results show the possibility and feasibility of blending DNTP with PLA for use in agricultural and packaging applications.

1. Introduction

The rise in the cost of petroleum based polymer has led to an increased trend in the replacement of the synthetic polymer with bio-based polymers. PLA, protein, starch and gluten are among the bio-based polymers that are very attractive as replacement due to their availability and properties [1-3]. PLA has experienced substantial growth in its application as a result of its unique properties such as glossy optical appearance, biodegradability, compostability, high tensile strength and good barrier properties toward carbon dioxide, oxygen and water [4-6]. PLA is a biodegradable thermoplastic polyester derived from corn starch, with several

applications in biomedical and pharmaceutical fields as a material used in surgical operations, tissue regeneration, and drug delivery systems [7]. PLA is also considered suitable for high-volume packaging applications [4, 8] because of its good barrier properties to aromas and permeability to carbon dioxide, oxygen and water vapour compared to synthetic polymers. However, PLA is expensive and has low heat deflection temperature which remains as limitations for wider application. Therefore PLA has often been blended with other polymers to reduce cost and improve blends properties [4, 9-11]

Decoloured Novatein thermoplastic protein (DNTP) is a newly developed biopolymer using bloodmeal as starting material [12, 13]. DNTP is best suited for agricultural and horticultural applications such as weasand clips, weed mat pegs, biodegradable plant pot and seedling trays. DNTP is a protein polymer consisting of complex molecules with strong intra- and intermolecular interactions. These strong interactions make the melt processing of DNTP such as extrusion and injection moulding very difficult unless an adequate amount of plasticizers are added to promote mobility and flexibility of the protein chains enabling flow and consolidation during processing. Low molecular weight polyols such as glycerol, propylene glycol, ethylene glycol and their derivatives [13-17] are used as plasticizers for proteins to reduce intermolecular interactions and glass transition temperature T_g . However, the amount of plasticizer used affects the material's mechanical properties as well as leads to phase separation [5, 9]. Previous research has shown that DNTP can be successfully processed using the extrusion and injection moulder [18]. However, like every other protein polymer, moisture evaporates during processing which leads to a highly brittle material and loss of functionality. Blending DNTP with other polymers can improve its processability and mechanical properties. Researches has shown that blending protein with other hydrophobic thermoplastic is an alternative to increase the processability and moisture resistance of the protein based polymer products. Therefore, DNTP will be blended with PLA. However, the problem with this blend system is the poor interfacial interaction between the hydrophilic DNTP and hydrophobic PLA. Compatibilizer such as poly-2-ethyl-2-oxazoline (PEOX) [9, 19], polymeric methylene diphenyl diisocyanate (pMDI) [5, 20], maleic anhydride [21, 22], methylene diphenyl diisocyanate (MDI) [23, 24] and itaconic anhydride [25] have been used to enhance the interfacial interaction between PLA and other protein polymers.

Research on compatibilized blends of protein thermoplastics and polybutylene succinate reported an improvement in water resistance and tensile strength [5]. Blends of soy protein and PLA was found to increase tensile strength, reduced water absorption of soy plastic and a co-

continuous phase was observed for soy protein concentrate (SPC) and PLA [9]. Blends of cereal protein and poly (hydroxyl ester ether) without compatibilizer was reported to exhibit acceptable mechanical properties due to the strong hydrogen bonding between the two components [26]. Using a small amount of maleic anhydride (MA) grafted on low-density polyethylene (LLDPE), An improvement in the compatibility between Novatein thermoplastic protein (NTP) was observed as well as improved tensile strength and reduction in water absorption of NTP [20].

Itaconic anhydride (IA) is a highly reactive monomer in free radical grafting as it has the ability to produce tertiary radicals [27]. Although IA has not been extensively studied but it has been used as a renewable monomer for synthesising bio-based copolymers through conventional copolymerization [28], also can be used for acetylating lysin, tyrosine and cysteine [29]. IA is extremely stable when reacted with proteins compared to MA.

In this study, blends of DNTP and PLA compatibilized with itaconic anhydride were investigated. The main objective of this study was an attempt to demonstrate that DNTP can be used for PLA blends, as other proteins and starch has already been used for PLA blends. It also considered the improvement of processibility and properties of DNTP based plastic through blending with PLA. The morphology, thermal, mechanical and water absorption properties of DNTP/PLA blends were investigated.

2. Experimental

2.1. Materials

Bloodmeal was obtained from Wallace Corporation Limited, New Zealand and used as received. Analytical grade itaconic anhydride (IA), dicumyl peroxide (DCP), acetone, 30 wt % hydrogen peroxide, technical grade sodium dodecyl sulphate (SDS), triethylene glycol (TEG) were purchased from Sigma Aldrich NSW, Australia. Peracetic acid (Peraclean 5) was purchased from Evonik Industries, Morrinsville, New Zealand. Poly(lactic acid) (PLA) grade 3051D was purchased from NatureWorks Ltd in pellet form. Distilled water was produce onsite.

2.2. Sample preparation

2.2.1. Interfacial modification of PLA

PLA was modified through free radical grafting of itaconic anhydride [6] to create reactive side-chain groups. PLA was dried at 80 °C for 4 hours to control moisture. 4.2 parts per hundred

PLA (pph) itaconic anhydride and 0.8 pph dicumyl peroxide were dissolved in 30 mL acetone. The preformed solution was poured over the oven dried PLA and was kept in the fume hood for about 2 hours. The solution was decanted before oven drying the PLA for 3 hours at 50 °C. The modified PLA (PLA-g-IA) was extruded using a LabTech twin screw co-rotating extruder having a screw diameter of 20 mm and L/D of 44:1, at temperature profile of 145 (feed zone), 145, 165, 165, 180, 180, 180, 180, 160, 160, 155 °C (die zone). A constant screw speed was maintained at 150 rpm. A vacuum pump was attached on the 7th heating zone of the extruder to get rid of vapour generated during extrusion. To avoid the crystallization of the extruded PLA-g-IA, it was collected in a water bath upon exiting the die and afterwards pelletized. The pelletized PLA-g-IA was oven dried for 12 hours prior to blending with Decoloured Novatein (DNTP) to minimise hydrolysis during melt processing.

2.2.2. Bloodmeal decolouring and Decoloured Novatein preparation

Bloodmeal was decoloured using the standard method with solution of peracetic acid (PAA) [30, 31]. 4 wt% PAA solution was prepared by diluting 5 wt% stock solution with distilled water with a constant percentage ratio of 80:20 respectively. 150 g bloodmeal was decoloured by adding 450 g of 4 wt% PAA in a high speed mixer. The mixture was allowed to mix continuously for 5 min to ensure homogenous decolouring of bloodmeal. 450 g of distilled water was added and mixed for another 5 min to ensure complete dilution of the slurry. The slurry was neutralized by adjusting to pH = 7 with sodium hydroxide solution. The neutralized slurry was filtered using a wire mesh sieve with aperture size 60 and subsequently washed by adding another 450 g of distilled water. The decoloured bloodmeal was dried approximately 15 hours in a 75 °C oven.

Decoloured Novatein (DNTP) was formulated by dissolving 6 part per hundred decoloured bloodmeal (pphD) SDS in 40 pphD water heated to 60 °C while stirring. The solution was added to decoloured bloodmeal powder in a high speed mixer and mixed for 5 min. 30 pphD TEG was added to the mixture and mixed for another 5 min to ensure homogeneous mixture is obtained. The mixed material was stored in an air tight bag overnight in a 2 °C fridge to equilibrate.

2.2.3. Blends preparation

DNTP was formulated prior to blending. Blends containing 30:70, 50:50, 70:30 and 90:10 (w/w) DNTP/PLA-g-IA or PLA were prepared. The prepared DNTP and PLA-g-IA or PLA blends were then compounded using a twin screw co-rotating extruder (LabTech). The extruder

barrel had eleven heating zones and the screw speed was maintained at 150 rpm. The compounding extrusion temperature varied from 100 (feed zone) to 180 °C (die zone) depending on the DNTP content which required a reduction in compounding temperature with an increase in DNTP content as it's formulation contained 40 parts of water that could lead to PLA hydrolysis. The extrudate was granulated using a Tri-blade granulator from Castin Manufacturing Limited.

2.2.4. Test specimens preparation

ASTM D638-14 Standard tensile test samples [32] and ISO 179-1:2010 impact test samples [33] of the blends were injection moulded using a BOY 35A injection moulding machine. The samples were injected through a cold runner into a 60 °C water heated mould. The injection moulder has five heating zones including the feed and the die zones. The feed temperature remained constant at 100 °C, the barrel temperature varied between 100 to 140 and the die temperature varied between 120 to 140 depending on the formulation. The screw speed was constant at 150 rpm. The sample specimens produced were also used for water absorption, thermal and morphology testing.

2.3. Sample Analysis

All samples were conditioned for 7 days at 23 °C and 50 % relative humidity before testing except otherwise stated.

2.3.1. Mechanical properties

The mechanical testing was performed according to ASTM D638 using Instron Universal Testinf machine (model 33R4204) at a crosshead speed of 5 mm/min and an extensometer guage length of 50 mm. 10 replicates were tested for each sample type to obtain an average value.

The impact testing bars produced from the injection moulder had diameter of 80 x 10 x 4 mm³. Charpy edgewise impact strength was performed according to ISO 179-1:2010 using a RAY-RAN Pendulum Impact System. The bars tested were notched according to standard. 10 bars were tested to obtain average impact strength of the material.

2.3.2. Thermal analysis

Dynamic mechanical analysis (DMA) was conducted using Elmer DMA 8000 fitted with a high temperature furnace and cooled with liquid nitrogen. Rectanglar samples (30 x 9 x 4 mm) were cut from injection moulded samples and tested in a single cantilever fixture using free

length of 12.5 mm and scanning temperature from -80 to 150 °C at 2 °C/min . data was collected at multiple oscillation frequencies (0.1 – 30 Hz). Tan δ peak values were recorded as glass transition temperatures.

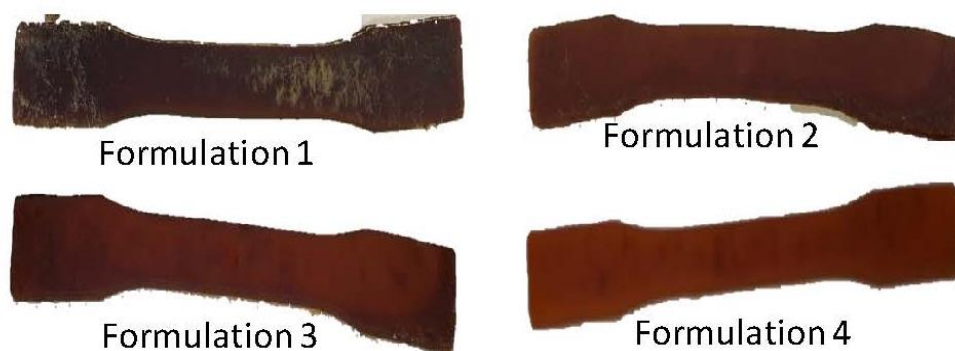
2.3.3. Wide angle X-ray scattering measurement (WAXS)

WAXS was used to measure the XRD pattern of the blends. WAXS was performed with a philips X-ray diffractometer operating at 40 Kv and 40 mA using CuK α radiation. The diffraction data was collected from 2θ values of 4° to 40° with a step size of 0.013°. a fixed 7.5 mm anti-scatter slit, fixed incidence beam mask of 10mm and a soller slit of 0.04 rad were used. *The data collected was baseline corrected from 5-40° and amorphous halo was fitted to this region to determine crystallinity of the blends.*

2.3.4. Fracture morphology

The phase structure of the blends was investigated using Hitachi S-4700 field emission scanning electron microscope (SEM). The injection molded specimens were cryofractured using liquid nitrogen. The specimens were sputter coated with platinum using Hitachi E-1030 Ion sputter before scanning.

3. Results and Discussion



Different formulations of DNTP were prepared based on varying the additives. Water was varied between 30 and 40 pphD, TEG was between 20 and 30 pphD and SDS was between 3 and 6 pphD to produce four sample formulations. The formulations were assessed for blend suitability with PLA based on ease of processing, mechanical and visible colour of produced sample. Formulation 2, 3 and 4 had ease of processing and were easily reproducible compared to formulation 1. They were easy to pull out of the mould and most were self-ejected. They showed reduced injection time and barrel refill time compared to formulation 1, which was

faced with spur and mould blockage. Comparing the visible clarity of samples, formulation 2, 3 and 4 were more transparent. Compromising tensile strength, formulation 2, 3 and 4 showed low modulus, impact strength and strain at break greater when compared. Similar mechanical properties have been reported for bioplastic produced from decoloured bloodmeal [13].

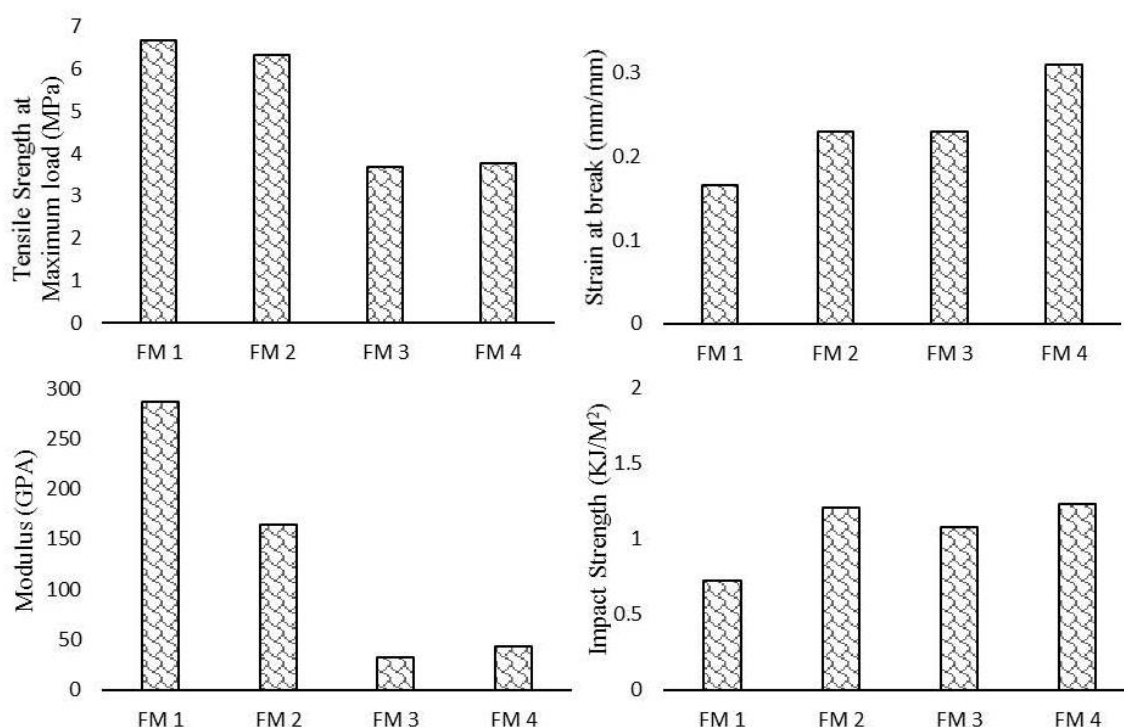


Figure 1: Mechanical properties of DNTP formulation with different ratio amount additives.

Flexibility, toughness and elongation are very important when considering a material for sheet production as they describe the material's ductility and are useful in the prediction of material performance during handling and storage. Therefore, formulation 4 was chosen to be investigated further as blends with PLA because it produced better extrudate, injection mouldable and brighter samples, having better strain at break, low modulus and good impact strength.

3.1 Blending and processing

Two different blend approaches were used to determine the best approach for DNTP/PLA-g-IA or PLA blends. In the first variation, PLA-g-IA or PLA was blended with pre-extruded

granules of DNTP and the second variation was to blend PLA-g-IA or PLA with DNTP powder.

3.1.1. Extrusion processing of the blended material

Extruding the blends of DNTP/PLA-g-IA or PLA produced either consolidated or semi-consolidated extrudate with semi or reasonably smooth surface. Extrudate flowed out of the extruder with moderate torque and pressure. The produced extrudate was flexible and rubbery prior to cooling. Small surface defects such as cracks and shark skinning were observed with the blends with high ratio of DNTP. The produced extrudate were granulated and injection moulded.

3.1.2. Injection moulding of the blended material

Injection moulding of blended DNTP granules and PLA-g-IA or PLA

The blends with pre-granulated DNTP could not be injection moulded due to excessive blockage of the injection moulder barrel and protein degradation. Adding of Struktol processing aid had no effect on the blend processing as it became more difficult to feed through the barrel. This was considered an effect of lack of plasticizer in the blend, which might be as a result of excess heat run on DNTP resulting to loss of plasticizers, considering that moisture was also controlled to avoid the hydrolysis of PLA. Therefore an approach to reduce DNTP heat run during processing was considered leading to blends of DNTP powder and PLA-g-IA or PLA.

Injection moulding of blended DNTP powder and PLA-g-IA or PLA

The injection moulding of DNTP powder and PLA-g-IA or PLA worked well without processing aid and produced flexible and consolidated sample bars. The injection of blends produced three type of sample bars as shown in Table 1.

Table 1: description of injection processing of blends

Injection type	Description
1	not self ejected out of the mould, longer injection time and barrel refill time, very difficult to pull out of the mould due to spur block.
2	not self injected out of the mould, reduced injection time and barrel refill time, easy to pull out of the mould unit and spur section.

- 3 | mostly self injected out of the mould and easy to remove from the mould unit manually, reduced injection time and barrel filling time.

Injection type 1 was observed mainly for blend having high amount of PLA while for blends having lower amount of PLA injection type 2 and 3 were observed and injection type 3 was observed for 50:50 blends. Blending PLA and DNTP powder was injection mouldable and showed ease of processing, therefore the second variation was chosen to be the optimal method for processing DNTP/PLA blends. The properties of the sample produced were investigated.

3.2 Phase morphology

The study of polymer blend morphology is important as it is related to the mechanical and barrier properties of the blend [14, 34] and it is essential in understanding property-structure relationship of the material. Most polymer blends are immiscible therefore produce a heterogeneous morphology [34]. Compatibilizers are used to reduce the interfacial tension in polymer blends thereby stabilizing the morphology, often resulting in a co-continuous structure [5]. Co-continuous morphology exhibits a combination of both polymer components characteristics [35], this is formed mainly around the point of phase inversions such that the matrix is undistinguishable from the dispersed phase.

Figure 2 shows the cryofractured phase structure of DNTP/PLA and DNTP/PLA-g-IA blends with DNTP/PLA-g-IA or PLA ratio varying between 30:70 to 90:10 (w/w). A dispersed phase morphology was observed with blends without itaconic anhydride showing one phase which is rich in DNTP and another that is rich in PLA (Figure 2.c, d, e). Also, the interstices between the DNTP phase and PLA matrix were clearly observed for the uncompatibilized blend indicating poor interfacial adhesion. This is expected, as DNTP contains 90% protein which is highly polar and hydrophilic while PLA is hydrophobic therefore will lead to poor interfacial interaction between the two phase. Blend of Novatein and polybutylene succinate (PBS) without compatibilizer was reported to have poor interfacial adhesion [5]. As DNTP content increased, the diameter of DNTP rich phase increased for blends without IA. This is attributed to the poor interfacial adhesion between DNTP and PLA phase. However, the addition of IA (Figure 2. c', d', e') showed an improved even dispersion of DNTP within the matrix. Even at high DNTP content (Figure 2. e'), a virtually undistinguishable DNTP phase was observed. Although some interstices were still observed in the compatibilized sample but they are fewer and smaller compared to the uncompatibilized blends.

The improved dispersion observed with blends compatibilized with IA arose from the formation of branched and crosslinked macromolecules initiated by the reaction of the anhydride group of PLA-g-IA with the amino groups of DNTP. Same phenomena had been reported for compatibilized PLA blends with protein and starch [10, 22]. It has been reported that addition of PEOX improved the interfacial adhesions between SPC/PLA blends resulting to finer structure and homogeneous phase structure [9]

Compatibilization showed no clear effect on 30:70 blend ratio (Figure 2. b and b'), this is believed to be due to the overwhelming effect of high PLA content in the matrix. This was further explored using thermal analysis and wide angle X-ray scattering (WAXS).

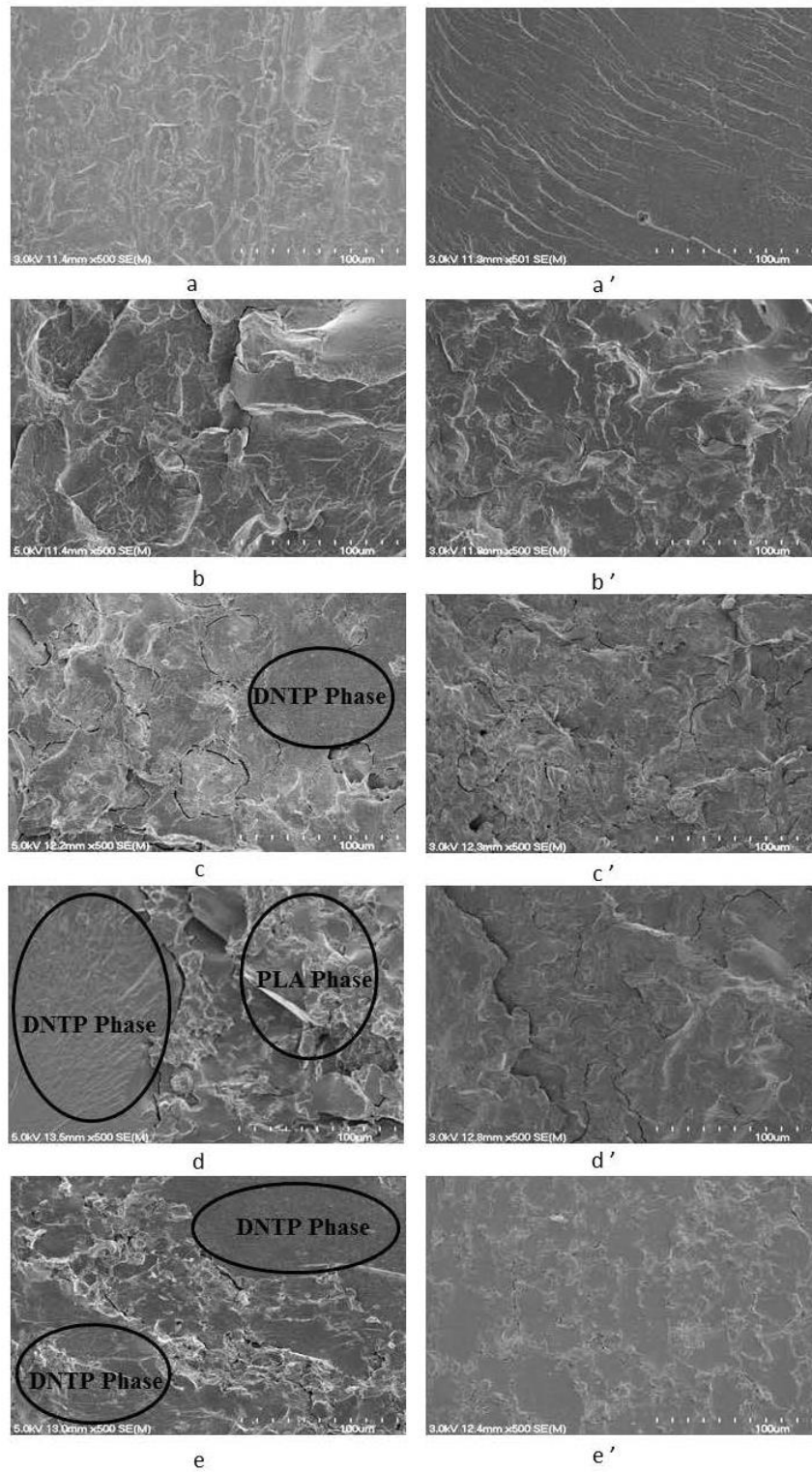


Figure 2: SEM micrographs of cryo-fractured surface of DNTP/ PLA-g-IA or PLA blends. a and a': PLA and DNTP; b and b': 3070DP and 3070DgP; c and c': 5050DP and 5050DgP; d and d': 7030DP and 7030DgP; e and e': 9010DP and 9010DgP

3.3. Dynamic mechanical properties

Understanding thermal transition of a polymer material is very important in the prediction of the material's performance under different end use conditions. DMA have been commonly used to study the molecular relaxation processes in polymers [14] and to determine inherent flow and mechanical properties such as modulus and damping of viscoelastic material over a spectrum of time (frequency) and temperature [36]. Figure 3 show the $\tan \delta$ and storage modulus (E') of neat PLA, PLA-g-IA and DNTP. PLA and DNTP showed broad and low damping peaks (T_g) while PLA-g-IA exhibited a sharp and high damping peak. The high damping peaks is suggested to be due to PLA-g-IA low crystallinity which makes it very soft when the temperature is above its α -transition. Similar observation have been reported for PLA grade used for blends with soy protein composites [9, 22].

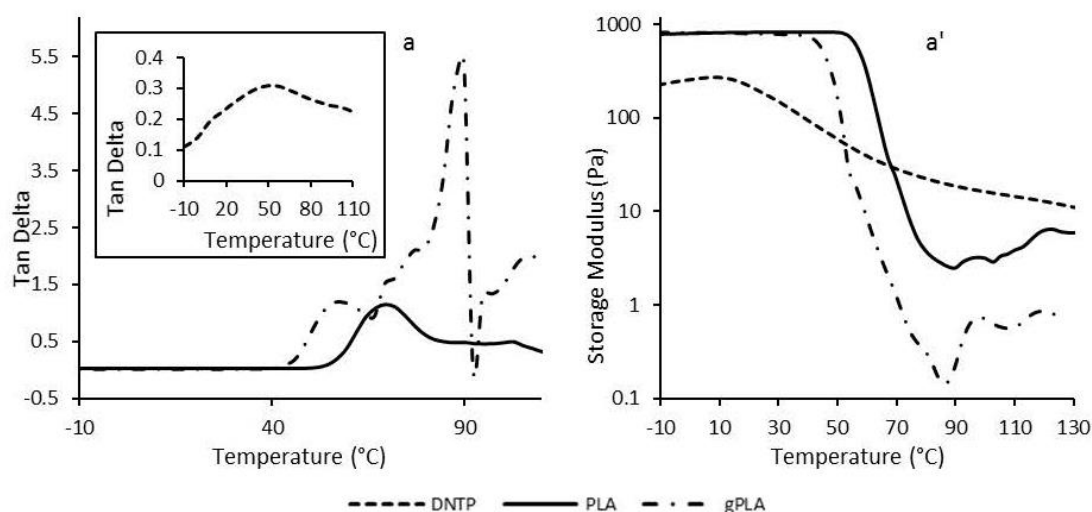


Figure 3: $\tan \delta$ and storage modulus (E') of neat PLA, PLA-g-IA and DNTP

The damping peak of PLA and PLA-g-IA in the blends were observed to be lower than that of the neat PLA and PLA-g-IA alone. This suggests that the DNTP component was still in glassy state in the α -transition range of PLA and PLA-g-IA. The compatibilized blends (Figure 4. a') show broader peaks compared to the uncompatibilized blends (Figure 4. a), which suggested that the blends had improved interactions between PLA and DNTP. The damping peak height decreased with increasing DNTP ratio, this is probably attributed to the effective contribution of the DNTP phase to the storage modulus in the rubbery region of PLA [9, 22, 37]. The decrease in T_g observed with the blends is thought to be due to the migration of small molecules of plasticisers from DNTP phase to the PLA matrix during compounding. No significant

difference was observed in the T_g of the compatibilizer and the uncompatibilizer blends therefore it suggests that compatibilization has no significant influence on the melting point of PLA in the blends.

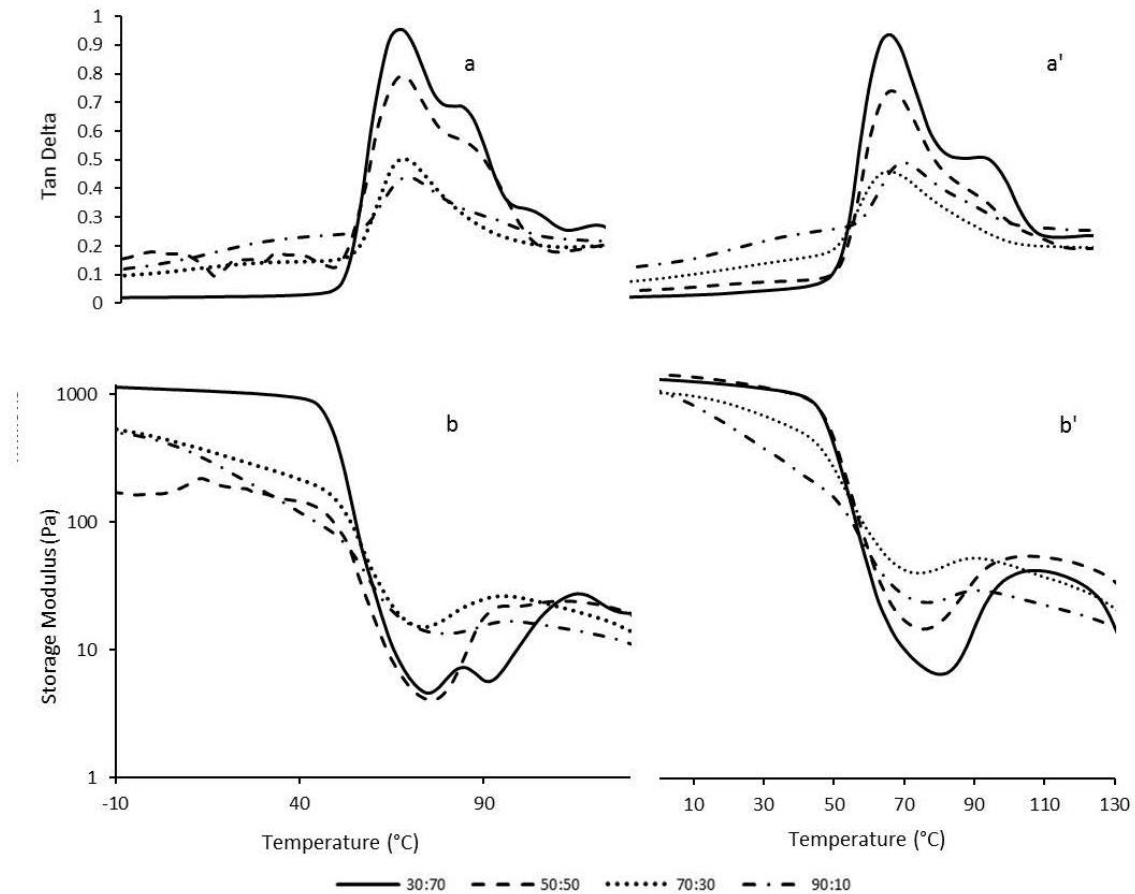


Figure 4: Tan δ and storage modulus (E') of blends. a and b: DNTP/ PLA, a' and b': DNTP/ PLA-g-IA

Two transitions (peak and a shoulder) was observed for the 30:70 and 50:50 blends (Figure 4. a). the first peak corresponds to the α -transition of PLA region and the second peak could be associated with the α -transition of the DNTP region in the blends. 30:70 and 50:50 blends with PLA-g-IA (Figure 4. a') showed a shift in the α -transition of DNTP region towards a lower temperature while the PLA region showed a slight change with compatibilization. This change is suggested to be due to the improved compatibility between both regions or as a result of miscibility of DNTP and the compatibilizer. Jinwen Zhang et al observed same trend with soy protein isolate/PLA compatibilizer with PEOX [9]. At higher content of DNTP, only a single peak was observed and no shift in peak temperature was observed. The storage modulus of the uncompatibilized blends dropped when the T_g of DNTP (≈ 60 °C) was reached, and then

recovered to a significant degree between 90 and 95 °C due to the cold crystallization of PLA. However, this recovery was not observed with the compatibilized blends. The compatibilized blends showed a lower storage modulus than both DNTP and PLA (Figure 3. a') at temperature below α -transition of PLA region. This might be associated with the compatibilization effect of IA on DNTP in the blends making DNTP more flexible in the blends. Ning Wang et al suggested that the addition of maleic anhydride improved the plasticization of starch in starch/PLA blends [10].

3.4. Wide angle X-ray scattering (WAXS) measurement

X-ray diffraction (XRD) is a technique used to measure the atomic arrangement of a material. The XRD data of polymers can be used to study the material's phase change. The WAXS of neat PLA, DNTP and DNTP/PLA blends with and without compatibilizer are shown in Figure 5. An amorphous peak at $16^\circ 2\theta$ was observed for PLA without a crystal and long-range order. PLA-g-IA clearly presents crystalline peaks at $2\theta = 16^\circ$ and 22° . The 2θ at 16° was recognized as (110)/(200) reflection of α -form homo-crystal structure and 2θ at 22° was recognized as (100)/(-120)/(-210) of stereo-complex crystals [38-40]. DNTP is semi-crystalline with less aggregated β -sheet and high number of disordered structure [13]. The peak at $2\theta = 9^\circ$ corresponds to helical spacing and inter- β -sheet and the peak at $2\theta = 22^\circ$ corresponds to repeated distance within each structure.

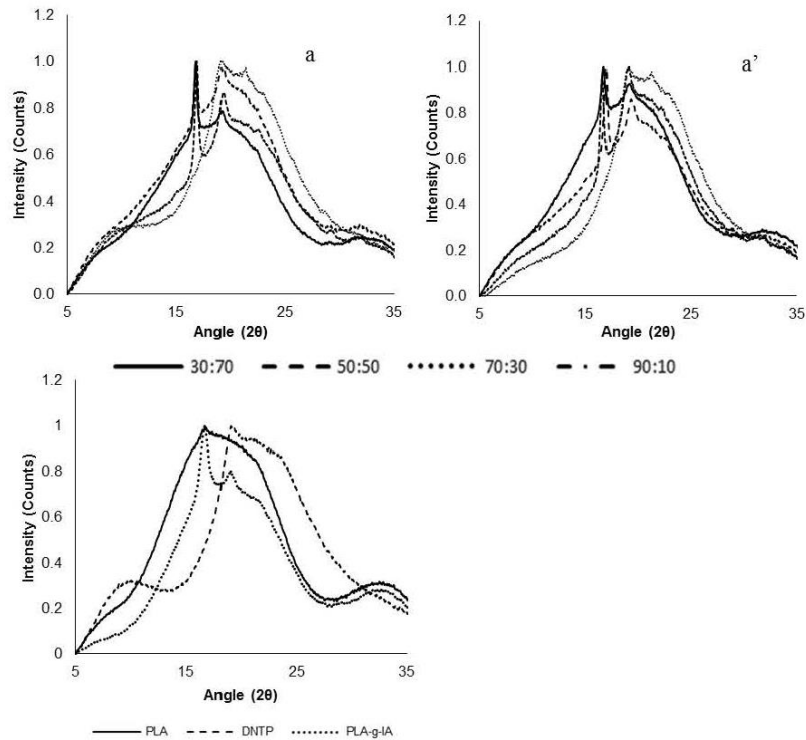


Figure 5: WAXS diffractograms of PLA, DNTP, PLA-g-MA and DNTP/PLA blends without (a) and with compatibilizer (a')

The summation of DNTP and PLA diffractogram looks exactly like the diffractogram of DNTP/PLA blends of both with and without compatibilizer. This suggests the existence of three phases in the blends, the amorphous DNTP, amorphous PLA and crystalline PLA. The compatibilized blends showed a slight reduction in the amorphous region suggesting an intergration of both PLA and DNTP amorphous region. This is probably due to the reduction in DNTP agglomerate observed with SEM thermogram (Figure 2).

No change was observed in 2θ for the two peak at 16° and 22° with the addition of compatibilizer. This suggests that Itaconic anhydride had no compatibilizing effect with the crystal region of the blend therefore may not be a good compatibilizer for DNTP/PLA blends or the degree of PLA grafting is not sufficient to compatibilize DNTP/PLA blends.

3.5 Mechanical properties

Mechanical testing provides valuable information on material's flexibility, toughness and elongation which is useful in the prediction of its performance during processing, handling, storage and final product performance. The mechanical properties of PLA, DNTP and DNTP/PLA blends are shown in Figure 6. PLA has been reported to have high tensile strength, impact strength, modulus and low elongation [41] while DNTP has low tensile strength, impact strength, modulus and high elongation [18]. Mechanical properties might be used to assess polymer blends miscibility as it depends on the intermolecular interaction chain stiffness and molecular symmetry of the individual polymer in the blend matrix [42]. Willemse et al. suggested that tensile modulus of polymer blends depends strongly on the composition and morphology of the blends [43].

Both DNTP/PLA blends with and without compatibilizer showed rigid and brittle behaviour. The modulus of the blends was higher than that of neat DNTP due to the incorporation of rigid PLA.

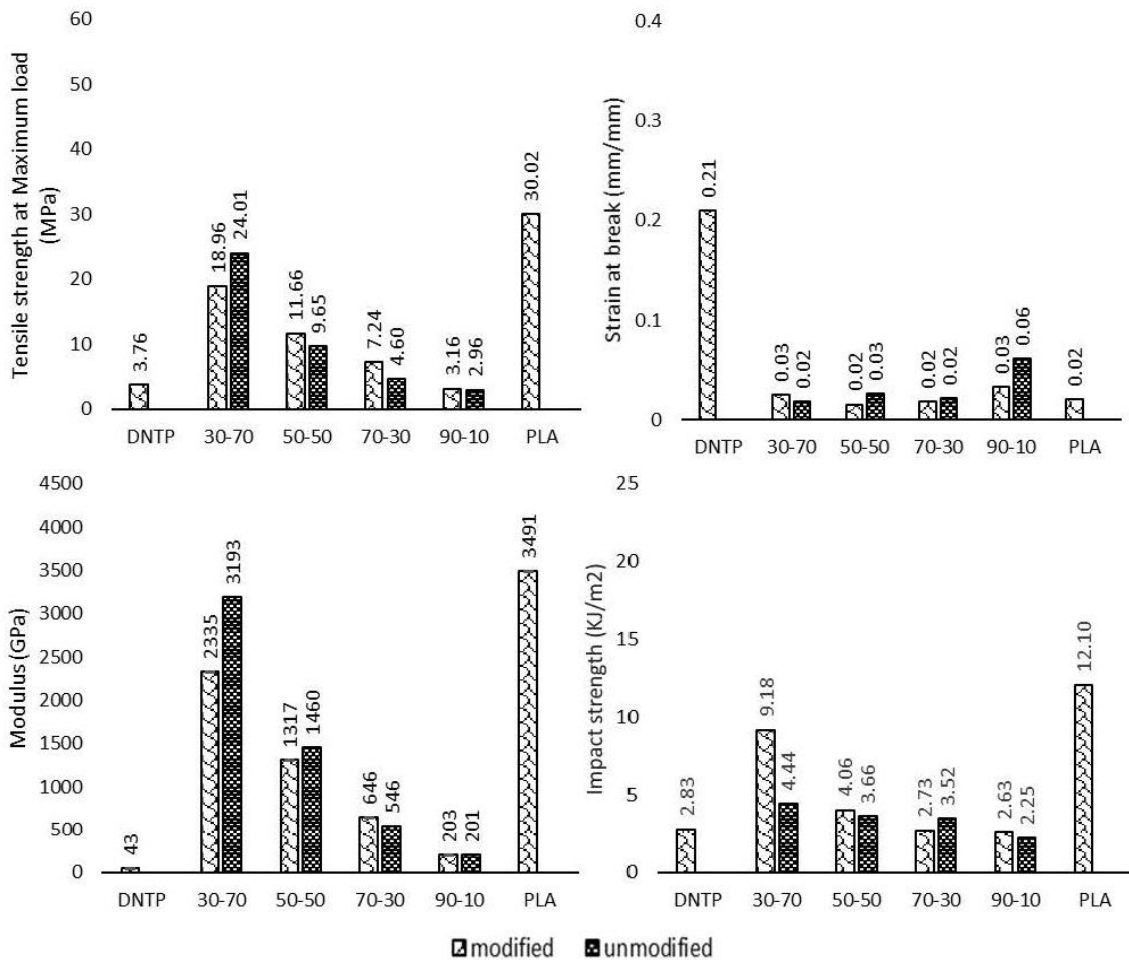


Figure 6: Mechanical properties of DNTP, PLA and DNTP/PLA blends with and without compatibilizer

Tensile strength observed for DNTP/PLA blends were inferior compare to neat PLA. This is as a result of weak interfacial adhesion between the two phases even with the addition of compatibilizer. Previous researches have reported inferior tensile strength for blends of PLA/Novatein [25] and PLA/soy protein [22]. However, all blends showed an improvement in tensile strength compared to DNTP. Further improvement was observed for 50-50 and 70-30 blends with the addition of itaconic anhydride. The mechanical properties of 30-70 compatibilized blends were very poor compared to the uncompatibilized blends while 90-10 blend showed no significant effect. It is assumed that below 50% and above 70% DNTP cotent, DNTP overwhelm the compatibiling effect of itaconic anhydride resulting in poor tensile strength.

The anhydride groups of Itaconic anhydride were likely to react with the amino groups of DNTP protein therefore enhancing the interfacial adhesion as observed with the SEM

micrographs (Figure 2) which played a role in reducing the size of DNTP phase in the compatibilized blends. However, this interfacial adhesion is considered to be very weak therefore wasn't strong enough to effect significant improvement in the mechanical properties. This is thought to be probably due to insufficient amount of compatibilizer (i.e. low degree of grafting) or an indication that Itaconic anhydride is not a suitable compatibilizer for DNTP/PLA blends. Rui Zhu et al, reported an increase in both tensile strength and elongation of PLA/Soy protein composite with an increase in compatibilizer content [22].

4. Conclusion

DNTP/PLA blends were successfully prepared by extrusion mixing. The processibility and flowability of DNTP increased after blending with PLA and it was injection mouldable without processing aids. The DNTP/PLA blends showed a co-continuous phase morphology with a wide range of compositions. Blends of DNTP/PLA compatibilized with itaconic anhydride led to significant change in morphology improving the interfacial adhesion between the blended material phases. however, the adhesion between the phases was not strong enough to improve mechanical properties. DMA results, WAXS diffractograms and mechanical properties indicated compatibility of PLA with DNTP and the possibility of improving their interfacial interactions. Itaconic anhydride can be used as compatibilizer for DNTP/PLA blends, leading to improved mixing of the two phases. However, the two transition observed in the blend's DMA (although the second transition shifted to lower temperature for 30:70 and 50:50 blends ratio) suggests that the amount of IA in PLA-g-IA is probably not sufficient enough to effect a significant improvement in the blend's mechanical properties. All blends showed low elongation at break and high brittle behaviour thereby creating room for material plasticization and toughening in future investigations. Investigation of DNTP formulation and plasticization will be necessary to optimize process and material's properties.

5. References

1. Sue, H.-J., S. Wang, and J.-L. Jane, *Morphology and mechanical behaviour of engineering soy plastics*. Polymer, 1997. **38**(20): p. 5035-5040.
2. Vaidya, U.R. and M. Bhattacharya, *Properties of blends of starch and synthetic polymers containing anhydride groups*. Journal of applied polymer science, 1994. **52**(5): p. 617-628.
3. Mohamed, A.A., et al., *Thermal characteristics of polylactic acid/wheat gluten blends*. Journal of food quality, 2006. **29**(3): p. 266-281.
4. Huneault, M.A. and H. Li, *Morphology and properties of compatibilized polylactide/thermoplastic starch blends*. Polymer, 2007. **48**(1): p. 270-280.
5. Ku-Marsilla, K. and C. Verbeek, *Compatibilization of Protein Thermoplastics and Polybutylene Succinate Blends*. Macromolecular Materials and Engineering, 2015. **300**(2): p. 161-171.

6. Marsilla, K.K. and C. Verbeek, *Modification of poly (lactic acid) using itaconic anhydride by reactive extrusion*. European Polymer Journal, 2015. **67**: p. 213-223.
7. Gorrasi, G. and R. Pantani, *Effect of PLA grades and morphologies on hydrolytic degradation at composting temperature: assessment of structural modification and kinetic parameters*. Polymer degradation and stability, 2013. **98**(5): p. 1006-1014.
8. Auras, R., B. Harte, and S. Selke, *An overview of polylactides as packaging materials*. Macromolecular bioscience, 2004. **4**(9): p. 835-864.
9. Zhang, J., et al., *Morphology and properties of soy protein and polylactide blends*. Biomacromolecules, 2006. **7**(5): p. 1551-1561.
10. Wang, N., J. Yu, and X. Ma, *Preparation and characterization of thermoplastic starch/PLA blends by one-step reactive extrusion*. Polymer International, 2007. **56**(11): p. 1440-1447.
11. Suyatma, N.E., et al., *Mechanical and barrier properties of biodegradable films made from chitosan and poly (lactic acid) blends*. Journal of Polymers and the Environment, 2004. **12**(1): p. 1-6.
12. Verbeek, C.J.R., M.C. Lay, and A.W.K. Low, *Methods of manufacturing plastic materials from decolorized blood protein*. 2013, Google Patents.
13. Low, A., *Decoloured bloodmeal based bioplastic*. 2012, University of Waikato.
14. Hernandez-Izquierdo, V. and J. Krochta, *Thermoplastic processing of proteins for film formation—a review*. Journal of food science, 2008. **73**(2).
15. Gennadios, A., *Protein-based films and coatings*. 2002: CRC Press.
16. Zhang, J., P. Mungara, and J.-I. Jane, *Mechanical and thermal properties of extruded soy protein sheets*. Polymer, 2001. **42**(6): p. 2569-2578.
17. Pickering, K.L., et al., *Plastics material*. 2012, Google Patents.
18. Verbeek, C.J.R., et al., *Processability and mechanical properties of bioplastics produced from decoloured bloodmeal*. Advances in Polymer Technology, 2017.
19. Smith, M.J. and C.J. Verbeek, *The relationship between morphology development and mechanical properties in thermoplastic protein blends*. Advances in Polymer Technology, 2017.
20. Marsilla, K. and C.J.R. Verbeek, *Properties of Bloodmeal/Linear Low-density Polyethylene Blends Compatibilized with Maleic Anhydride Grafted Polyethylene*. Journal of Applied Polymer Science, 2013. **130**(3): p. 1890-1897.
21. John, J. and M. Bhattacharya, *Properties of reactively blended soy protein and modified polyesters*. Polymer international, 1999. **48**(11): p. 1165-1172.
22. Zhu, R., H. Liu, and J. Zhang, *Compatibilizing effects of maleated poly (lactic acid)(PLA) on properties of PLA/Soy protein composites*. Industrial & Engineering Chemistry Research, 2012. **51**(22): p. 7786-7792.
23. Zhong, Z. and X.S. Sun, *Properties of soy protein isolate/polycaprolactone blends compatibilized by methylene diphenyl diisocyanate*. Polymer, 2001. **42**(16): p. 6961-6969.
24. Huang, J., et al., *Soy protein isolate/kraft lignin composites compatibilized with methylene diphenyl diisocyanate*. Journal of applied polymer science, 2004. **93**(2): p. 624-629.
25. Walallavita, A., C.J. Verbeek, and M. Lay. *Blending Novatein® thermoplastic protein with PLA for carbon dioxide assisted batch foaming*. in *AIP Conference Proceedings*. 2016. AIP Publishing.
26. Wang, C., C. Carriere, and J. Willett, *Processing, mechanical properties, and fracture behavior of cereal protein/poly (hydroxyl ester ether) blends*. Journal of Polymer Science Part B: Polymer Physics, 2002. **40**(19): p. 2324-2332.
27. Sharabasht, M.M. and R.L. Guile, *Copolymerization Parameters of Itaconic Anhydride in Free-Radical Polymerization*. Journal of Macromolecular Science: Part A-Chemistry, 1976. **10**(6): p. 1039-1054.

28. Okuda, T., et al., *Renewable biobased polymeric materials: facile synthesis of itaconic anhydride-based copolymers with poly (L-lactic acid) grafts*. *Macromolecules*, 2012. **45**(10): p. 4166-4174.
29. Fischer, L. and F. Peissker, *A covalent two-step immobilization technique using itaconic anhydride*. *Applied microbiology and biotechnology*, 1998. **49**(2): p. 129-135.
30. Low, A., C.J.R. Verbeek, and M.C. Lay, *Treating Bloodmeal with Peracetic Acid to Produce a Bioplastic Feedstock*. *Macromolecular Materials and Engineering*, 2014. **299**(1): p. 75-84.
31. Hicks, T.M., et al., *The role of peracetic acid in bloodmeal decoloring*. *Journal of the American Oil Chemists' Society*, 2013. **90**(10): p. 1577-1587.
32. Properties, A.S.D.o.M. *Standard test method for tensile properties of plastics*. 1996. American Society for Testing and Materials.
33. ISO, E., *179-1 (2010)*.". *Plastics. Determination of Charpy impact properties. Part. 1*.
34. Willemse, R., et al., *Co-continuous morphologies in polymer blends: a new model*. *Polymer*, 1998. **39**(24): p. 5879-5887.
35. Xie, H.-Q., J. Xu, and S. Zhou, *Polymer blends with two kinds of elastomeric ionomers*. *Polymer*, 1991. **32**(1): p. 95-102.
36. Menczel, J.D. and R.B. Prime, *Thermal analysis of polymers: fundamentals and applications*. 2014: John Wiley & Sons.
37. Sumita, M., et al., *Dynamic mechanical properties of polypropylene composites filled with ultrafine particles*. *Journal of applied polymer science*, 1984. **29**(5): p. 1523-1530.
38. Furuhashi, Y., Y. Kimura, and H. Yamane, *Higher order structural analysis of stereocomplex-type poly (lactic acid) melt-spun fibers*. *Journal of Polymer Science Part B: Polymer Physics*, 2007. **45**(2): p. 218-228.
39. Tsuji, H., H. Takai, and S.K. Saha, *Isothermal and non-isothermal crystallization behavior of poly (l-lactic acid): effects of stereocomplex as nucleating agent*. *Polymer*, 2006. **47**(11): p. 3826-3837.
40. Mittal, V., et al., *PLA, TPS and PCL binary and ternary blends: structural characterization and time-dependent morphological changes*. *Colloid and Polymer Science*, 2015. **293**(2): p. 573-585.
41. Martin, O. and L. Averous, *Poly (lactic acid): plasticization and properties of biodegradable multiphase systems*. *Polymer*, 2001. **42**(14): p. 6209-6219.
42. Joseph, S. and S. Thomas, *Modeling of tensile moduli in polystyrene/polybutadiene blends*. *Journal of Polymer Science Part B: Polymer Physics*, 2002. **40**(8): p. 755-764.
43. Willemse, R., et al., *Tensile moduli of co-continuous polymer blends*. *Polymer*, 1999. **40**(24): p. 6645-6650.

Appendix 2

Decoloured Novatein® and PLA blends compatibilized with itaconic anhydride

Sandra C. P. Izuchukwu^{1,a*}, Casparus J. R. Verbeek^{1,b}, and James Michael Bier²

*Corresponding author; sciokoro@gmail.com, scpi1@students.waikato.ac.nz

¹ School of Engineering, University of Waikato, Private bag 3105, Hamilton 3240, New Zealand

² Aduro Bioploymers LP, Private Bag 3105, Hamilton 3240, New Zealand

Keywords: PLA, Decoloured Novatein, Bloodmeal, Bio-based polymer, Blends, Itaconic anhydride.

Abstract

Poly (lactic acid) (PLA) was modified through free radical grafting of itaconic anhydride to create reactive side-chain groups. Modified PLA was blended with Decoloured Novatein® (DNTP), a thermoplastic protein material using reactive extrusion to produce a degradable material with improved properties compared to neat Decoloured Novatein®. Varying ratios of blends were prepared. DNTP/PLA blends was found to increase tensile strength between 22% to 538% and modulus between 201 GPa to 3193 GPa, whereas the strain at break decreased between 80% to 94% depending on the blend ratio. The glass transition temperature of the blends which was measured as the $\tan \delta$ peak, also revealed an increase when compared to neat DNTP. Scanning electron microscope revealed an enhanced interfacial adhesion between the two phases in the blends with PLA-g-IA suggesting a more homogenous microstructure. The results show the possibility and feasibility of blending DNTP with PLA for use in agricultural and packaging applications.

1. Introductions

The rise in the cost of petroleum based polymer has led to an increased trend in the replacement of the synthetic polymer with bio-based polymers. PLA, protein, starch and gluten are among the bio-based polymers that are very attractive as replacement due to their availability and properties [1-3]. PLA has experienced substantial growth in its application as a result of its unique properties such as glossy optical appearance, biodegradability, compostability, high tensile strength and good barrier properties toward carbon dioxide, oxygen and water [4-6]. PLA is a biodegradable thermoplastic polyester derived from corn starch, with several applications in biomedical and pharmaceutical fields as a material used in surgical operations,

tissue regeneration, and drug delivery systems [7]. PLA is also considered suitable for high-volume packaging applications [4, 8] because of its good barrier properties to aromas and permeability to carbon dioxide, oxygen and water vapour compared to synthetic polymers. However, PLA is expensive and has a low heat deflection temperature which remains as limitations for wider application. Therefore PLA has often been blended with other polymers to reduce cost and improve blends properties [4, 9-11].

Decoloured Novatein thermoplastic protein (DNTP) is a newly developed biopolymer using bloodmeal as a starting material [12, 13]. DNTP is best suited for agricultural and horticultural applications such as weasand clips, weed mat pegs, biodegradable plant pot and seedling trays. DNTP is a protein polymer consisting of complex molecules with strong intra- and intermolecular interactions. These strong interactions make the melt processing of DNTP such as extrusion and injection moulding very difficult unless an adequate amount of plasticizers are added to promote mobility and flexibility of the protein chains enabling flow and consolidation during processing. Low molecular weight polyols such as glycerol, propylene glycol, ethylene glycol and their derivatives [13-17] are used as plasticizers for proteins to reduce intermolecular interactions and glass transition temperature T_g . However, the amount of plasticizer used affects the material's mechanical properties as well as leads to phase separation [5, 9]. Previous research has shown that DNTP can be successfully processed using the extrusion and injection moulder [18]. However, like every other protein polymer, moisture evaporates during processing which leads to a highly brittle material and loss of functionality. Blending DNTP with other polymers can improve its processability and mechanical properties. Researches have shown that blending protein with other hydrophobic thermoplastic is an alternative to increase the processability and moisture resistance of the protein based polymer products. Therefore, DNTP will be blended with PLA. However, the problem with this blend system is the poor interfacial interaction between the hydrophilic DNTP and hydrophobic PLA. Compatibilizer such as poly-2-ethyl-2-oxazoline (PEOX) [9, 19], polymeric methylene diphenyl diisocyanate (pMDI) [5, 20], maleic anhydride [21, 22], methylene diphenyl diisocyanate (MDI) [23, 24] and itaconic anhydride [25] have been used to enhance the interfacial interaction between PLA and other protein polymers.

Research on compatibilized blends of protein thermoplastics and polybutylene succinate reported an improvement in water resistance and tensile strength [5]. Blends of soy protein and PLA was found to increase tensile strength, reduced water absorption of soy plastic and a co-continuous phase was observed for soy protein concentrate (SPC) and PLA [9]. Blends of

cereal protein and poly (hydroxyl ester ether) without compatibilizer was reported to exhibit acceptable mechanical properties due to the strong hydrogen bonding between the two components [26]. Using a small amount of maleic anhydride (MA) grafted on low-density polyethylene (LLDPE), An improvement in the compatibility between Novatein thermoplastic protein (NTP) was observed as well as improved tensile strength and reduction in water absorption of NTP [20].

Itaconic anhydride (IA) is a highly reactive monomer in free radical grafting as it has the ability to produce tertiary radicals [27]. Although IA has not been extensively studied but it has been used as a renewable monomer for synthesizing bio-based copolymers through conventional copolymerization [28], also can be used for acetylating lysin, tyrosine and cysteine [29]. IA is extremely stable when reacted with proteins compared to MA.

In this study, blends of DNTP and PLA compatibilized with itaconic anhydride were investigated. The main objective of this study was an attempt to demonstrate that DNTP can be used for PLA blends, as other proteins and starch has already been used for PLA blends. It also considered the improvement of processibility and properties of DNTP based plastic through blending with PLA. The morphology, thermal, and mechanical properties of DNTP/PLA blends were investigated.

2. Experimental

2.1. Materials

Bloodmeal was obtained from Wallace Corporation Limited, New Zealand and used as received. Analytical grade itaconic anhydride (IA), dicumyl peroxide (DCP), acetone, 30 wt % hydrogen peroxide, technical grade sodium dodecyl sulphate (SDS), triethylene glycol (TEG) were purchased from Sigma Aldrich NSW, Australia. Peracetic acid (Peraclean 5) was purchased from Evonik Industries, Morrinsville, New Zealand. Poly(lactic acid) (PLA) grade 3051D was purchased from NatureWorks Ltd in pellet form. Distilled water was produce onsite.

2.2. Sample preparation

2.2.1. PLA grafting

itaconic anhydride was grafted unto PLA through free radical grafting [6] to create reactive side-chain groups. PLA was dried at 80 °C for 4 hours to control moisture. 4.2 parts per hundred PLA (pph) itaconic anhydride and 0.8 pph dicumyl peroxide were dissolved in 30 mL acetone.

The preformed solution was poured over the oven dried PLA and was kept in the fume hood for about 2 hours. The solution was decanted before oven drying the PLA for 3 hours at 50 °C. The modified PLA (PLA-g-IA) was extruded using a LabTech twin screw co-rotating extruder having L/D 44:1 with a screw diameter of 20 mm, at temperature profile of 145 (feed zone), 145, 165, 165, 180, 180, 180, 180, 160, 160, 155 °C (die zone). A constant screw speed was maintained at 150 rpm. A vacuum pump was attached on the 7th heating zone of the extruder to get rid of vapour generated during extrusion. To avoid the crystallization of the extruded PLA-g-IA, it was collected in a water bath upon exiting the die and afterwards pelletized. The pelletized PLA-g-IA was oven dried for 12 hours at 50 °C prior to blending with Decoloured Novatein (DNTP) to minimise hydrolysis during melt processing.

2.2.2. Bloodmeal decolouring and Decoloured Novatein preparation

Bloodmeal was decoloured using the standard method with solution of peracetic acid (PAA) [30, 31]. 4 wt% PAA solution was prepared by diluting 5 wt% stock solution with distilled water with a constant percentage ratio of 80:20 respectively. 150 g bloodmeal was decoloured by adding 450 g of 4 wt% PAA in a high speed mixer. The mixture was allowed to mix continuously for 5 min to ensure homogenous decolouring of bloodmeal. 450 g of distilled water was added and mixed for another 5 min to ensure complete dilution of the slurry. The slurry was neutralized by adjusting to pH = 7 with sodium hydroxide solution. The neutralized slurry was filtered using a wire mesh sieve with aperture size 60 and subsequently washed by adding another 450 g of distilled water. The decoloured bloodmeal was dried approximately 15 hours in a 75 °C oven.

Decoloured Novatein (DNTP) was formulated by dissolving 6 part per hundred decoloured bloodmeal (pphD) SDS in 40 pphD water heated to 60 °C while stirring. The solution was added to decoloured bloodmeal powder in a high speed mixer and mixed for 5 min. 30 pphD TEG was added to the mixture and mixed for another 5 min to ensure homogeneous mixture is obtained. The mixed material was stored in an air tight bag overnight in a 2 °C fridge to equilibrate.

2.2.3. Blends preparation

DNTP was formulated prior to blending. Blends containing 30:70, 50:50, 70:30 and 90:10 (w/w) DNTP/PLA-g-IA or PLA were prepared. The performed DNTP and PLA-g-IA or PLA blends were then compounded using a twin screw co-rotating extruder (LabTech). The extruder barrel had eleven heating zones and the screw speed was maintained at 150 rpm. The

compounding extrusion temperature varied from 100 (feed zone) to 180 °C (die zone) depending on the DNTP content which required a reduction in compounding temperature with an increase in DNTP content as it's formulation contained 40 parts of water that could lead to PLA hydrolysis. The extrudate was granulated using a Tri-blade granulator from Castin Manufacturing Limited.

2.2.4. Test specimens preparation

ASTM D638-14 Standard tensile test samples [32] and ISO 179-1:2010 impact test samples [33] of the blends were injection moulded using a BOY 35A injection moulding machine. The samples were injected through a cold runner into a 60 °C water heated mould. The injection moulder has five heating zones including the feed and the die zones. The feed temperature remained constant at 100 °C, the barrel temperature varied between 100 to 140 and the die temperature varied between 120 to 140 depending on the formulation. The screw speed was constant at 150 rpm. The sample specimens produced were also used for thermal and morphology analysis.

2.3. Sample Analysis

All samples were conditioned for 7 days at 23 °C and 50 % relative humidity before testing except otherwise stated.

2.3.1. Mechanical properties

The mechanical testing was performed according to ASTM D638 using Instron Universal Testing machine (model 33R4204) at a crosshead speed of 5 mm/min and an extensometer gauge length of 50 mm. 10 replicates were tested for each sample type to obtain an average value.

The impact testing bars produced from the injection moulder had diameter of 80 x 10 x 4 mm³. Charpy edgewise impact strength was performed according to ISO 179-1:2010 using a RAY-RAN Pendulum Impact System. The bars tested were notched according to standard. 10 bars were tested to obtain average impact strength of the material.

2.3.2. Thermal analysis

Dynamic mechanical analysis (DMA) was conducted using Elmer DMA 8000 fitted with a high temperature furnace and cooled with liquid nitrogen. Rectangular samples (30 x 9 x 4 mm) were cut from injection moulded samples and tested in a single cantilever fixture using free length of 12.5 mm and scanning temperature from -80 to 150 °C at 2 °C/min . data was collected

at multiple oscillation frequencies (0.1 – 30 Hz). Tan δ peak values were recorded as glass transition temperatures.

2.3.3. Fracture morphology

The phase structure of the blends was investigated using Hitachi S-4700 field emission scanning electron microscope (SEM). The injection molded specimens were cryofractured using liquid nitrogen. The specimens were sputter coated with platinum using Hitachi E-1030 Ion sputter before scanning.

3. Results and Discussion

3.1 Phase morphology

The study of polymer blend morphology is important as it is related to the mechanical and barrier properties of the blend [14, 34] and it is essential in understanding property-structure relationship of the material. Most polymer blends are immiscible therefore produce a heterogeneous morphology [34]. Compatibilizers are used to reduce the interfacial tension in polymer blends thereby stabilizing the morphology, often resulting in a co-continuous structure [5]. Co-continuous morphology exhibits a combination of both polymer components characteristics [35], this is formed mainly around the point of phase inversions such that the matrix is undistinguishable from the dispersed phase.

Figure 1 shows the cryofractured phase structure of DNTP/PLA and DNTP/PLA-g-IA blends with DNTP/PLA-g-IA or PLA ratio varying between 30:70 to 90:10 (w/w). A dispersed phase morphology was observed with blends without itaconic anhydride showing one phase which is rich in DNTP and another that is rich in PLA (Figure 1.c, d, e). Also, the interstices between the DNTP phase and PLA matrix were clearly observed for the uncompatibilized blend indicating poor interfacial adhesion. This is expected, as DNTP contains 90% protein which is highly polar and hydrophilic while PLA is hydrophobic therefore will lead to poor interfacial interaction between the two phases. Blend of Novatein and polybutylene succinate (PBS) without compatibilizer was reported to have poor interfacial adhesion [5]. As DNTP content increased, the size of DNTP rich phase increased for blends without IA. This is attributed to the poor interfacial adhesion between DNTP and PLA phase. However, the addition of IA (Figure 1. c', d', e') showed an improved even dispersion of DNTP within the matrix. Even at high DNTP content (Figure 1. e'), a virtually undistinguishable DNTP phase was observed. Although some interstices were still observed in the compatibilized sample but they are fewer and smaller compared to the uncompatibilized blends.

The improved dispersion observed with blends compatibilized with IA arose from the formation of branched and crosslinked macromolecules initiated by the reaction of the anhydride group of PLA-g-IA with the amino groups of DNTP. Same phenomena had been reported for compatibilized PLA blends with protein and starch [10, 22]. It has been reported that addition of PEOX improved the interfacial adhesions between SPC/PLA blends resulting to finer structure and homogeneous phase structure [9]

Compatibilization showed no clear effect on 30:70 blend ratio (Figure 1. b and b'), this is believed to be due to the overwhelming effect of high PLA content in the matrix. This was further explored using thermal.

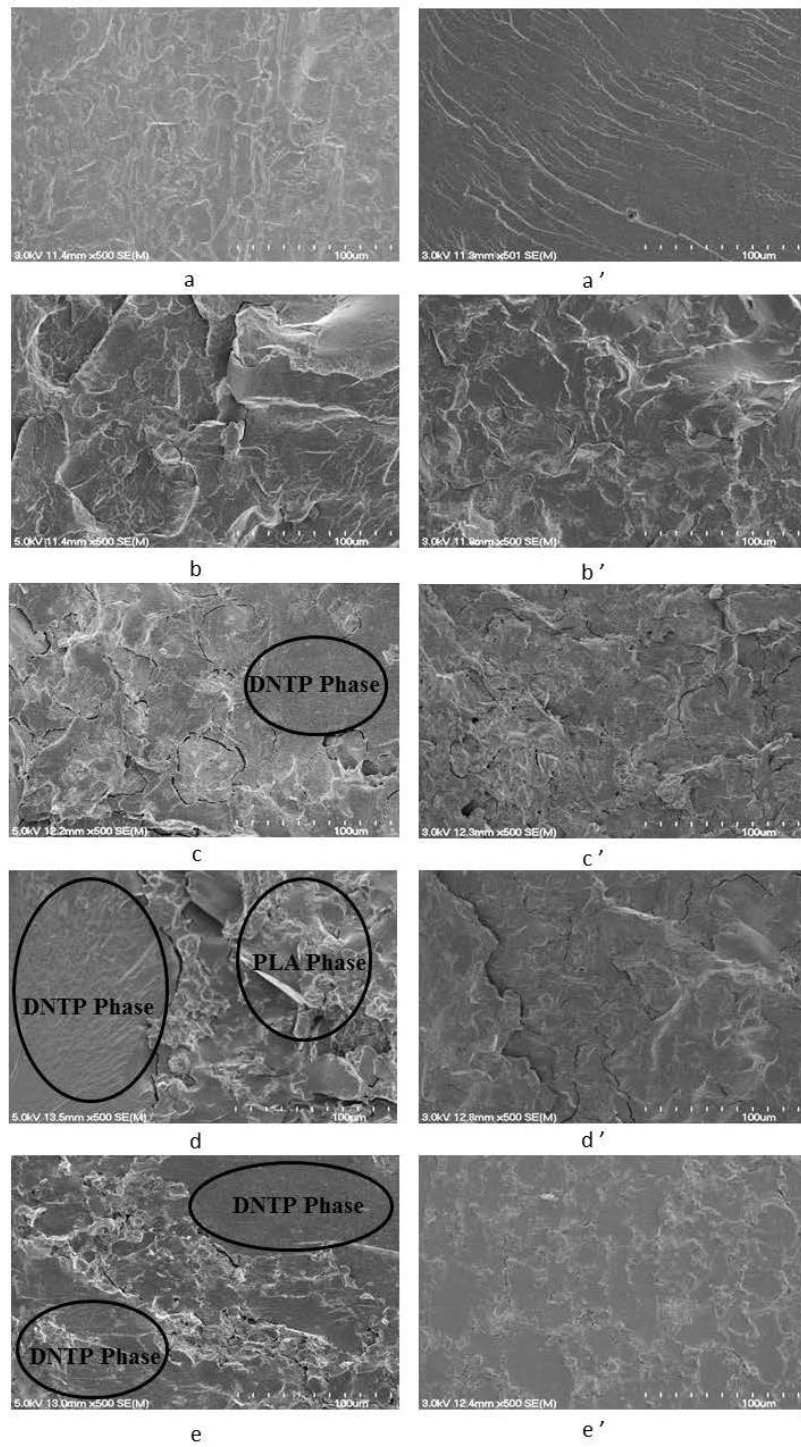


Figure 1: SEM micrographs of cryo-fractured surface of DNTP/ PLA-g-IA or PLA blends. a and a': PLA and DNTP; b and b': 3070DP and 3070DgP; c and c': 5050DP and 5050DgP; d and d': 7030DP and 7030DgP; e and e': 9010DP and 9010DgP

3.2. Dynamic mechanical properties

Understanding thermal transition of a polymer material is very important in the prediction of the material's performance under different end use conditions. DMA have been commonly used to study the molecular relaxation processes in polymers [14] and to determine inherent flow and mechanical properties such as modulus and damping of viscoelastic material over a spectrum of time (frequency) and temperature [36]. Figure 2 show the $\tan \delta$ and storage modulus (E') of neat PLA, PLA-g-IA and DNTP. PLA and DNTP showed broad and low damping peaks (T_g) while PLA-g-IA exhibited a sharp and high damping peak. The high damping peaks is suggested to be due to PLA-g-IA low crystallinity which makes it very soft when the temperature is above its α -transition. Similar observation have been reported for PLA grade used for blends with soy protein composites [9, 22].

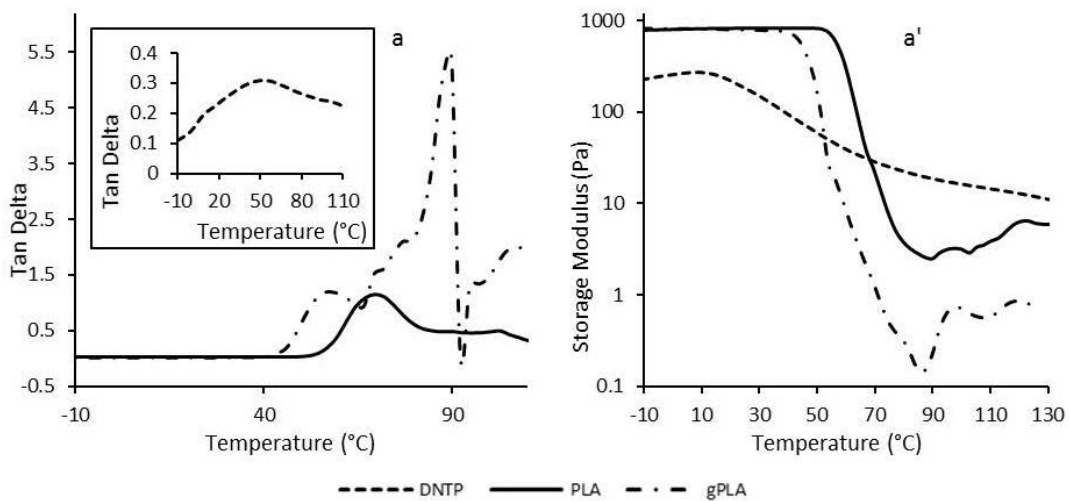


Figure 2: $\tan \delta$ and storage modulus (E') of neat PLA, PLA-g-IA and DNTP

Figure 3 shows the $\tan \delta$ and storage modulus (E') of blends with and without compatibilizer. The damping peak of PLA and PLA-g-IA in the blends were observed to be lower than that of the neat PLA and PLA-g-IA alone. This suggests that the DNTP component was still in glassy state in the α -transition range of PLA and PLA-g-IA. The compatibilized blends (Figure 3. a') show broader peaks compared to the uncompatibilized blends (Figure 3. a), which suggested that the blends had improved interactions between PLA and DNTP. The damping peak height decreased with increasing DNTP ratio, this is probably attributed to the effective contribution of the DNTP phase to the storage modulus in the rubbery region of PLA [9, 22, 37]. The decrease in T_g observed with the blends is thought to be due to the migration of small molecules

of plasticisers from DNTP phase to the PLA matrix during compounding. No significant difference was observed in the T_g of the compatibilizer and the uncompatibilizer blends therefore it suggests that compatibilization has no significant influence on the melting point of PLA in the blends.

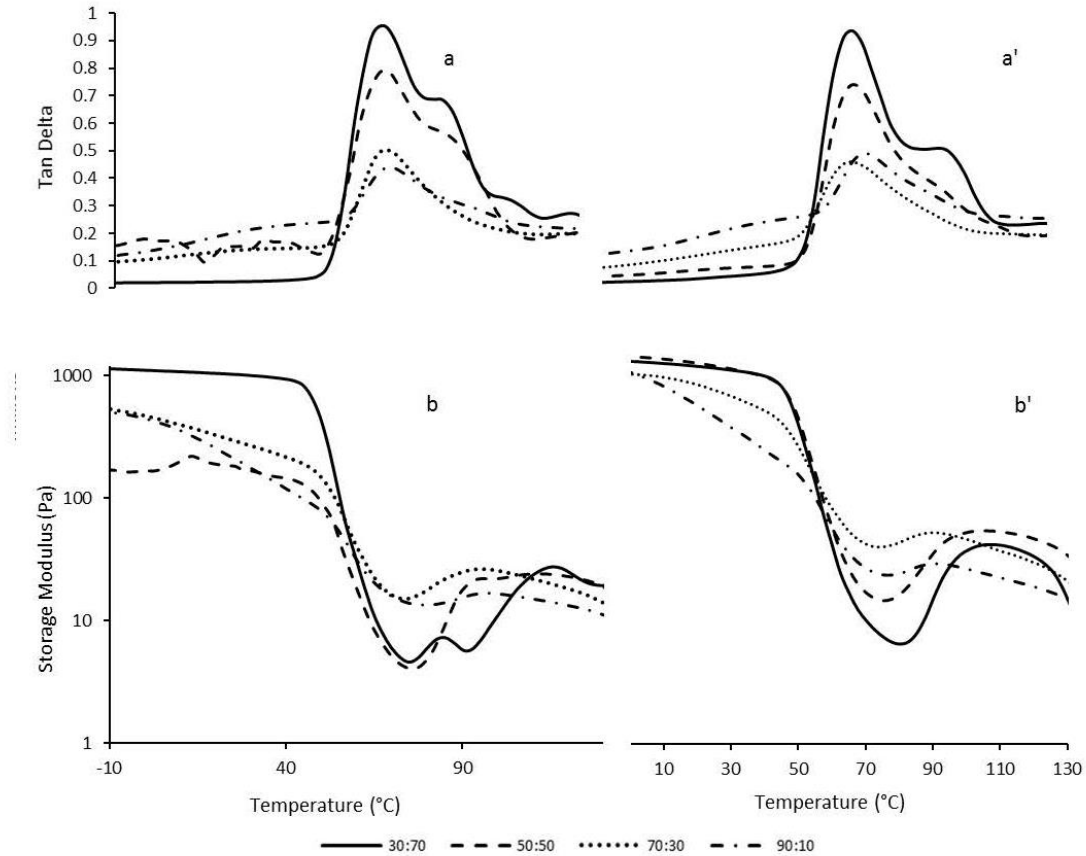


Figure 3: Tan δ and storage modulus (E') of blends. a and b: DNTP/ PLA, a' and b': DNTP/ PLA-g-IA

Two transitions (peak and a shoulder) was observed for the 30:70 and 50:50 blends (Figure 3. a). the first peak corresponds to the α -transition of PLA region and the second peak could be associated with the α -transition of the DNTP region in the blends. 30:70 and 50:50 blends with PLA-g-IA (Figure 3. a') showed a shift in the α -transition of DNTP region towards a lower temperature while the PLA region showed a slight change with compatibilization. This change is suggested to be due to the improved compatibility between both regions or as a result of miscibility of DNTP and the compatibilizer. Jinwen Zhang et al observed same trend with soy protein isolate/PLA compatibilizer with PEOX [9]. At higher content of DNTP, only a single

peak was observed and no shift in peak temperature was observed. The storage modulus of the uncompatibilized blends dropped when the T_g of DNTP (≈ 60 °C) was reached, and then recovered to a significant degree between 90 and 95 °C due to the cold crystallization of PLA. However, this recovery was not observed with the compatibilized blends. The compatibilized blends showed a lower storage modulus than both DNTP and PLA (Figure 2. a') at temperature below α -transition of PLA region. This might be associated with the compatibilization effect of IA on DNTP in the blends making DNTP more flexible in the blends. Ning Wang et al suggested that the addition of maleic anhydride improved the plasticization of starch in starch/PLA blends [10].

3.3. Mechanical properties

Mechanical testing provides valuable information on material's flexibility, toughness and elongation which is useful in the prediction of its performance during processing, handling, storage and final product performance.

PLA has been reported to have high tensile strength, impact strength, modulus and low elongation [38] while DNTP has low tensile strength, impact strength, modulus and high elongation [18]. Mechanical properties might be used to assess polymer blends miscibility as it depends on the intermolecular interaction, chain stiffness and molecular symmetry of the individual polymer in the blend matrix [39]. Willemse et al. suggested that tensile modulus of polymer blends depends strongly on the composition and morphology of the blends [40].

The mechanical properties of pure DNTP, PLA and DNTP/PLA blends with and without PLA-g-IA are show in Figure 4. Both DNTP/PLA blends with and without compatibilizer showed rigid and brittle behaviour. The modulus of the blends was higher than that of neat DNTP due to the incorporation of rigid PLA.

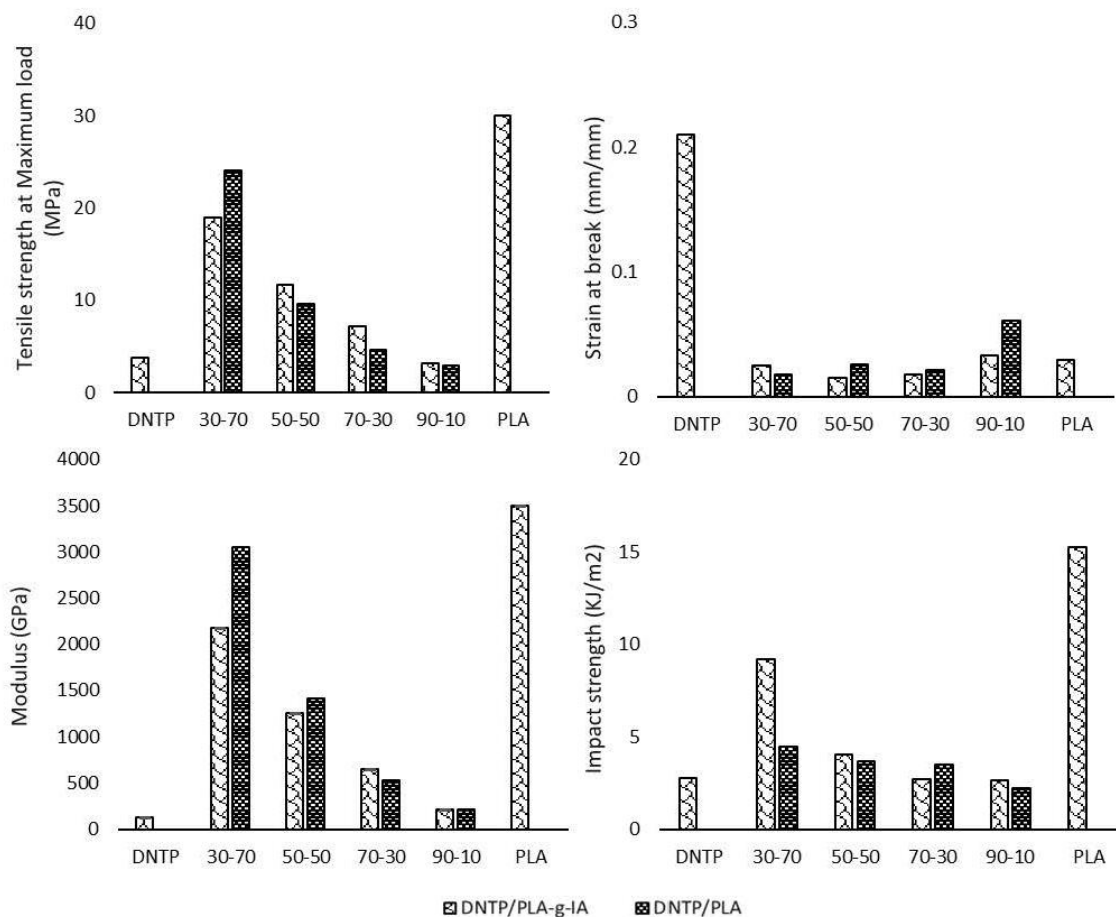


Figure 4: Mechanical properties of DNTP, PLA and DNTP/PLA blends with and without compatibilizer

Tensile strength observed for DNTP/PLA blends were inferior compare to neat PLA. This is as a result of weak interfacial adhesion between the two phases even with the addition of compatibilizer. Previous researches have reported inferior tensile strength for blends of PLA/Novatein [25] and PLA/soy protein [22]. However, all blends showed an improvement in tensile strength compared to DNTP except for 90-10. Further improvement was observed in tensile strength for 50-50 and 70-30 blends with the addition of itaconic anhydride. The tensile strength of 30-70 compatibilized blends were very poor compared to the uncompatibilized blends while 90-10 blend showed no significant effect. It is assumed that below 50% and above 70% DNTP content, DNTP overwhelm the compatibilizing effect of itaconic anhydride resulting in poor tensile strength.

The anhydride groups of Itaconic anhydride were likely to react with the amino groups of DNTP protein therefore enhancing the interfacial adhesion as observed with the SEM micrographs (Figure 1) which played a role in reducing the size of DNTP phase in the compatibilized blends. However, this interfacial adhesion is considered to be very weak therefore wasn't strong enough to effect significant improvement in the mechanical properties. This is thought to be probably due to insufficient amount of compatibilizer (i.e. low degree of grafting) or an indication that Itaconic anhydride is not a suitable compatibilizer for DNTP/PLA blends. Rui Zhu et al, reported an increase in both tensile strength and elongation of PLA/Soy protein composite with an increase in compatibilizer content [22].

4. Conclusion

DNTP/PLA blends were successfully prepared by extrusion mixing. The processibility and flowability of DNTP increased after blending with PLA and it was injection mouldable without processing aids. The DNTP/PLA blends showed a co-continuous phase morphology with a wide range of compositions. Blends of DNTP/PLA compatibilized with itaconic anhydride led to significant change in morphology improving the interfacial adhesion between the blended material phases; however, the adhesion between the phases was not strong enough to improve mechanical properties. DMA results and mechanical properties indicated compatibility of PLA with DNTP and the possibility of improving their interfacial interactions. Itaconic anhydride can be used as compatibilizer for DNTP/PLA blends, leading to improved mixing of the two phases. However, the two transition observed in the blend's DMA (although the second transition shifted to lower temperature for 30:70 and 50:50 blends ratio) suggests that the amount of IA in PLA-g-IA is probably not sufficient enough to effect a significant improvement in the blend's mechanical properties. All blends showed low elongation at break and high brittle behaviour thereby creating room for material plasticization and toughening in future investigations. Investigation of DNTP formulation and plasticization will be necessary to optimize process and material's properties.

5. References

1. Sue, H.-J., S. Wang, and J.-L. Jane, *Morphology and mechanical behaviour of engineering soy plastics*. Polymer, 1997. **38**(20): p. 5035-5040.
2. Vaidya, U.R. and M. Bhattacharya, *Properties of blends of starch and synthetic polymers containing anhydride groups*. Journal of applied polymer science, 1994. **52**(5): p. 617-628.
3. Mohamed, A.A., et al., *Thermal characteristics of polylactic acid/wheat gluten blends*. Journal of food quality, 2006. **29**(3): p. 266-281.
4. Huneault, M.A. and H. Li, *Morphology and properties of compatibilized polylactide/thermoplastic starch blends*. Polymer, 2007. **48**(1): p. 270-280.

5. Ku-Marsilla, K. and C. Verbeek, *Compatibilization of Protein Thermoplastics and Polybutylene Succinate Blends*. *Macromolecular Materials and Engineering*, 2015. **300**(2): p. 161-171.
6. Marsilla, K.K. and C. Verbeek, *Modification of poly (lactic acid) using itaconic anhydride by reactive extrusion*. *European Polymer Journal*, 2015. **67**: p. 213-223.
7. Gorrasi, G. and R. Pantani, *Effect of PLA grades and morphologies on hydrolytic degradation at composting temperature: assessment of structural modification and kinetic parameters*. *Polymer degradation and stability*, 2013. **98**(5): p. 1006-1014.
8. Auras, R., B. Harte, and S. Selke, *An overview of polylactides as packaging materials*. *Macromolecular bioscience*, 2004. **4**(9): p. 835-864.
9. Zhang, J., et al., *Morphology and properties of soy protein and polylactide blends*. *Biomacromolecules*, 2006. **7**(5): p. 1551-1561.
10. Wang, N., J. Yu, and X. Ma, *Preparation and characterization of thermoplastic starch/PLA blends by one-step reactive extrusion*. *Polymer International*, 2007. **56**(11): p. 1440-1447.
11. Suyatma, N.E., et al., *Mechanical and barrier properties of biodegradable films made from chitosan and poly (lactic acid) blends*. *Journal of Polymers and the Environment*, 2004. **12**(1): p. 1-6.
12. Verbeek, C.J.R., M.C. Lay, and A.W.K. Low, *Methods of manufacturing plastic materials from decolorized blood protein*. 2013, Google Patents.
13. Low, A., *Decoloured bloodmeal based bioplastic*. 2012, University of Waikato.
14. Hernandez-Izquierdo, V. and J. Krochta, *Thermoplastic processing of proteins for film formation—a review*. *Journal of food science*, 2008. **73**(2).
15. Gennadios, A., *Protein-based films and coatings*. 2002: CRC Press.
16. Zhang, J., P. Mungara, and J.-I. Jane, *Mechanical and thermal properties of extruded soy protein sheets*. *Polymer*, 2001. **42**(6): p. 2569-2578.
17. Pickering, K.L., et al., *Plastics material*. 2012, Google Patents.
18. Verbeek, C.J.R., et al., *Processability and mechanical properties of bioplastics produced from decoloured bloodmeal*. *Advances in Polymer Technology*, 2017.
19. Smith, M.J. and C.J. Verbeek, *The relationship between morphology development and mechanical properties in thermoplastic protein blends*. *Advances in Polymer Technology*, 2017.
20. Marsilla, K. and C.J.R. Verbeek, *Properties of Bloodmeal/Linear Low-density Polyethylene Blends Compatibilized with Maleic Anhydride Grafted Polyethylene*. *Journal of Applied Polymer Science*, 2013. **130**(3): p. 1890-1897.
21. John, J. and M. Bhattacharya, *Properties of reactively blended soy protein and modified polyesters*. *Polymer international*, 1999. **48**(11): p. 1165-1172.
22. Zhu, R., H. Liu, and J. Zhang, *Compatibilizing effects of maleated poly (lactic acid)(PLA) on properties of PLA/Soy protein composites*. *Industrial & Engineering Chemistry Research*, 2012. **51**(22): p. 7786-7792.
23. Zhong, Z. and X.S. Sun, *Properties of soy protein isolate/polycaprolactone blends compatibilized by methylene diphenyl diisocyanate*. *Polymer*, 2001. **42**(16): p. 6961-6969.
24. Huang, J., et al., *Soy protein isolate/kraft lignin composites compatibilized with methylene diphenyl diisocyanate*. *Journal of applied polymer science*, 2004. **93**(2): p. 624-629.
25. Walallavita, A., C.J. Verbeek, and M. Lay. *Blending Novatein® thermoplastic protein with PLA for carbon dioxide assisted batch foaming*. in *AIP Conference Proceedings*. 2016. AIP Publishing.
26. Wang, C., C. Carriere, and J. Willett, *Processing, mechanical properties, and fracture behavior of cereal protein/poly (hydroxyl ester ether) blends*. *Journal of Polymer Science Part B: Polymer Physics*, 2002. **40**(19): p. 2324-2332.
27. Sharabasht, M.M. and R.L. Guile, *Copolymerization Parameters of Itaconic Anhydride in Free-Radical Polymerization*. *Journal of Macromolecular Science: Part A-Chemistry*, 1976. **10**(6): p. 1039-1054.

28. Okuda, T., et al., *Renewable biobased polymeric materials: facile synthesis of itaconic anhydride-based copolymers with poly (L-lactic acid) grafts*. *Macromolecules*, 2012. **45**(10): p. 4166-4174.
29. Fischer, L. and F. Peissker, *A covalent two-step immobilization technique using itaconic anhydride*. *Applied microbiology and biotechnology*, 1998. **49**(2): p. 129-135.
30. Low, A., C.J.R. Verbeek, and M.C. Lay, *Treating Bloodmeal with Peracetic Acid to Produce a Bioplastic Feedstock*. *Macromolecular Materials and Engineering*, 2014. **299**(1): p. 75-84.
31. Hicks, T.M., et al., *The role of peracetic acid in bloodmeal decoloring*. *Journal of the American Oil Chemists' Society*, 2013. **90**(10): p. 1577-1587.
32. Properties, A.S.D.o.M. *Standard test method for tensile properties of plastics*. 1996. American Society for Testing and Materials.
33. ISO, E., *179-1 (2010)*.". *Plastics. Determination of Charpy impact properties. Part. 1*.
34. Willemse, R., et al., *Co-continuous morphologies in polymer blends: a new model*. *Polymer*, 1998. **39**(24): p. 5879-5887.
35. Xie, H.-Q., J. Xu, and S. Zhou, *Polymer blends with two kinds of elastomeric ionomers*. *Polymer*, 1991. **32**(1): p. 95-102.
36. Menczel, J.D. and R.B. Prime, *Thermal analysis of polymers: fundamentals and applications*. 2014: John Wiley & Sons.
37. Sumita, M., et al., *Dynamic mechanical properties of polypropylene composites filled with ultrafine particles*. *Journal of applied polymer science*, 1984. **29**(5): p. 1523-1530.
38. Martin, O. and L. Averous, *Poly (lactic acid): plasticization and properties of biodegradable multiphase systems*. *Polymer*, 2001. **42**(14): p. 6209-6219.
39. Joseph, S. and S. Thomas, *Modeling of tensile moduli in polystyrene/polybutadiene blends*. *Journal of Polymer Science Part B: Polymer Physics*, 2002. **40**(8): p. 755-764.
40. Willemse, R., et al., *Tensile moduli of co-continuous polymer blends*. *Polymer*, 1999. **40**(24): p. 6645-6650.

Appendix 3

Blending Decoloured Novatein® with Modified PLA

Sandra C. P. Izuchukwu^{a*}, Casparus J. R. Verbeek^a

*Corresponding author; sciokoro@gmail.com, scpi1@students.waikato.ac.nz

^a School of Engineering, University of Waikato, Private bag 3105, Hamilton 3240, New Zealand

Abstract

Blends of semi-crystalline poly (lactic acid) (PLA), a thermoplastic polyester and decoloured Novatein® (DNTP), a thermoplastic protein material, were prepared using reactive extrusion. Free radical grafting was used to graft itaconic anhydride unto PLA, creating a reactive side group. The compatibility between DNTP and PLA blends was investigated by mechanical testing, scanning electron microscopy (SEM), differential scanning calorimetry (DSC) and wide-angle X-ray scattering (WAXS). SEM revealed a co-continuous phase structure existed in the blends. The addition of itaconic anhydride improved the dispersion of DNTP in the PLA matrix. DNTP accelerated cold crystallization of PLA in the blend and increase crystallinity of PLA in the blends. Tensile strength exceeding that of DNTP was observed for the blends. Secant modulus, elongation at break and impact strength were also improved.

Keywords: PLA, Decoloured Novatein, Bloodmeal, Bio-based polymer, Blends, Itaconic anhydride.

Introduction

Renewed interest in bio-based polymer has been due to their environmentally friendly nature and potential use in packaging and agricultural industries [1-4]. Biopolymers have been considered an attractive alternative for petroleum-based polymers because they are abundant, inexpensive, biodegradable, renewable and environmental friendly. Biopolymers such as protein, cellulose and starch are obtained from animal and plant sources.

Bloodmeal is one of the animal sources of protein, containing 90 to 95 % dry weight of protein [5-7]. Bloodmeal can potentially be used as an alternative resource for bioplastics in agricultural and horticultural applications such as weasand clip, weed pegs, biodegradable plant pots and biopolymer foams [8-10]. There are some limitations to wider application of bloodmeal based polymer due to their offensive odour and colour. However, the colour and odour were

successfully eliminated through a pre-treatment with peracetic acid (PAA) [7] resulting to a bio-feed stock referred to as decoloured bloodmeal (DBM). Decoloured bloodmeal has been processed into thermoplastic known as Decoloured Novatein® (DNTP), using Triethylene glycol (TEG), water and sodium dodecyl sulphate (SDS) [11]. However, its properties are relatively poor compared to other polymers used in sheet production due to its hydrophilicity [12], also processibility is difficult due to strong intra- and inter-molecular interactions between the protein chains. Therefore, the improvement of its properties and processibility becomes imperative.

Studies have concentrated on property improvement of protein-based polymers through association with other hydrophobic polyesters with desirable properties [13-18]. Association with other polymers can be achieved through blending, coating or lamination. Blending is the most effective and easier way of modifying polymer properties, although poor interfacial adhesion between the polymer phases will result in a material with poor properties [19]. Poor interfacial adhesion in polymer-polymer blends is as a result of incompatibility between the two phases. However, this can be addressed using compatibilizers to create reactive functional groups capable of reacting with both polymer phases resulting in improved properties [13, 15, 17, 18, 20].

PLA is one of the suitable polymers for blend with other protein bio-polymers because of its biodegradability, high strength and hydrophobic properties. PLA is a thermoplastic polyester synthesized from lactic acid, which is derived from corn starch and sugar beets [21]. Most polyesters are immiscible with proteins because of the different polarities [16, 17, 20, 22]. DNTP and PLA blends are thermodynamically immiscible having weak interfacial adhesion, resulting in inferior mechanical properties because of the large difference in their hydrophilicities. Interfacial modification plays an important role in manipulating the solid-state adhesion between the components of two incompatible material blend [23]. Therefore, compatibilization of DNTP and PLA blend is essential.

Poly(2-ethyl-2-oxazoline) (PEOX) and methylene diphenyl diisocyanate (MDI) have been used widely as compatibilizers for natural polymers and PLA blends [18, 22, 24, 25]. Recent developments in interfacial modification of PLA and natural polymer blends has been explored. This involved grafting a reactive moiety, such as maleic anhydride [10, 20, 23, 26-29], or itaconic anhydride [9, 30] onto PLA matrix to create functional reactive groups for the natural polymers.

The amide and amino groups of DNTP protein components would possibly react with the anhydride group of itaconic anhydride. The aim of this study was to identify the quantity of additives for DNTP formulation and processing conditions required to produce a homogenous blend of DNTP/PLA with an improved property. This was achieved by investigating varying combination of water, TEG and SDS to determine the best formulation for blending with PLA.

1.1 Material and Methods

1.1.1 Materials

Bloodmeal was obtained from Wallace Corporation Limited, New Zealand and used as received. Analytical grade itaconic anhydride (IA), dicumyl peroxide (DCP), acetone, 50 wt% hydrogen peroxide, technical grade sodium dodecyl sulphate (SDS) and triethylene glycol (TEG) were purchased from Sigma Aldrich NSW, Australia. Peracetic acid (Peraclean 5) was purchased from Evonik Industries, Morrinsville, New Zealand. Poly (lactic acid) (PLA) grade 3051D was purchased from NatureWorks Ltd in pellet form. Distilled water was produced onsite.

1.1.2 Sample preparation

1.1.2.1 Interfacial modification of PLA

PLA was modified through free radical grafting of itaconic anhydride [30] to create reactive side-chain groups. PLA was dried at 80 °C for 4 hours to control moisture. 4.2 parts per hundred PLA (pph) Itaconic anhydride and 0.8 pph dicumyl peroxide were dissolved in 30 mL acetone. The preformed solution was poured over the oven dried PLA and was kept in the fume hood for about 2 hours. The solution was decanted before oven drying the PLA for 3 hours at 50 °C. The modified PLA (PLA-g-IA) was extruded using a LabTech twin screw co-rotating extruder having a screw diameter of 20 mm and L/D of 44:1, at temperature profile of 145 (feed zone), 145, 165, 165, 180, 180,180, 180, 160, 160, 155 °C (die zone). A constant screw speed was maintained at 150 rpm. A vacuum pump was attached on the 7th heating zone of the extruder to get rid of vapour generated during extrusion. The pelletized PLA-g-IA was oven dried for 12 hours prior to blending with Decoloured Novatein (DNTP) to minimise hydrolysis during melt processing.

1.1.2.2 Bloodmeal decolouring and decoloured Novatein preparation

Bloodmeal was decoloured using a solution of peracetic acid (PAA) according to previous methods [7, 31]. 4 wt% PAA solution was prepared by diluting 5 wt% PAA stock solutions with

distilled water at a constant ratio of 80:20 respectively. 150 g bloodmeal was decoloured by adding 450 g of 4 wt% PAA in a high-speed mixer. The mixture was allowed to mix continuously for 5 min to ensure homogenous decolouring of bloodmeal. 450 g of distilled water was added and mixed for another 5 min to ensure complete dilution of the slurry. The slurry was neutralized by adjusting to pH = 7 with sodium hydroxide solution. The neutralized slurry was filtered using a wire mesh sieve with aperture size 60 and subsequently washed by adding another 450 g of distilled water. The decoloured bloodmeal was dried approximately 15 hours in a 75 °C oven.

Decoloured Novatein (DNTP) was formulated by dissolving SDS in water heated to 60 °C while stirring. The solution was added to decoloured bloodmeal powder in a high-speed mixer and mixed for 5 min. TEG was added to the mixture and mixed for another 5 min to ensure homogeneous mixture is obtained. The mixed material was stored in an air tight bag overnight in a 2 °C fridge to equilibrate.

1.1.2.3 Blend preparation

Different DNTP formulations are shown in TABLE 1 and PLA grafting was performed prior to blending. All blends contained 50 wt% DNTP and 50 wt% PLA or PLA-g-IA. Blends were compounded using the same extruder as for grafted. The extrusion temperature varied from 100 to 180 °C (having the lowest temperature at the feed zone and the highest at die zone) depending on the DNTP content. The extrudate were granulated using a Tri-blade granulator from Castin Manufacturing Limited.

TABLE 1: Varying formulations contents of DNTP, dried bloodmeal and TEG plasticized used for PLA blends.

Components	Formulations				
	Dried decoloured bloodmeal (D)	TEG plasticized (T)	F2	F3	F4
Water	0	0	40	30	40
TEG	0	30	20	30	30
SDS	0	0	3	6	6

Note: all formulations contained 100 parts decoloured bloodmeal

1.1.3 Test specimen preparation

ASTM D638-14 Standard tensile test samples [32] and ISO 179-1:2010 impact test specimens [33] were injection moulded using a BOY 35A injection moulding machine. The samples were injected through a cold runner into a 60 °C water heated mould. The injection moulder has five heating zones including the feed and the die zone. The feed temperature remains constant at 100 °C, the barrel temperature varied between 100 to 140, and the die temperature varied from 120 to

140 depending on the formulation. The screw speed was constant at 150 rpm. The sample specimens produced were also used for thermal, moisture content and morphology testing.

1.1.4 Sample Analysis

All samples were conditioned for 7 days at 23 °C and 50% relative humidity before testing except otherwise stated.

1.1.4.1 Mechanical properties

Mechanical testing was performed according to ASTM D638 using Instron Universal Testing machine (model 33R4204) at a crosshead speed of 5 mm/min and an extensometer gauge length of 50 mm. 10 replicates were tested for each sample type to obtain an average value.

The impact testing bars produced from the injection moulder has diameter of 80 x 10 x 4 mm³. Charpy edgewise impact strength was performed according to ISO 179-1:2010 using a RAY-RAN Pendulum Impact System. The bar tested was notched according to standard. 10 bars were tested to obtain average impact strength of the material.

1.1.4.2 Thermal analysis

Differential scanning calorimetry was conducted using a Perkin Elmer DSC 8500. About 5 mg of sample was crimp sealed in 30µL DSC aluminium pans. All samples were heated from 25 to 200 °C at 10 °C/min and kept on isothermal for 5mins before cooling to 25 °C at 10 °C/min. The data collected was analysed using Pyris software version 11.1.1.0492. The reported values were average of three replicates.

1.1.4.3 Wide angle X-ray scattering measurement (WAXS)

WAXS was used to measure the XRD pattern of the blends. WAXS was performed with a philips X-ray diffractometer operating at 40 Kv and 40 mA using CuK α radiation. The diffraction data was collected from 2 θ values of 4° to 40° with a step size of 0.013°. A fixed 7.5 mm anti-scatter slit, fixed incidence beam mask of 10mm and a soller slit of 0.04 rad was used. The data collected was baseline corrected from 5° to 40° and amorphous halo was fitted to this region to determine crystallinity of the blends.

1.1.4.4 Phase Morphology

The phase structure of the blends was investigated using Hitachi S-4700 field emission scanning electron microscope (SEM). The injection moulded specimens were cryo-fractured using liquid nitrogen. The specimens were sputter coated with platinum using Hitachi E-1030 Ion sputter before scanning. For the digested surface, the samples were extracted with chloroform and then

rinsed with hot water to remove PLA phase as DNTP is not soluble in chloroform. The extracted surface was dried, and sputter coated prior to examination.

1.2 Results and Discussion

1.2.1 Morphological Characterisation

The fracture and digested morphologies of the DNTP/PLA or PLA-g-IA blends samples with different DNTP formulations are shown in FIGURE 1 and FIGURE 2 respectively.

The cryo-fractured surface of blends without itaconic anhydride (IA) showed a relatively large and unevenly distributed DNTP agglomerates because of the inherent immiscibility. However, addition of PLA-g-IA revealed a much finer and more homogeneously dispersed matrix indicating improved mixing and good interfacial adhesion as the DNTP agglomerate observed in the blends without IA are not distinct. Interstices were clearly observed in the blends without IA, indicating poor interfacial adhesion. Some interstices were still visible in the blends with PLA-g-IA but they are much smaller and fewer compared to the blends without IA. PLA is hydrophobic with poor polarity while DNTP has strong polarity and is hydrophilic. Therefore, the poor interfacial adhesion between the two phases led to coarse phase structure for both phases in the material matrix.

The clear phase separation observed in the blends without IA, is an indication of poor blend compatibility. Blending different formulation of DNTP with PLA-g-IA improved the morphology of the blend significantly as the reduction of the DNTP rich phase size was observed. In the modified PLA blend, the two polymers are proposed to form co-continuous phases, one that is rich in DNTP and another that is rich in PLA with sufficient adhesion between both phases. This is further investigated through SEM digested surface morphology of the blends.

Larger voids were observed in blends without IA (FIGURE 2) indicating a poor dispersion of PLA in the blends, corresponding to the DNTP agglomerates observed in FIGURE 1 for blends without IA. Blends with PLA-g-IA exhibited a much finer phase structure with relatively uniform voids having small dimension. This fine structure confirms an improved interfacial adhesion between the two phases are suggested in FIGURE 1 with PLA-g-IA. This suggests that blending immiscible polymer without compatibilization will result in a material with undesired properties due to the high interfacial tension between both material phases. F3P, DP and DgP disintegrated in chloroform suggesting that DNTP was the dispersed phase while PLA formed a continuous phase in the blends matrix.

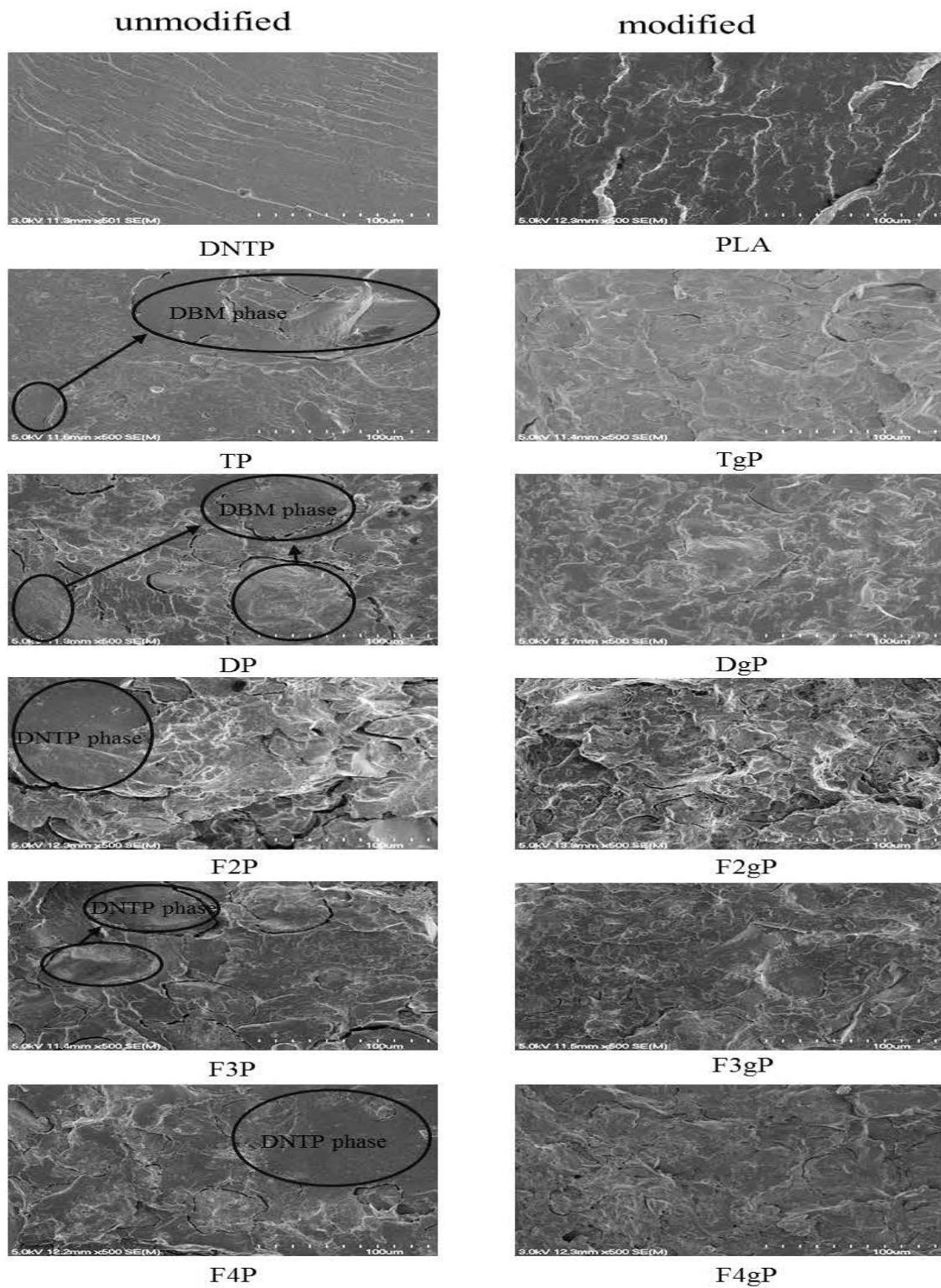


FIGURE 1: SEM cryo-fracture surface of DNTP/PLA blends with and without Itaconic anhydride. (DNTP) Decoloured Novatein, (TP) TEG plasti zed decoloured bloodmeal, (DP) dried decoloured bloodmeal, (F2, F3 and F4) varied additives for DNTP

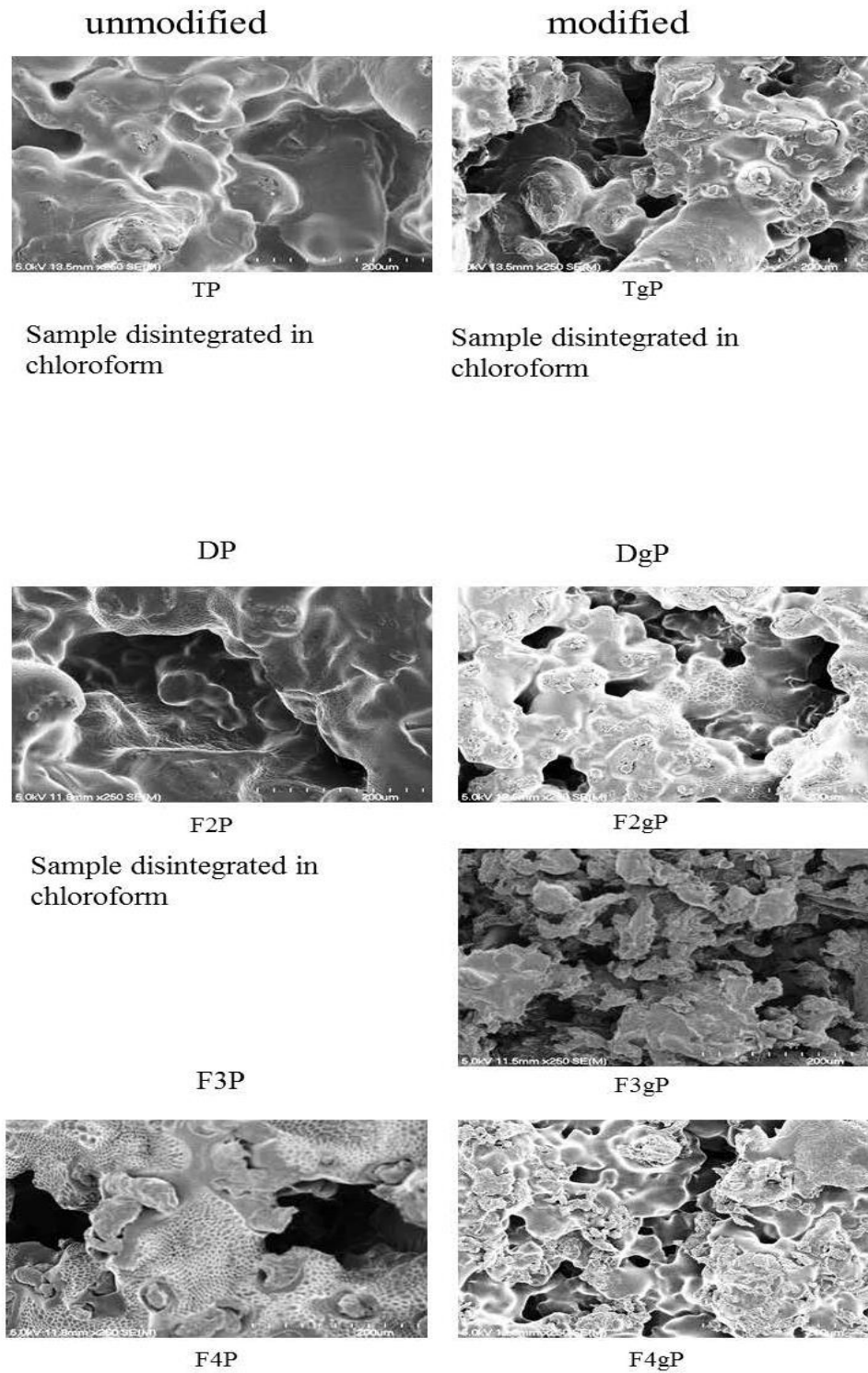


FIGURE 2: SEM Digested surface micrograph of DNTP/PLA blends with and without Itaconic anhydride. (DNTP) Decoloured Novatein, (TP) TEG plasticized decoloured bloodmeal, (DP) dried decoloured bloodmeal, (F2, F3 and F4) varied additives for DNTP

1.2.2 Mechanical properties

Properties of polymer blends are strongly influenced by its morphology. Materials performance during processing, storage and handling can be predicted through its mechanical properties as a function of flexibility, toughness and elongation. FIGURE 3 shows the mechanical properties of neat materials and blends (with and without PLA-g-IA). DNTP and PLA are known to be rigid polymers and show brittle behaviour which was reflected in the blend's elongation and modulus. The mechanical properties of blends were compared with that of the neat DNTP.

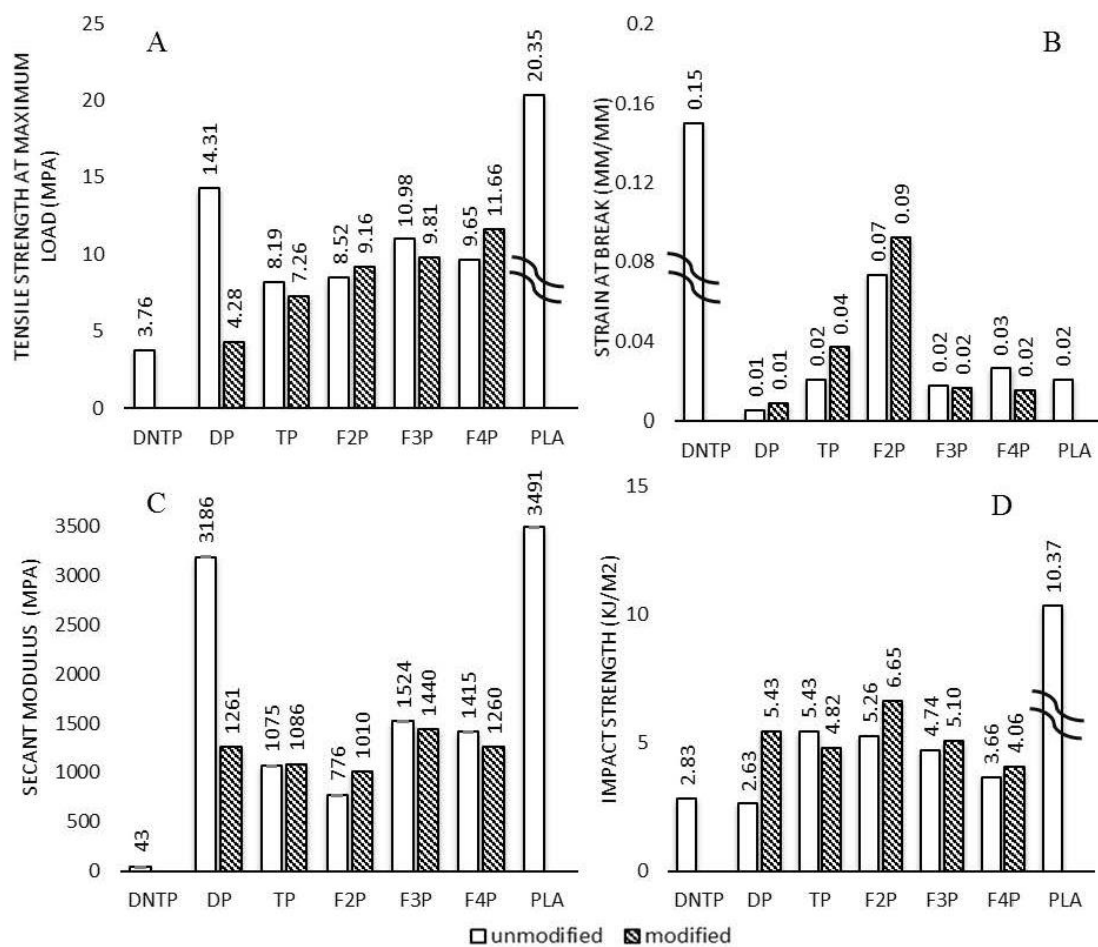


FIGURE 3: Mechanical property of DNTP/PLA blends with and with Itaconic anhydride

Tensile strength and modulus of both blends with and without PLA-g-IA increased while the elongation decreased when compared to neat DNTP. However, there was no significant difference observed in the mechanical properties of both compatibilized blends compared to the uncompatibilized blends except for DP blend which showed a drastic decrease in the tensile strength of the modified blends. This can be attributed to the interfacial adhesion as affected by

the addition of Itaconic anhydride. It is thought that itaconic anhydride improved the interfacial adhesion between the both phases as observed in FIGURE 1 (modified). However, the interaction between both phases was weak resulting in slightly low or insignificant increase in tensile strength compared to uncompatibilized blends. The agglomerates of dispersed DNTP phase (FIGURE 1 unmodified) in DP blend are believed to act as stress concentrations, absorbing a similar level of stress as the PLA phase (i.e. stress was effectively transferred between both phases) resulting in high strength. Blending of DNTP and PLA led to a reduction in elongation compared to DNTP. This is due to the addition of the rigid PLA which restricted the movement of polymer chains, thereby decreasing the elongation at break. The interactions between the phases may also have caused a reduction in elongation. Marsilla et al, suggested same with the blends of protein thermoplastic and polybutylene succinate blends [17].

The secant modulus increased compared to neat DNTP suggested that interfacial adhesion was not sufficient to maintain the stiffness of each blend's components. An increase in impact strength of blends compared to neat DNTP was observed suggesting the blends ability to absorb energy before rupturing.

F2P modified blend had considerable increase in elongation at break exceeding that of all blends, an increase in tensile strength and impact strength more than double fold compared to neat DNTP with a lower modulus more than all the blends. This suggests better compatibility between PLA and this DNTP formulation.

1.2.3 Differential scanning calorimetry (DSC)

DSC thermograms of neat PLA, DNTP and their blends are shown in FIGURE 4, FIGURE 5 and there results are listed in TABLE 2. The glass transition, cold crystallization and melting endotherm can be observed in the DSC curve of neat PLA and each blend. However, there was no exothermic peak in the DSC curve for DNTP. Small water molecules act as plasticizers in the protein system reducing protein exothermic temperature [22, 34]. A single peak is observed for all blends suggesting a degree of miscibility. Double Tg have been reported as evidence of immiscibility by other researchers [35, 36]. The presence of a single peak in the cold crystallization and double-melting peaks for DNTP/PLA blends suggests that DNTP acted as a heterogenous nucleating agent for the PLA matrix, inducing and accelerating PLA crystallization. A glass transition temperature of 49.8 °C and cold crystallization temperature of 102.86 °C were observed for DP (dried bloodmeal/PLA blend) suggesting slower crystallization kinetics and the involvement of less flexible macromolecules. Similar Tg and cold crystallization temperature have been observed for other protein/ PLA blends [22]. However, with the addition of itaconic

anhydride both T_g and cold crystallization shifted to lower temperature of 47.94 °C and 95.81 °C respectively. The blends of DNTP/PLA showed a slight increase in both T_g and cold crystallization temperature with the addition of Itaconic anhydride, except for F4P with an insignificant decrease in T_g . The increase observed is attributed to the restricted slippage and mobility of the PLA macromolecular segment due to an increased interaction between PLA and DNTP phases.

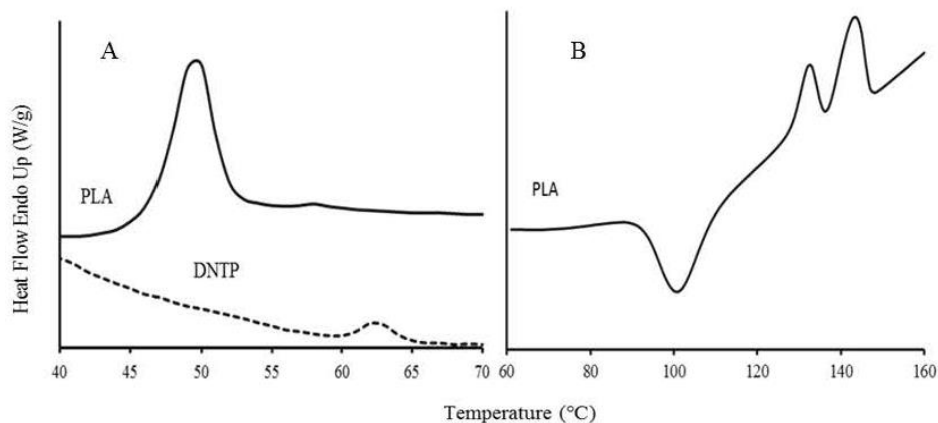


FIGURE 4: Glass transition temperature (T_g), crystallization peak (T_{cc}) and melting endotherms (T_m) of Pure PLA and DNTP

The PLA in the compatibilized blends exhibited cold crystallization at lower temperature compared to the neat PLA and uncompatibilized blends. This suggested that PLA-g-IA accelerated the crystallization of PLA and substantially increased PLA crystallinity. The melting of the PLA in the blend was reflected by the bimodal endotherm transition observed at ~ 120 – 145 °C. The peak at lower temperature reflects the melting of less paragon crystal in the boundary regions followed by the melting of recrystallized PLA at higher temperature [13, 35]. The ΔH_m values observed in the blends (TABLE 2) are larger than the ΔH_{cc} values. This indicates that the addition of DNTP promoted a certain degree of PLA crystallinity. Crystallization and melting temperatures of all blends showed a decrease compared to neat PLA except for DP with a T_g slightly higher than neat PLA. This could be attributed to the residual moisture in the blends which plasticizes the PLA molecules and increases its flexibility resulting in lower crystallization and melting temperatures. Zhang et al, observed a continuous decrease in T_g , T_{cc} and T_m with an increase in moisture content of SPI/PLA containing 3 phr PEOX conditioned at different relative humidity [13]. The blends showed a decrease in ΔH_{cc} with the addition of IA suggesting that Itaconic anhydride probably reduced the interfacial tension as a result of interaction between phases such as hydrogen bonding promoting the crystallization of PLA.

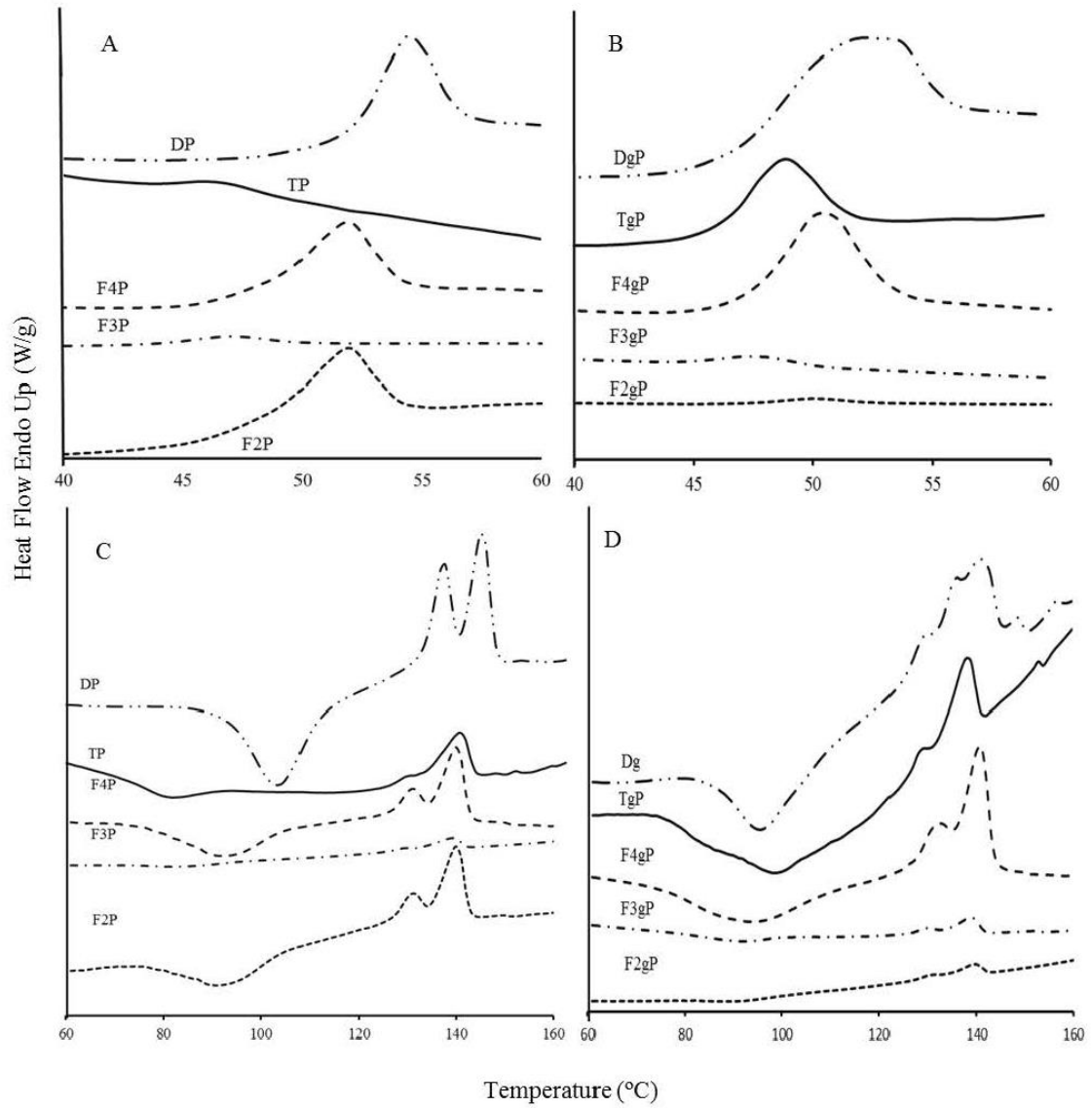


FIGURE 5: DSC first heat scan thermograms of different DNTP/PLA blends showing glass transition temperature (T_g), crystallization peak (T_{cc}) and melting endotherms (T_m) of the blends. (DNTP) Decoloured Novatein, (TP) TEG plasticized bloodmeal, (DP) dried bloodmeal, (F2, F3 and F4) DNTP with varying additives, (P) Neat PLA and (gPLA) modified PLA

TABLE 2: Glass transition temperature, cold crystallization peak and melting endotherms of blends

Sample	T_g (°C)	Cold Crystallization		Melting T_m (°C)		Δh_m (J/G)
		T_{cc} (°C)	Δh_{cc}^a (J/G)	1	2	
PLA ^a	41.78	99.48	-2.736	131.81	142.89	2.4303
DNTP	60.5			nd	nd	
DP	49.8	102.86	-3.122	135.6	142.27	3.4074
DgP	47.94	95.81	-2.456	135.55	140.62	1.6384
TP	39.53	81.32	-0.6967	124	138.78	1.0073
TgP	45.51	99.38	-3.09	128.49	138.19	0.8297
F2P	47.37	92.08	-10.133	130.97	140.06	10.8316
F2gP	47.43	92.2	-0.6146	130.18	139.32	0.7878
F3P	43.59	83.98	-0.9813	129.29	139.21	1.601
F3gP	44.14	91.42	-0.6898	129.79	138.92	1.1314
F4P	47.51	91.58	-11.068	130.97	140.06	11.0577
F4gP	47.47	91.75	-5.3824	131.8	141.19	10.4048

^a Data collected on the second heat scan of samples, T_g : glass transition temperature, T_{cc} : cold crystallization temperature, T_m : melting endotherm

1.2.4 Wide angle X-ray scattering (WAXS) measurement

WAXS analysis has been performed on the blends for better insight into the blend morphology. Data obtained for the XRD of a material can be used to study the material's phase change. FIGURE 6 presents the wide-angle X-ray diffractogram for neat PLA and DNTP, and blends of DNTP/PLA with and without compatibilizer. It can be observed the neat PLA shows only amorphous halo.

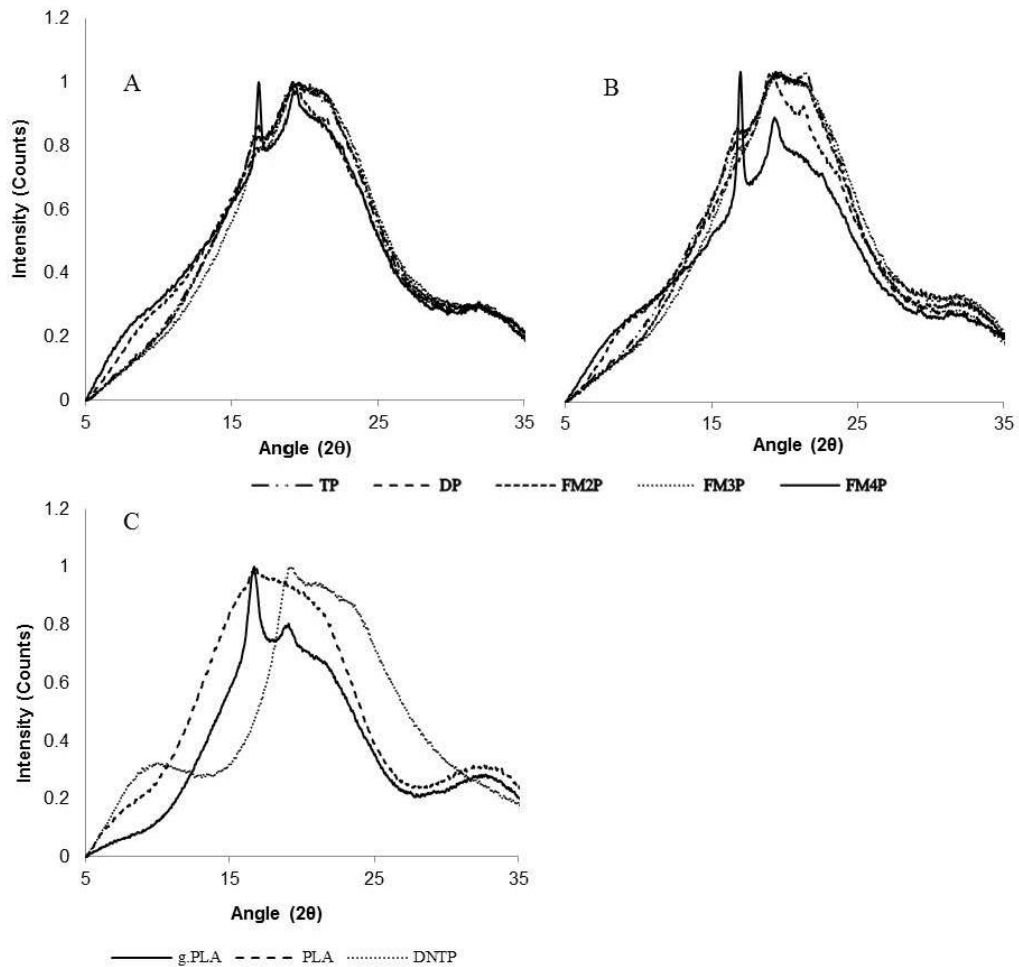


FIGURE 6: WAXS diffraction patterns for DNTP/PLA blends with and without Itaconic anhydride

Clear crystalline peaks were observed at 16° and 20° for PLA-g-IA, the peak at $2\theta = 16^\circ$ has been reported to be associated with (110)/(020) which is a reflection of α -form homo-crystal structure and $2\theta = 22^\circ$ was indexed as (100)/(-120)/(-210) which is a reflection of stereo-complex crystals [37-42]. The formation of stereo-complex crystal as well as α -form homo-crystal structure observed in PLA-g-IA suggests that significant chain orientations occurred during the grafting of PLA because of hydrolytic degradation probably due to decrease in molecular weight. These peaks were very strong and sharp in blends with formulation 4. This indicates the presence of significant crystallinity in the blends. The presence of stable crystal structure observed has been suggested to be evidence of some degree of PLA hydrolytic degradation during modification which is probably, reflected in the low tensile properties observed for the blends modified with itaconic anhydride FIGURE 3.

The peaks at $2\theta = 9^\circ$ observed in the diffractogram of DNTP corresponds to helical spacing and inter β -sheet while the peak at $2\theta = 20^\circ$ corresponds to the repeated distance within each structure. The amorphous region of the compatibilized blends showed a slight reduction probably due to the integration of both PLA and DNTP amorphous regions as confirmed by the reduction of DNTP agglomerate in SEM thermogram **FIGURE 1**.

Peaks were observed at 2θ , 19° and 20° with an appearance of a shoulder at 22° for F2P, F3P and TP blends. However, with the addition of Itaconic anhydride, the peak at 19° became slightly broader for F3P and TP, and the shoulder at 22° for TP became clearer. There was a slight shift in the 2θ of both peaks for TP blend. A sharp peak at 2θ 19° and shoulders at 16° and 20° were observed for DP blends. The shoulder at 16° became broader and an appearance of a shoulder at 9° was observed while the shoulder observed at 2θ 22° became clearer. F4P showed a sharp peak at 2 16° and another clear peak at 19° . The peaks became sharper and had reduced intensity with the addition of itaconic anhydride.

1.3 Conclusion

Blends of PLA/DNTP with varying additives were successfully prepared through reactive extrusion. The processibility and flowability of DNTP increased with the addition of PLA and was injection mouldable without processing aids. Co-continuous phase morphology was observed in the blends. The mechanical properties of DNTP were greatly enhanced by the addition of PLA. The mechanical properties, SEM and DSC indicated compatibility of DNTP and PLA-g-IA. Adding itaconic anhydride led to improved mixing of the two phases, which resulted in finer phase structure. However, no significant effect was observed in the blend's mechanical properties with the addition of itaconic anhydride. This was attributed to itaconic anhydride, improving the dispersion of DNTP as observed in SEM thereby enhancing the interfacial adhesion. However, the interfacial adhesion is thought to be weak resulting in low mechanical properties compared to the uncompatibilized blends. All blends showed low elongation at break and brittle fracture failure in tensile testing, suggesting a gap for toughening and plasticization in future investigation. However, the data obtained from mechanical properties F2P modified with Itaconic anhydride seems to be the best DNTP formulation for blend with PLA as it showed better tensile strength, elongation at break and flexibility favourable for sheet processing. The crystallization temperature of compatibilized blends occurred at higher temperature indicating reduction of chain mobility. DNTP /PLA blends showed an improved thermal stability compared to neat DNTP. The addition of Itaconic anhydride showed a further improvement in thermal stability of DNTP/PLA blends. WAXS of DNTP/PLA blends showed the formation of stereo-complex crystal as well as α -form homo-crystal structure on the PLA in the blends, suggesting the occurrence of significant chain

orientations due to PLA hydrolysis. With the addition of Itaconic anhydride, the presence of these crystal structure became clearer which is thought to be responsible for the insignificant effect of Itaconic anhydride on the mechanical properties of DNTP/PLA blends. This suggests the manipulation of processing and blend conditions to better control for hydrolysis of PLA in the blends.

1.4 References

1. Rhim, J.-W., et al., *Preparation and properties of biodegradable multilayer films based on soy protein isolate and poly (lactide)*. *Industrial & engineering chemistry research*, 2006. **45**(9): p. 3059-3066.
2. Rhim, J.-W., J.H. Lee, and P.K. Ng, *Mechanical and barrier properties of biodegradable soy protein isolate-based films coated with polylactic acid*. *LWT-Food Science and Technology*, 2007. **40**(2): p. 232-238.
3. Briassoulis, D., *An overview on the mechanical behaviour of biodegradable agricultural films*. *Journal of Polymers and the Environment*, 2004. **12**(2): p. 65-81.
4. Petersen, K., et al., *Potential of biobased materials for food packaging*. *Trends in food science & technology*, 1999. **10**(2): p. 52-68.
5. Grant, R., *Applied protein chemistry*. 1980: Applied Science Publishers.
6. Pickering, K.L., et al., *Plastics material*. 2012, Google Patents.
7. Low, A., C.J.R. Verbeek, and M.C. Lay, *Treating Bloodmeal with Peracetic Acid to Produce a Bioplastic Feedstock*. *Macromolecular Materials and Engineering*, 2014. **299**(1): p. 75-84.
8. van der Merwe, D.W., *The Environmental and Economic Impacts for Producing the Port Jackson from Novatein®*. 2014, University of Waikato.
9. Walallavita, A.S., C.J.R. Verbeek, and M.C. Lay, *Biopolymer foams from Novatein thermoplastic protein and poly (lactic acid)*. *Journal of Applied Polymer Science*.
10. Gavin, C., M.C. Lay, and C.J. Verbeek. *Extrusion foaming of protein-based thermoplastic and polyethylene blends*. in *AIP Conference Proceedings*. 2016. AIP Publishing.
11. Low, A., C.J.R. Verbeek, and M.C. Lay, *Processing peracetic acid treated bloodmeal into bioplastic*. *Chemeca 2012: Quality of life through chemical engineering: 23-26 September 2012, Wellington, New Zealand, 2012*: p. 1433.
12. Low, A., *Decoloured bloodmeal based bioplastic*. 2012, University of Waikato.
13. Zhang, J., et al., *Morphology and properties of soy protein and polylactide blends*. *Biomacromolecules*, 2006. **7**(5): p. 1551-1561.
14. Zhong, Z. and S.X. Sun, *Properties of soy protein isolate/poly (ethylene - co - ethyl acrylate - co - maleic anhydride) blends*. *Journal of applied polymer science*, 2003. **88**(2): p. 407-413.
15. Li, Y.-D., et al., *Structure and properties of soy protein/poly (butylene succinate) blends with improved compatibility*. *Biomacromolecules*, 2008. **9**(11): p. 3157-3164.
16. Mungara, P., et al., *Processing and physical properties of plastics made from soy protein polyester blends*. *Journal of Polymers and the Environment*, 2002. **10**(1): p. 31-37.
17. Ku - Marsilla, K. and C. Verbeek, *Compatibilization of Protein Thermoplastics and Polybutylene Succinate Blends*. *Macromolecular Materials and Engineering*, 2015. **300**(2): p. 161-171.
18. Marsilla, K. and C.J.R. Verbeek, *Properties of Bloodmeal/Linear Low - density Polyethylene Blends Compatibilized with Maleic Anhydride Grafted Polyethylene*. *Journal of Applied Polymer Science*, 2013. **130**(3): p. 1890-1897.
19. Wang, L., R. Shogren, and C. Carriere, *Preparation and properties of thermoplastic starch - polyester laminate sheets by coextrusion*. *Polymer Engineering & Science*, 2000. **40**(2): p. 499-506.
20. Zhu, R., H. Liu, and J. Zhang, *Compatibilizing effects of maleated poly (lactic acid)(PLA) on properties of PLA/Soy protein composites*. *Industrial & Engineering Chemistry Research*, 2012. **51**(22): p. 7786-7792.

21. Garlotta, D., *A literature review of poly (lactic acid)*. Journal of Polymers and the Environment, 2001. 9(2): p. 63-84.
22. Fang, K., et al., *Properties and morphology of poly (lactic acid)/soy protein isolate blends*. Journal of applied polymer science, 2009. 114(2): p. 754-759.
23. Huneault, M.A. and H. Li, *Morphology and properties of compatibilized polylactide/thermoplastic starch blends*. Polymer, 2007. 48(1): p. 270-280.
24. Aoi, K. and M. Okada, *Polymerization of oxazolines*. Progress in polymer science, 1996. 21(1): p. 151-208.
25. Wang, H., X. Sun, and P. Seib, *Strengthening blends of poly (lactic acid) and starch with methylenediphenyl diisocyanate*. Journal of Applied Polymer Science, 2001. 82(7): p. 1761-1767.
26. Carlson, D., et al., *Maleation of polylactide (PLA) by reactive extrusion*. Journal of applied polymer science, 1999. 72(4): p. 477-485.
27. Nyambo, C., A.K. Mohanty, and M. Misra, *Effect of maleated compatibilizer on performance of PLA/wheat Straw - Based green composites*. Macromolecular Materials and Engineering, 2011. 296(8): p. 710-718.
28. Zhang, J.-F. and X. Sun, *Mechanical properties of poly (lactic acid)/starch composites compatibilized by maleic anhydride*. Biomacromolecules, 2004. 5(4): p. 1446-1451.
29. Orozco, V.H., et al. *Preparation and characterization of poly (Lactic acid) - g - maleic anhydride+ starch blends*. in *Macromolecular symposia*. 2009. Wiley Online Library.
30. Marsilla, K.K. and C. Verbeek, *Modification of poly (lactic acid) using itaconic anhydride by reactive extrusion*. European Polymer Journal, 2015. 67: p. 213-223.
31. Hicks, T.M., et al., *The role of peracetic acid in bloodmeal decoloring*. Journal of the American Oil Chemists' Society, 2013. 90(10): p. 1577-1587.
32. Properties, A.S.D.o.M. *Standard test method for tensile properties of plastics*. 1996. American Society for Testing and Materials.
33. ISO, E., *179-1 (2010)*.". Plastics. Determination of Charpy impact properties. Part. 1.
34. Mo, X., X.S. Sun, and Y. Wang, *Effects of molding temperature and pressure on properties of soy protein polymers*. Journal of applied polymer science, 1999. 73(13): p. 2595-2602.
35. Jiang, L., M.P. Wolcott, and J. Zhang, *Study of biodegradable polylactide/poly (butylene adipate-co-terephthalate) blends*. Biomacromolecules, 2006. 7(1): p. 199-207.
36. Signori, F., M.-B. Coltelli, and S. Bronco, *Thermal degradation of poly (lactic acid)(PLA) and poly (butylene adipate-co-terephthalate)(PBAT) and their blends upon melt processing*. Polymer degradation and stability, 2009. 94(1): p. 74-82.
37. Mihai, M., et al., *Extrusion Foaming of Semi - Crystalline PLA and PLA/Thermoplastic Starch Blends*. Macromolecular bioscience, 2007. 7(7): p. 907-920.
38. Gorrasi, G. and R. Pantani, *Effect of PLA grades and morphologies on hydrolytic degradation at composting temperature: assessment of structural modification and kinetic parameters*. Polymer degradation and stability, 2013. 98(5): p. 1006-1014.
39. Zhang, X., et al., *Morphological behaviour of poly (lactic acid) during hydrolytic degradation*. Polymer Degradation and Stability, 2008. 93(10): p. 1964-1970.
40. Furuhashi, Y., Y. Kimura, and H. Yamane, *Higher order structural analysis of stereocomplex - type poly (lactic acid) melt - spun fibers*. Journal of Polymer Science Part B: Polymer Physics, 2007. 45(2): p. 218-228.
41. Tsuji, H., H. Takai, and S.K. Saha, *Isothermal and non-isothermal crystallization behavior of poly (l-lactic acid): effects of stereocomplex as nucleating agent*. Polymer, 2006. 47(11): p. 3826-3837.
42. Mittal, V., et al., *PLA, TPS and PCL binary and ternary blends: structural characterization and time-dependent morphological changes*. Colloid and Polymer Science, 2015. 293(2): p. 573-585.

Appendix 4

Chemeca 2018

Paper: 102

30 September – 3 October 2018, Queenstown, New Zealand

Mechanical Properties of Decoloured Bloodmeal and PLA blends

Sandra C. P. Izuchukwu^{a*} and Casparus J. R. Verbeek^a

^a School of Engineering, University of Waikato, Private bag 3105, Hamilton 3240, New Zealand

*Corresponding author; sciokoro@gmail.com, scpi1@students.waikato.ac.nz

Abstract

Blends of decoloured bloodmeal thermoplastic (DBT), a thermoplastic protein material from slaughter house by-product, and poly (lactic acid) (PLA), a thermoplastic polyester, was prepared using reactive extrusion. Itaconic anhydride grafted PLA (PLA-g-IA), poly (2-ethyl-2-oxazoline) (PEOX) and poly (phenyl isocyanate)-co-formaldehyde (pMDI) were used as compatibilizers. The compatibility between DBT and PLA blends were investigated by mechanical testing and scanning electron microscopy (SEM). SEM revealed a co-continuous phase structure. The addition of compatibilizers improved the dispersion of DBT in the PLA matrix indicating improved interfacial adhesion between both material phases. Tensile strength and impact strength exceeding that of DBT was observed for the blends excluding the impact strength for the PEOX systems. PLA-g-IA showed better tensile strength and impact strength improvement compared to PEOX/pMDI and PEOX only system indicating that PLA-g-IA is the best compatibilizer for DBT and PLA blend systems.

Keywords: PLA, Decoloured bloodmeal, Novatein, Bloodmeal, Bio-based polymer, Blends, Itaconic anhydride.

1 Introduction

The recent environmental awareness and known effect of petroleum resources on the environment have attracted more attention on the development of biodegradable, environmentally friendly and renewable materials.

Bloodmeal is a protein byproduct of the meat processing industry and consist of complex macromolecules containing 20 different amino acids with strong intra- and intermolecular interactions.[1]. Based on New Zealand industry alone 350,000 tonnes of lamb, 341,000 tonnes of beef and 165,000 tonnes of meat and their products are exported yearly [2]. Bloodmeal has been successfully processed into thermoplastic known as Novatein [3] and used to produce end use products in agriculture and horticulture [4, 5]. Bloodmeal has been treated with peracetic acid to eliminate its odour and dark colour and subsequently, processed into thermoplastic using conventional methods. However, the mechanical properties of the produced thermoplastic known as decoloured bloodmeal thermoplastic (DBT) are very poor compared to conventional polymers. Efforts have been made to blend protein material and other polymers to produce fully biodegradable materials with improved mechanical properties from renewable resources [6-14]. PLA is one of such polymers that have been used for blend with protein [6, 7, 15, 16].

PLA is an aliphatic polyester derived from lactic acid, obtained from fermentation of renewable resources such as corn, sugar cane [17]. PLA has shown to be a good alternative to petroleum-based polymers due to its attractive properties such as high strength, good gas permeability, high transparency, high modulus, biodegradability and renewable origin [18-20]. PLA has found applications in the biomedical, disposable and food packaging industries [18]. Although blending is an effective way of improving polymer properties [9], however blending two polymers will results in an incompatible and inferior material because of poor interfacial adhesion between both distinct polymer phases.

Polymer blend compatibility can be improved by either the addition of a third component, or by grafting a reactive group capable of interacting with each polymer phase. Previous research reported a significant improvement in the mechanical properties of PLA and wheat blend with 0.5 wt% methylene diphenyl diisocyanate (MDI) compared to the blend without MDI [21]. An increase in tensile strength, finer domain size of SPC and lower damping peak were reported for PLA/Soy protein concentrate (SPC) blend with maleic anhydride grafted PLA (PLA-g-MA) compared to the uncompatibilized blend [13]. Rui Zhu et al suggested that the observations were evidences of good interfacial adhesion between the blend surfaces. Yi Dong Li et al reported a finer phase structure with good dispersion of poly(butylene succinate) (PBS) in the blend matrix, improved tensile strength and modulus of soy protein isolate (SPI)/poly(butylene succinate) (PBS) blends with pretreated PBS (pretreated with urethane and isocyanate group) compared to blends without pretreated PBS [9]. Poly(2-ethyl-2-oxazoline) (PEOX) was used as compatibilizer to improve compatibility of soy protein and PLA [11].

Addressing the issue of blend compatibility in our blend system, we grafted itaconic anhydride unto PLA to produce a material that is referred to as PLA-g-IA [22] and introduced it into the blends component as compatibilizer as well as poly (2-ethyl-2-oxazoline) (PEOX) and poly (phenyl isocyanate)-co-formaldehyde (pMDI). The objective of this study was to evaluate the effects of different compatibilizers commonly used for protein blend system on the mechanical and structural properties of DBT and PLA blend for the optimization of DBT based plastics.

2 Material and Methods

2.1 Materials

Bloodmeal was obtained from Wallace Corporation Limited, New Zealand and used as received. Analytical grade itaconic anhydride (IA), dicumyl peroxide (DCP), acetone, 50 wt% hydrogen peroxide, technical grade sodium dodecyl sulphate (SDS), Triethylene glycol (TEG), PEOX and pMDI were all acquired from Sigma Aldrich Auckland, New Zealand. Peracetic acid (Peraclean 5) was purchased from Evonik Industries, Morrinsville, New Zealand. Poly (lactic acid) (PLA) grade 3052D was purchased from NatureWorks LLC USA, sourced from Clariant New Zealand Ltd, Auckland, New Zealand in pellet form. Distilled water was produced onsite at the University of Waikato.

2.2 Sample Preparation

2.2.1 PLA grafting

PLA was modified with itaconic anhydride through free radical grafting [22] to create reactive side-groups. PLA was dried at 80 °C for 4 hours to control moisture. 4.2 parts per hundred PLA (pph) itaconic anhydride and 0.8 pph dicumyl peroxide were dissolved in 30 mL acetone. The preformed solution was poured over the oven dried PLA and was kept in the fume hood for about 2 hours. The solution was decanted before oven drying the PLA for 3 hours at 50 °C. The material was reactively extruded to produce PLA-g-IA using a LabTech twin screw co-rotating extruder having a screw diameter of 20 mm and L/D of 44:1. The temperature profile increased along the barrel from 145 (feed zone) to 180 °C, having the highest temperature at midzone and 155 °C at die zone. A constant screw speed was maintained at 150 rpm. A vacuum pump was attached on the 7th heating zone of the extruder to get rid of vapour generated during extrusion. The pelletized PLA-g-IA was oven dried for 12 hours prior to blending to minimise hydrolysis during melt processing.

2.2.2 Bloodmeal decolouring

Bloodmeal was decoloured using a solution of peracetic acid (PAA) according to previous methods [23, 24]. 4 wt% PAA solution was prepared by diluting 5 wt% PAA stock solutions with distilled water at a constant ratio of 80:20 respectively. 150 g bloodmeal was decoloured by adding 450 g of 4 wt% PAA in a high-speed mixer. The mixture was allowed to mix continuously for 5 min to ensure homogenous decolouring of bloodmeal. 450 g of distilled water was added and mixed for another 5 min to ensure complete dilution of the slurry. The slurry was neutralized by adjusting to pH = 7 with sodium hydroxide solution. The neutralized slurry was filtered using a wire mesh sieve with aperture size 60 and subsequently washed by adding another 450 g of distilled water. The decoloured bloodmeal (DBM) was dried approximately 15 hours in a 75 °C oven.

2.2.3 Decoloured bloodmeal thermoplastic powder preparation

Decoloured bloodmeal thermoplastic powder (DBTP) was formulated by dissolving SDS in water heated to 60 °C while stirring. The solution was added to decoloured bloodmeal in a high-speed mixer and mixed for 5 min. TEG was added to the mixture and mixed for another 5 min to ensure homogeneous mixture is obtained. The prepared DBTP was stored in an air tight bag overnight in a 2 °C fridge to equilibrate.

2.2.4 Blend Preparation

DBTP and PLA grafting were performed prior to blending. All blends contained 50 wt% DBTP, 40 wt% PLA and 10 wt% compatibilizer (PLA-g-IA, PEOX or pMDI) as presented in Table 1. Blends were compounded using the same extruder profile used for grafting PLA. The extrusion temperature varied from 70 to 145 °C (having the lowest temperature at the feed zone and the highest at die zone). The extrudates were granulated using a Tri-blade granulator from Castin Manufacturing Limited.

Table 1: Composition of the blends sampled

Sample Name	Composition				
	DBTP	PLA	Compatibilizer		
IA			PEOX	pMDI	
463	100	0	0	0	0
PLA	0	100	0	0	0
436.PLA	50	50	0	0	0
463.IA	50	40	10	0	0
463.PEOX	50	40	0	10	0
463.PP	50	40	0	3	7

2.2.5 Test Specimen Preparation

ASTM D638-14 Standard tensile test samples [25] and ISO 179-1:2010 impact test specimens [26] were injection moulded using a BOY 35A injection moulding machine. The samples were injected through a cold runner into a 60 °C water heated mould. The injection moulder has five heating zones including the feed and the die zone. The temperature profile increased along the barrel, from 100 °C at the feed zone to 140 °C at the injection nozzle. The screw speed was constant at 150 rpm. The sample specimens produced were also used for morphology testing.

2.3 Sample Analysis

All samples were conditioned for 7 days at 23 °C and 50% relative humidity before testing.

2.3.1 Mechanical Properties

Mechanical testing was performed according to ASTM D638 using Instron Universal Testing machine (model 33R4204) at a crosshead speed of 5 mm/min and an extensometer gauge length of 50 mm. 5 replicates were tested for each sample type to obtain an average value.

The impact testing bars produced from the injection moulder have diameter of 80 x 10 x 4 mm³. Charpy edgewise impact strength was performed according to ISO 179-1:2010 using a RAY-RAN Pendulum Impact System. The bar tested was notched according to standard. 5 bars were tested to obtain average impact strength of the material.

2.3.2 Morphology

The phase structure of the blends was investigated using Hitachi S-4700 field emission scanning electron microscope (SEM). The injection moulded specimens were cryo-fractured using liquid nitrogen. The specimens were sputter coated with platinum using Hitachi E-1030 Ion sputter before scanning. For the digested surface, the samples were extracted with chloroform and then rinsed with hot water to remove PLA phase as DBT is not soluble in chloroform. The extracted surface was dried, and sputter coated prior to examination.

2.3.3 Dynamic Mechanical Analysis (DMA)

Dynamic mechanical analysis (DMA) was conducted using Elmer DMA 8000 fitted with a high temperature furnace and cooled with liquid nitrogen. Rectangular samples (30 x 9 x 4 mm) were cut from injection moulded samples and tested in a single cantilever fixture using free length of 12.5 mm and scanning temperature from -80 to 150 °C at 2 °C/min. data was collected at a single oscillation frequency of 1 Hz. Tan δ peak values were recorded as glass transition temperatures.

3 Results and Discussion

3.1 Morphology

Microstructure of blends are generally associated with their mechanical properties. Blends of almost equal proportions of immiscible polymer often leads to a co-continuous morphology [27]. Normally compatibilizers are used to stabilize the blend's morphology through reduction of the interfacial tension between both immiscible polymer phases. The cryo-fractured surface of PLA, DBT and DBT/PLA blends with different compatibilizers are shown in Figure 1. Presence of interstices and clear agglomerates of DBT particles embedded in the PLA matrix were revealed for blend without compatibilizer (463.PLA). This indicates lack of interfacial adhesion.

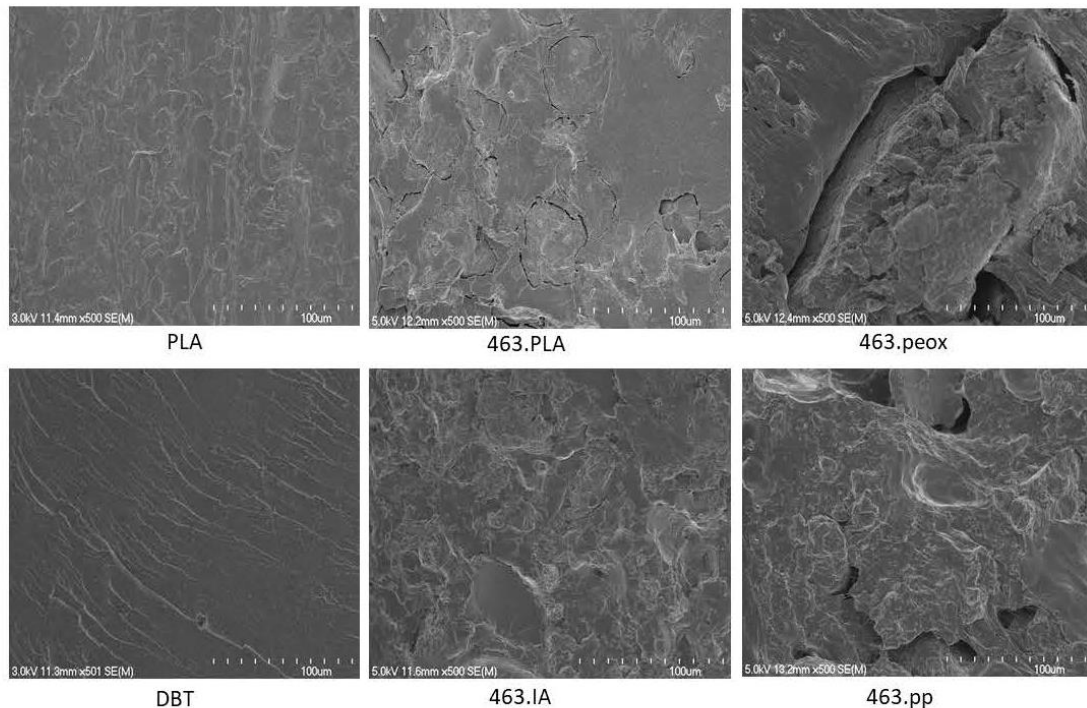


Figure 1: Scanning electron cryo-fractured surface micrographs of both pure and blends of DBT and PLA with different compatibilizers

Blends containing compatibilizer show fewer agglomerated DBT particles compared to the uncompatibilized blend. However, blend 463.peox containing only PEOX revealed a clear interstice and at higher magnification (not included) revealed bridging between phases rich in DBT and PLA. This is indicative of poor interfacial adhesion.

The blend with both PEOX and pMDI showed an improved morphology, although voids were also revealed for this blend. At higher magnification (not included) fewer elongated strand-like structures were observed. This is evidence of an improvement in the interfacial interaction between both DBT and PLA compared to using PEOX alone.

Using PLA-g-IA showed a more improved morphology compared to all blends having much finer and evenly dispersed DBT particles within the blend matrix. Although few agglomerates of DBT were observed. It is thought that DBT rich phase was encapsulated in PLA rich phase resulting in a finer phase structure and improved adhesion compared to using pMDI and PEOX or PEOX alone. Rui Zhu et al [13] reported an improved tensile strength, finer domain sizes of soy protein concentrate and improved interfacial adhesion between PLA/Soy protein composite compatibilized with maleated poly (lactic acid) (PLA-g-MA).

3.2 Mechanical Properties

The morphology of individual polymers in a blend plays an important role in the properties of the polymer blends. This is evident as the mechanical properties of the blends and the pure material as shown in Figure 2 confirmed that the morphologies of both DBT and PLA influenced the mechanical properties of the blends significantly. Blending DBT/PLA without compatibilizer showed a decrease in the tensile strength of the blend compared to both the pure PLA and DBT. This was suggested in literature as a result of poor interfacial interaction due to incompatibility between the two polymer phases. DBT/PLA blend without compatibilizer showed clear interstices between PLA matrix and DBT domain (Figure 1). As suggested by previous researchers [19, 28], it is thought that DBT and the interstices observed acted as stress concentrations in the blend inducing cracks and subsequently resulting in a lower tensile strength. The blends of Novatein Thermoplastic protein and Polybutylene succinate showed an improved compatibility using both PEOX and pMDI as reported by Marsilla and Verbeek [29], suggesting that PEOX improved the dispersion of NTP and pMDI strengthened the adhesion between both material phases.

It could be observed from Figure 2 that incorporating compatibilizers showed an improvement in the tensile strength of the blends. The blend with PLA-g-IA had the highest tensile strength while blend with PEOX had the lowest strength which was also observed in their morphologies. Strain at break showed no significant change for the blends compared to pure PLA. All compatibilizers showed no significant change in strain at break.

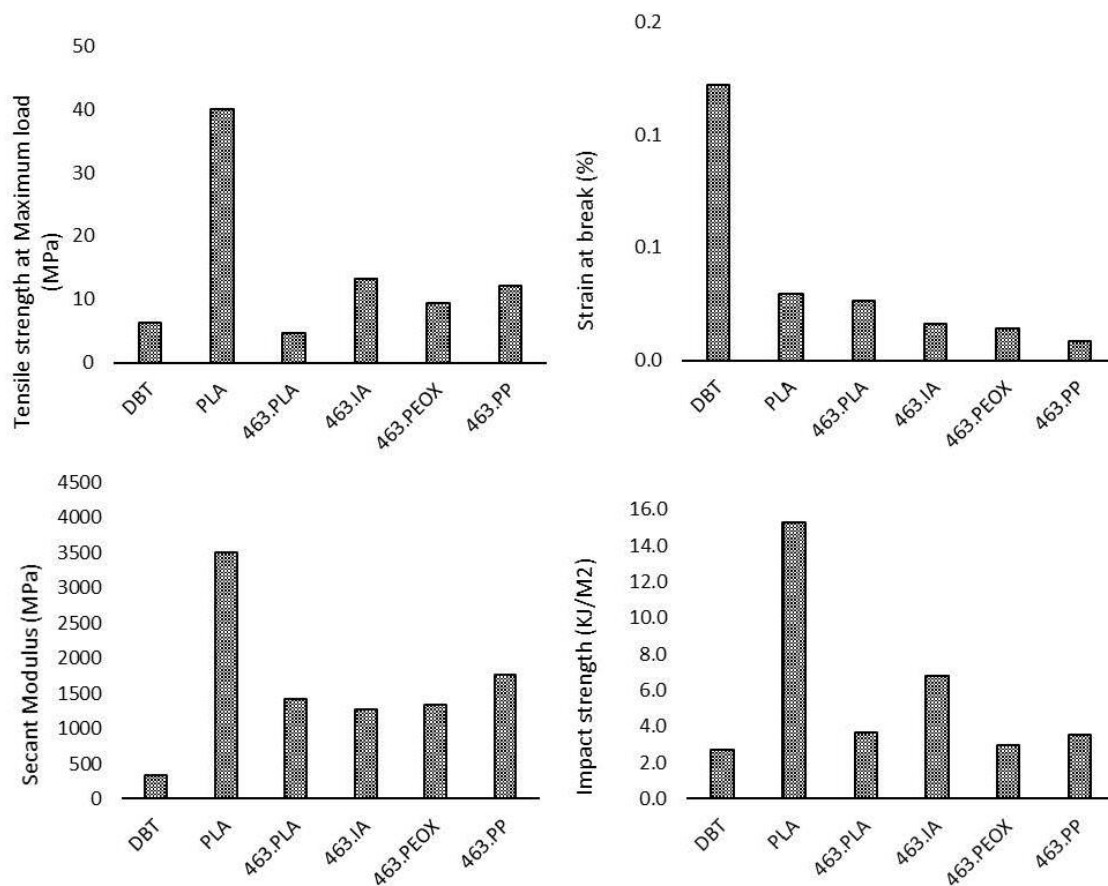


Figure 2: Mechanical properties of PLA, DBT and DBT/PLA blends with different compatibilizers

Secant Modulus increased for all blends compared to DBT. However, a decrease was observed in Secant Modulus of the blends with the incorporation of compatibilizer except for the blend with pMDI suggesting that incorporation of pMDI makes the blend more rigid, although it showed better dispersion in blend's morphology and increased tensile strength compared to using only PEOX as compatibilizer. Blend with PLA-g-IA is less brittle, and rigid compared to blends with PEOX and pMDI as observed in its low secant Modulus compared to the other compatibilizers.

The blend with PLA-g-IA has higher toughness than PEOX alone or PEOX and pMDI. pMDI has isocyanate group that might react with both carboxyl and hydroxyl groups on PLA to produce urethane linkage [30], also can react with amine or probably hydroxyl groups in DBT. The poor interfacial adhesion and low toughness observed might be due to some reaction resulting in secondary chemical bonds between DBT surface and PLA. This was supported by other researchers, which reported high mechanical properties and interfacial adhesion as a result of some of these reactions probably resulting in primary chemical bonding [19]. It was also shown that there was possibility of pMDI reacting predominantly with hydroxyl groups of water rather than starch [31].

The tensile strength and toughness observed for blend with only PEOX was the lowest for all blends suggesting PEOX interacted with DBT through hydrogen bonded water molecule. Previous research by Ku-Marsilla [27] suggested that PEOX interacted with NTP through the arrangement of hydrogen bonded water molecules and the addition of pMDI further strengthened the interactions between PBS and NTP.

3.3 Dynamic Mechanical Analysis (DMA)

Damping temperature (T_g), molecular mobility and material stiffness under dynamic mode can be evaluated through DMA measurement [32]. The movement and broadening of damping temperature helps to predict the

degree of miscibility in a polymer blend. Tan delta ($\tan \delta$), storage modulus and loss modulus as a function of temperature for PLA, DBT and DBT/PLA blends without and with different compatibilizers are shown in Figure 3. PLA showed a sharp and high Tg at approximately 70 °C while DBT exhibited a broad and low Tg at approximately 50 °C. The high damping peak observed for PLA is thought to be associated with PLA low crystallinity as PLA becomes very soft when temperatures are above its α -transition of approximately 70 °C thereby presenting a high damping peak within the transition zone [13]. DBT is in its glassy state, having a low damping temperature compared to PLA. This suggests that DBT behaved more like a rigid material in the blends reducing the damping peak of PLA in the blends compared to pure PLA.

Good interaction and compatibility between two polymer phases in a blend, is usually determined by the movement of each damping temperature towards each other [9, 27, 31]. A peak and a shoulder were observed for blends. The peak is consistent with DBT damping temperature while the shoulder observed is consistent with PLA phase. This confirms that DBT restricted the movement of PLA chain thereby reduced the Tg of PLA resulting in broadening of the peak. The shoulder decreased in intensity with the addition of compatibilizers. This might be due to more effective contribution of DBT phase to the storage modulus in the rubbery region of PLA with the addition of compatibilizer. Blends with compatibilizers showed a slight decrease in Tg of PLA and an increase in the Tg of DBT in the blends, coming closer to each other with 463.IA (blend with PLA-g-IA) having the highest shift towards each other. This indicates better interaction between DBT and PLA with the addition of PLA-g-IA.

High storage modulus was observed for blends with compatibilizers indicating an improvement in interaction between DBT and PLA phases. Comparing the compatibilizers used, PLA-g-IA was less rigid than PEOX alone or PEOX and pMDI.

The loss modulus curve of PLA showed a sharp peak at 60 °C while DBT showed a broader peak at approximately 15 °C. It is expected that the modulus curve of a polymer blend will be similar to the modulus curve of the continuous phase as it provides greater contribution to modulus of the blend. The blend of DBT/PLA without compatibilizer showed a peak at appropriately 55 °C with a drop when the Tg of PLA was reached, then recovered to a significant degree of between 90 to 130 °C. However, with the addition of compatibilizer, the peak intensity increased significantly compared to the uncompatibilized blend. The loss modulus curve of the blends with compatibilizer resembles that of PLA, although there is a decrease in peak's intensity and an apparent recovery between 100 to 120 °C. This recovery is thought to be due to cold crystallization of PLA [33]. The similarity in the curves of PLA and blends with compatibilizer suggested that PLA coalesced and encapsulated DBT making PLA the continuous phase and DBT, the dispersed phase as observed in their morphologies.

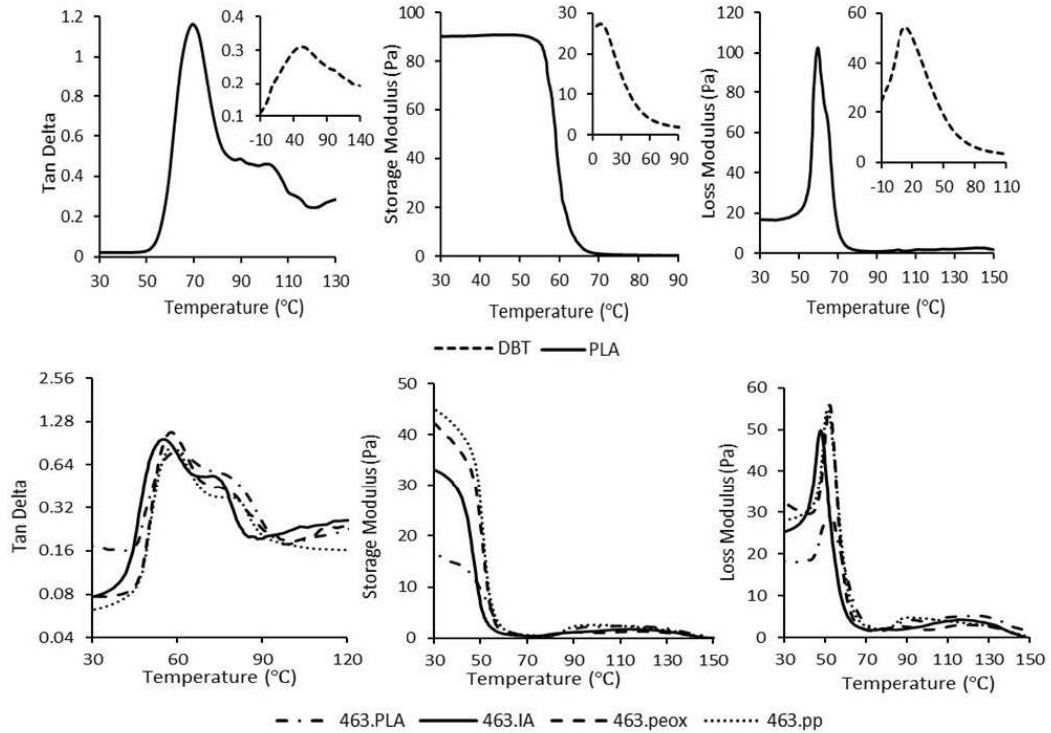


Figure 3: Tan δ , storage modulus and loss modulus of DBT, PLA and DBT/PLA blends without (463.PLA) and with different compatibilizer (463.IA, 463.peox and 463.pp)

4 Conclusion

The morphology of DBTP/PLA blend without compatibilizer revealed the presence of interstices and clear agglomerates of DBT embedded in the PLA matrix indicating the presence of interfacial tension and leading to poor mechanical properties. However, with the addition of compatibilizer an even distribution of the DBT particles and reduced interstices were observed. The morphology also suggested that PLA is the continuous phase while DBT is the dispersed phase. This is supported by the similarity in the loss modulus curves of PLA and the blends. Comparing the different compatibilizers, PLA-g-IA showed a more improved morphological structure compared to all compatibilizers used (pMDI and PEOX or PEOX alone) having much finer and evenly dispersed DBT particles within the blend matrix. It is thought that DBT rich phase was encapsulated in PLA rich phase which resulted in the finer phase structure and improved adhesion observed in the SEM.

Uncompatibilized blend showed a decrease in mechanical properties because of the interstices and phase separation observed in the morphology due to the restriction of strong protein-protein interaction. Comparing the different compatibilizers sampled, PEOX alone and PEOX/pMDI showed a decrease in tensile strength, impact strength and an increase in the secant modulus compared to PLA-g-IA compatibilized blend.

The peak and the shoulder observed in the Tan δ of uncompatibilized blend shifted towards each other with addition of compatibilizers. The blend with PLA-g-IA had the highest shift towards each other, suggesting that better interfacial adhesion was achieved in the presence of PLA-g-IA.

This study successfully demonstrated that PLA-g-IA served as the most effective compatibilizer for DBT/PLA blends. Using PLA-g-IA showed significant effect on the morphology and properties of DBT/PLA blends compared to PEOX alone and PEOX/pMDI.

5 References

1. van den Berg, L.E., *Development of 2nd generation proteinous bioplastics*. 2009, The University of Waikato.
2. Izuchukwu, S.C.P., *The Effect of Moisture Content and Extrusion Temperature on the Processing, Thermal and Mechanical Properties of Novatein®*. 2015, University of Waikato: Hamilton, New Zealand.
3. Pickering, K.L., et al., *Plastics material*. 2012, Google Patents.
4. Walallavita, A., C.J. Verbeek, and M. Lay. *Blending Novatein® thermoplastic protein with PLA for carbon dioxide assisted batch foaming*. in *AIP Conference Proceedings*. 2016. AIP Publishing.
5. van der Merwe, D.W., *The Environmental and Economic Impacts for Producing the Port Jackson from Novatein®*. 2014, University of Waikato.
6. Fang, K., et al., *Properties and morphology of poly (lactic acid)/soy protein isolate blends*. *Journal of applied polymer science*, 2009. **114**(2): p. 754-759.
7. Graiver, D., et al., *Biodegradable soy protein–polyester blends by reactive extrusion process*. *Journal of applied polymer science*, 2004. **92**(5): p. 3231-3239.
8. John, J. and M. Bhattacharya, *Properties of reactively blended soy protein and modified polyesters*. *Polymer international*, 1999. **48**(11): p. 1165-1172.
9. Li, Y.-D., et al., *Structure and properties of soy protein/poly (butylene succinate) blends with improved compatibility*. *Biomacromolecules*, 2008. **9**(11): p. 3157-3164.
10. Rhim, J.-W., J.H. Lee, and P.K. Ng, *Mechanical and barrier properties of biodegradable soy protein isolate-based films coated with polylactic acid*. *LWT-Food Science and Technology*, 2007. **40**(2): p. 232-238.
11. Zhang, J., et al., *Morphology and properties of soy protein and polylactide blends*. *Biomacromolecules*, 2006. **7**(5): p. 1551-1561.
12. Zhong, Z. and X.S. Sun, *Properties of soy protein isolate/polycaprolactone blends compatibilized by methylene diphenyl diisocyanate*. *Polymer*, 2001. **42**(16): p. 6961-6969.
13. Zhu, R., H. Liu, and J. Zhang, *Compatibilizing effects of maleated poly (lactic acid)(PLA) on properties of PLA/Soy protein composites*. *Industrial & Engineering Chemistry Research*, 2012. **51**(22): p. 7786-7792.
14. Marsilla, K. and C.J.R. Verbeek, *Blends of linear-low-density polyethylene and thermoplastic bloodmeal using maleic anhydride grafted polyethylene as compatibilizer*. 2012.
15. Liu, B., et al., *Synergetic effect of dual compatibilizers on in situ formed poly (lactic acid)/soy protein composites*. *Industrial & Engineering Chemistry Research*, 2010. **49**(14): p. 6399-6406.
16. Rhim, J.-W., et al., *Preparation and properties of biodegradable multilayer films based on soy protein isolate and poly (lactide)*. *Industrial & engineering chemistry research*, 2006. **45**(9): p. 3059-3066.
17. Yang, S.-I., et al., *Thermal and mechanical properties of chemical crosslinked polylactide (PLA)*. *Polymer Testing*, 2008. **27**(8): p. 957-963.
18. Ali, F., et al., *Thermal, mechanical and rheological properties of poly (lactic acid)/epoxidized soybean oil blends*. *Polymer Bulletin*, 2009. **62**(1): p. 91-98.
19. Wang, H., X. Sun, and P. Seib, *Mechanical properties of poly (lactic acid) and wheat starch blends with methylenediphenyl diisocyanate*. *Journal of applied polymer science*, 2002. **84**(6): p. 1257-1262.
20. Noori, F.T.M. and N.A. Ali, *Study the mechanical and thermal properties of biodegradable polylactic acid/poly ethylene glycol nanocomposites*. *Int J Appl Innov Eng Manag*, 2014. **3**(1): p. 459-464.
21. Wang, H., X. Sun, and P. Seib, *Properties of poly (lactic acid) blends with various starches as affected by physical aging*. *Journal of applied polymer science*, 2003. **90**(13): p. 3683-3689.
22. Marsilla, K.K. and C. Verbeek, *Modification of poly (lactic acid) using itaconic anhydride by reactive extrusion*. *European Polymer Journal*, 2015. **67**: p. 213-223.
23. Low, A., C.J.R. Verbeek, and M.C. Lay, *Treating Bloodmeal with Peracetic Acid to Produce a Bioplastic Feedstock*. *Macromolecular Materials and Engineering*, 2014. **299**(1): p. 75-84.
24. Hicks, T.M., et al., *The role of peracetic acid in bloodmeal decoloring*. *Journal of the American Oil Chemists' Society*, 2013. **90**(10): p. 1577-1587.
25. Properties, A.S.D.o.M. *Standard test method for tensile properties of plastics*. 1996. American Society for Testing and Materials.
26. ISO, E., *179-1 (2010)*.". *Plastics. Determination of Charpy impact properties. Part. 1*.
27. Ku-Marsilla, K. and C. Verbeek, *Compatibilization of Protein Thermoplastics and Polybutylene Succinate Blends*. *Macromolecular Materials and Engineering*, 2015. **300**(2): p. 161-171.
28. Smith, M.J. and C.J. Verbeek, *Compatibilization effects in thermoplastic protein/polyester blends*. *Journal of Applied Polymer Science*, 2018. **135**(6).

29. Marsilla, K.K. and C. Verbeek, *Properties of Blends of Novatein Thermoplastic Protein from Bloodmeal and Polybutylene Succinate Using Two Compatibilizers*.
30. Dieteroch, D., E. Grigat, and W. Hahn, *In Polyurethane Handbook*, Oertel, G. Hanser, New York, 1985. 7.
31. Mohamed, A., et al., *Thermal and mechanical properties of compression-molded pMDI-reinforced PCL/gluten composites*. *Journal of applied polymer science*, 2010. **118**(5): p. 2778-2790.
32. Menczel, J.D. and R.B. Prime, *Thermal analysis of polymers: fundamentals and applications*. 2014: John Wiley & Sons.
33. Jiang, L., M.P. Wolcott, and J. Zhang, *Study of biodegradable polylactide/poly (butylene adipate-co-terephthalate) blends*. *Biomacromolecules*, 2006. **7**(1): p. 199-207.